GA-A15144
UC-77

GAS-COOLED FAST BREEDER REACTOR

QUARTERLY PROGRESS REPORT FOR THE PERIOD AUGUST 1, 1978 THROUGH OCTOBER 31, 1978

by
PROJECT STAFF

Prepared under
Contract EY-76-C-03-0167
Project Agreement No. 23
for the San Francisco Operations Office
Department of Energy

GENERAL ATOMIC PROJECT 3228
DATE PUBLISHED: NOVEMBER 1978

GENERAL ATOMIC COMPANY

PROGRESS REPORT SERIES

GA-5537	November 1, 1963 through July 31, 1964
GA-6667	August 1, 1964 through July 31, 1965
GA-7645	August 1, 1965 through July 31, 1966
GA-8107	August 1, 1966 through July 31, 1967
GA-8787	August 1, 1967 through July 31, 1968
GA-8895	August 1, 1968 through October 31, 1968
GA-9229	November 1, 1968 through January 31, 1969
GA-9359	February 1, 1969 through April 30, 1969
GA-9639	May 1, 1969 through July 31, 1969
GA-9811	August 1, 1969 through October 31, 1969
GA-9838	November 1, 1969 through January 31, 1970
GA-10517	February 1, 1970 through January 31, 1971
GA-10645	February 1, 1971 through April 30, 1971
GA-A10803	May 1, 1971 through July 31, 1971
GA-A10906	August 1, 1971 through July 31, 1972
GA-A12003	November 1, 1971 through January 31, 1972
GA-A12165	February 1, 1972 through April 30, 1972
GA-A12252	May 1, 1972 through July 31, 1972
GA-A12421	August 1, 1972 through October 31, 1972
GA-A12530	November 1, 1972 through January 31, 1973
GA-A12635	February 1, 1973 through April 30, 1973
GA-A12728	May 1, 1973 through July 31, 1973
GA-A12824	August 1, 1973 through October 31, 1973
GA-A12894	November 1, 1973 through January 31, 1974
GA-A13021	February 1, 1974 through April 30, 1974
GA-A13148	May 1, 1974 through July 31, 1974
GA-A13238	August 1, 1974 through October 31, 1974
GA-A13379	November 1, 1974 through January 31, 1975
GA-A13458	February 1, 1975 through April 30, 1975
GA-A13565	May 1, 1975 through July 31, 1975

GA-A13766	August 1, 1975 through October 31, 1975
GA-A13815	November 1, 1975 through January 31, 1976
GA-A13868	February 1, 1976 through April 30, 1976
GA-A13975	May 1, 1976 through July 31, 1976
GA-A14112	August 1, 1976 through October 31, 1976
GA-A14240	November 1, 1976 through January 31, 1977
GA-A14358	February 1, 1977 through April 30, 1977
GA-A14492	May 1, 1977 through July 31, 1977
GA-A14613	August 1, 1977 through October 31, 1977
GA-A14771	November 1, 1977 through January 31, 1978
GA-A14928	February 1, 1978 through April 30, 1978
GA-A15054	May 1, 1978 through July 31, 1978

ABSTRACT

The tasks of the gas-cooled fast breeder reactor (GCFR) program which are supported by the Department of Energy include development of GCFR fuel, blanket, and control assemblies; development of the pressure equalization system for GCFR fuel; out-of-pile loop facility test programs; fuels and materials development; fuel, blanket, and control rod analyses and development; nuclear analysis and reactor physics for GCFR core design; shielding requirements for the GCFR; reactor engineering to assess the thermal, hydraulic, and structural performance of the core and the core support structure; plant systems control; systems engineering; development of reactor components, including reactor vessel, control and locking mechanisms, fuel handling equipment, core support structure, shielding assemblies, main helium circulator, steam generator, circulator test facility, and auxiliary circulator; development of a helium circulator test facility; reactor safety, environment, and risk analyses, including planning and support of an in-pile and out-of-pile safety test program; nuclear island engineering design; and development of a reliability data bank.

CONTENTS

ABSTRACT v

1. INTRODUCTION 1-1

2. CORE ASSEMBLY DEVELOPMENT (189a No. 00502) 2-1

2.1. Core Assembly Thermal-Hydraulic Analysis 2-1

2.1.1. Introduction 2-1

2.1.2. Fuel Assembly Analysis 2-1

2.1.3. Control Assembly Analysis 2-6

2.1.4. Radial Blanket Analysis 2-6

2.1.5. Integral Core Performance of Demonstration Plant Core 2-7

2.2. Core Assembly Mechanical Analysis 2-8

2.2.1. Up-Flow Core Design 2-8

2.2.2. Core Distortion Analysis 2-17

2.2.3. Outlet Nozzle Mechanical Analysis 2-21

2.2.4. Core Assembly Flow-Induced Vibration 2-23

2.2.5. Core Seismic Engineering 2-25

2.3. Core Assembly Structural Design Criteria 2-28

2.4. Core Assembly Mechanical Testing 2-28

2.5. Heat Transfer and Fluid Flow Testing 2-30

References 2-30

3. PRESSURE EQUALIZATION SYSTEM FOR FUEL (189a No. 00582) 3-1

3.1. Core Assembly and PES Seals 3-1

3.2. Analysis, Models, and Code Development 3-1

3.3. Plateout and Plugging 3-1

3.4. Fission Product Release and Transport 3-2

3.5. Monitor Station and Instrumentation 3-3

3.6. PES Up-Flow Core Assessment 3-3

References 3-5

4. CORE ASSEMBLY DESIGN VERIFICATION (189a No. 00582) 4-1
4.1. Core Flow Test Loop Program 4-2
4.1.1. Program Planning 4-2
4.1.2. CFTL Analysis 4-6
4.1.3. CFTL Liaison 4-9
4.2. GCFR Prototype Assembly Test Program 4-9
4.3. Helium Flow Test 4-11
4.4. Depressurized Accident Condition Test 4-15
4.5. In-Pile Loop for GRIST-2 Fuel Rod Conditioning 4-15
4.6. Fast Test Reactor Helium Loop Study 4-16
References 4-16
5. FUELS AND MATERIAL ENGINEERING (189a No. 00582) 5-1
5.1. Oxide Fuel and Blanket Technology 5-1
5.2. Cladding Technology 5-2
5.2.1. Mechanical Testing Program 5-2
5.2.2. Helium Loop Test Program 5-3
5.3. F-1 (X094) Fast Flux Irradiation Experiment 5-4
5.4. F-3 (X206) Fast Flux Irradiation Experiment 5-5
5.5. F-5 (X317) Grid-Spaced Fuel Rod Bundle Fast Flux Irradiation Experiment 5-5
5.6. GB-10 Vented Fuel Rod Experiment 5-6
References 5-9
6. FUEL ROD ENGINEERING (189a No. 00583) 6-1
6.1. Fuel, Blanket, and Control Rod Analytical Methods 6-1
6.2. Analysis of Irradiation Tests 6-5
6.3. Rod Analysis and Performance 6-5
6.3.1. Steady-State Operating Conditions 6-6
6.3.2. Transient Operating Conditions 6-7
6.4. Fuel Rod Mechanical Tests 6-8
References 6-8
7. NUCLEAR ANALYSIS AND REACTOR PHYSICS (189a No. 00584) 7-1
7.1. Critical Assembly Planning 7-1
7.2. Distorted Core Analysis 7-3
7.2.1. Description of Reference Configuration 7-3

7.2.2. Generation of Cross Sections 7-4
7.2.3. Derivation of Streaming Correction Factors 7-5
7.2.4. Diffusion Theory Calculations 7-5
7.2.5. Transport Theory Calculations and Method Studies 7-5
References 7-6
8. SHIELDING REQUIREMENTS (189a No. 00584) 8-1
8.1. One-Dimensional Analysis of Radial Shielding for Conceptual Shielding Configuration 1 8-1
8.2. Material Damage Response Functions for GA and ORNL Shielding Analysis 8-7
8.3. Radial Shielding Experiment Requirements 8-8
8.4. Data Requirements for Structural Material Irradiation Effects 8-9
References 8-10
9. SYSTEMS ENGINEERING (189a No. 00585) 9-1
9.1. Systems Design 9-1
9.1.1. Up-flow/Down-flow Core Studies 9-1
9.1.2. Main Circulator Drive Study 9-3
9.1.3. Residual Heat Removal 9-3
9.1.4. Primary Coolant System 9-4
9.1.5. Parametric Model for the Steam and Circulating Water Systems 9-4
9.2. Systems Integration 9-5
10. COMPONENT DEVELOPMENT (180a No. 00585) 10-1
10.1. Reactor Vessel 10-1
10.2. Control and Locking Mechanisms 10-12
10.3. Fuel Handling Development 10-15
10.4. Core Support Structure 10-17
10.4.1. Stress and Dynamic Analyses of Up-Flow Core Support Structure 10-18
10.4.2. Interim Up-Flow Core Study Input 10-18
10.5. Reactor Shielding Assemblies 10-20
10.6. Main Helium Circulator, Valve and Service System 10-22

10.6.1. Main Helium Circulator 10-22
10.6.2. Shaft and Bearings 10-24
10.6.3. Electric Motor Drive Design Recommendations 10-24
10.6.4. Motor Reliability 10-30
10.6.5. Motor and Controller Experience 10-31
10.7. Steam Generator 10-32
10.8. Auxiliary Circulator, Valve and Service System 1035
10.8.1. Aerodynamic Design and Performance 10-38
10.8.2. Rotor Dynamics of the Hydraulic Drive Auxiliary Circulator 10-42
10.8.3. Core Auxiliary Heat Exchanger 10-52
10.9. Helium Processing Components 10-53
10.10. Control and Electric Components 10-55
10.10.1. Main Circulator Electric Drive Study 10-55
10.10.2. Separation of IE Power Sources: Safety Residual Heat Removal System 10-56
10.10.3. Plant Protection System Trip on Core Reactivity and Delayed Neutron Activity . . . 10-61
10.10.4. Plant Protection System Response to Six Accident Cases 10-61
References 10-62
11. CIRCULATOR TEST FACILITY (189a No. 00586) 11-1
Reference 11-5
12. PLANT DYNAMICS (189a No. 00586) 12-1
12.1. Control Systems 12-1
12.1.1. Main Steam Temperature and Neutron Flux Control 12-1
12.1.2. Main Steam Pressure and Feedwater Flow Control 12-4
12.1.3. Steam Generator Module Outlet Temperature and Helium Circulator Speed Control 12-4
12.2. Seismic Engineering 12-5
12.3. Flow-Induced and Acoustically Induced Vibrations 12-5

13. REACTOR SAFETY, ENVIRONMENT, AND RISK ANALYSIS (189a No. 00589) 13-1

13.1. Reactor Safety Program Coordination 13-1

13.1.1. Safety Evaluation of Up-Flow Core 13-1

13.1.2. General Safety Assessment 13-2

13.2. Probabilistic Safety Analysis: Reliability Evaluation of Residual Heat Removal by Natural Circulation 13-3

13.3. Core Accident Analysis 13-5

13.3.1. Core Disruptive Accident Consequences for Up-Flow Versus Down-Flow Concepts 13-5

13.3.2. Protective Loss of Flow Accident Analysis 13-6

13.3.3. Loss of Flow Analysis 13-13

13.3.4. Transient Overpower Analysis 13-18

13.3.5. Single-Assembly Blockage Analysis 13-21

13.4. Post Accident Fuel Containment 13-23

13.4.1. Initial PAFC Conditions 13-24

13.4.2. Retention Volume Required 13-24

13.4.3. Upward Heat Removal 13-25

13.4.4. Potential Reduction of Retention Volume . . . 13-25

13.4.5. Stored Heat Effect and the Possibility of Fuel Boiling 13-25

13.4.6. Steel Bath Core Retention Concept 13-26

13.4.7. Emphasis in PAFC System Design 13-26

13.4.8. Downward Heat Removal and Refueling Penetration 13-26

13.4.9. Planned PAFC Analysis 13-26

13.5. Engineering Reliability Integration 13-27

13.6. Gas-Cooled Reactor Reliability Bank 13-27

14. GCFR SAFETY TEST PROGRAM (189a No. 00588) 14-1

14.1. GRIST-2 Program 14-1

14.2. GRIST-2 Preliminary Test Plan Fuel Fabrication and Preirradiation Requirements 14-3

14.3. Duct Melting and Fallaway Test Program 14-7

14.3.1. FLS-1 Experiment 14-7

14.3.2. FLS-1 Analytical Support 14-12
References 14-12
15. GCFR NUCLEAR ISLAND DESIGN (189a No. 00615) 15-1
16. ALTERNATE DESIGN STUDY (189a No. 00759) 16-1
16.1. Alternate Residual Heat Removal System Study 16-1
16.1.1. Residual Heat Removal Requirements 16-1
16.1.2. Reference Design 16-2
16.2. Alternate RHR Concepts 16-2
16.2.1. Screening Evaluation 16-4
16.2.2. Candidate Concepts 16-5
References 16-6
17. ALTERNATE FUEL CYCLES (189a No. 00761) 17-1
17.1. Approximate Sensitivity Analysis 17-1
17.2. Detailed Mass Flow Information 17-5
17.3. Alternate Fuel Cycle Materials 17-5
References 17-5

FIGURES

2-1. 104-mm pitch fuel assembly with fueled corner rod 2-3
2-2. Edge rod temperature drop 2-4
2-3. Average cladding midwall temperature 2-5
2-4. Pneumatic balancing for fuel assembly inlet nozzle (KWU design) 2-11
2-5. Standing assembly mechanical lock 2-12
2-6. Fuel assembly inlet nozzle mechanical latching 2-14
2-7. Fuel assembly outlet shielding 2-15
2-8. Control assembly outlet shielding 2-16
2-9. Fuel assembly general arrangement (up-flow core) 2-18
2-10. Up-flow core concept 2-19
2-11. Relative duct displacements with bulging points (750 h) 2-22
2-12. Finite element mesh of fuel assembly outlet nozzle 2-24

FIGURES (Continued)

2-13. Core restraint support locations for down-flow core GCFR 2-29

4-1. Conceptual design of helium flow test rig 4-12

4-2. Helium flow test rig 4-13

4-3. Schedule of flow/vibration testing of GCFR core assemblies in the helium flow test rig 4-14

5-1. Depressurization and resealing concept 5-7

5-2. Proposed disassembly and examination sequence for subassembly X317 5-8

6-1. Release-to-birth ratio for Kr-87 6-3

6-2. Release-to-birth ratio for Xe-138 6-4

8-1. Model of down-flow demonstration plant shielding system and reactor internal components, conceptual shielding configuration 1 8-3

8-2. Nuclear heating profile through the radial shielding, PCRV liner, and PCRV for conceptual shielding configuration 1 8-6

10-1. 300-MW(e) GCFR PCRV configuration with up-flow core, concept No. 4A 10-2

10-2. 300-MW(e) GCFR PCRV configuration with up-flow core, concept No. 7A 10-3

10-3. 300-MW(e) GCFR PCRV up-flow core with rotating plug 10-5

10-4. 300-MW(e) GCFR PCRV with horizontally mounted helium circulator 10-6

10-5. 300-MW(e) GCFR PCRV arrangement with rotating refueling plug 10-7

10-6. Conceptual up-flow core configuration 10-19

10-7. Lower plenum shielding reference design 10-21

10-8. GCFR main helium circulator 10-23

10-9. Comparison of Westinghouse and GA results (all bearings have same stiffness and zero damping) 10-25

10-10. Comparison of Westinghouse and GA results for the exciter 10-26

10-11. Comparison of GA results with Westinghouse data for the motor rotor 10-27

10-12. Comparison of Westinghouse and GA results for the coupling 10-28

FIGURES (Continued)

10-13. General arrangement of top exhaust steam generator 10-33

10-14. Expansion loop stresses and frequencies with respect to geometry and allowable values 10-36

10-15. GCFR auxiliary loop isolation valve 10-37

10-16. Compressor performance (nondimensional parameters); GCFR auxiliary circulator designed for DBDA (no air ingress) 10-41

10-17. Auxiliary circulator electric drive 10-43

10-18. Auxiliary circulator shaft assembly 10-45

10-19. Critical speed map for GCFR electric drive auxiliary circulator 10-46

10-20. Hydraulic drive auxiliary circulator 10-49

10-21. Critical speed map for GCFR hydraulic drive auxiliary circulator 10-51

10-22. Radially free support plate concept for core auxiliary heat exchangers 10-54

10-23. IE power system for loop 1 of core auxiliary cooling system (typical of loops 2 and 3; loop 2 is IE Division II 2, loop 3 is IE Division 3) 10-58

10-24. IE power system for loop A of shutdown cooling system (typical of loops B and C; loop B is IE Division V, loop C is IE Division VI) 10-59

10-25. Trip on increase of trip parameter 10-63

10-26. Trip on decrease of trip parameter 10-64

11-1. GCFR helium circulator test facility 11-2

11-2. Schematic diagram of GCFR helium circulator test facility 11-3

12-1. Plant schematic indicating control system measurements 12-2

12-2. Control system structure 12-3

13-1. Up-flow/down-flow core disruptive accident assessment program 13-7

13-2. PLOF event sequence diagram 13-9

13-3. LOF event sequence diagram 13-15

13-4. TOP event sequence diagram 13-19

13-5. Total flow blockage of an individual subassembly 13-22

FIGURES (Continued)

14-1. Proposed GRIST-2 testing schedule to meet needs of tests outlined in preliminary test plan 14-5

14-2. Fuel preirradiation program to support tests outlined in preliminary GRIST-2 test plan 14-6

14-3. Estimated schedule for designing and constructing a preirradiation loop facility for the GRIST-2 program 14-8

17-1. Characteristics of 1200-MW(e) GCFR, Pu/U/U/UO_2 17-3

17-2. Energy potential of a Pu/U/U/U/ GCFR influenced by fuel rod diameter 17-4

TABLES

2-1. Design basis core data for the up-flow/ down-flow comparison 2-9

2-2. Flow parameters for alternate helium flow test rigs 2-26

2-3. Summary of preliminary helium flow test program 2-27

4-1. Input for experimentally modeling the GCFR DBDA 4-4

4-2. Activities for defining experimental modeling of the GCFR DBDA 4-5

4-3. Comparison of heaters with CFTL power supply 4-7

4-4. CFTL 61-rod blanket bundle duct bowing steady-state design margin test with maximum power skew (test 951, maximum bowing) 4-8

6-1. Fuel cladding mechanical test matrix 6-9

8-1. Exposure margins for conceptual shielding configuration 1 (core midplane level) 8-5

10-1. Major GCFR closures 10-10

10-2. GCFR auxiliary circulator compressor design 10-40

10-3. Main parameters of GCFR hydraulic drive auxiliary circulator. 10-47

10-4. Class IE separation 10-60

14-1. GRIST-2 preliminary test plan outline (first 5 years) 14-4

TABLES (Continued)

14-2. Preirradiation requirements that need further definition prior to initiating preirradiation facilities survey 14-9

14-3. List of fuel requirements needing definition in order to define the scope of the GRIST-2 fuel fabrication and preirradiation task 14-11

16-1. Alternate RHR configurations 16-3

17-1. Comparison of GCFR round 1 and round 2 physics parameters in the NASAP study 17-6

1. INTRODUCTION

The various tasks of the gas-cooled fast breeder reactor (GCFR) program for the period August 1, 1978 through October 31, 1978 sponsored by the Department of Energy (DOE) are discussed in this quarterly progress report. The GCFR utility program, which is sponsored by a large number of electric utility companies, rural electric cooperatives, and General Atomic (GA), is primarily directed toward the development of a GCFR demonstration plant. The utility-sponsored work and the DOE-sponsored work are complementary.

Analytical, experimental, and fabrication development is being accomplished under the core assembly development task to establish the basis for the design of GCFR fuel, blanket, and control assemblies. Methods development for structural, thermal-hydraulic, and mechanical analyses is discussed, and the results of structural analysis of the fuel assembly components and thermal-hydraulic analysis of the blanket assembly during low power are presented. Current progress on rod-spacer interaction tests, fuel assembly seismic and vibration test planning, and development of assembly fabrication techniques is also presented. The various subtasks of core assembly development and the work accomplished during this reporting period are discussed in Section 2.

The technology to support the design and construction of the pressure equalization system (PES) for GCFR fuel is being developed. This includes (1) the development of analytical models and computer codes which will be verified by test programs and testing of materials and seals and (2) the development of fabrication processes for the PES. These are discussed in Section 3.

To demonstrate the ability of GCFR fuel, control, and blanket assembly designs to meet design goals and verify predictions of analytical models, a

series of out-of-pile simulation tests will be performed. The emphasis of the tests will be on obtaining thermal-structural data for steady-state, transient, and margin conditions using electrically heated rod bundles in a dynamic helium loop. These are discussed in Section 4.

In the fuels and materials development program, thermal flux and fast flux irradiation studies are being conducted to establish conditions and design features specific to GCFR fuel rods, such as vented fuel, fission product traps, and surface-roughened cladding. In addition, an irradiation test program of smooth and surface-roughened GCFR cladding specimens will be conducted to determine how these materials behave under irradiation. The fuels and materials tests, the analytical studies, and the results to date are presented in Section 5.

Under the fuel rod engineering task, performance of the fuel and blanket rods under steady-state and transient conditions is being evaluated to determine performance characteristics, operating limits, and design criteria. In addition, surveillance of the fuel rod and blanket rod technology of other programs is being carried out. These studies are presented in Section 6.

The objectives of the nuclear analysis and reactor physics task are to verify and validate the nuclear design methods which will be applied to the GCFR core design. Data from a critical assembly experimental program at the ZPR-9 facility at Argonne National Laboratory (ANL) are being used for this purpose. Critical assembly design, analysis, and methods development are discussed in Section 7.

Verification of the physics and engineering analytical methods and the data for design of the GCFR shields is being conducted under the shielding requirements task along with an evaluation of the effectiveness of various shield configurations. The results of radial shield analyses and the work being done on structural analysis are presented in Section 8.

Section 9 discusses systems engineering for the GCFR. This includes systems integration; coordination of interface requirements between plant systems; and development and implementation of effective documentation management.

Section 10 discusses the evaluation and development of the main components of the GCFR, including reactor vessel, control and locking mechanisms, fuel handling, core support structure, shielding assemblies, main helium circulator, steam generator, auxiliary circulator, and helium processing components. Section 11 is concerned with the engineering required to design and develop the circulator test facility, and Section 12 reports on the development of control systems and the assessment of seismically induced and flow-induced vibration behavior for the GCFR demonstration plant.

The reactor safety task, which is discussed in Section 13, includes (1) maintenance of liaison between GA and other organizations and integration of the overall GCFR safety analysis effort; (2) formulation and review of the GCFR safety program plan; (3) performance of detailed safety, environmental, and risk analyses of the GCFR; (4) evaluation of the post-accident fuel containment (PAFC) capability of the GCFR; (5) integration of the results of DOE safety studies into the licensing reviews; and (6) evaluation of probabilistic design methods for use in the GCFR program. Procurement, supply, and storage of reliability data are also reported along with estimates in support of probabilistic analyses of accident events being analyzed for gas-cooled reactors.

Section 14 discusses the safety test program, which involves quantification of fuel and cladding behavior during accidents leading to core damage and identification of safety test information required for licensing and commercialization of the GCFR. The GRIST-2 and duct melting and fall-away test programs (DMFT) are also examined.

Section 15 discusses the nuclear island. The purposes of this task are to accomplish engineering design work on the nuclear island portion

of the demonstration plant and to resolve the interface requirements of major nuclear steam supply (NSSS) and balance of plant (BOP) systems.

Development of an alternate design concept for the NSSS and related BOP facilities and equipment is discussed in Section 16, and the characteristics of a GCFR fueled with combinations of U-233, U-235, U-238, plutonium, and thorium are reported in Section 17.

2. CORE ASSEMBLY DEVELOPMENT
(189a No. 00502)

2.1. CORE ASSEMBLY THERMAL-HYDRAULIC ANALYSIS

2.1.1. Introduction

Experimental data are being evaluated to develop the analytical basis for the design and development of the GCFR fuel, control, and blanket assemblies. Because complete prototype in-pile tests cannot be conducted, a strong analytical base supported by development tests is required to design the core assemblies. The current effort is devoted to the development of an adequate steady-state and transient analysis capability in the areas of thermal-hydraulic and structural analysis to provide a basis for assembly design criteria and specific test requirements. The main efforts have focused on improvement of thermal-hydraulic correlations and development of methods for applying these correlations to the design and analysis of GCFR core assemblies.

2.1.2. Fuel Assembly Analysis

2.1.2.1. Correlation for Biot Number Correction. The GCFR reference correlations (Ref. 2-1) give the following relation for Biot number correction:

$$St = St^{o} \cdot K_{\infty}; \quad K_{\infty} = 1 - Bi \cdot C_{B} \quad , \tag{2-1}$$

where St = Stanton number,

St^{o} = Stanton number for infinite thermal conductivity of cladding,

C_B = correction coefficient,

Bi = Biot number = $\bar{h}e/k_c$.

Reference 2-1 recommends a value of $C_B = 1.2$. This value was based on the Biot number correction used in the BR-2 calibration experiment and AGATHE-IC experiment calculations. Reference 2-2 (see Fig. 2-1) indicates that C_B is a function of the parameter t/e (cladding thickness based on tip diameter/rib height). The results in Ref. 2-2 are used to obtain the following correlation for C_B:

$$C_B = \frac{t/e}{3} - 0.433 \quad . \tag{2-2}$$

Hence, for a GCFR rod (t/e = 3.92), $C_B = 0.87$. Thus, the Biot number correction for GCFR fuel assembly analysis will be slightly less than that proposed in Ref. 2-1.

If Eq. 2-2 is used to calculate the Biot number correction instead of using a constant value of $C_B = 1.2$, the Stanton number for GCFR conditions will be 2.8% higher. Equation 2-2 will be included in the set of reference correlations.

2.1.2.2. Corner Rod Analysis. In connection with fuel rod bowing studies, a larger edge spacing (80%) is being considered for the fuel assembly design. This opens the corner subchannel area (to 50% of the internal subchannel area). The possibility of having a fueled corner rod under these conditions was investigated.

A fuel assembly with a 10.4-mm pitch and 80% edge spacing was analyzed with the COBRA-4 code (Ref. 2-3) (Fig. 2-1). Figure 2-2 shows the temperature gradients across the corner rod (No. 17) and a peripheral rod (No. 16). The gradients are almost alike, showing overcooling on the duct wall side (negative ΔT). Figure 2-3 shows that the average midwall cladding temperatures of these two rods are also very close.

With 80% edge spacing, the temperature and the gradients of a fueled corner rod are no better or worse than those of the other

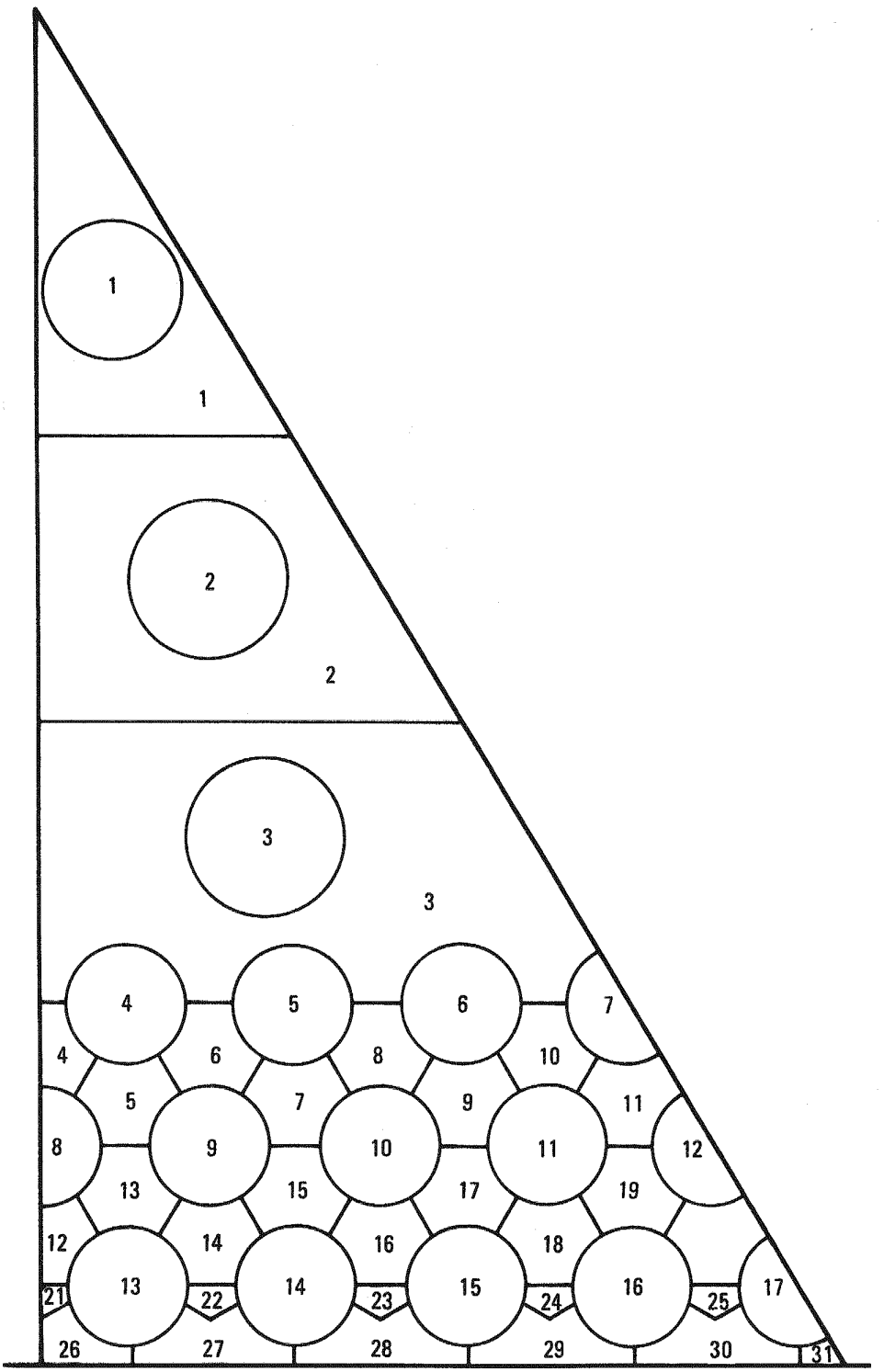

Fig. 2-1. 104-mm-pitch fuel assembly with fueled corner rod

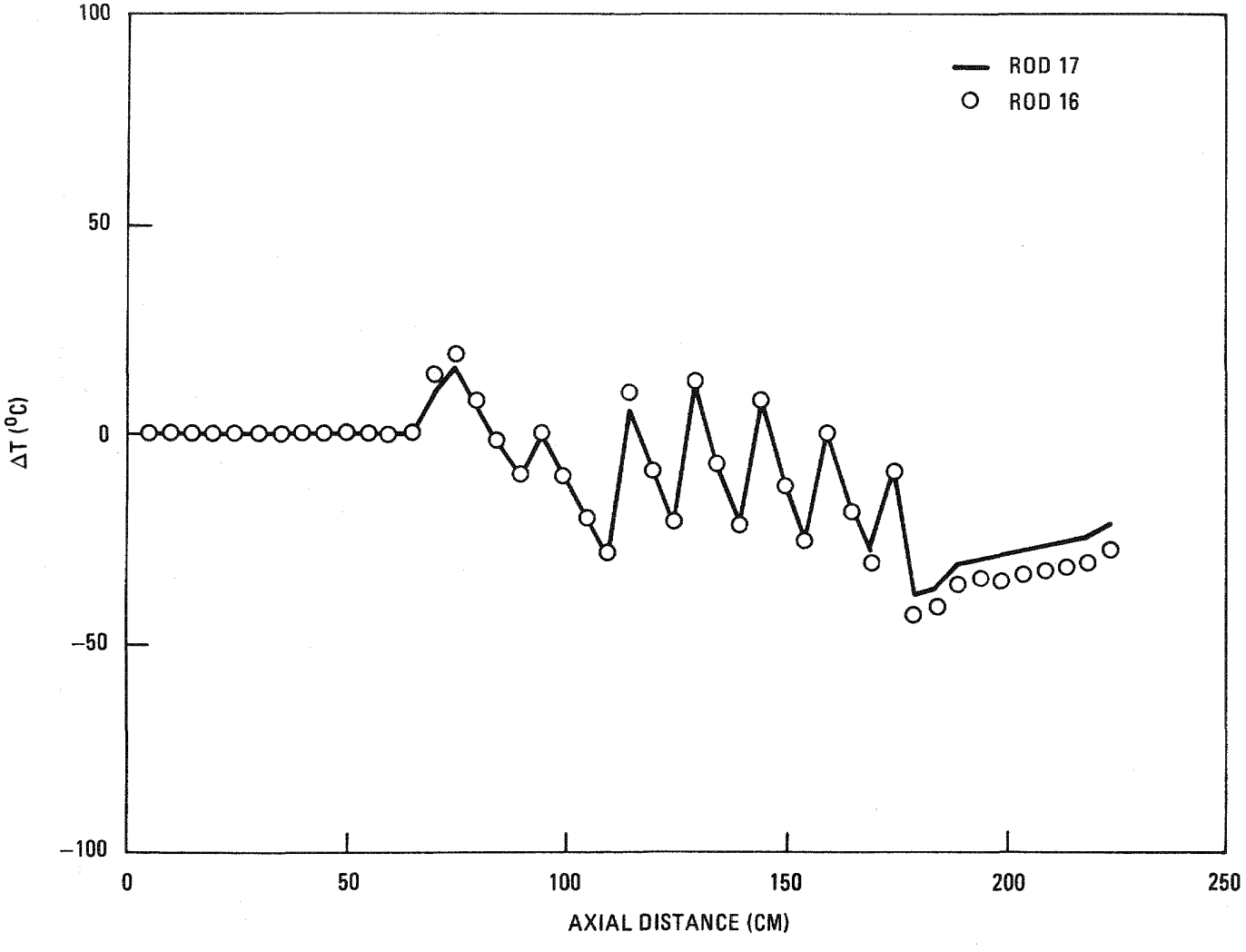

Fig. 2-2. Edge rod temperature drop

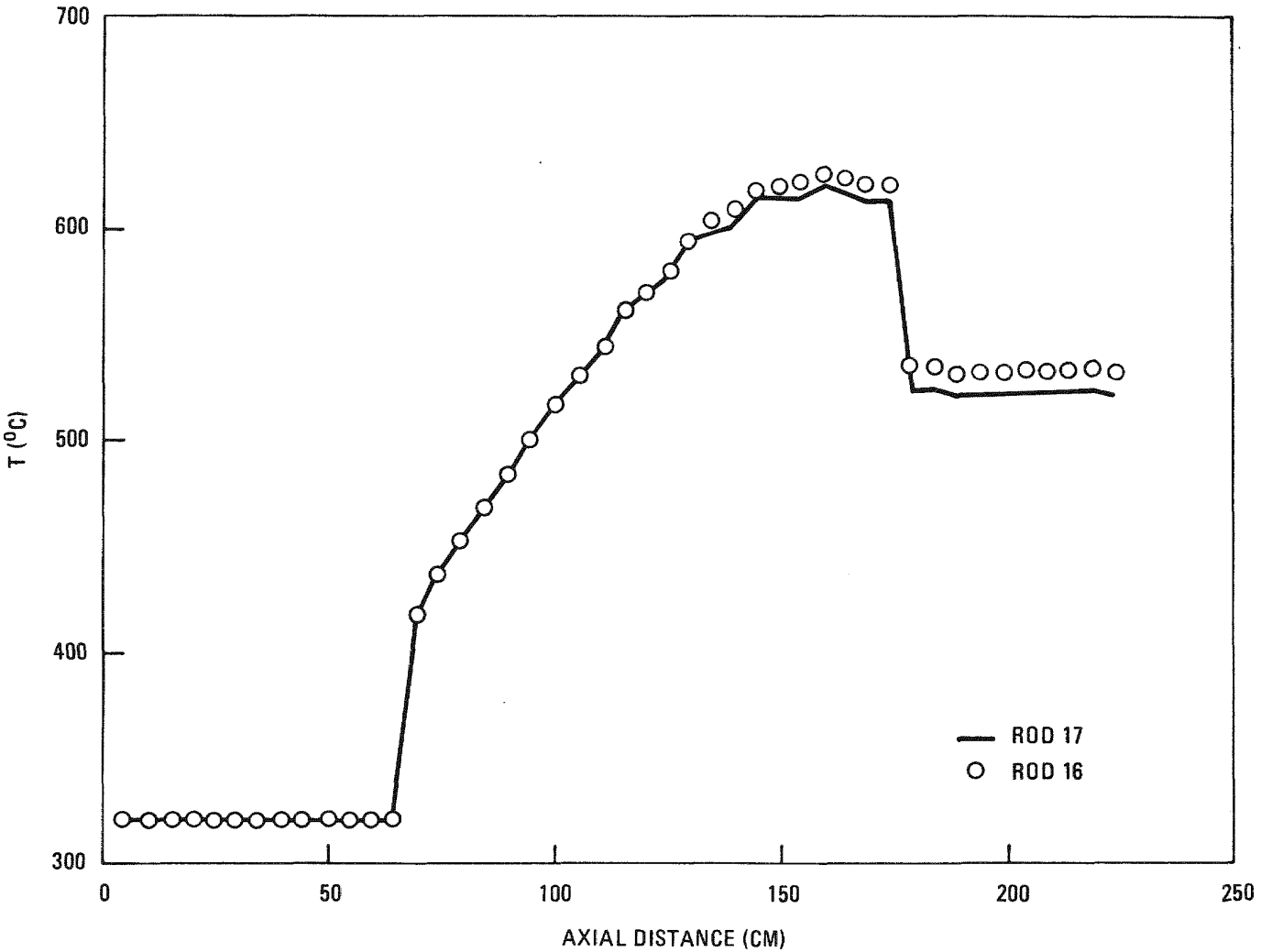

Fig. 2-3. Average cladding midwall temperature

peripheral rods. Placing a fuel rod in the corner would eliminate the need for designing the odd shaped spacer sleeves. However, instead, the spacers could be supported by hanger rods placed within the fuel bundle. These would then be of circular section, larger than the fuel rod diameter, and easily roughened. Although for the nominal geometry, under laminar flow conditions, edge rod cooling appears to be acceptable under full-power and full-flow conditions, fabrication tolerances may have an impact on the temperature gradients. This is being investigated.

2.1.3. Control Assembly Analysis

An approximate analysis was performed to estimate the flow rate and flow velocity through the control assembly cluster. The geometry and data are as follows:

Number of rods in control assembly cluster	37
Diameter of rods (cm)	1.21
Heated length (cm)	113.0
Pitch-to-diameter ratio	1.3
Peak linear power (W/cm)	154

The results of the analysis are

Flow rate through the 37-rod cluster (kg/s)	0.73
Average flow velocity (m/s)	33
Average coolant outlet temperature (°C)	453

2.1.4. Radial Blanket Analysis

There was no activity on this subtask during this quarter.

2.1.5. Integral Core Performance of Demonstration Plant Core

Recent core system performance analyses have indicated that future core designs will attain a somewhat reduced performance compared with previous data, such as those reported in Ref. 2-4. The reasons for the performance reduction are (1) updated thermal-hydraulic correlations, (2) corrected performance analysis models, and (3) design changes that are responsive to minimization of development work and core disruptive accident (CDA) mitigating design proposals.

Incorporating the above changes into the demonstration plant core performance analysis without making any other efforts to balance core design and performance would reduce the core outlet temperature of the down-flow core from 552° to 503°C. An attempt was made to recover some of the thermal performance losses by changing core length and width, rod pitch, assembly size, etc. Analyses show that the thermal performance can be restored, but only at the cost of nuclear performance in terms of linear rating, fissile rating, and doubling time. Overall system optimization studies are expected to yield a core design with balanced plant, thermal, and nuclear performance characteristics. However, current cost information yields a rather flat optimum, so there is sufficient freedom for emphasizing one performance characteristic over the other. An attempt is currently under way to identify core design configurations for which the performance penalty of the imposed design changes is minimum. These studies are being conducted in parallel with the up-flow/down-flow evaluation so that revised core and system operating parameters can be defined subsequent to selection of either the up-flow or down-flow configuration.

The reactor design parameters for a larger breeder reactor plant were reviewed. Earlier studies were used to set the rod size at 8.0 mm to obtain a minimum doubling time. Subsequent fuel strategy studies

demonstrate that the energy potential is maximized for a rod diameter which is slightly less than 8.0 mm. Calculations to determine the optimum rod size for a GCFR symbiotic system are under way. A series of calculations was made for cores with differing length-to-diameter ratios, resulting in the selection of a 397-assembly core, including 31 control assemblies. Limiting the rod rating to 39.37 kW/m made it possible to produce an outlet helium temperature of 566°C, which was judged necessary for good steam plant performance. However, this resulted in a reactor rating of only 0.58 MW(t)/kg fissile; the desired value is around 0.7. The only feasible way to increase this rating is to allow the outlet temperature to drop to 543°C, which would increase the rating to 0.68 MW(t)/kg. The breeding ratio and doubling time are satisfactory for both conditions described above.

2.2. CORE ASSEMBLY MECHANICAL ANALYSIS

2.2.1. Up-Flow Core Design

During the previous quarter, alternate designs for the core assemblies of an up-flow core GCFR were developed. The efforts to date have primarily centered on development of three areas: (1) alternate locking concepts, (2) outlet end shielding for the fuel and control assemblies, and (3) rod bundle support schemes for top- and bottom-end venting of fuel rods.

The main assembly parameters were developed in Ref. 2-5 to give approximately the same nuclear and thermal performance as that given for the 300-MW(e) GCFR demonstration plant in Ref. 2-4. Design basis core data for the up-flow and the down-flow cores are given in Table 2-1. As can be seen, the main assembly parameters are quite similar for the two designs. However, because of slightly larger inlet and exit losses in the up-flow core, the rod-to-rod pitch must be slightly (approximately 0.2 mm) greater than that in the down-flow core. In addition, to compensate for the thermal performance drop due to the larger pitch, the active core length of the up-flow core must be increased approximately 7.0 mm over that in the down-flow core.

TABLE 2-1
DESIGN BASIS CORE DATA FOR THE UP-FLOW/DOWN-FLOW COMPARISON[a]

	Up-flow	Down-flow
Core length (mm)	1200	1130
Each axial blanket (mm)	450	450
Roughened length (%)	75	75
Rod o.d. (mm)	7.46	7.46
Rod pitch (mm)	10.6	10.4
Rod-to-duct gap (%)	51.36	51.36
Duct wall thickness (mm)	4	3.9
Duct width outside dimension across flap (mm)	184.0	180.4
Duct-to-duct gap (mm)	6.9	6.7
Assembly pitch (mm)	190.8	187.1
Assembly overall length (mm)	4650.0[b]	4208.0
Outlet temperature (°C)	552	552
Breeding ratio	1.36	1.36
Doubling time (yr)	17.5	16.7
MW(t)/kg fissile	0.517	0.549
Average enrichment (%)	16.7	16.6
Maximum linear rating (kW/m)	36.7	39.0
In-pile time	3.3	3.11
Peak fast fluence (n/cm^2)	2.22×10^{23}	2.22×10^{23}

[a] From Ref. 2-5. Cladding midwall temperature and core ΔP adjusted to give performance in Ref. 2-4 (T = 720°C, ΔP = 250 kPa). Number of assemblies: 108 fuel, 15 control, 4 shutdown, 90 blanket, 180 shield (up-flow core only).

[b] Includes 840-mm-long outlet shielding.

2.2.1.1. Assembly Axial Restraint. Several concepts for core assembly axial restraint have been investigated, including pneumatic balancing (sometimes called hydraulic hold-down) and mechanical latching. The inlet nozzle region of a pneumatically balanced core assembly is illustrated in Fig. 2-4. Although this concept has the advantage of being a basically passive system, it also has several drawbacks which seem to make it undesirable for an up-flow core GCFR. At best, such a hold-down scheme can only just balance out the fluid lifting force exerted on the core assemblies, leaving the assembly weight as the only hold-down force available for core axial restraint. Because of space limitations in the GCFR, only about one-half the fluid lifting force could be removed, and thus the hold-down force would only be about 50% to 60% of the assembly weight. This would restrict the seismic capability of the core. Furthermore, because of the unique requirements of the GCFR pressure equalization system (PES), a positive mechanical seating is considered to be required for the PES vent connection to the grid plate (or the PES plate). Pneumatic balancing schemes do not ensure that the vent connection will always be made, since there is a possibility of individual assemblies ratcheting upward as a result of interassembly interactions. The design of the PES vent connection for accommodating such travel does not appear practical at this time.

One alternative to pneumatic balancing for core axial restraint is a locking concept proposed by Kraftwerk Union (KWU) (Fig. 2-5). Although the design of the lock is somewhat mechanically complex, it appears to be feasible. In common with most other mechanical latch designs considered, the KWU design requires pulling of a latch actuator rod from above by the fuel handling equipment to release the assembly. A possible deficiency of this design is that it does not appear to apply very much seating force; instead, it just prevents assembly lift-off. As noted above, PES considerations make a seating force desirable.

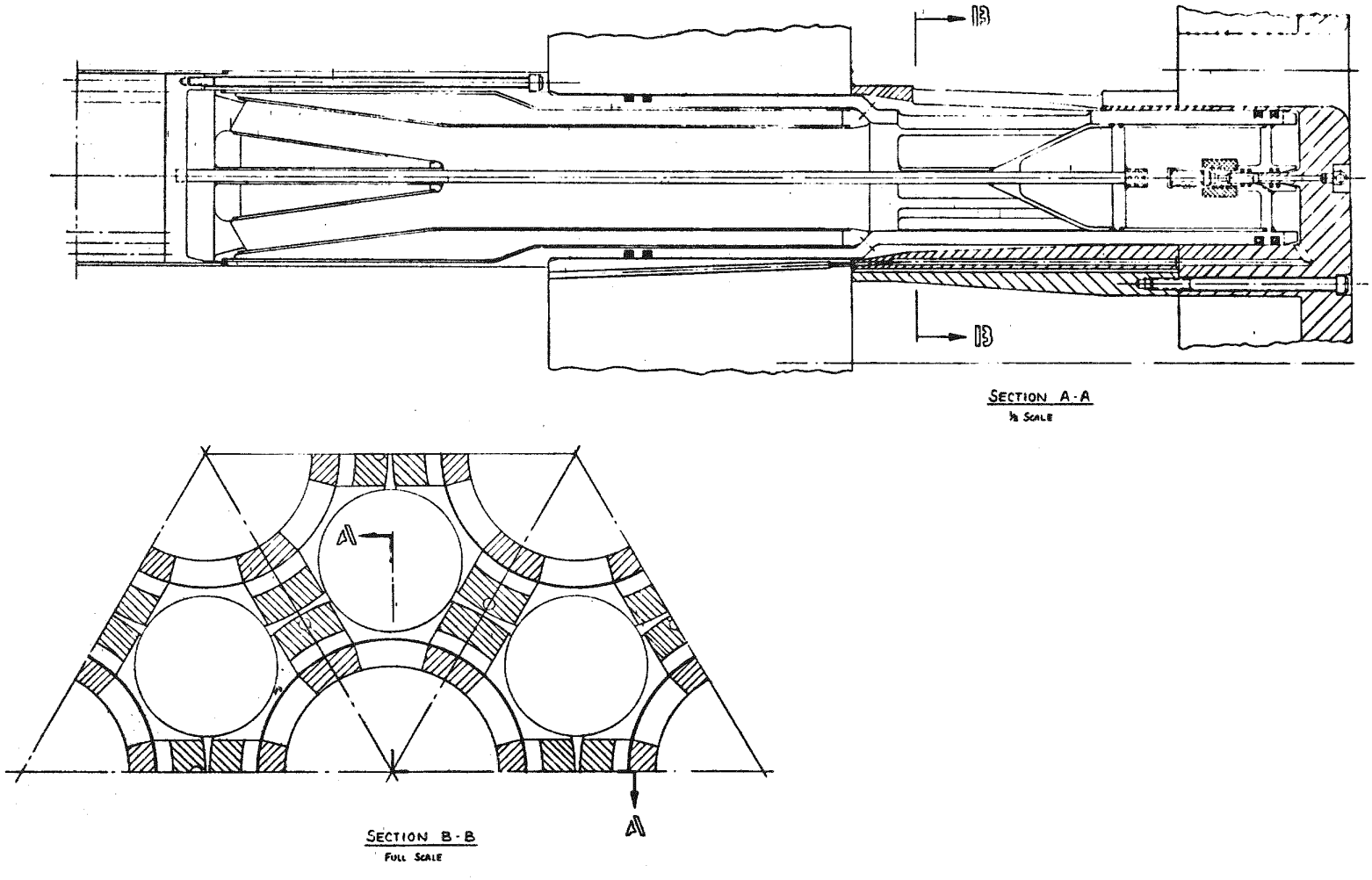

Fig. 2-4. Pneumatic balancing for fuel assembly inlet nozzle (KWU design)

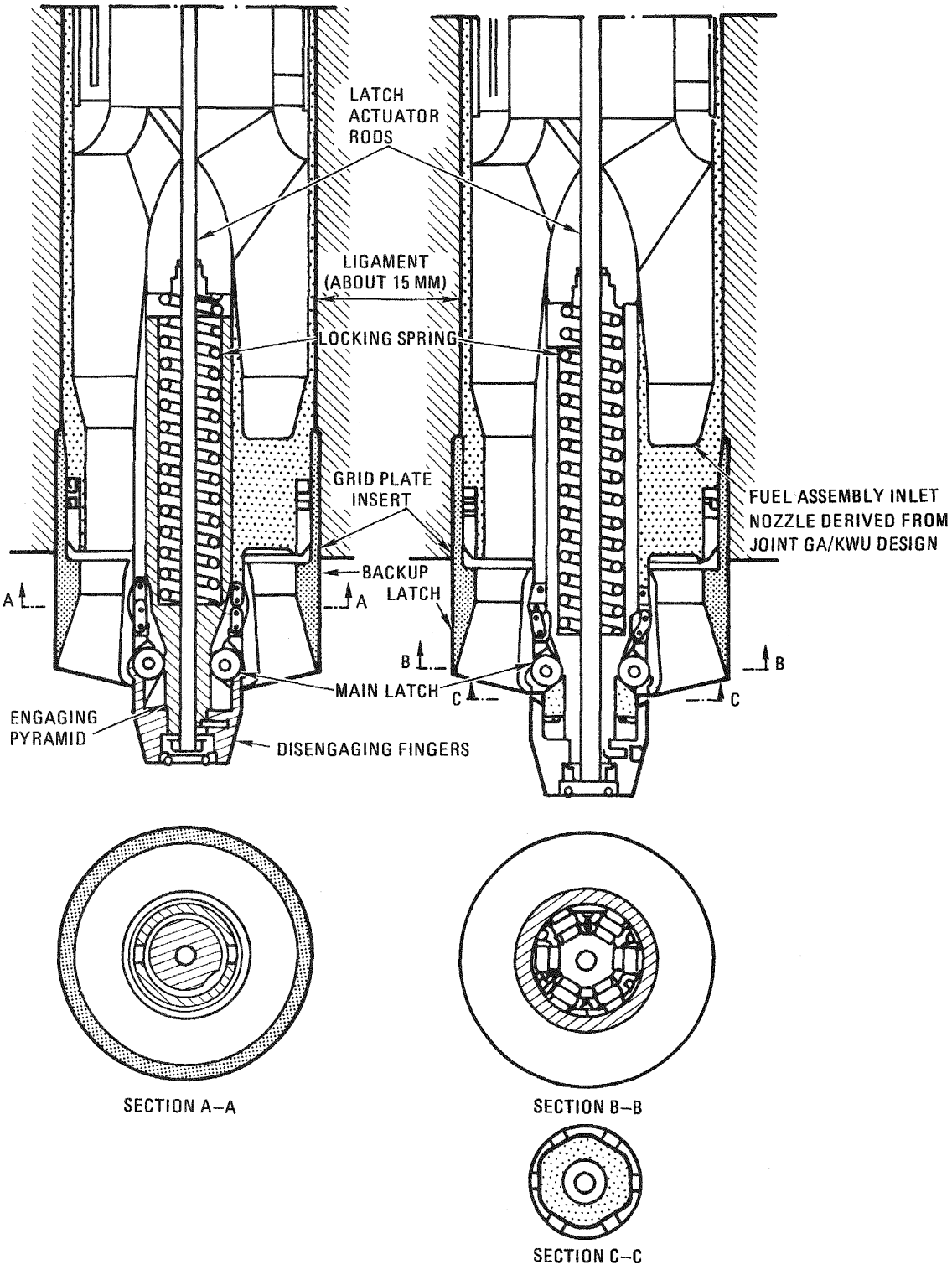

Fig. 2-5. Standing assembly mechanical lock

The latching concept selected for the interim design is shown in Fig. 2-6. This is an individual mechanical latch similar in concept to the KWU design. It was selected because of its relative simplicity and because it conceptually differs the least from the down-flow core locking concept. The lock consists of three cams which engage an insert in the core support plate. The cams are actuated by a spring-loaded plunger, which in turn is actuated by a 10-mm rod passing up through the core to the top of the assembly. If necessary, this actuation rod could be made out of one of the radiation-resistant alloys currently under development. No backup lock is provided (although one could easily be incorporated) because of the redundancy provided by the three cams and because secondary restraint is expected to be provided by the control rod drive guide mechanisms.

2.2.1.2. Shielding. The shielding for the core support plate is located in the inlet region of the core assemblies and is essentially identical to that used to protect the grid plate in the down-flow core. Additional protection of the core support from the effects of radiation is provided by the 100-mm-thick, segmented PES manifold plate which is directly attached to the top of the support plate and which can be removed and replaced if necessary.

Additional axial shielding is provided at the outlet end of the core assemblies to protect the control rod drive mechanisms. The exit shielding for the fuel assembly is shown in Fig. 2-7 and that for the control assembly is shown in Fig. 2-8. Both the fuel assembly exit shielding and the control assembly exit shielding have been subjected to detailed nuclear analysis (Ref. 2-6) and have been shown to be sufficient to reduce the effective fast fluence to the outlet plenum structures to below damage limits. Pressure drop calculations have been performed for both designs and their pressure drop performance has been found acceptable.

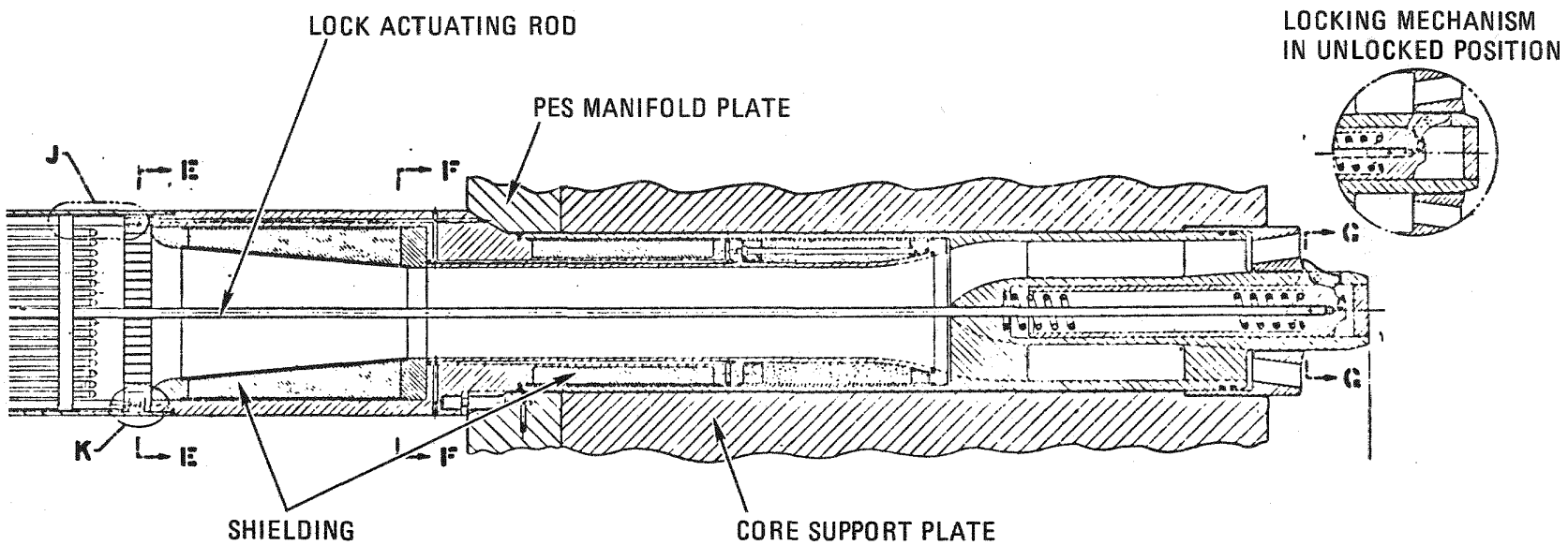

Fig. 2-6. Fuel assembly inlet nozzle mechanical latching

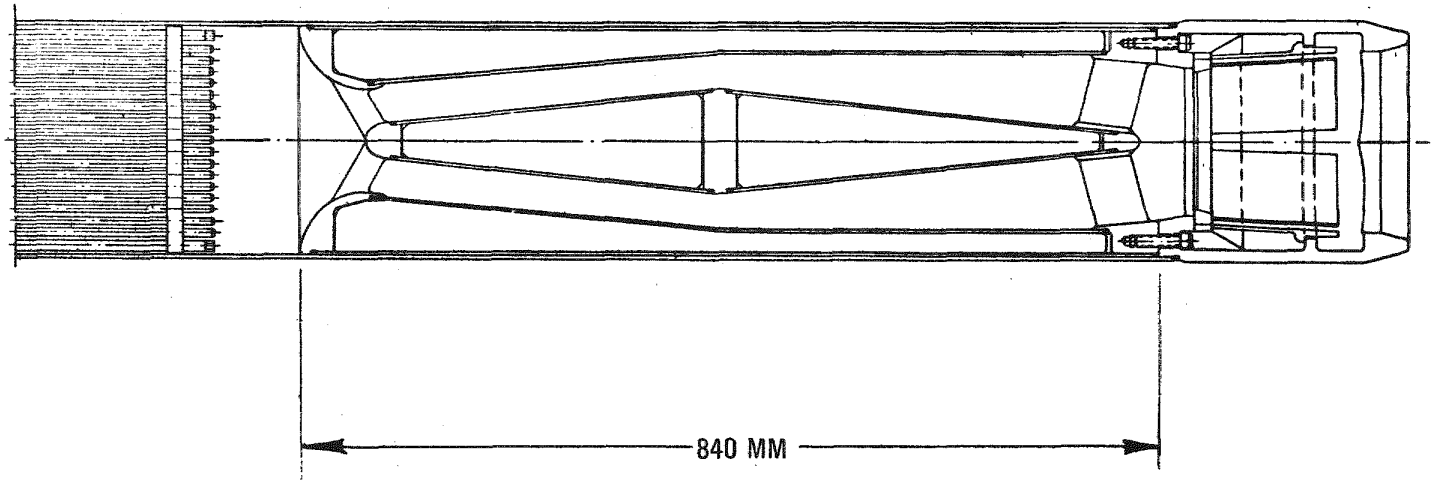

Fig. 2-7. Fuel assembly outlet shielding

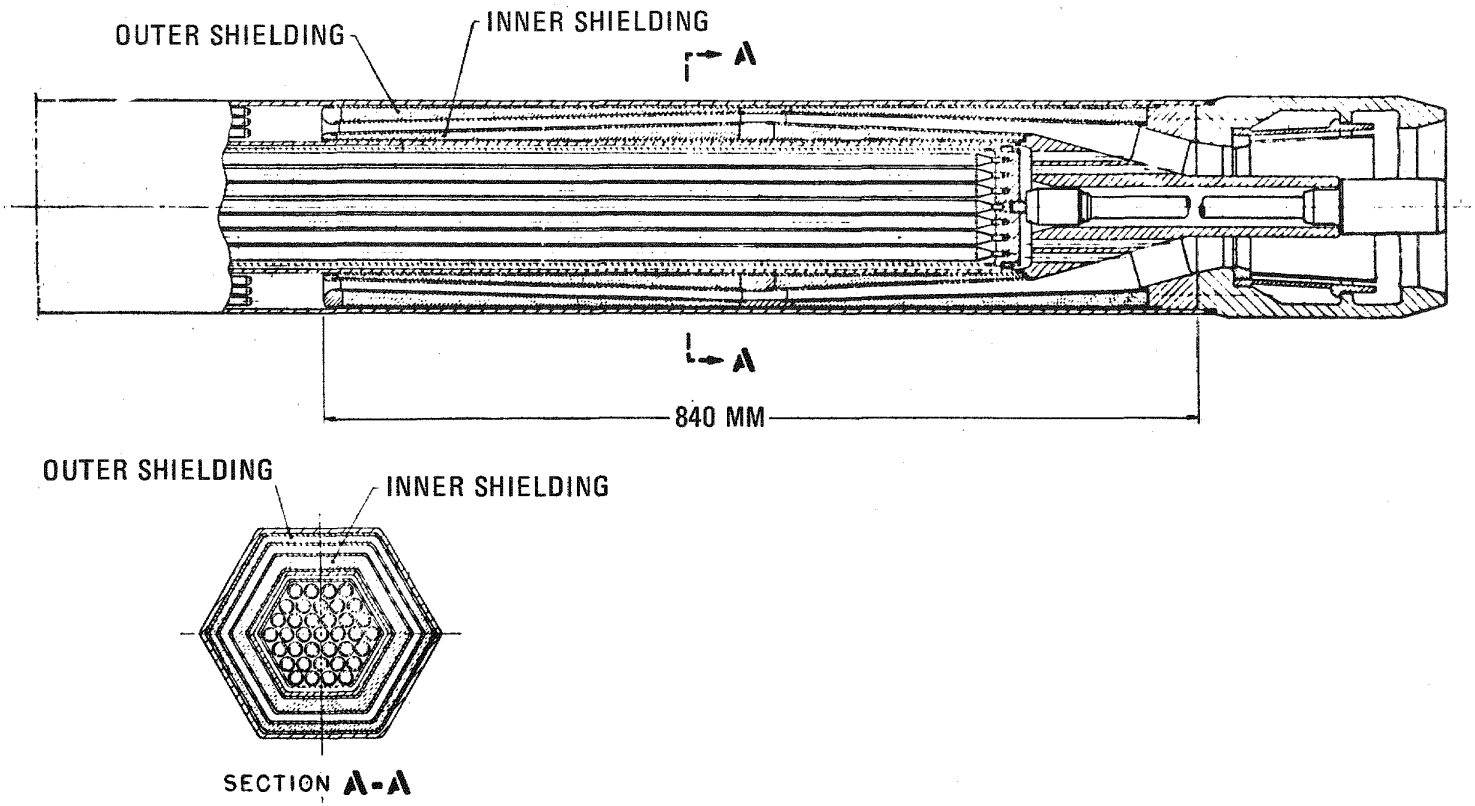

Fig. 2-8. Control assembly outlet shielding

The radial shielding required to protect the (30-yr) core restraint structure is provided by three rows of radial shielding assemblies containing a 50/50 mix of graphite and steel.

2.2.1.3. Bundle Venting and Manifolding. Rod bundle arrangements for both top- and bottom-end venting of rods were developed. Based on the recommendations in Ref. 2-7, which concluded that rod venting should be done at the hot end and/or the upper end, a rod arrangement incorporating top end venting was selected. Reference 2-7 concluded that no change in length would be required as a result of temperature changes. Thus, the rod charcoal trap length for the up-flow core need not differ from that of the down-flow core.* The fuel assembly is shown in Fig. 2-9, and an overall view of the up-flow core is given in Fig. 2-10.

2.2.2. Core Distortion Analysis

In support of the up-flow core design concept, a study of core-wide distortion in two and three dimensions has been undertaken. Prior work in this area for the down-flow core utilized a single assembly code, CRASIB (Ref. 2-8). The interactions between assemblies in a radial spoke were computed by manually combining individual assembly analyses. Recently, however, two codes, NUBOW-2D (Ref. 2-9) and NUBOW-3D (Ref. 2-10), have become available which systematically perform an inelastic analysis of a radial spoke and a three-dimensional sector of a complete core, respectively. Three phases of work were identified: (1) obtaining the code, implementing it on the GA computer, and making the modifications and improvements necessary for the GCFR system and this particular study; (2) for verification purposes, running sample problems and GCFR models

*Reference 2-7 recommended an increase in the length of the rod charcoal trap for both the down-flow and the up-flow core based on recent test data. Since this is a generic issue, the up-flow core rod trap length in this study was based on the down-flow core trap length given in Ref. 2-4.

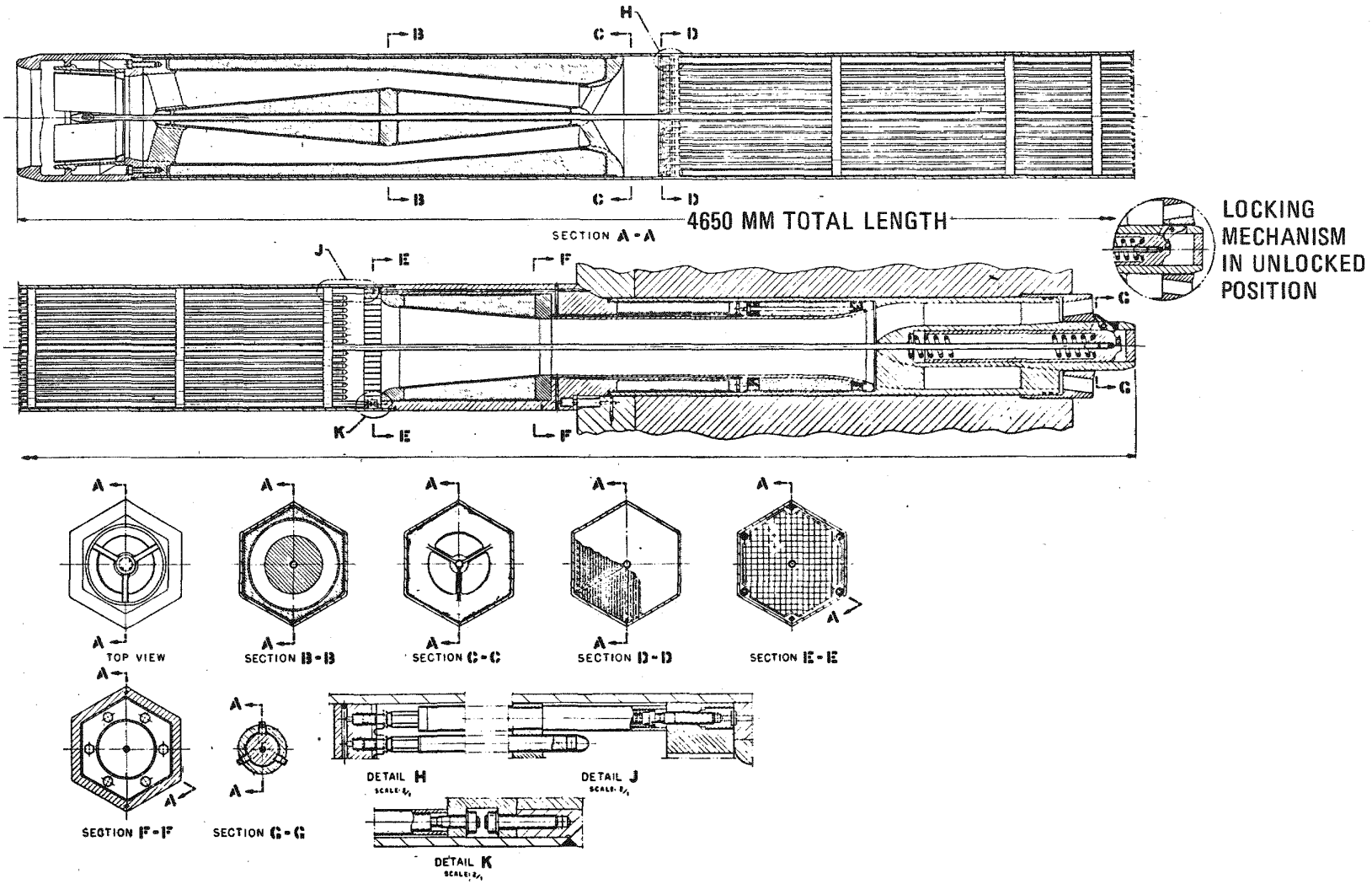

Fig. 2-9. Fuel assembly general arrangement (up-flow core)

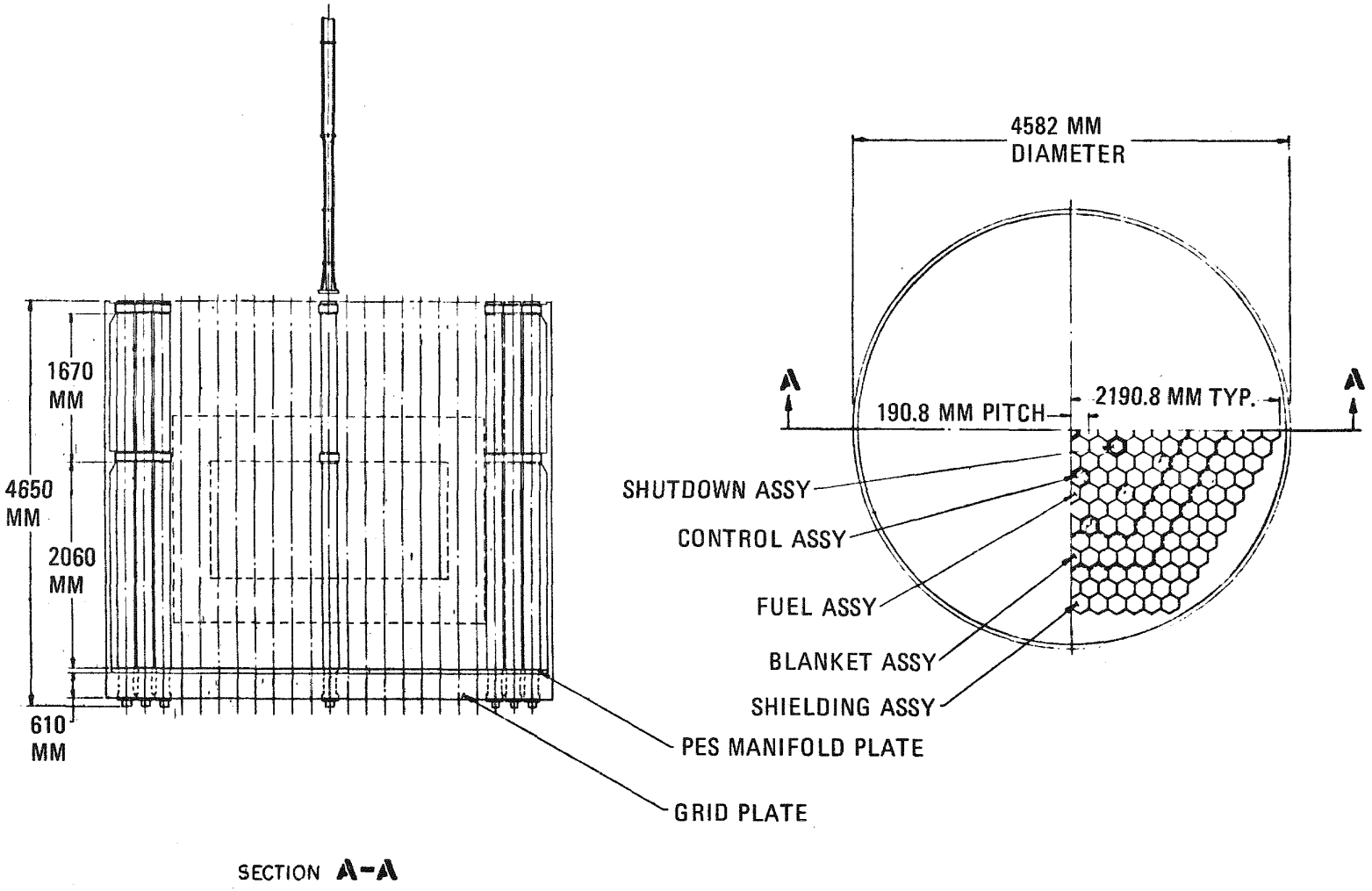

Fig. 2-10. Up-flow core concept

in a manner similar to prior studies; and (3) modeling and analyzing various up-flow configurations. During this quarter the first two phases and half of the third were completed with NUBOW-2D. The first phase is in progress for NUBOW-3D.

As received, NUBOW-2D required some modification to make it compatible with the UNIVAC operating system. Once this was done and the modeling process was understood, it became obvious that four areas were in need of improvement. First, the irradiation creep and swelling correlations contained in the code were outdated, and these were replaced by the current ones from Ref. 2-11 (and revision 5 of Ref. 2-11). Second, it was desirable to have the code compatible in either British or metric units. Minor coding modifications were required to accomplish this. Third, a systematic method of handling the voluminous output was required, and an additional subroutine was developed to scan the output data for relevance and additional files for storage. This enabled post-plotting routines to be easily accommodated. Because of the lack of a core restraint system and the currently accepted fuel management concept, the ability to model replacement and 180-deg rotation of fuel assemblies was required. Most of the routines necessary had been informally written by ANL for previous GCFR work. These were obtained, incorporated, and verified.

Two models were generated. The first was a model identical to that used in previous core distortion studies. Up to the point of first interassembly contact, NUBOW-2D predicted somewhat smaller displacements than CRASIB. Inherent modeling differences between the two account for some of the discrepancy, but further investigation is being made as to the exact causes of the differences. When refueling and rotation were considered, the position of interassembly contact occurred at the same locations as in previous studies for an equilibrium core configuration. The loads predicted were somewhat higher however, giving a maximum refueling side load of 13,780 N. The cause of this discrepancy is probably related to the difference in the computed displacement fields.

The second model was generated to analyze the current down-flow GCFR core. It was initially used to validate the compatibility of metric/British versions (which proved to be compatible). The results also gave an indication of the expected bowing interference within the current design. The outer five rows are shown in Fig. 2-11. The ordinate is the radial position of the assembly less the undistorted across-flats dimensions of all the preceding assemblies. Thus, only pertinent thermal growth, bowing displacement, and duct wall bulging are plotted; i.e., an assembly with no displacement or distortion would appear as two vertical superimposed straight lines. The bulging appears as triangular discontinuities on the otherwise smooth profile. This is the result of only computing the bulging at two axial locations. In reality, a smooth curve should be passed through the peaks tapering back to the displaced duct wall profile above and below these two points. Rows 8a and 9 are blanket assemblies. Analysis of this system with replacement and rotation will commence upon resolution of the discrepancies noted above.

The third phase of the study has been initiated. A model of the up-flow core has been completed and debugged, and a parametric analysis considering support point locations and initial gaps is in progress.

2.2.3. Outlet Nozzle Mechanical Analysis

Previous analysis of the outlet nozzle section approximated the structure using flat plates to investigate the thermal stress fields. To validate these results and extend the analysis to considerations of mechanical loading, a three-dimensional model of a 120-deg sector of the nozzle section was constructed. It will provide detailed thermal and mechanical stress fields which cannot be obtained in any other way. The THREED computer code will be used on the model for heat transfer and stress analysis.

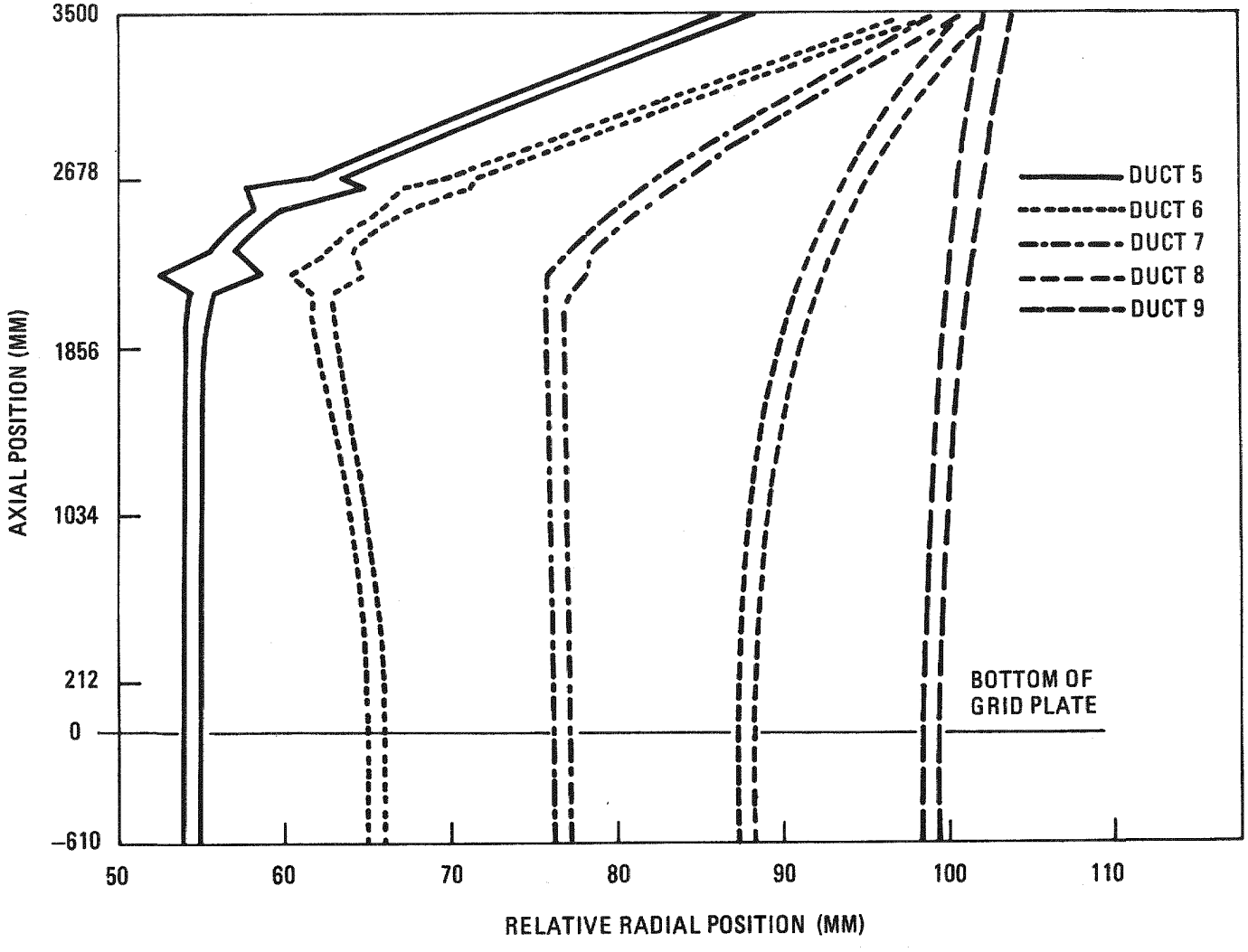

Fig. 2-11. Relative duct displacements with bulging points (750 h)

The model (Fig. 2-12) consists of 212 brick elements and 1528 node points. As generated, a large, sparsely coupled system of equations would have to be solved; this would be a prohibitively time consuming operation. A bandwidth optimization code (Ref. 2-12) has been used to reduce the bandwidth to manageable proportions. Calculation of the temperature field is now in progress.

2.2.4. Core Assembly Flow-Induced Vibration

During the previous quarter a core assembly vibration analysis and test program were developed to provide analytic and experimental evidence to ensure the absence of potentially damaging flow-induced vibrations in the GCFR fuel, blanket, control, and shutdown assemblies. The helium flow test rig (HFTR) is a major part of this program. The specific objective of the experimental program planned for the HFTR is to obtain the following information:

1. Natural frequencies, damping coefficients, and vibrational modes of individual components and complete assemblies in static air at ambient conditions and in flowing helium at simulated reactor conditions.

2. Amplitudes of flow-induced vibrations for a range of coolant conditions.

3. Evaluation of available design margins, including determination of maximum allowable span between spacer grids, maximum allowable rattle space in blanket assemblies, maximum allowable clearance between fuel rods and spacer grids, and maximum gap allowed between the control rod duct wear pads and the control rod guide duct.

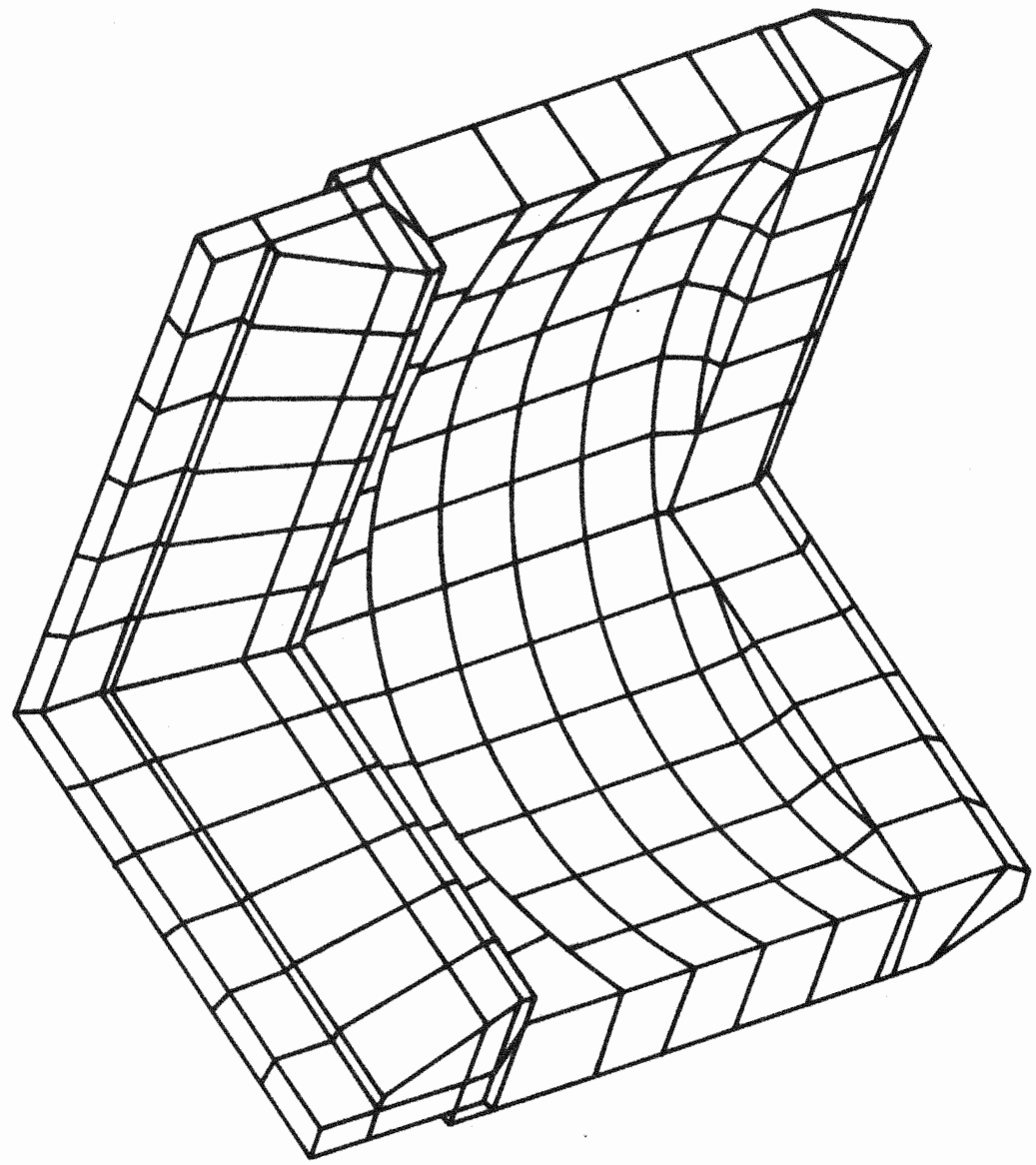

Fig. 2-12. Finite element mesh of fuel assembly outlet nozzle

To obtain this information, a combined analytic and experimental program consisting of the following principal tasks has been proposed:

Task I:	Analytic consideration of core assembly flow-induced vibrations.
Task II:	Single-rod tests.
Task III:	Full-length, partial-bundle tests.
Task IV:	Full-scale assembly tests.

Task I, analytic consideration of flow-induced vibrations, has been an ongoing task at GA for the last several years. In addition to providing predictions of the flow-induced vibration response of GCFR core assemblies, the principal objectives of this task have been to provide pretest predictions of the vibrational behavior of the test assemblies for equipment and instrument design, to perform dynamic similitude studies, to analytically validate test results, and to develop or adapt existing analytic techniques to describe rod vibration performance for future component design enhancement or changes.

The experimental tasks (tasks II through IV) are arranged in order of increasing complexity to allow early definition and correction of potential problems. In general, experiments will be performed with full-length rod bundles using flowing helium at the temperature, pressure, and flow conditions of test rig III in Table 2-2 (from Ref. 2-13). A summary of the preliminary test program is presented in Table 2-3.

2.2.5. Core Seismic Engineering

Over the past several years, the length of the core assemblies for the down-flow core has steadily increased as a reuslt of design changes. This increase in assembly length has caused the seismic response of the core to increase to the point where it is felt that a core restraint system may be required. As a first step toward the design and evaluation of a core

TABLE 2-2
FLOW PARAMETERS FOR ALTERNATE HELIUM FLOW TEST RIGS

	Pressure (MPa)	Temperature (°C)	Velocity (m/s)	Flow Rate (kg/s)	Density (kg/m^3)	Viscosity x 10^5 [(N-s)/m^2]	Young's Modulus (GPa)	Speed of Sound [m/s (c/c_{nom})]	Reynolds No.	Mach No.	ω/ω_{nom} [a] (rods)
300-MW(e) GCFR core											
Inlet	9.0	316	53.6	5.37	7.36	3.16	∿177	1428	98,000	0.04	1.07
Outlet	8.71	552	74.4	5.37	5.08	3.99	∿154	1690	74,500	0.04	1.00
Average	8.86	434	64.0	5.37	6.22	3.58	∿166	1562 (1.0)	87,400	0.04	1.04
Test rig 1 (helium, full pressure, full temperature)											
Nominal	8.86	434	64.0	5.37	6.22 (at 434)	3.58	∿166	1562 (1.0)	87,000	0.04	1.04
Design	9.0	550	100	7.16	7.36 (at 316°C)			1690			1.00
Test rig 2 (helium, reduced pressure, reduced temperature											
Nominal	7.37	425	75	5.37	5.08 (at 425°C)	3.55	∿166	1554 (1.0)	84,400	0.05	1.04
Design	7.37	425	100	7.16	6.22 (at 300°C)						
Test rig 3 (helium, reduced pressure, low temperature)											
Nominal	5.79	175	64.0	5.37	6.22 (at 175°C)	2.62	∿185	1245 (0.80)	119,400	0.05	1.10
Design	5.79		100								
Test rig 4 (air, low pressure, low temperature)											
Nominal inlet	0.66	40	54	5.37	7.37	1.96	193	355 (0.23)	159,000	0.15	1.12
Nominal outlet	0.44	∿30	75	5.37	5.06	1.90	192	350 (0.23)	168,000	0.21	
Design outlet	0.4		100	7.16						0.29	

[a] Natural frequency/(natural frequency)$_{nominal}$.

TABLE 2-3
SUMMARY OF PRELIMINARY HELIUM FLOW TEST PROGRAM

Test Model[a]	Objectives	Test Duration	Comments
Single rod F, B, C, S Simulator and instrumented rods (total of 16 rod models)	Obtain natural frequencies and damping coefficients of simulator rods under static and flowing conditions; calibrate and verify instrument rods	1 week per test series (approximately 5 runs/model)	Static tests in air; flowing tests in helium at simulated reactor conditions
Partial bundle 3 each F and B 1 each possible C, S (total of 8 bundle models)	Measure flow-induced vibration response of rods in a rod bundle environment in flowing helium at simulated conditions; assess effects of parameters, including spacer grid type, spacer grid spacing, rod-spacer clearance, and wire-wrapped bundle rattle space	4 weeks per test series (approximately 20 runs/bundle)	37-rod fuel and blanket bundles; testing of partial bundle control and shutdown rod bundles may also be required. Parallel programs should evaluate flow-induced vibration response of other core assembly internal components (e.g., inlet nozzle, outlet nozzle, and orifice) and blanket assembly flow control device.
Full-scale assembly 1 each F, B, C, S (total of 4 models)	Measure flow-induced vibration response of fuel, control, blanket, and shutdown rods; measure flow-induced vibration response of control rod subassembly and shutdown rod subassembly; measure gross assembly motions; measure flow-induced vibration response of installed internal components; evaluate assembly acoustic resonances	5 weeks per test series (approximately 30 runs/bundle)	

[a] F = fuel, B = blanket, C = control, S = shutdown.

restraint system for the down-flow core, two core restraint system concepts were proposed (Fig. 2-13). The first concept is a dual-support concept similar to that employed in the Clinch River breeder reactor (CRBR) and the fast flux test facility (FFTF). The second is a single-support concept, which has the potential advantage of being able to reduce the core seismic response without affecting core distortions under normal operation; in addition, the safety characteristics of the top-supported unconstrained core are retained.

2.3. CORE ASSEMBLY STRUCTURAL DESIGN CRITERIA

There was no activity on this task during this quarter.

2.4. CORE ASSEMBLY MECHANICAL TESTING

The objective of this task is to conduct mechanical tests of core assembly components and subassemblies to simulate the mechanical loads anticipated during normal and abnormal reactor operating conditions. The current phase of this program involves testing of fuel assembly components. All core component mechanical test programs are being discontinued except for the rod-spacer interaction tests.

The current phase of interaction tests has been designed to evaluate the effect of angular misalignment of spacer cells during axial rod movement. It has been postulated that deflection of core components due to assembly tolerances, rod bowing, and swelling could cause angular misalignment on the order of a few degrees rotation. The testing equipment has been assembled in the furnace, and initial temperature profiles have been run. The best peak-to-peak value obtained so far is about 60°C, which represents an approximate 12% span. This profile is currently being evaluated. Tentative indications are that this profile may not be unreasonable, since the significant comparisons made will be from test to test and not from spacer to spacer within each test.

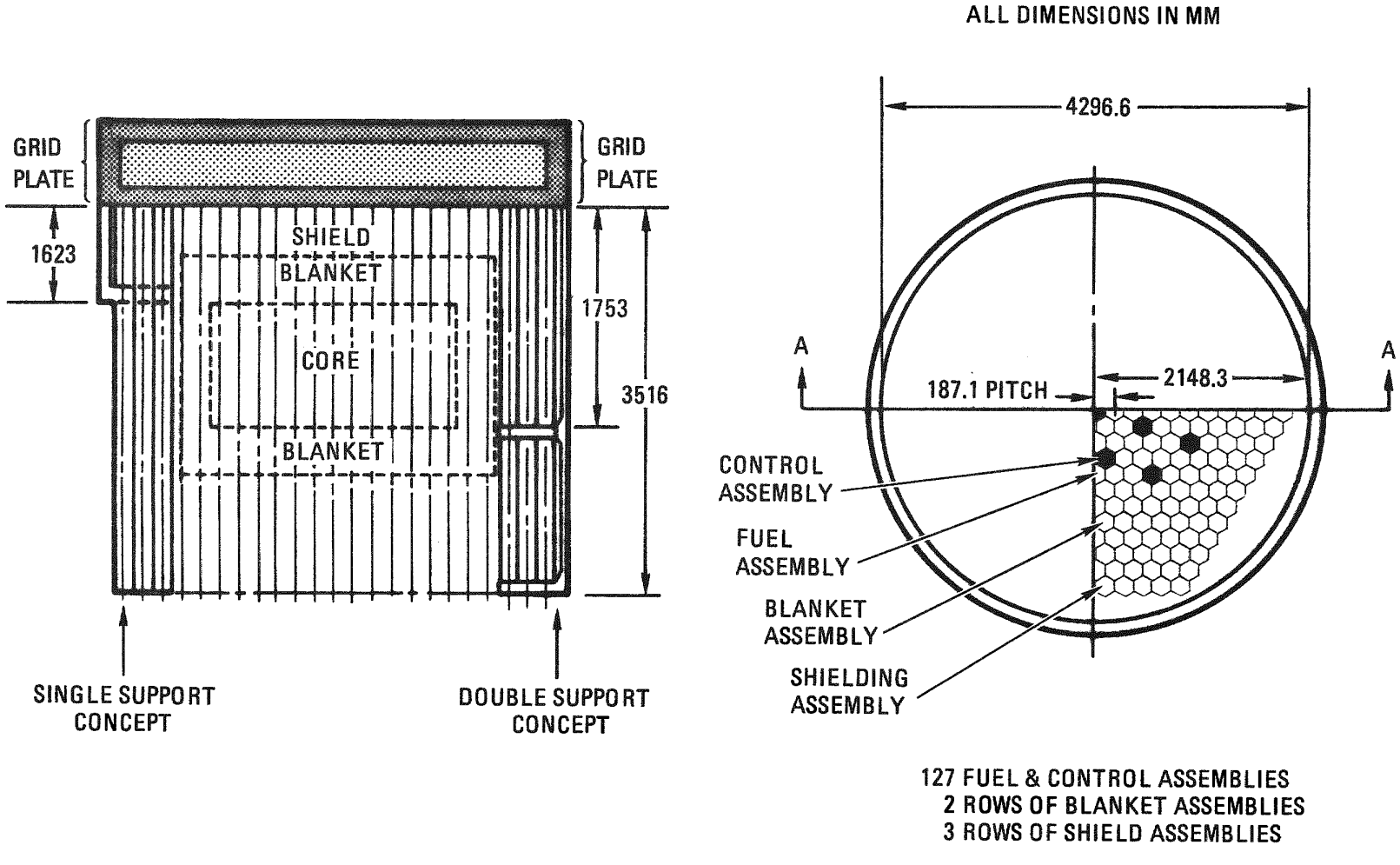

Fig. 2-13. Core restraint support locations for down-flow core GCFR

2.5. HEAT TRANSFER AND FLUID FLOW TESTING

These tests have been indefinitely postponed.

REFERENCES

2-1. Baxi, C. B., "Reference Thermal-Hydraulic Correlations for Turbulent Flow Analysis of GCFR Fuel Assembly," General Atomic Company, unpublished data.

2-2. Hudina, M., and S. Yanar, "The Influence of Heat Conduction on the Heat Transfer Performance of Some Ribbed Surfaces Tested in ROHAN Experiment," Swiss Federal Institute for Reactor Research Report TM-IN-572, 1974.

2-3. Wheeler, C. L., et al., "COBRA-IV-1: An Interim Version of COBRA of Thermal-Hydraulic Analysis of Rod Bundle Nuclear Fuel Elements and Cores," Battelle Northwest Laboratory Report BNWL-1962, March 1976.

2-4. "Baseline Data Book," General Atomic Company, unpublished data.

2-5. Baxi, C. B., and G. Schlueter, "1. Upflow Core Design, 2. Revision of Downflow Core Design," General Atomic Company, unpublished data.

2-6. Rouse, C. A., et al., "Approximate Neutron Transport Solutions for Proposed Fuel and Control Assembly Exit Shields," General Atomic Company, unpublished data.

2-7. Campana, R. J., "PES Upflow Core Study Results," General Atomic Company, unpublished data.

2-8. Rector, J. D., and W. H. Sutherland, "CRASIB Users Guide and Program Manual," Battelle Northwest Laboratory, March 23, 1970.

2-9. Cha, B. K., G. A. McLennan, and P. J. Fulford, "NUBOW 2-D Inelastic: A Fortran Program for Static Two-Dimensional Structural Analysis of Bowed Reactor Cores," Argonne National Laboratory Report ANL-CT-77-34, June 1977.

2-10. Cha, B. K., G. A. McLennan, and P. J. Fulford, "NUBOW 3-D Inelastic: A Fortran Program for Static Three-Dimensional Structural Analysis of Bowed Reactor Cores," Argonne National Laboratory Report ANL-CT-78-19, March 1978.

2-11. Nuclear Systems Materials Handbook, Hanford Engineering Development Laboratory (TID-26666).

2-12. "MARC-CDC, A General Purpose Finite Element Analysis Program," v. I, Rev. H, Control Data Corporation Publication 17309500, 1976.

2-13. Lee, G. E., "Selection of Flow Conditions and Model Parameter for GCFR Core Component Flow Tests," General Atomic Company, unpublished data.

3. PRESSURE EQUALIZATION SYSTEM FOR FUEL (189a No. 00582)

3.1. CORE ASSEMBLY AND PES SEALS

There was no activity on this subtask during this quarter.

3.2. ANALYSIS, MODELS, AND CODE DEVELOPMENT

The GCFR is designed with pressure-equalized and vented fuel and blanket assemblies. A PES is provided to perform these functions and contains one unit of the helium purification system (HPS). The PES, described in Ref. 3-1, is a complex flow network consisting of manifolded fuel rods, fuel and blanket assemblies, monitor lines through which vented fission gases are swept by inflowing coolant to the HPS unit, and check valves leading to the suctions of the main and auxiliary circulators which power the system.

Programming of the transient PES flow code continued during this quarter. The remaining program elements (mass and heat sources and output section) were completed, and input instructions for the code are being prepared. Some model application and debugging must still be done.

3.3. PLATEOUT AND PLUGGING

Volatile fission products, particularly cesium and iodine, vented from the core assemblies and produced by decay of noble gas precursors also vented from the core assemblies may plate out on the walls of the monitor lines. These fission products will be swept through the monitor lines into the HPS traps by helium entering at the core subassembly vent connections. If deposited material accumulates, it may constrict the

sweep gas flow passages and could potentially lead to flow restrictions in the lines. The conditions under which plateout or plugging could occur in the GCFR, the means of minimizing or eliminating these conditions, and the methods for removing deposits, should they form, are being investigated. A small high-pressure loop has been built and is being used for this purpose. Components for injection, control, and measurement of impurities (i.e., H_2 and H_2O) and sources for simulating venting of volatile fission products and their compounds have been developed.

The first successful experiment simulating cesium vapor transport in PES monitor lines has been completed. A 7-day run using a redesigned cesium source which allows flowing helium to come into direct contact with a pool of liquid cesium resulted in the transport of ∿6% of the source inventory to the monitor line test section. Although this is not a large fraction of the loop inventory, it nonetheless confirms the basic operation of the apparatus. A major stumbling block in this and previous runs was the need to carry out wet chemistry analyses to determine cesium loadings in loop components. Since it was the aim of the experimental plan to use gamma spectroscopy to monitor nuclide movement, the loop configuration was altered to allow for introduction of a shielded NaI detector into the hood containing the apparatus. This improvement should offer much faster turnaround times for loop data and solution of the problem of determining the time during the experiment (early, late, continuously) at which cesium migrates. It will also provide quantitative data on the relative location of fission products within the test section, which wet chemistry analysis cannot do.

3.4. FISSION PRODUCT RELEASE AND TRANSPORT

The purpose of this subtask is to obtain experimental data on (1) interdiffusion of fission gases in helium, and (2) gas and surface back diffusion of gaseous and volatile fission products into the primary coolant. The interdiffusion coefficient data will be used to validate or improve the fission product release code used to model gas phase diffusion transport

(including radioactive decay). Surface transport and back diffusion data will be used to establish a model for predicting the importance of these mechanisms to contamination of the reactor coolant system.

Planned out-of-pile studies modeling fission gas interdiffusion in GCFR rods are nearing an end. A series of experiments modeling Kr-85 diffusion in the blanket and charcoal trap regions of a fuel rod were completed. The blanket tests were carried out using depleted UO_2 pellets to provide a fuel cladding-blanket gap of 0.25 mm. In the charcoal trap tests, a simulated rod trap was placed in the lower region of the diffusion tube in such a manner that all the Kr-85 was forced to diffuse through it to reach the counting region. The data obtained are currently being analyzed to provide krypton diffusion coefficients for SLIDER (Ref. 3-2) input. Remaining work includes several open tube runs using both Kr-85 and Xe-133. The latter nuclide is being utilized to ensure that the proper ratio of krypton to xenon diffusion coefficients is being used as input into code predictions.

3.5. MONITOR STATION AND INSTRUMENTATION

There was no activity on this subtask during this quarter.

3.6. PES UP-FLOW CORE ASSESSMENT

A study of the impact of an up-flow core on PES design and operation has been completed. In this study it was assumed that the core flow direction and configuration would not affect the noncore components of the PES. Consequently, the scope of the study was limited to the effects of the up-flow core configuration on the pressure equalization and venting considerations of the core assemblies. Three experimental observations were factored into the PES up-flow core study: (1) the presence of significant levels of cesium in the charcoal traps of high-burnup rods F-1 (low-pressure, sealed) and GB-10 (high-pressure, vented); (2) the 30% to

60% volumetric shrinkage of charcoal at peak fast neutron fluences; and (3) the plugging of the GB-10 fuel rod after 90 MWd/kg burnup when operated at steady conditions for long times.

The results of this study indicate that (1) the rod traps are required and should be based on cesium rather than iodine containment (iodine reaches the traps in only insignificant amounts); (2) cesium sorption on charcoal and graphite is relatively insensitive to core temperature levels; (3) sorption of cesium on charcoal degraded by radiation-induced shrinkage is probably better than cesium sorption on graphite enhanced by radiation (charcoal has an initial unirradiated advantage factor of 1000 over graphite in the sorption of cesium); (4) the lengths of the degraded charcoal traps are feasible ($\leq$300 mm), but those of the graphite traps are not; (5) plugging at the bottom, nonvented cold end of the GB-10 rod suggested that gravity and/or temperature (condensation) effects may be operative in plug formation; and (6) plugging at the nonvented end of the rods does not affect their pressure equalization or venting capabilities. It is indicated that top venting (manifolding of rods) is always preferable for avoiding any possible gravity effect which could lead to plug formation, and hot end venting is always preferable for minimizing any condensation effect leading to plug formation. Thus, the up-flow core is preferred because top and hot venting can be simultaneously realized. Although increased transport of cesium to the traps and gaseous fission product activity to the assembly vents may be consequences of hot-end venting, the design will be conservative with respect to the potential for rod plugging (if any).

These results reflect the most conservative design based on the current state of knowledge. However, there is also evidence to the contrary. If it is accepted that the plugging in GB-10 applies to the GCFR design, it can logically be assumed that the other characteristics observed in GS-10 should also be applied to the GCFR, namely

1. Plugging will occur only at the nonvented end.
2. Plugging will occur only at burnups >90 MWd/kg.

3. Plugging will never be present during reduced power transients.

Plugging of the nonvented end, as found in capsule GB-10, should not be considered as plugging. If burnup is limited to <90 MWd/kg, then plugging at either end would not be expected. If power level changes occur at short intervals (average of 1 every 3 h), relative to significant fission gas pressure accumulation times (∿1 month), the collected gas would be harmlessly vented and the rod pressure equalized. Programmed power cycling operation could also obviate any problem. If the plug found in GB-10 is characteristic of mixed oxide fast breeder reactor rods, the fact that no plugging has been observed in LMFBR rod irradiations may be explained by venting at reduced power. Plugging has not been reported in the fast breeder reactor R&D programs, nor is any known to have been reported from operation of BN-350 [150-MW(e) LMFBR], Phenix, or PFR [250-MW(e) LMFBR]. This suggests that plugging is not a significant fast breeder reactor design problem. The PES designs in both up- and down-flow core configurations are feasible and practical; i.e., PES considerations should not enter strongly into the core flow direction decision.

REFERENCES

3-1. "Gas-Cooled Fast Breeder Reactor Quarterly Progress Report for the Period May 1, 1976 through July 31, 1976," ERDA Report GA-A13975, General Atomic Company, August 31, 1976.

3-2. Jadhov, K. B., and B. W. Roos, "SLIDER, A FORTRAN-V Program for the Computation of Release of Fission Products from One-Dimensional Multi-Layer Fuel Configurations," USAEC Report GA-8566, Gulf General Atomic Company, August 1969.

4. CORE ASSEMBLY DESIGN VERIFICATION
(189a No. 00582)

Core assembly design verification consists of planning and executing the principal GCFR test programs to demonstrate satisfactory performance of the GCFR core assemblies. Model assemblies will be tested over a range of simulated GCFR environments, and the resultant performance data will be used to establish the GCFR design data base, to verify design analyses and predictive design computer codes, and to explore for design faults. The goals of these activities are to provide assurance of design performance and to generate the information necessary to support licensing. The current task scope includes

1. Core flow test loop (CFTL).
2. Prototype assembly tests.
3. Helium flow tests.
4. Depressurized accident condition tests.
5. In-pile loop to provide irradiated fuel rod for GRIST 2.
6. Fast test reactor helium loop study.

The principal achievements for this quarter were as follows:

1. DOE officially recognized the CFTL Coordinating Committee and its activities.

2. A simplified data prediction package was completed for the blanket bundle tests in the CFTL.

3. The helium flow test plan for core assemblies was completed (Ref. 4-1).

4.1. CORE FLOW TEST LOOP PROGRAM

A series of out-of-pile simulation tests will be performed to (1) demonstrate the ability of the GCFR fuel, control, and blanket assembly designs to meet design goals and (2) verify predictions of analytical models which describe design operation and accident behavior. The emphasis of the tests will be on obtaining thermal-structural data for steady-state, transient, and marginal conditions using electrically heated rod bundles in a dynamic helium loop. Final margin tests will be progressively extended to the highest possible temperature until the heater elements fail. The CFTL program plan (Ref. 4-2) describes the requirements for the test program to be conducted in the CFTL, which will be constructed and operated by Oak Ridge National Laboratory (ORNL).

4.1.1. Program Planning

4.1.1.1. CFTL Coordinating Committee. The CFTL Coordinating Committee achieved official status with the approval of the management plan (Ref. 4-3) for the CFTL by DOE. The committee is responsible for determining and resolving CFTL issues and reports to DOE Headquarters, as shown in Fig. 4-1 of Ref. 4-4. The CFTL Coordinating Committee will meet as necessary, but at least once a year. The functions of the committee are

1. Coordination of the detailed program responsibilities of all participants in the CFTL program.

2. Review and recommendation of the technical program, budget, and schedule.

3. Provision of assurance that the program meets GCFR development requirements.

4. Provision of information and being responsive to DOE.

5. Recommendation of revisions, as necessary, to the management plan and quality assurance principles.

6. Modification of the committee's functions and composition as required to accomplish the program objective.

The execution of these functions is in large part accomplished by overseeing program documentation (see Table 4-1 of Ref. 4-2). The committee has reviewed the control documents.

4.1.1.2. CFTL Documentation. GA accepted the ORNL revision of Ref. 4-5 except in the area of instrumentation. This document identifies three GA-ORNL interface areas, i.e., (1) design and fabrication of test bundles, (2) analysis and prediction, (3) test bundle instrumentation, and denotes the organization responsible for each. Subject to ORNL approval, GA has revised the test bundle instrumentation responsibilities to achieve efficient execution of measurement requirements by making one organization, namely ORNL, responsible for design, procurement, installation, and inspection.

A task document index (TDI), which contains information on reports, letters, and memos pertinent to the CFTL, was prepared. The current TDI lists about 300 items and serves as a forerunner of planned compiled reference information which can be retrieved by the computer program ORLOOK (Ref. 4-6) at ORNL.

4.1.1.3. Test Planning. Modeling of the GCFR design basis depressurization accident (DBDA) in the CFTL has received increased attention, and the modeling input and activities for defining experimental modeling of the GCFR DBDA have been established (Tables 4-1 and 4-2).

Consideration has been given to the use of the Los Alamos Scientific Laboratory (LASL) heater for the DBDA test. The CFTL power supply for driving the ORNL fuel rod simulators is also capable of driving the LASL heater. The CFTL ac power supply consists of 13 circuits, with a maximum

TABLE 4-1
INPUT FOR EXPERIMENTALLY MODELING THE GCFR DBDA

GCFR design to be referenced

DBDA test simulations conducted on models of fuel, control, and blanket assemblies

Size(s) (number of rod simulators) for each assembly model

Required test conditions expected to provide representative data for a GCFR DBDA

Test measurement data needed and how it will be used

Date(s) test results are needed

Rod simulator heating as a function of axial position and time.

Assembly model duct heating and net allowable heat loss as a function of position and time.

TABLE 4-2
ACTIVITIES FOR DEFINING EXPERIMENTAL MODELING OF
THE GCFR DBDA

Selection of a reference GCFR design

Technical justification and cost of duct wall heating and guard heaters/ insulation

Design of test bundle(s), including duct heating mechanism

Analysis of bundle(s) with GCFR codes (or the necessary modifications of codes)

Evaluation of ORNL and LASL rod simulators for high-temperature operation

Evaluation of thermocouples for use in rod simulators at high temperatures

Evaluation of flow instrumentation hardware and/or methods for subchannel measurements

Evaluation of temperature instrumentation for subchannel measurements

of 10 heaters per circuit, and a nominal rod rating of 150 A and 300 V. Voltage levels via transformer taps are 100%, 50%, 25%, 12.5%, 6.25%, 3%, 1.6%, 0.8%, 0.4%, and 0.2%. The power supplied to a row of heaters at any voltage level is linearly divided into 16 levels at a 6-2/3% power change per step. Each circuit supplies a row of heater rods, and operation may simulate a uniform power distribution or a GCFR transverse power distribution. The operating resistance of the ORNL heater is 1.7 ohms and that of the LASL heater is 1.0 ohm. A sample power input for both heaters is compared in Table 4-3. Table 4-3 indicates that the LASL heaters can be used in the CFTL if ORNL heaters cannot achieve the high temperature required, which is approximately 1260°C.

4.1.2. CFTL Analysis

The TSPEC code (Ref. 4-7), which provides a simplified analysis of thermal-hydraulic characteristics and duct bowing due to differential thermal expansion, was used to predict CFTL blanket rod assembly duct bowing. The code was developed to analyze fuel assemblies but has been modified to permit analysis of blanket assemblies. Reference 4-8 describes the modifications (eliminating approximations) incorporated into TSPEC to provide more accurate results.

The amount of blanket test bundle duct bowing under various simulated flow and power conditions has been predicted using the modified version of TSPEC. For extreme conditions, blanket test bundle bowing of up to 75 mm may occur if the assembly could survive a predicted maximum cladding temperature of 1460°C. By interpolating the data in Table 4-4 to a cladding melting temperature of 1370°C, the maximum bowing is predicted to be about 67 mm, which is within the value of 80 mm that was set as a clearance allowance. Based on the present stage of design and analysis for the GCFR and CFTL, the following test section space envelope for the blanket assembly is valid:

Length = 3000 mm,
Diameter = 300 mm,
Margin for bowing = 80 mm.

TABLE 4-3
COMPARISON OF HEATERS WITH CFTL POWER SUPPLY

Electrical Input	ORNL (kW)	Single Heater Output	
		LASL Single Heater (kW)	Two LASL Heaters in Series (kW)
150 A[(a)]	38.2	22.5	22.5
75 V	3.3	5.6	1.4
37.5 V	0.8	1.4	0.3

[(a)]Nominal maximum current.

TABLE 4-4
CFTL 61-ROD BLANKET BUNDLE DUCT BOWING
STEADY-STATE DESIGN MARGIN TEST WITH MAXIMUM POWER SKEW
(TEST 951, MAXIMUM BOWING)

Flow		Power (kW)			Maximum Cladding Temperature (°C)	Maximum Helium Temperature (°C)	Minor diamater Bowing[a] (mm)		Major Diameter Bowing[b] (mm)	
Fraction	kg/s	Avg	Max	Min			TSPEC	Modified TSPEC	TSPEC	Modified TSPEC
1.1	1.76	28	44	18	674	644	16.4	20.3	14.2	17.6
1.0	1.60	28	44	18	705	673	18.1	22.4	15.7	19.5
0.9	1.44	28	44	18	743	709	20.1	24.9	17.4	21.6
0.8	1.28	28	44	18	789	754	22.6	28.0	19.6	24.3
0.7	1.12	28	44	18	848	812	25.8	32.0	22.3	27.6
0.6	0.96	28	44	18	927	889	30.1	37.3	26.1	32.4
0.5	0.80	28	44	18	1036	996	36.2	44.9	31.3	38.8
0.4	0.64	28	44	18	1197	1158	45.2	56.0	39.1	48.5
0.3	0.48	28	44	18	1464[c]	1427	60.4	74.9	52.3	64.9

[a] Across the flats.

[b] Across the corners.

[c] Exceeds cladding melting temperature (see Section 4.1.2).

4.1.3. CFTL Liaison

A large coolant flow range must be accommodated by the CFTL control and measurement systems. Problems in attempting to meet the control and measurement requirements stated in the test specifications arose from the following conditions: (1) high volumetric flow at low pressure, (2) unmatched power and flow conditions, (3) low flow at high pressure, and (4) measurement of low flow at low pressure. To alleviate these problems, changes have been made to some of the test conditions in Ref. 4-9.

Four pieces of GCFR-type ribbed cladding were furnished to ORNL for continuing near-term evaluation activities on the nonswaged fuel rod simulator, which is currently preferred over the swaged simulator for CFTL test bundle use.

4.2. GCFR PROTOTYPE ASSEMBLY TEST PROGRAM

Program planning for testing of the prototype core assemblies is continuing. The tests will be conducted on full-size core assemblies to ensure that they meet design qualification requirements prior to fabrication of the demonstration plant initial core. The prototype assemblies will be the same as the GCFR demonstration plant core assemblies except that the PuO_2-UO_2 fuel in the GCFR fuel rods will be simulated by depleted UO_2. The assemblies will be subjected to maximum GCFR helium flow conditions to closely simulate the reactor core environment; however, there will be no radiation. One assembly of each type (fuel, control, and blanket) will be subjected to the equivalent of approximately one year of reactor operation in a hot helium test loop. The helium test loop temperature will be maintained external to the test section, since fuel rod heating will not be simulated in these tests.

The test facility and operation are planned as part of the German contribution to the GCFR program. Several options are being considered, including (1) a new facility which would most likely be situated in Germany;

(2) the CARMEN-2 loop at Saclay, France; and (3) upgrading of the proposed GCFR core assembly helium flow test rig. The Commissariat a L'Energie Atomique (CEA) has indicated that with minimal loop changes, the CARMEN-2 loop can provide a helium flow of 8 kg/s with a test assembly Δp of 290 kPa at 75 bars and 550°C. With additional changes, particularly upgrading of the recuperator/reheater and test vessel, the loop would meet the desired prototype test condition requirements of 8 kg/s with a Δp of 290 kPa at 90 bars and 450°C.

Idaho Nuclear Engineering Laboratory (INEL) has conducted a GCFR engineering test loop feasibility study (Ref. 4-10) which indicates that a helium flow facility at INEL which is capable of testing prototype assemblies is technically feasible. The study does not include sufficient cost information to permit updating of the prototype test program cost estimates.

A feasibility study on upgrading the proposed GCFR core assembly helium flow test rig to permit prototype testing has been initiated. The proposed helium flow test rig (which will be located in the U.S.) will be capable of relatively low-pressure and low-temperature test conditions and will be used for design evaluation testing of full-size core assemblies. The design evaluation work will include vibration, acoustic, and pressure drop testing. Upgrading will include raising the system pressure from 6 to 9 MPa and the test assembly temperature from 175° to 550°C. This may be accomplished by using the same circulator as that used for the helium flow tests, but a helium heater and a regenerator/recuperator will have to be added to the system to attain the desired prototype assembly test conditions.

Germany has agreed to complete an engineering design assessment of the prototype facility by the end of 1978 so that the funding and schedule requirements necessary for the program can be established. Implementation requirements will be defined by the Fuels, Materials, and Core Components Technical Coordinating Committee under the umbrella agreement, and a test

site will be selected. The prototype test schedule is being interfaced with other GCFR program schedules to ensure its compatibility with the overall GCFR schedule. The prototype Resource Evaluation and Control System (RECS) test and summary task definition have been completed.

4.3. HELIUM FLOW TEST

Helium flow testing is planned for the design evaluation of full-size core assemblies; Ref. 4-11 describes the need for conducting flow tests on the GCFR core assemblies. The objectives of the tests are to determine local and overall pressure drops and local flow distributions and to explore for acoustic excitation phenomena and flow-induced vibration characteristics. The results of these tests will be used to establish satisfactory flow performance of the core assemblies. Therefore, it is required that these tests be accomplished during the preliminary design phase of the core assembly to provide input for completion of the preliminary core design effort. Figures 4-1 and 4-2 are simplified flow diagrams of the test assembly and include the major test parameters and test section envelope dimensions.

The specification for the helium compressor/driver assembly for the helium flow test rig was prepared and sent with a request for proposal to compressor manufacturers. The responses are being evaluated. One manufacturer suggested that the helium circulator fabricated for the EBOR facility at INEL very nearly matches the circulator described, and refurbishment of this circulator may be the most economical way to obtain a circulator system for the helium flow test rig. (The EBOR circulator has been removed from the EBOR facility and placed in storage.) The manufacturer of the EBOR circulator has indicated that refurbishment of the EBOR circulator is feasible.

A Core Assembly Helium Flow Test Program Plan (Ref. 4-1) has been written and issued. The program plan includes a description of the flow-induced-vibration problem, the test objectives, the test program, the schedule, and a summary RECS. The helium flow test schedule is shown in Fig. 4-3.

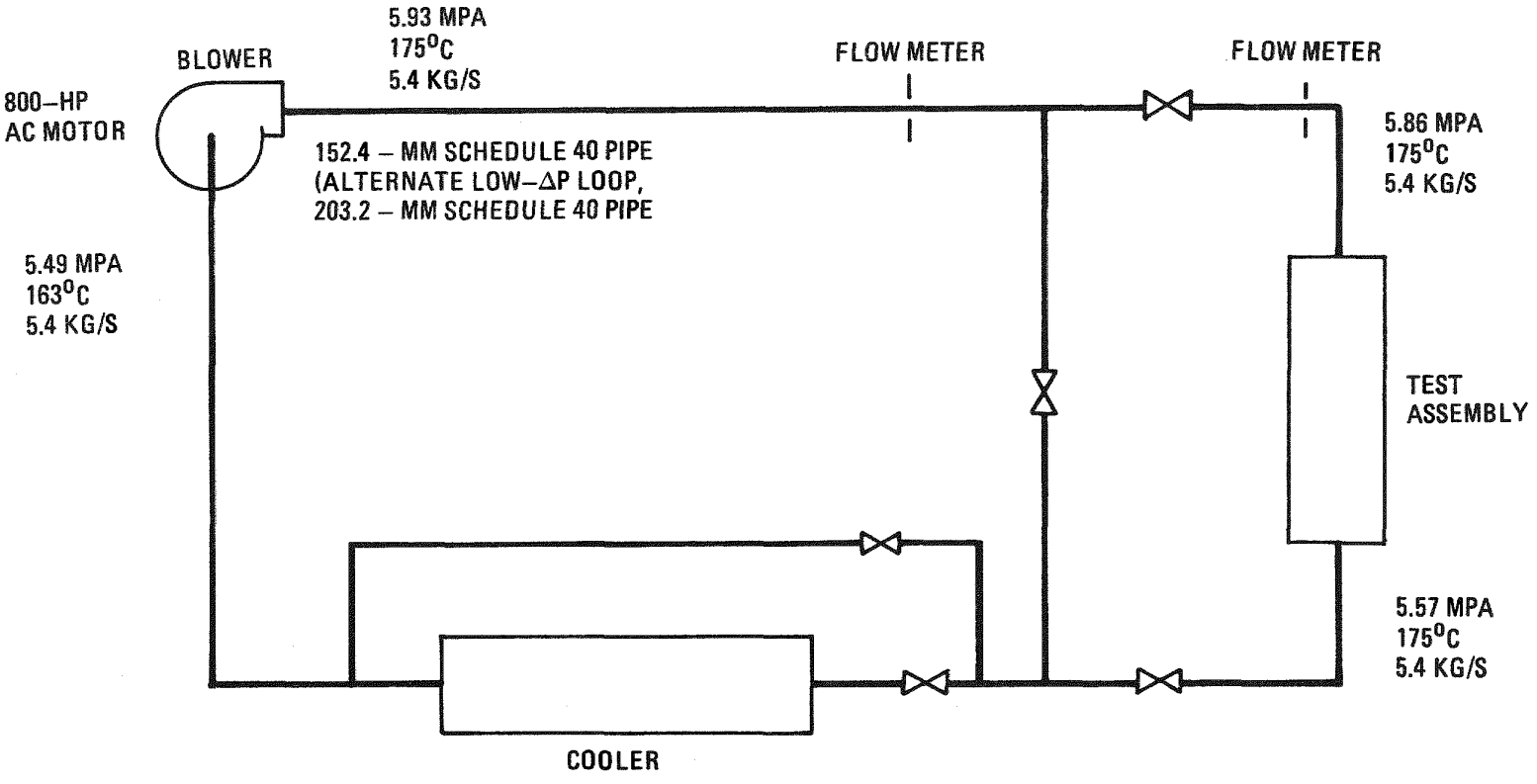

	REACTOR CORE	TEST RIG
TEMPERATURE	300° - 550°C	175°C
PRESSURE (AVERAGE)	8.86 MPA	5.86 MPA
FLOW	5.4 KG/S	5.4 KG/S
DENSITY (AVERAGE)	6.22 KG/M^3	6.22 KG/M^3
ACOUSTIC VELOCITY	1400 - 1700 M/S	1240 M/S

Fig. 4-1. Conceptual design of helium flow test rig

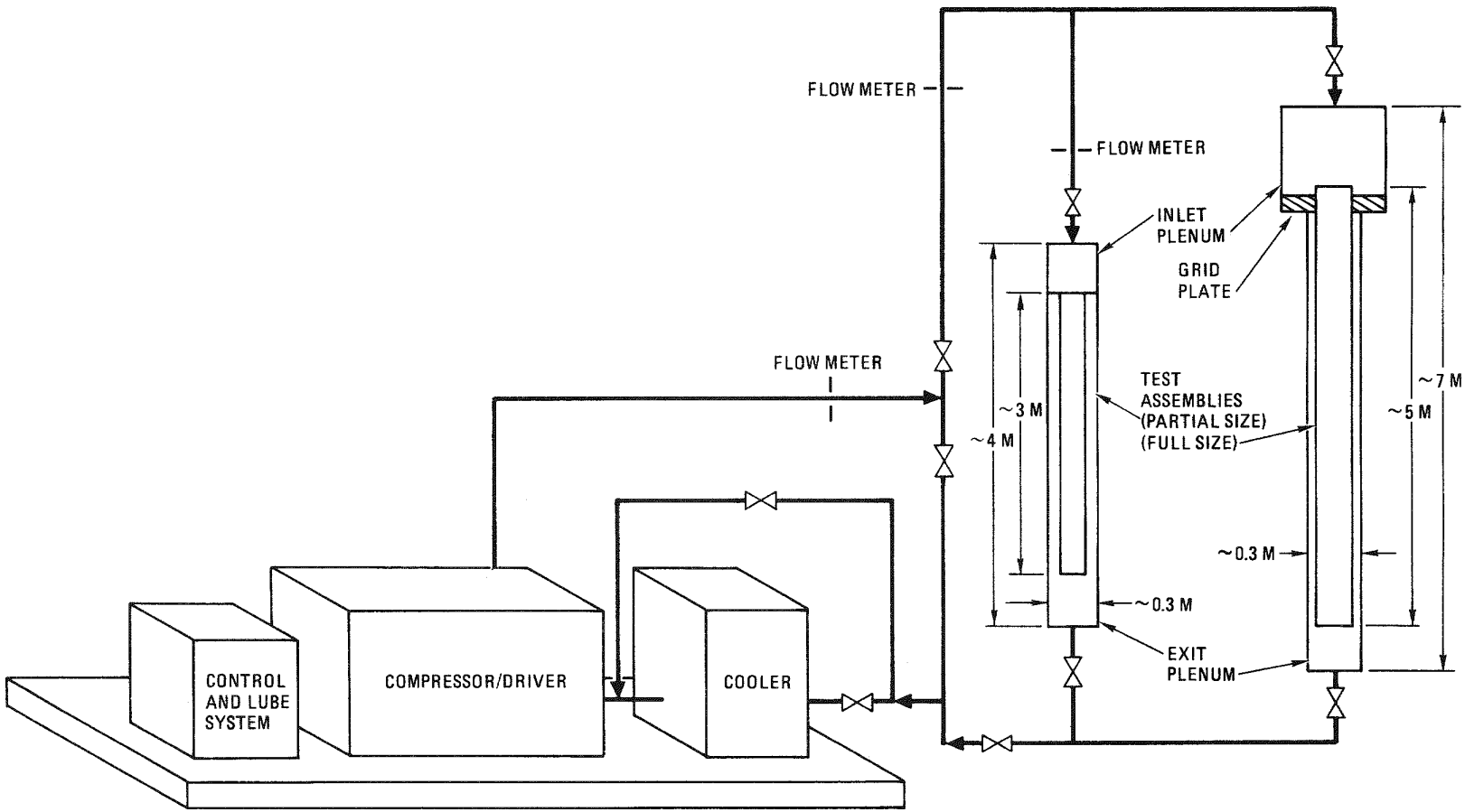

Fig. 4-2. Helium flow test rig

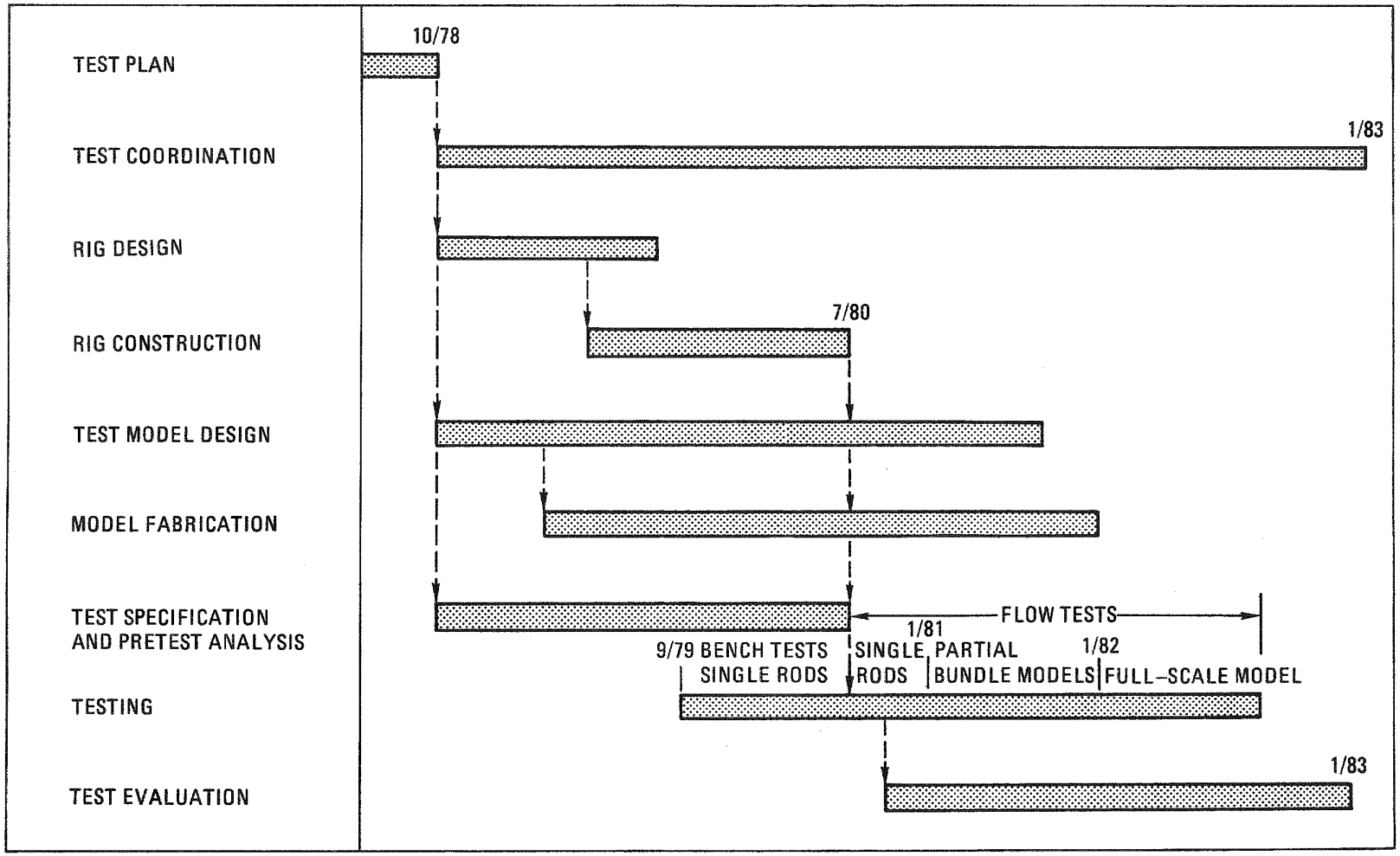

Fig. 4-3. Schedule of flow/vibration testing of GCFR core assemblies in the helium flow test rig

4.4. DEPRESSURIZED ACCIDENT CONDITION TEST

The depressurized accident condition test (DACT) will provide core cooling safety margin information under low-pressure, pseudo-steady-state DBDA conditions. The test is designed to provide experimental information on potential GCFR core assembly edge channel problems and flow and temperature distributions within the bundles under depressurized conditions. In addition, DACT will be capable of investigating natural convection effects within the core assemblies. Since recently developed experimental equipment for the duct melting fallaway test (DMFT) can be adapted to DACT, it is proposed that DACT be conducted at LASL, which is including the DACT requirements in the design of the DMFT test vessel. DACT will be run in FY 79 and 80 and thus will be ahead of the CFTL DBDA tests and will provide the near-term information required for licensing reviews.

The requirements for the DACT were being developed, but lack of funding has stopped the preparation of these requirements. Since LASL is in the process of designing the test fixtures which may be used for both the DMFT and DACT, development of the information required by LASL for incorporating DACT requirements into the test fixture design was emphasized. The two DMFT requirements which affect the LASL fixture design are instrumentation and bundle requalification. It appears that DACT will require about twice the amount of instrumentation as DMFT. Bundle requalification may be achieved by either (1) establishing a certain moderate temperature test condition data point and periodically returning to this point during testing to ensure that the bundle and/or the bundle instrumentation is still within specified test limits or (2) disassembling the test fixture to inspect and requalify the bundle.

4.5. IN-PILE LOOP FOR GRIST-2 FUEL ROD CONDITIONING

The need for irradiation conditioning of fuel rods for the GRIST-2 program is discussed in Ref. 4-12. Planning information was prepared for the program which provides preirradiated rods for the loss of flow tests in GRIST-2.

4.6. FAST TEST REACTOR HELIUM LOOP STUDY

Reference 4-12 states that preirradiation of fuel rods in a fast reactor may be required to simulate cladding neutron damage effects which qualify the fuel rods for transient overpower tests. Planning information was also prepared for this part of the program.

REFERENCES

4-1. Strong, W. R., and H. C. Hopkins, "Core Assembly Helium Flow Test Program Plan," General Atomic Company, unpublished data, September 14, 1978.

4-2. Hopkins, H. C., Jr., "Program Plan for GCFR Core Flow Test Loop," USAEC Report GA-A13080, General Atomic Company, August 9, 1974.

4-3. Kasten, P. R., and U. Gat, "Management Plan for the Core Flow Test Loop," Oak Ridge National Laboratory, unpublished data, May 1978.

4-4. "Gas-Cooled Fast Breeder Reactor Quarterly Progress Report for the Period February 1, 1978 through April 30, 1978," DOE Report GA-A14928, General Atomic Company, May 1978.

4-5. Hopkins, H. C., and U. Gat, "Core Flow Test Loop - Division of Responsibility," General Atomic Company, unpublished data, July 14, 1978.

4-6. Singletary, V., "An Outline Conversational Retrieval System for ORCHIS Text-Oriented Data Bases – A User's Manual," Rev. 1, Oak Ridge National Laboratory Report No. 4951, May 1975.

4-7. Hopkins, H. C., Jr., "TSPEC - A Computer Program to Predict Approximate Model Performance in the Core Flow Test Loop," ERDA Report GA-A14057, General Atomic Company, 1975.

4-8. Sanders, J. P., "Calculated Deflection of Test Assemblies in CFTL," Appendix A, ORNL unpublished data, June 26, 1978.

4-9. Hopkins, Harvey C., Jr., "Scope of Total CFTL Test Specifications," General Atomic Company, unpublished data, January 4, 1978.

4-10. Porter, E. H., "GCFR Engineering Test Loop Feasibility Study," EG&G, unpublished data, May 1978.

4-11. "Core-Element Development Program Plan for the Gas-Cooled Fast Breeder Reactor Demonstration Plant," ERDA Report GA-A13312, General Atomic Company, November 1976.

4-12. "Gas-Cooled Fast Breeder Reactor Quarterly Progress Report for the Period May 1, 1978 through July 31, 1978," DOE Report GA-A15054, General Atomic Company, August 1978.

5. FUELS AND MATERIAL ENGINEERING (189a No. 00582)

5.1. OXIDE FUEL AND BLANKET TECHNOLOGY

The purposes of this subtask are to (1) maintain liaison with and surveillance of other DOE and non-DOE programs, especially the liquid metal fast breeder reactor (LMFBR) program, to enable utilization of the information on fuel and blanket materials obtained in these programs in the GCFR design; (2) participate in the fast breeder reactor Fuel Element Development Working Group and its subsidiary task groups; and (3) guide the laboratory and irradiation test programs for the GCFR.

During the present quarter, comments were submitted to the Fuel Properties Task Group on the fuel-cladding chemical interaction (FCCI) correlation proposed by Hanford Engineering Development Laboratory (HEDL) for inclusion in the Nuclear Systems Materials Handbook (Ref. 5-1). Comments on the HEDL recommendation of Nd-148 fission yields for determination of fuel burnup were also presented to the Steady-State Irradiation Task Group.

Studies were initiated on the development during FY-79 of an integrated and coordinated irradiation testing program which would take into account the following programmatic requirements:

1. Steady-state irradiation design verification testing.

2. Supply of irradiated fuel rods for the GCFR safety testing program proposed for GRIST-II.

3. Supply of irradiated fuel rods for the GCFR design basis testing program proposed for GRIST-II.

5.2. CLADDING TECHNOLOGY

5.2.1. Mechanical Testing Program

The objective of the ANL mechanical testing program is to determine the effects of the following factors on the behavior and properties of GCFR ribbed and smooth cladding:

1. Ribs, rib geometry, fabrication technique, and stress state.

2. Helium impurity levels typical of the environment expected in the GCFR demonstration plant.

These tests are biaxial creep rupture tests with a hoop to axial tensile stress ratio of 2. Tests at a hoop to axial tensile stress ratio of unity and pure tensile tests are planned in support of the irradiated cladding test program. Two tests at 650°C and a hoop stress of ∿238 MPa in a purified helium atmosphere (i.e., O_2 partial pressure of $<10^{-1}$ Pa) were completed, and a third test in impure helium was also completed at ANL prior to this quarter (Ref. 5-2). In general, ribs increase the rupture life and do not affect strain at failure. Various types of ribbed and smooth cladding were tested, and the ribs were found to strengthen the cladding in terms of rupture life.

During this quarter, ANL and GA agreed on the design of the test matrix for test ANL-IV. Cladding fabrication for this test has been completed, specimen fabrication has been initiated, and the test is expected to start during the first quarter of FY-79.

Recent fuel rod and fuel assembly analyses indicate that fuel assembly life is limited by bowing of the edge rods in the assembly. Bowing is caused by differential swellings of the 20% cold-worked 316 reference cladding. Performance improvements are possible if alloys with low swelling characteristics are used, and therefore data on six candidate

advanced alloys were obtained from HEDL. Analysis of these data from a materials point of view has been completed and the following observations have been made.

The vented fuel rod design of the GCFR removes the only source of primary stress on the cladding. This fact allows consideration of two low-strength ferritic alloys (HT-9 and D-57) for cladding. The other advanced alloys which can be considered are a modified stainless steel alloy (D-9) and three high-nickel precipitation-strengthened alloys. The swelling rate of the modified stainless steel alloy D-9 is too high, and significant improvements cannot be achieved by its use. The high-nickel alloys have very low ductility at high temperatures, and a significant neutronic penalty has to be paid. These considerations narrow the field to the ferritic alloys, i.e., commercial alloy HT-9 and developmental alloy D-57.

Comparisons of the properties of these two alloys show that a higher hot spot temperature can be used with alloy D-57. Both have excellent ductility, and use of ferritic alloys should improve neutron economy. Based on mechanical properties, D-57 appears to be better, although it has to be hot drawn, which may increase the fabrication cost. Presently, duct fabrication is feasible only with HT-9. Thus, alloy D-57 appears to be a good choice for the cladding, and HT-9 appears good for the spacers and ducts.

5.2.2. Helium Loop Test Program

The primary objective of the Pacific Northwest Laboratory (PNL) helium loop test program is to compare the mechanical properties of GCFR ribbed cladding in recirculating helium, determined at PNL, with those in quasi-static helium, determined at ANL. The loop was modified for unattended operation, and the first test was initiated. Significant problems in measuring and controlling impurity levels caused this test to be terminated at the end of 100 h. Additional equipment was purchased and installed to rectify these problems. This program has been plagued by various failures

of the system and instrumentation, and therefore there was no significant progress achieved during this quarter.

5.3. F-1 (X094) FAST FLUX IRRADIATION EXPERIMENT

The encapsulated fuel rods in the F-1 (X094B) experiment received burnup exposures in the range of 8 to 13.6 at. % (8×10^{26} n/m^2 total fluence and 6.1×10^{26} n/m^2, E > 0.1 MeV). Postirradiation examination of the seven fuel rods removed at the termination of the experiment is continuing at ANL, and examination of special components (dosimetry and charcoal traps) continues at GA.

Tritium analysis data from the lower third of the fuel section of rod G-4 for a fuel sample taken at approximately 8.6 cm from the bottom of the fuel column have been received from ANL-W. The residual tritium content of this fuel section was determined to be 8.6×10^{-2} μCi/g fuel, which translates to a residual content of 29 ppm, or 2.9×10^{-3}% retained, based on the calculated tritium inventory. This is in the range expected from other fast breeder reactor irradiations.

Budget restraints have made it necessary to reduce the number of analytical samples submitted by ANL-E to ANL-W. A minimum number of samples (three samples/rod) from the designated priority rods G-4 (high burnup), G-11 (low oxygen to metal ratio), and G-13 (high temperature) will be analyzed for burnup. Single midplane samples from each of the remaining rods will also be analyzed for burnup. Since initial measurements have indicated no significant tritium content, additional analyses of the fuel for tritium or cladding are not contemplated at this time.

Postirradiation analysis of the charcoal removed from the fission product traps of the F-1 irradiation experiment fuel rods is continuing at GA. Gamma ray spectral analysis of aliquots from all F-1 trap sections has been completed, and variance analysis of the gamma measurements indicates large error bands, typically 20% to 40%. Hence, a direct measure of the fission product content of the entire trap section charcoal by gamma ray

spectral analysis using an appropriate lead container was initiated. Several lead casks (3.80-cm wall thickness) were fabricated for this task. The activity content of the sample within the cask was measured with a high-resolution, low-sensitivity GeLi spectrometer. The spectrometer system was calibrated by subdivision of a cask sample and counting of the sample fractions using the GA Sigma-2 Standard GeLi System. Direct gamma ray spectral measurements of the entire charcoal mass from each trap section have been completed, and analysis of the results is in progress.

5.4. F-3 (X206) FAST FLUX IRRADIATION EXPERIMENT

There was no activity on this subtask during this quarter.

5.5. F-5 (X317) GRID-SPACED FUEL ROD BUNDLE FAST FLUX IRRADIATION EXPERIMENT

As reported previously (Ref. 5-3), the F-5 experiment was designed to study the performance of fuel rods irradiated under simulated GCFR conditions to determine (1) the reliability of the GCFR design and (2) the effect of a step power increase which simulates a 180-deg rotation of a subassembly at the core-blanket interface in the proposed GCFR demonstration plant. The irradiation of the F-5 (X317) grid-spaced bundle was begun in EBR-II run 93 in January 1978. At the end of EBR-II run 96, the experiment had achieved a peak exposure of 22 MWd/kg (2.5 at. %) burnup [2.5×10^{26} n/m^2 ($E > 0.1$ MeV)], with a goal of 50 MWd/kg in the first phase of its irradiation at 400 W/cm and a cladding midwall temperature of 700°C. Approval has been granted by the EBR-II project for irradiation of F-5 (X317) to 50 MWd/kg burnup prior to the first scheduled interim examination. Based on the current schedule, the start of the first interim examination will occur in April 1979.

Depressurization of the fuel rod is required prior to reconstitution of F-5 as a 19-rod subassembly. A laser technique used by HEDL on some

irradiated fuel rods which were later subjected to transient testing was adopted to accomplish depressurization and rewelding. However, there have been no reirradiations in flowing sodium of fuel rods which have been laser punctured and resealed were carried out. Thus, this procedure is not considered to be qualified for use in EBR-II. In addition, laser puncture and seal welding trials by HEDL on tubing with a wall thickness similar to that of F-5 cladding resulted in unacceptable welds as determined by metallography. Subsequent discussions with ANL and HEDL produced an alternate plan to remove the top compartment of the fuel rod and weld on an adapter fitting with a capillary tube and then a top fitting as shown in Fig. 5-1. The capillary tube will be used for xenon gas tagging. HEDL has successfully performed girth welds between irradiated tubing and fresh end fittings. HEDL presently possesses all the equipment and capabilities for carrying out this plan, and cutting, drilling, and welding trials are being planned to verify the design and procedures. This concept has been discussed with ANL Material Science Division, EBR-II, and hot fuel examination facility (HFEF) personnel and is acceptable to all parties. A schedule for the first interim examination was agreed upon and is shown in Fig. 5-2.

5.6. GB-10 VENTED FUEL ROD EXPERIMENT

During this quarter destructive examination of GB-10 vented fuel rod GA-21, which achieved a burnup exposure of 11.0 at. % in the Oak Ridge Reactor (ORR), continued at ANL. Examination of the charcoal trap is continuing at GA. Burnup analysis data for the GB-10 fuel rod have been received from ANL-W. The peak (midplane) burnup is at 11.0 at. %.

Radiochemical analysis of the GB-10 charcoal trap for Sr-89 and Sr-90 indicates that transport of these isotopes to the charcoal trap is in the same (low-ppm) range as that of GB-9. However, Cs-137 transport appears to be 500 times as high, which may be a consequence of the "flow-through" feature of the GB-10 fuel rod which was not present in GB-9. The Cs-133 and Cs-135 loadings [expected shortly from Idaho Nuclear Engineering Laboratory (INEL)] will aid in analyzing the reasons for the enhanced Cs-137 transport.

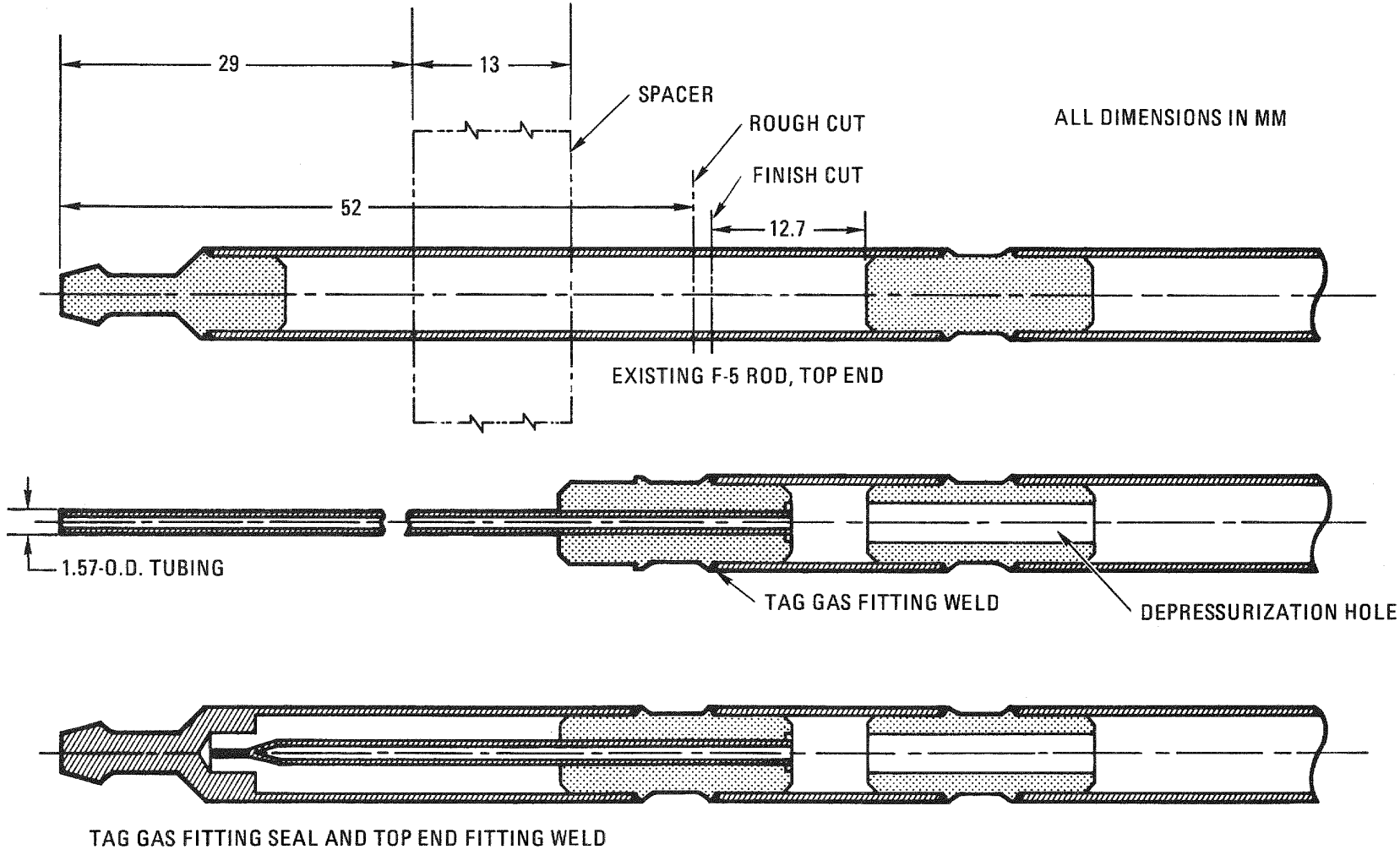

Fig. 5-1. Depressurization and resealing concept

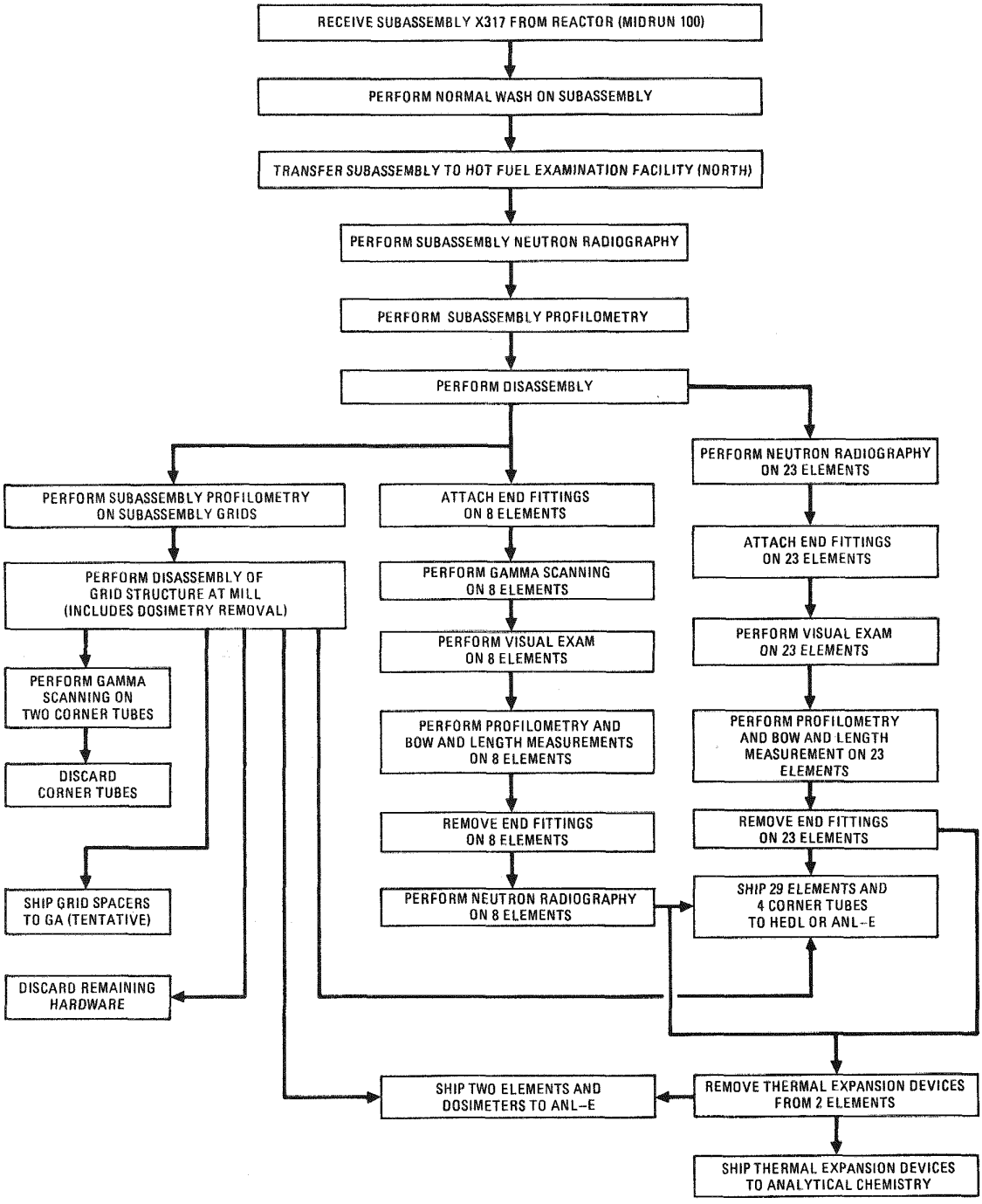

Fig. 5-2. Proposed disassembly and examination sequence for subassembly X317

Tritium analysis data for the midplane fuel section have been received from ANL-W. The residual tritium content of this fuel section was determined to be 2.1×10^{-2} μCi/g fuel, which translates to 16.5 ppm, or 1.65×10^{-3}% retention, based on the tritium inventory. This low retention is in line with results from the F-1 experiment and also other irradiations.

Budget restraints have made it necessary to reduce the number of analytical samples submitted by ANL-E to ANL-W. Since initial measurements have indicated no significant tritium content, no additional analyses of the fuel or cladding for tritium are contemplated at this time.

REFERENCES

5-1. Nuclear Systems Materials Handbook, Hartford Engineering Development Laboratory (TID-26666).

5-2. "Gas-Cooled Fast Breeder Reactor Quarterly Progress Report for the Period May 1, 1978 through July 31, 1978," DOE Report GA-A15054, General Atomic Company, August 1978.

5-3. "Gas-Cooled Fast Breeder Reactor Quarterly Progress Report for the Period August 1, 1976 through October 31, 1976," ERDA Report GA-A14112, General Atomic Company, November 1976.

6. FUEL ROD ENGINEERING (189a No. 00583)

The objective of this task is to evaluate the steady-state and transient performance of the fuel, blanket, and control rods for the determination of performance characteristics, operating limits, and design criteria. To this end, analytical tools such as the LIFE code (Ref. 6-1) are being adapted and/or developed and applied to the analysis of GCFR prototypical rods and experimental rods. In addition, continuous surveillance of the LMFBR fuels and materials development program and technology is maintained to maximize the use of development technology and material properties. Support is also given to planning and designing irradiation experiments.

6.1. FUEL, BLANKET, AND CONTROL ROD ANALYTICAL METHODS

The GB-10 sweep gas capsule test was irradiated in the thermal flux environment of the Oak Ridge Research Reactor (ORR) (Ref. 6-2). One of the major objectives of this experiment was to generate information on the release, transport, and trapping of the gaseous and volatile fission products for use in the design of the GCFR PES. To obtain the fission gases released directly from the mixed oxide fuel during irradiation, one of the sweep gas lines was connected at the bottom of the upper blanket region. Thus, the fission gases released from the fuel could be directly swept out of the fuel rod without transport through the upper blanket and charcoal trap. The fission gas release data from this sweeping mode have been analyzed to evaluate the diffusion of xenon and krypton gases in the mixed oxide fuel.

The analysis was performed using a combination of the LIFE-III code and the subroutine GAREL. LIFE-III is a fuel rod thermomechanical performance code which provides the fuel temperature and power histories to

GAREL. The fission gas release model used in GAREL is based on Booth's spherical particle diffusion model and is documented in Ref. 6-3. The input data for the LIFE-III fuel rod analysis were obtained from Ref. 6-2.

The effective diffusion coefficients of krypton and xenon isotopes in the fuel determined from the GB-10 data and the LIFE-III and GAREL analysis are in the form

$$D = D_o \exp [-Q/KT], \qquad (6\text{-}1)$$

where D_o = 0.12074×10^{-9} cm^2/s for krypton isotopes,

= 0.7521×10^{-9} cm^2/s for xenon isotopes,

Q = 1.53 - 0.08763 burnup eV/atom for krypton isotopes,

= 1.55 - 0.05258 burnup eV/atom for xenon isotopes,

Bu = burnup in at. %,

K = Boltzmann's constant,

T = absolute temperature.

With these diffusion coefficients the calculated and measured fission gas release-to-birth ratios for the krypton and xenon isotopes are in good agreement, as shown in Figs. 6-1 and 6-2 for Kr-87 and Xe-138, respectively.

The analytical method developed to permit the calculation of the release of isotopic fission gases from the fuel of a fuel rod under irradiation consists of the fission gas release subroutine GAREL, the fuel rod thermomechanical performance code LIFE-III, and the effective diffusion coefficients of Eq. 6-1 determined from GB-10. This method has been applied to the HELM-2 irradiation test in BR-2. The calculated fission gas release from the fuel matrix was used to predict the fission gas venting rate from the fuel rod, and the results were in good agreement with the measured fission gas venting rate (Ref. 6-4).

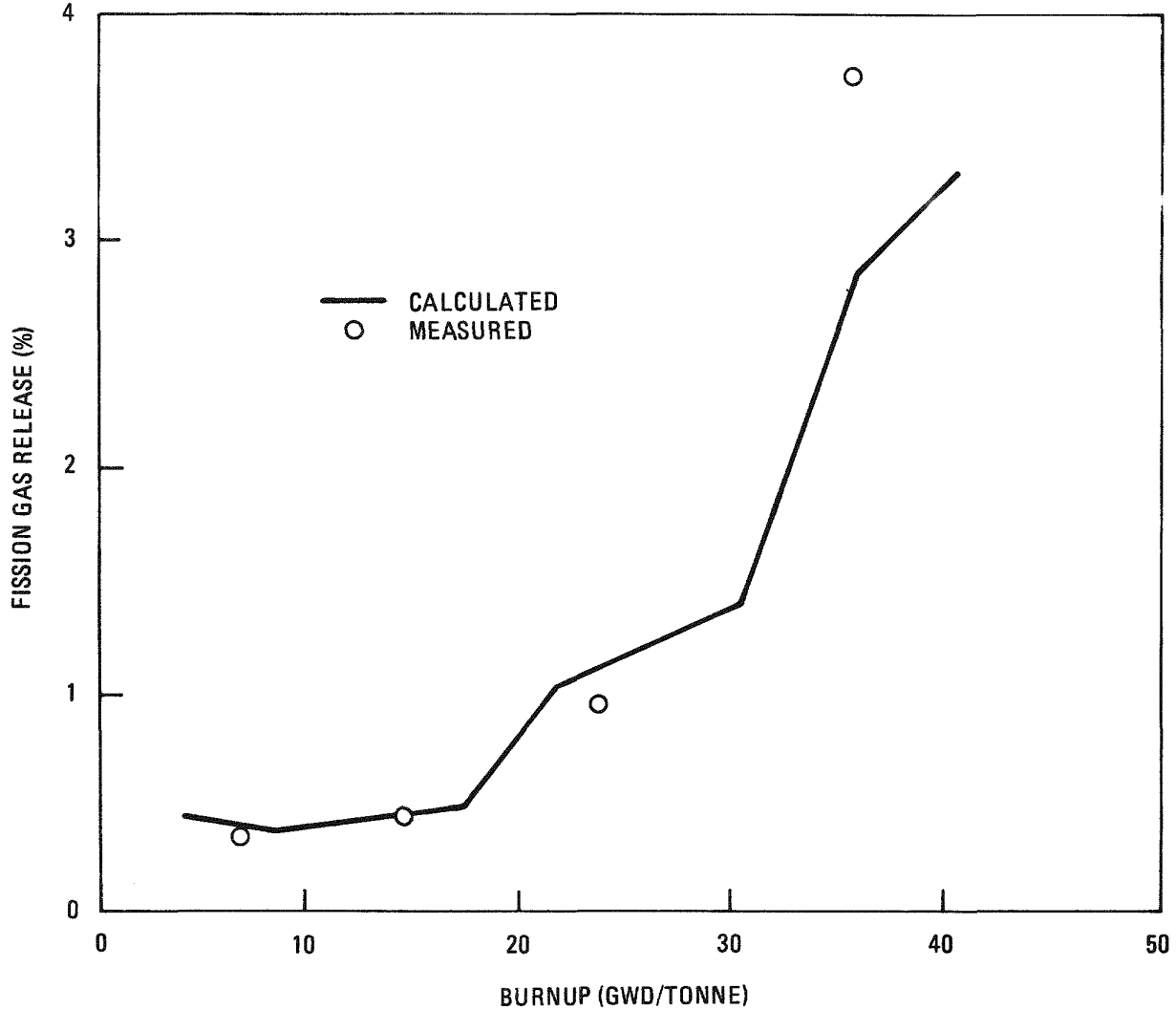

Fig. 6-1. Release-to-birth ratio for Kr-87

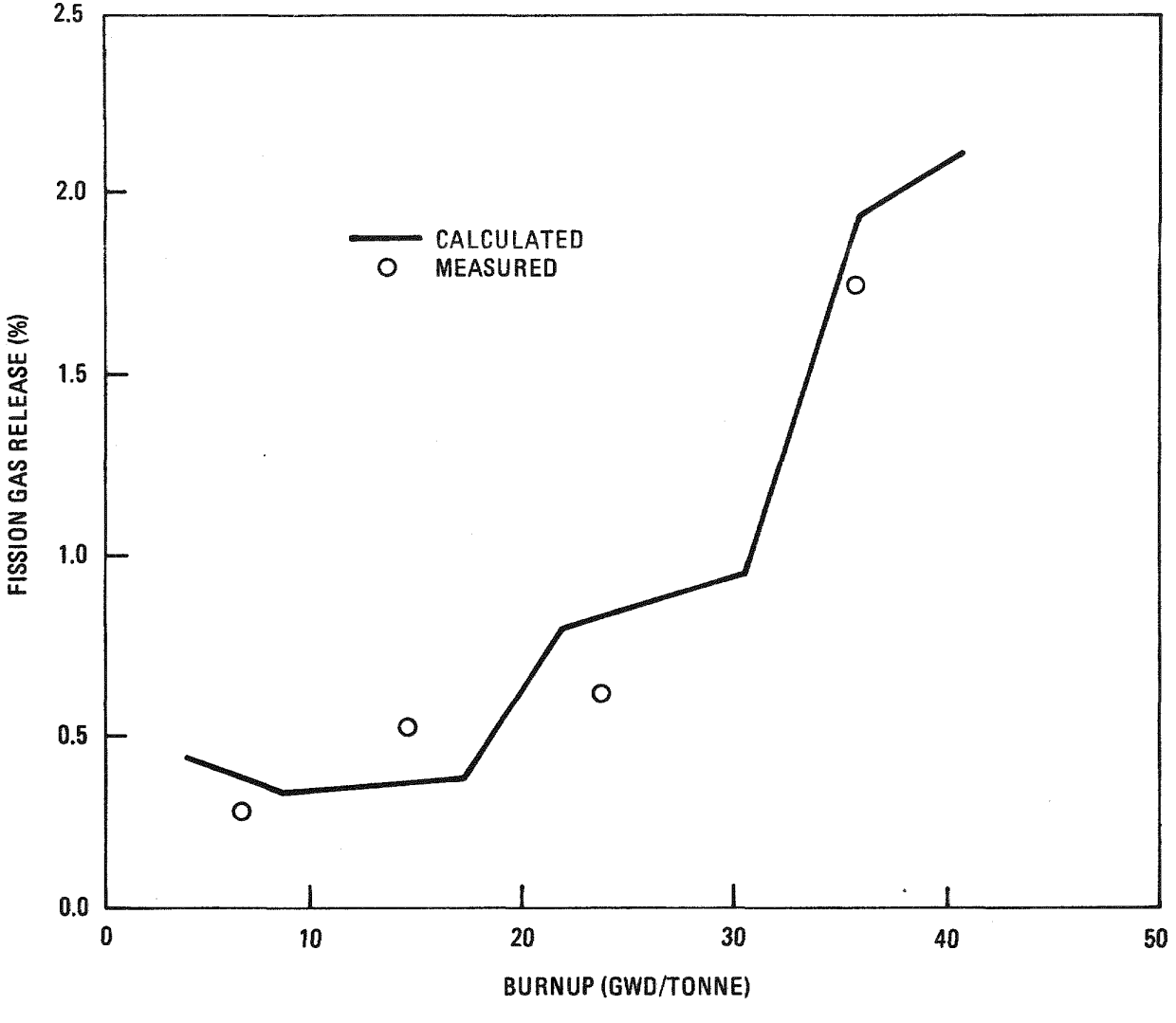

Fig. 6-2. Release-to-birth ratio for Xe-138

6.2. ANALYSIS OF IRRADIATION TESTS

The steady-state fission gas release-to-birth ratio from the HELM-2 irradiation test was calculated using a combination of the fuel rod thermomechanical performance code LIFE-III and the isotopic fission gas release subroutine GAREL. The diffusion coefficients used in the GAREL subroutine were derived from the GB-10 measured data described in Section 6.1. The linear power and coolant conditions are given as bundle-averaged values so that the bundle-averaged fission gas release can be characterized. The results indicate that the release-to-birth ratio increases with increasing half life; for stable isotopes, this ratio is exactly equal to 1.00. In addition, the release-to-birth ratio decreases with increasing burnup because of the reduction of fuel temperature due to fuel-to-gap closure.

6.3. ROD ANALYSIS AND PERFORMANCE

There has been a great deal of concern about identifying the state of the GCFR clad primary stresses for application to the cladding mechanical testing program. By definition, primary stress is any normal or shear stress developed by an imposed loading necessary to satisfy the laws of equilibrium of external and internal forces and moments. Therefore, stresses which arise from constraints such as thermal expansion, swelling, or fuel-cladding mechanical interaction (FCMI) are excluded from this category and in theory should not be included in the discussion. However, the stress induced by FCMI is an exception. In dealing with the problem of fuel rod structural integrity, FCMI has long been considered as one of the major sources of cladding failure. The exertion caused by fuel expansion on the cladding could severely damage the cladding beyond the elastic range before the stress has time to relax. In view of the important role of FCMI stress in cladding damage, it is included in the discussion of primary stresses, which are evaluated for the steady-state and transient operating conditions described below.

6.3.1. Steady-State Operating Conditions

As was shown in Ref. 6-5, FCMI is not expected in the GCFR vented fuel rod during steady-state operation. Consequently, the cladding primary stress can only arise from the pressure loading external and internal to the cladding and loading from the fuel rod dead weight. Based on Lame's solution for a long, thick-walled cylinder, the three principal stresses ($\bar{\sigma}_{rr}$, $\bar{\sigma}_{\theta\theta}$, $\bar{\sigma}_{zz}$) averaged across the cladding cross section caused by the external and internal pressures can be found:

$$\bar{\sigma}_{rr} = -8.77 \text{ MPa},$$

$$\bar{\sigma}_{\theta\theta} = -11.24 \text{ MPa},$$

$$\bar{\sigma}_{zz} = -10.00 \text{ MPa}.$$

The additional loading due to fuel rod dead weight produces stress only in the axial direction. The cladding midsection is subject to the dead weights of the fuel column, upper and lower blankets, lower end plug, and lower half of the cladding, which produce the following axial stress (Ref. 6-6):

$$\sigma_{zz} = 0.85 \text{ MPa}.$$

Therefore, the three total principal primary stresses at the cladding midsection are

$$\bar{\sigma}^{t}_{rr} = -8.77 \text{ MPa},$$

$$\bar{\sigma}^{t}_{\theta\theta} = -11.24 \text{ MPa},$$

$$\bar{\sigma}^{t}_{zz} = -9.15 \text{ MPa}.$$

Their triaxial ratio is

$$\bar{\sigma}^t_{rr}:\bar{\sigma}_{\theta\theta}:\bar{\sigma}^t_{zz} = 0.96: 1.23: 1:00.$$

6.3.2. Transient Operating Conditions

Although FCMI is not expected to occur in the GCFR vented fuel rod during steady-state operation, it could occur under a combination of steady-state and transient conditions. In particular, at the time when the fuel-to-cladding gap reaches a minimum after a period of steady-state operation, a step power increase (e.g., resulting from fuel assembly rotation) could introduce FCMI as a result of differential thermal expansion between the fuel and cladding.

For instance, it was reported in Ref. 6-7 that the fuel-to-cladding gap closed owing to thermal expansion during a step power change from 60% to 115% power for the GCFR fuel rod subjected to the following power history: (1) 13,000 h at 60% power and flux, (2) a rise to 115% power in 9 h followed by a 1-h hold and a 1-h decrease to 100% power; and (3) 500 h at 100% power. The fuel-cladding interface pressure increased to approximately 5.52 MPa above the plenum pressure, and the stress ratio (primary and secondary) in the outer ring of the cladding was $\sigma_\theta/\sigma_z = 1.22$. The gap reopened during the decrease in power. On the other hand, another LIFE analysis indicated that FCMI did not occur for a 100% steady-state power operation superimposed by a 15% overpower for 0.5 h at the time (7000 h) when the gap reached the minimum. The FCMI occurred in the case of 60% but not 100% steady-state power operations because of the cladding swelling effect.

It should be noted that the above step power analyses were performed by LIFE-III, which is a steady-state code. The response of the fuel rod temperature to the step power increase is instantaneous achievement of the steady-state temperature. This implies that the FCMI obtained in

this fashion is an instantaneous buildup and thus conservative, because there is no transient time allowed for stress relaxation. These results are preliminary. Further analyses will be performed when LIFE-IV, a transient version of LIFE, becomes available and more realistic transient power histories are defined.

6.4. FUEL ROD MECHANICAL TESTS

Testing of the fuel rod cladding tubing according to the test matrix given in Table 6-1 is in progress. All tests are progressing satisfactorily except for the tensile tests at elevated temperatures. The initial elevated temperature tensile tests were not successful owing to the loss of the cladding cold work properties because of the attachment of testing fixtures. Present plans are to develop an alternate method during the next quarter.

REFERENCES

6-1. Billone, M. C., et al., "LIFE-III Fuel-Element Performance Code," ERDA Report 77-56, Argonne National Laboratory, July 15, 1977.

6-2. Longest, A. W., et al., "Results from Irradiation of Vented GCFR Fuel Rods in the GB-9 and GB-10 Capsule Experiments," Oak Ridge National Laboratory Draft Report, February 17, 1977.

6-3. Chang, K. H., "A Theory of Radioactive Fission Gas Release and Its Application to the Fuel Rod Analysis," General Atomic Company, unpublished data, June 15, 1977.

6-4. Campana, R. J., General Atomic Company, private communication.

6-5. Chang, K. H., "Comparison of Fuel-to-Clad Gap Size Between Vented and Sealed Rods," General Atomic Company, unpublished data, July 1977.

6-6. Veca, A. R., "Structural Basis for Clad Damage Limit," General Atomic Company, unpublished data, April 13, 1977.

6-7. Billone, M. C., "Fuel-Cladding Mechanical Interaction in GCFR Fuel Rods," Argonne National Laboratory, unpublished data, April 11, 1977.

TABLE 6-1
FUEL CLADDING MECHANICAL TEST MATRIX

Test	Number of Tests			Remarks
	Ribbed	Smooth 1[(a)]	Smooth 2[(b)]	
Flexure	8	8	8	4 tests each at length of 10 and 20 cm
Compression	4	4	4	Sample length = 50 cm
Tensile room temperature	9	9	9	3 tests at length of 20 cm
300°C	3	3	3	Use procedure ASTM E-21-70; all tests at length of 20 cm
600°C	3	3	3	
1000°C	3	3	3	
Hertzian stress	3	3	3	All tests at length of 20 cm

(a) Smooth 1 = tubing ground to root diameter (0.73-cm o.d.).

(b) Smooth 2 = 0.75-cm o.d.

7. NUCLEAR ANALYSIS AND REACTOR PHYSICS
(189a No. 00584)

The scope of activities planned under this subtask encompasses the validation and verification of the nuclear design methods which will be applied to the GCFR core design. This will primarily be done by evaluating the methods using a critical assembly experimental program specifically directed toward GCFR development. Program planning and coordination activites, critical assembly design and analysis, and the necessary methods development will be carried out.

During the previous quarter, work centered on continued postanalysis of measurements in the phase II assembly of the benchmark series of GCFR critical experiments. During the present quarter, efforts were directed at two areas pertinent to design and licensing of the GCFR demonstration plant: (1) planning for the pre-engineering mock-up critical (pre-EMC) series of GCFR critical assemblies and (2) physics calculations needed for analysis of postulated distorted core configurations in a protected loss of flow accident.

7.1. CRITICAL ASSEMBLY PLANNING

A program has been mapped out for the pre-EMC series of critical experiments in support of the design efforts for the 300-MW(e) GCFR demonstration plant. This program and the proposed assembly designs were formulated considering requirements for four basic activities:

1. Updating of the GCFR reference design, which requires a core with only three enrichment zones but with an expanded total volume of about 4300 liters, an increased blanket fertile density and thickness (possibly a third row), and the potential addition of axial shield regions.

2. Experiments deleted from the previous benchmark series of GCFR critical assemblies. These include studies of the effects of high Pu-240 fuel mixtures, extensive control rod design and interaction studies, gamma heating measurements, and attempts at determining the intensity and spectra of neutron leakage from the balnkets.

3. Investigations of the alternate fuel cycle materials U-233 and thorium and core zones using plutonium plus thorium. U-233 and thorium may also be studied along with blanket zones in which thorium replaces U-238.

4. Safety impact studies which include the effects of fuel decladding, Doppler measurements for U-238 and thorium in different locations and environments, and the central worths of steam entry and helium in different fuel environments.

The proposed pre-EMC program consists of four configuration phases of increasing complexity, with the last approaching a close clean-geometry mock-up of the demonstration plant core. Phase I is a two-zone-core reference configuration for basic physic studies and benchmark-type experiments; control rod design studies and the decladding experiment are planned for this phase. Phase II consists of the phase I configuration modified by the addition of a large central core zone with a simulated fuel mixture having a higher Pu-240 fraction. Experiments will characterize the effects of the different plutonium isotopic makeup, and several basic physics measurements will be repeated. The phase III assembly is proposed as a study of alternate fuel cycle materials. This would consist of a central core zone fueled with plutonium and thorium coupled with a corresponding axial blanket zone utilizing a ThO_2 simulation. Small-core zone studies with a simulated U-233/thorium fuel are also possible in phase III. The final configuration, phase IV, contains a core of three enrichment zones to simulate the 300-MW(e) GCFR (according to Ref. 7-1). The experimental program includes evaluation of (1) power

profiles through the zones; (2) U-238 Doppler mapping; (3) full-core breeding ratios; (4) gamma heating rates. Studies with prototypical control rod designs and insertion patterns will be accomplished during phase IV. Work on a ThO_2 radial blanket sector and other blanket experiments will also be done.

Reference 7-2 gives a detailed account of pre-EMC planning, including basic program requirements, details of the reference design for the demonstration plant, proposed loading arrangements for the assemblies, a program of measurements, and a tentative schedule. Currently, the projected starting date for ZPR loading of the GCFR pre-EMC, phase I assembly is October 1, 1979.

7.2. DISTORTED CORE ANALYSIS

A program of physics calculations was initiated during this quarter as part of the safety analysis for the 300-MW(e) GCFR during a protected loss of flow incident. The analysis concerns the potential for recriticality in the event of melting and fallaway of core cladding with subsequent progressive slumping of assembly ducts and fuel pellets. Several distorted core configurations have been modeled for physics calculations to evaluate the effect of reactivity changes upon motion of the core steel components and fuel compaction. For this particular study (protected loss of flow), all control and safety rods are assumed to be fully inserted into the core, giving a hot, subcritical ($k \sim 0.90$) reference configuration. A five-stage procedure was formulated for the distorted core analysis. These stages are described in Sections 7.2.1 through 7.2.5.

7.2.1. Description of Reference Configuration

During the first stage, design data were completed to establish geometric specifications for calculational models. Data for the 289.6-kPa

pressure drop core design (from Ref. 7-1) were used and core zone fuel enrichments were selected on the basis of recent fuel cycle studies using the FEVER code (Ref. 7-3), with a core average value of 16.7% fissile plutonium in the mixed oxide blend. In addition, on the basis of recent rod design calculations, a total of 19 control and safety rods were assumed. All rods contained B_4C which was 77% enriched with B-10 to yield a total combined worth of about $40.

7.2.2. Generation of Cross Sections

Specifications were drawn up for several runs of the GGC-5 spectrum code (Ref. 7-4) to derive multigroup cross section sets which were appropriately averaged over the spectra in the different media for various standard and distorted core configuration regions. This stage of the analytical procedure has been completed and includes the following GGC-5 cases:

1. Standard core element at 300 K (cold).

2. Standard core element at hot operating conditions (fuel at 1300 K average).

3. Axial blanket at operating temperature.

4. A protected loss of flow case for the average core (fully rodded with fuel cladding and duct walls melted away and temperature of 2000 K).

5. The lower core region (corresponding to item 4) with coolant channels flooded with molten duct metal.

6. An axial blanket case with coolant channels blocked with refrozen cladding metal (from the core).

7. A slumped core case with fuel compacted to a packing fraction of 50% in molten steel.

8. A slumped core case with fuel compaction of 86% in molten steel.

7.2.3. Derivation of Streaming Correction Factors

For each of the fuel rod geometries defined for various normal and distorted regions, evaluations of corrections to diffusion theory problems are needed to account for neutron streaming down coolant channels. For cases with intact fuel rod bundles, the streaming effects are provided by the use of bidirectional modifiers to diffusion coefficients. A Benoist theory code, PINDF3 (Ref. 7-5), was utilized to calculate these modifiers. For compacted fuel situations in which random arrangements of fuel pellets and chunks in molten steel are assumed, a homogenized, isotropic diffusion coefficient will be used. This stage of the procedures is nearly complete.

7.2.4. Diffusion Theory Calculations

Two-dimensional diffusion theory calculations will be utilized to evaluate reactivity changes during hypothesized accident scenarios. The 2DB diffusion code (Ref. 7-6) will be used with 10-group cross sections and RZ geometry. Modeling of the reference configuration 2DB case was initiated during this quarter.

7.2.5. Transport Theory Calculations and Method Studies

Additional calculations will be needed using transport theory to reduce uncertainties for reactivity evaluations for configurations involving large voided regions, as in the upper core when fuel has slumped away and compacted on top of the lower axial blanket. Comparative 2DB and TWOTRAN (Ref. 7-7) cases will probably be run using 4-group cross sections to study the problem. Various schemes for approximating leakage through voids in the diffusion cases might also be investigated.

REFERENCES

7-1. "Baseline Data Book," General Atomic Company, April 1978, unpublished data.

7-2. Hess, A., "Pre-Engineering Mock-Up Critical Experiment Design Requirements Status," General Atomic Company, August 31, 1978, unpublished data.

7-3. Todt, F. W., and L. J. Todt, "FEVER/M1, A One-Dimensional Depletion Program for Reactor Fuel Cycle Analysis," Gulf General Atomic Report GA-9780, October 1969.

7-4. Mathews, D. R., et al., "GGC-5, A Computer Program for Calculating Neutron Spectra and Group Constants," Gulf General Atomic Report GA-8871, September 27, 1971.

7-5. Mathews, D. R., "Directional Diffusion Coefficients in Two-Region Cylindrical Geometry Cells - the Code PINDF3," General Atomic Company, April 12, 1978, unpublished data.

7-6. Little, W. W., Jr., and R. W. Hardie, "2DB, A Two-Dimensional Diffusion-Burnup Code for Fast Reactor Analysis," USAEC Report BNWL-640, Battelle Northwest Laboratory, January 1968.

7-7. Lathrop, K. D., and F. W. Brinkley, "Theory and Use of the General-Geometry TWOTRAN Program," USAEC Report LA-4432, Los Alamos Scientific Laboratory, May 1970.

8. SHIELDING REQUIREMENTS (189a No. 00584)

The purposes of the shielding task are to verify the adequacy of the methods and data for the nuclear design of GCFR shields, to evaluate the effectiveness of various shield configurations, and to provide an interface for mechanical and nuclear shield design activities. This task also coordinates and provides liaison with the analytical and experimental shielding program at ORNL.

During the last quarter, generic studies for radial shielding material arrangement and thickness were completed, and a full reactor RZ model of a candidate revised shield was determined for subsequent analyses at ORNL. Preliminary results from the lower plenum streaming study were obtained, and a preliminary study of heating rates in a proposed depleted uranium core catcher was completed.

During this quarter, the one-dimensional analysis of the down-flow demonstration plant shielding system (conceptual shielding configuration 1) was completed, and a material damage response function library for use in GA and ORNL shielding analyses was evaluated. The applicability of EBR-II as an appropriate test vehicle for simulating radiation damage accumulation in GCFR lower plenum components was evaluated. A review of the GCFR program schedule and the fast breeder reactor structural materials program resulted in a request for EBR-II irradiation experiments on candidate alloys and weldments at high temperatures (550° to 650°C).

8.1. ONE-DIMENSIONAL ANALYSIS OF RADIAL SHIELDING FOR CONCEPTUAL SHIELDING CONFIGURATION 1

A one-dimensional discrete ordinates calculation was performed for conceptual shielding configuration 1 (Section 8.2 of Ref. 8-1) in radial

geometry at the core midplane level as indicated by cut A-A' in Fig. 8-1. The conceptual shielding configuration 1 is a full RZ model of a down-flow demonstration plant shielding system and reactor internal components and has been transmitted to ORNL, where a two-dimensional (RZ) discrete ordinates analysis will be performed. Analysis of conceptual shielding configuration 1 will provide guidance for preanalysis and planning of the GCFR radial shield experiment (see Section 8.3).

The calculation was performed with the DTFX code (Ref. 8-2) using S_8 quadrature (Ref. 8-3) and 36 energy groups (26 neutron and 10 gamma). The core and blanket distributed fission source was obtained from a one-dimensional eigenvalue calculation using core midplane nuclide densities corresponding to reference end of equilibrium cycle (EOEC) core model A (Section 8.2 of Ref. 8-4 and Section 8.4 of Ref. 8-5) with the addition of a beginning of life (BOL) third blanket row. Response functions used to evaluate material damage are described in Section 8.2, and the radiation exposure criteria applied in the analysis are described in Section 8.1.2 of Ref. 8-1.

The radiation exposure criteria applied to the shielding structures were

1. An allowable 1-appm* helium gas concentration in structural steel.
2. $\leq 10^{21}$ total fluence exposure to the outer radial shield.
3. Assurance of no graphite swelling.

The exposure criteria applied to the primary coolant system boundary (PCSB) were

1. PCRV liner nil ductility temperature shift (NDTS) $\leq 47°C$.
2. PCRV tendon lubricant gamma ray dose $\leq 10^9$ rad.

*Absolute parts per million.

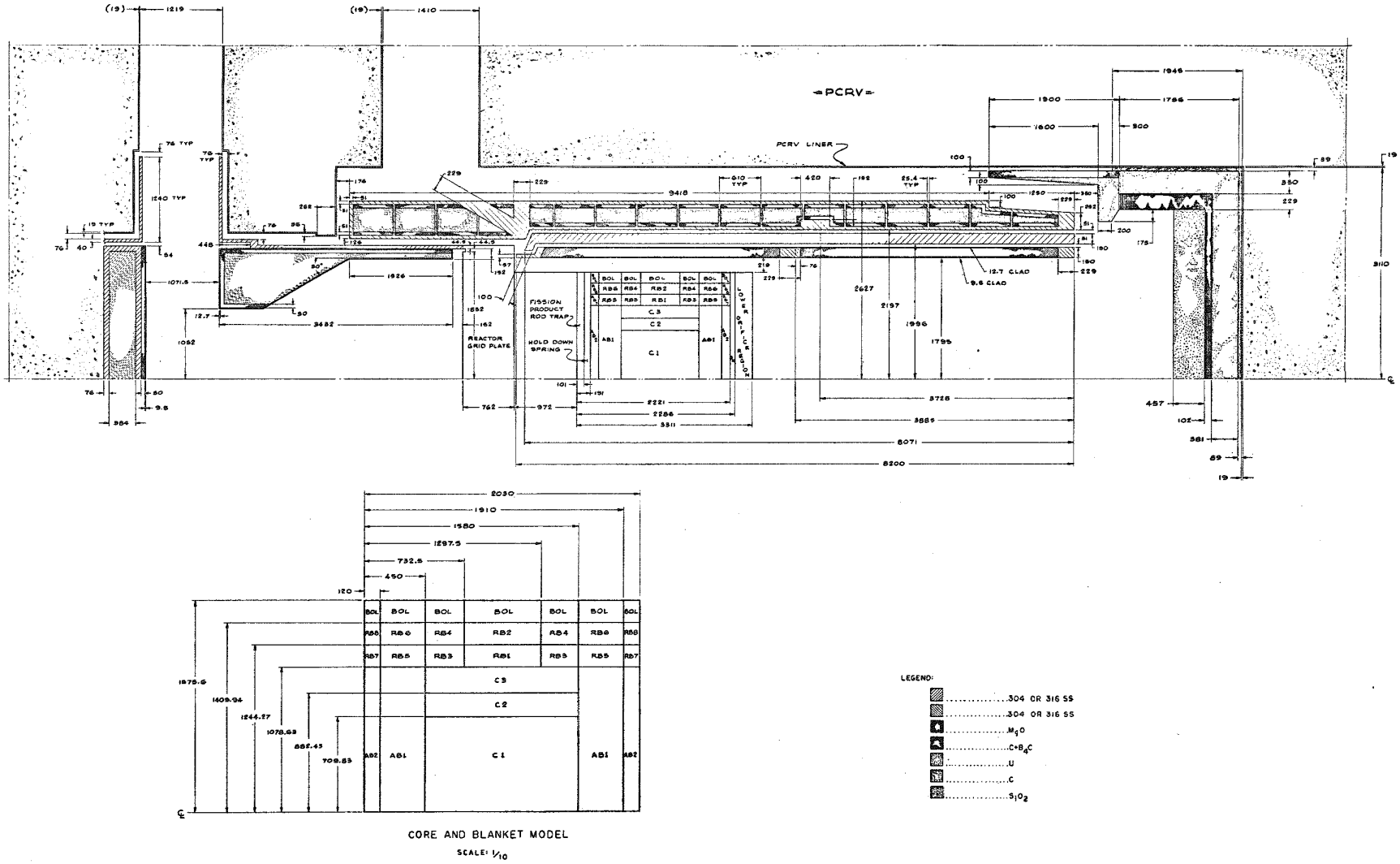

Fig. 8-1. Model of down-flow demonstration plant shielding system and reactor internal components, conceptual shielding configuration 1

Margins* of 0.5, 1.0, and 4.0 were considered necessary to account for uncertainties in radiation exposure to the inner radial shield assemblies, outer radial shield, and PCSB, respectively (see Section 8.1.3 of Ref. 8-1). Table 8-1 gives the exposure margins for the inner radial shields, outer radial shield, and the PCSB for conceptual shielding configuration 1. Figure 8-2 is a plot of the nuclear heating profile through the shielding and PCRV. The analysis indicates that all exposure criteria for shield structures and the PCSB are met by margins exceeding the desired margins except for the 10^{21}-n/cm^2 total fluence limit for the permanent outer radial shield. The 30 effective power year (EPY) exposure to the outer shield was calculated to be 1.03×10^{21} n/cm^2 (margin = -0.03). However, it is recommended that no measures be taken (e.g., addition of another row of inner radial shielding) to lower the calculated outer shield total fluence exposure below the desired amount of 5×10^{20} because

1. Calculations based on forthcoming core and blanket designs incorporating radial blanket management schemes with inward or modified inward shuffling of blanket assemblies will probably result in a lower radial blanket leakage source than obtained in the currently assumed core and blanket model.

2. It could be recommended that the outer radial shield be designed with the option that the components be replaceable (Ref. 8-7), although not as readily replaceable as the inner radial shield assemblies.

3. The 10^{21}-n/cm^2 fluence limit is considered highly conservative, and it is anticipated that the limit will be increased when data on irradiation effects become available (see Section 8.4).

*Margin = (exposure limit/calculated exposure) - 1.

TABLE 8-1
EXPOSURE MARGINS[a] FOR CONCEPTUAL SHIELDING
CONFIGURATION 1 (CORE MIDPLANE LEVEL)

Component	Exposure Time (EPY)	Exposure Criterion	Margin
Inner radial shield row 1	3	1-appm helium concentration in 316 stainless steel	6.17
		1.4×10^{22} n/cm^2 EFFGD[b] in H-451 graphite at 800°C	16.9
Inner radial shield row 2	6	1-appm helium concentration in 316 stainless steel	2.45
Outer radial shield	30	10^{21}-n/cm^2 total fluence	-0.03
		1-appm helium concentration in 316 stainless steel	9.10
		2.5×10^{22} n/cm^2 EFFGD[b] in H-451 graphite at 600°C	166
PCSB	30	PCRV liner 47°C NDTS	11.0
		10^9-rad tendon lubricant dose	16.6

[a] Margin = Limit/exposure - 1.

[b] EFFGD = Equivalent fission fluence for graphite damage (Section 8.3 of Ref. 8-6).

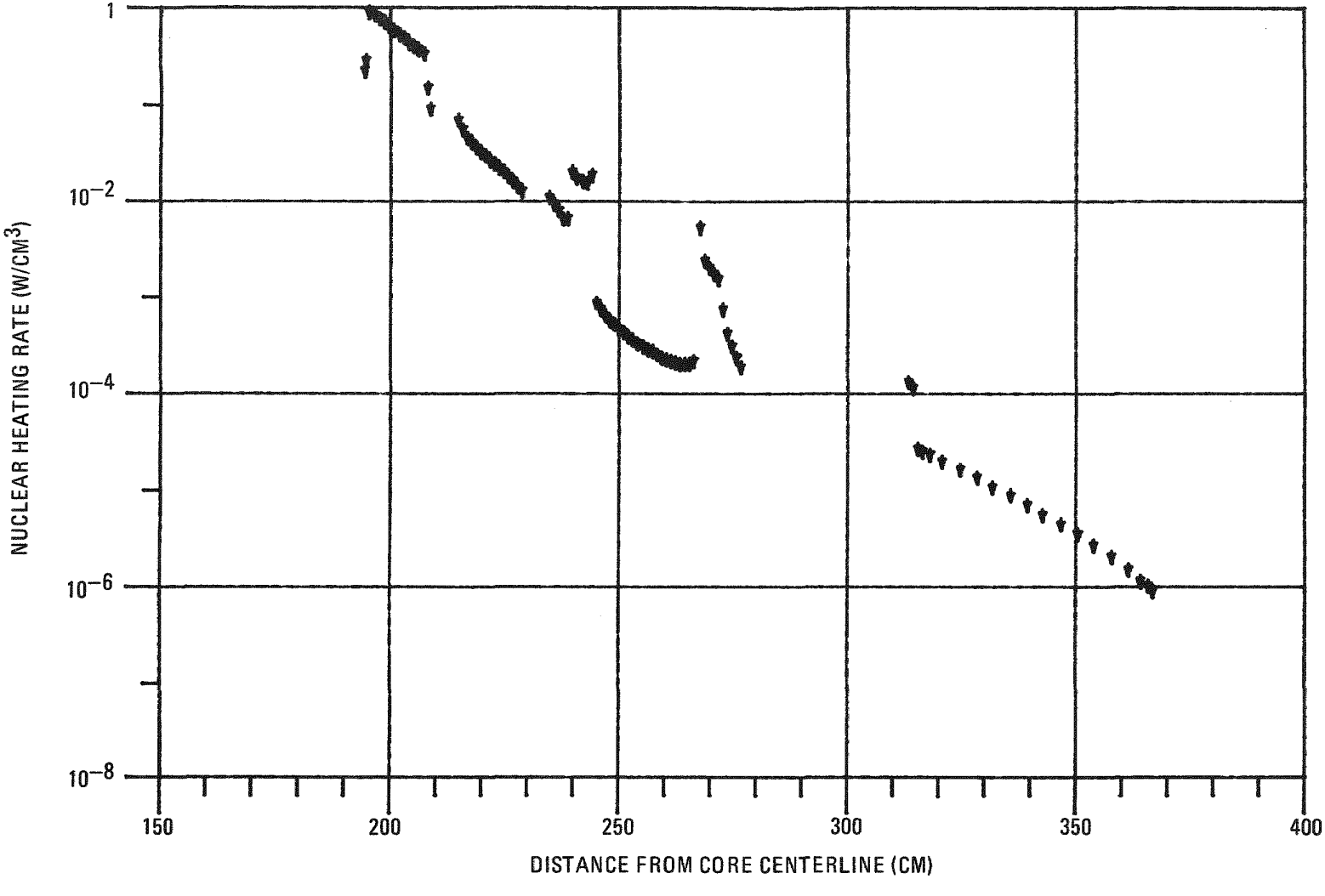

Fig. 8-2. Nuclear heating profile through the radial shielding, PCRV liner, and PCRV for conceptual shielding configuration 1

Reference 8-8 provides detailed data for neutron and gamma flux and spectrum, material damage accumulation (including helium production in stainless steel), and nuclear heating for conceptual shielding configuration 1.

8.2. MATERIAL DAMAGE RESPONSE FUNCTIONS FOR GA AND ORNL SHIELDING ANALYSIS

The following response functions were collapsed to multigroup energy structures corresponding to both the 26-neutron, 10-gamma library used at GA and the 51-neutron, 25-gamma cross section library used at ORNL.

1. Graphite atom displacement cross section, barns (Refs. 8-9, 8-10).

2. Stainless steel 316 atom displacement cross section, barns (Ref. 8-11).

3. Iron (PCRV liner) atom displacement cross section, barns (Ref. 8-11).

4. Upper-bound damage function to compute the fluence required to attain a residual 5% ductility based on uniform elongation in type 316 stainless steel irradiated at 593°C, $(n/cm^2 \times 10^{22})^{-1}$ (Ref. 8-12).

5. Nominal damage function to compute the fluence limit to attain a 75°C NDTS in A-212B medium carbon steel irradiated at less than 140°C, $(n/cm^2 \times 10^{22})^{-1}$ (Ref. 8-12).

6. Ni-58 (n,γ) Ni-59 cross section (unboronated region), barns (Ref. 8-13).

7. Ni-59 (n,γ) Ni-60 cross section (unboronated region), barns (Ref. 8-13).

8. Ni-59 (n,α) Fe-56 cross section (unboronated region), barns (Ref. 8-13).

9. Stainless steel 316 composite threshold (n,α) cross section (unboronated region), barns (Ref. 8-13).

10. B-10 (n,α) Li-7 cross section (unboronated region), barns (Ref. 8-13).

11. Ni-58 (n,γ) Ni-59 cross section (boronated region), barns (Ref. 8-13).

12. Ni-59 (n,γ) Ni-60 cross section (boronated region), barns (Ref. 8-13).

13. Ni-59 (n,α) Fe-56 cross section (boronated region), barns (Ref. 8-13).

14. Stainless steel 316 composite threshold (n,α) cross section (boronated region), barns (Ref. 8-13).

15. B-10 (n,α) Li-7 cross section (boronated region), barns (Ref. 8-13).

The fine-group response functions were collapsed to the (26, 10) and (51, 25) broad-group structures with fine-group fluxes from appropriate GGC-5 code (Ref. 8-14) single-region calculations. Reference 8-15 gives tables and plots of the broad-group response functions.

8.3. RADIAL SHIELDING EXPERIMENT REQUIREMENTS

The objectives and proposed test requirements, measurements, and configurations for the radial shielding experiment were documented

(Ref. 8-16) and transmitted to ORNL. This report is considered a working document which will be revised as radial shield design and experiment preanalysis progresses and constraints of fabrication and measurement costs are identified. Reference 8-16 also specifies that quality assurance activities will be in compliance with the applicable requirements of 10CFR50, Appendix B, or ANSI, 45.2.

The primary objective of the experiment is to validate analytical methods and data for calculating neutron and photon transport and heating through successive thicknesses of blanket, radial shield materials, and the PCRV. Uranium and thorium blankets will be measured.

8.4. DATA REQUIREMENTS FOR STRUCTURAL MATERIAL IRRADIATION EFFECTS

A previous evaluation of GCFR out-of-core structural component irradiation data requirements (Ref. 8-17) indicated that the highest priority need was high-temperature (550° to 650°C) data on candidate materials and weldments for lower plenum shielding and related components. According to the GCFR program schedule, this information will be required by October 1981 to fix the GCFR inner and outer radial shield envelope. The required data could be obtained in fast test reactor (FTR) irradiations, but the results would not be available until late 1981 and therefore could not be utilized in the shielding envelope decision process. Because of the impact of the spatial shield envelope on GCFR design (and the possible requirement for boronating the shield) and the need for irradiation data to make this decision, it was requested that HEDL develop a proposed scope for a pertinent EBR II irradiation experiment, including schedule and budget information.

Rates of production of helium gas and displacement per atom in stainless steel 316 in the EBR II core and in the GCFR radial shielding (at core midplane level) of GCFR conceptual shielding configuration 1

were compared to determine the possibility of using EBR-II as the irradiation test device for simulating the radiation damage accumulation expected in the GCFR demonstration lower plenum components. The ratio of helium gas concentration to accumulated displacement per atom was found to vary from 0.36 to 2.4 appm/dpa in the GCFR radial shielding compared with 0.56 appm/dpa in the EBR II core. However, rates for both helium gas generation and radiation damage accumulation per unit fluence in the EBR II core are much greater than those in the GCFR radial shielding, thus ensuring that data on irradiation effects from the EBR II core which are based on total fluence will provide a conservative prediction of material performance in the GCFR lower plenum components.

REFERENCES

8-1. "Gas-Cooled Fast Breeder Reactor Quarterly Progress Report for the Period May 1, 1978 through July 31, 1978," DOE Report GA-A15054, General Atomic Company, August 1978.

8-2. Archibald, R., K. D. Lathrop, and D. Mathews, "1DFX - A Revised Version of the 1DF (DTF-IV) S_N Transport Theory Code," Gulf General Atomic Report Gulf-GA-B10820, September 27, 1971.

8-3. Perkins, R. G., and J. Hom, "Sensitivity of Boronated Radial Shielding Response Values to Group Structure and Quadrature," General Atomic Company, unpublished data.

8-4. "Gas-Cooled Fast Breeder Reactor Quarterly Progress Report for the Period February 1, 1978 through April 30, 1978," DOE Report GA-A14928, General Atomic Company, May 1978.

8-5. "Gas-Cooled Fast Breeder Reactor Quarterly Progress Report for the Period August 1, 1977 through October 31, 1977," DOE Report GA-A14613, General Atomic Company, November 1977.

8-6. "Gas-Cooled Fast Breeder Reactor Quarterly Progress Report for the Period February 1, 1977 through April 30, 1977," DOE Report GA-A14358, General Atomic Company, May 1977.

8-7. Rodkin, S., "Replacement Requirements for GCFR Internal Components," General Atomic Company, unpublished data.

8-8. Perkins, R. G., "One-Dimensional Analysis of Radial Shielding for Conceptual Shielding Configuration 1," General Atomic Company, unpublished data.

8-9. Thompson, M., and S. Wright, "A New Damage Function for Predicting the Effect of Reactor Irradiation on Graphite in Different Neutron Spectra," J. Nucl. Mater. 16, 146-154 (1965).

8-10. Genthon, J. P., "Les Travaux Du Sous-Groupe Dommages D'Irradiation Du Groupe De Travail D'Euratom/Sur La Dosimetrie Du Reacteur De Recherche," Nucl. Eng. Design 33, 7-9 (1975).

8-11. Doran, D., and N. Graves, "Displacement Cross Sections for Fe, Cr, Ni, 18/10 SS, Mo, V, Nb, and Ta," USAEC Report HEDL-TME 73-59, Hanford Engineering Development Laboratory, July 1973.

8-12. Nuclear Systems Materials Handbook, v. I, II, Hanford Engineering Development Laboratory (TID-26666).

8-13. Simons, R. L., "Helium Production in FBR Out-of-Core Structural Components," Paper Presented at the Ninth ASTM International Symposium on Effects of Radiation on Structural Materials, Richland, Washington, July 11-14, 1978.

8-14. Mathews, D. R., et al., "GGC-5, "A Computer Program for Calculating Neutron Spectra and Group Constants," Gulf General Atomic Report GA-8871, September 27, 1971.

8-15. Perkins, R. G., and J. Hom, "Material Damage Response Functions for GA and ORNL Shielding Analysis," General Atomic Company, unpublished data.

8-16. Perkins, R. G., D. T. Ingersoll, and C. J. Hamilton, "Radial Shielding Experiment Requirements," General Atomic Company, unpublished data.

8-17. Rosenwasser, S. N., and R. G. Perkins, "Assessment of Materials Irradiation Effects Data Requirements for GCFR Out of Core Structural Components," General Atomic Company, unpublished data.

9. SYSTEMS ENGINEERING
(189a No. 00585)

9.1. SYSTEMS DESIGN

9.1.1. Up-flow/Down-flow Core Studies

System design work for the up-flow/down-flow core studies has concentrated on three areas: (1) overall technical coordination and liaison, (2) analysis of the system design aspects of the up-flow core, and (3) evaluation of the impact of ongoing down-flow tasks on the up-flow core plant design.

9.1.1.1. Up-flow Natural Circulation RHR. Natural circulation cooling, which is practical only with the up-flow core, has the potential to increase the reliability and diversity of residual heat removal (RHR). This has been a major incentive for performing up-flow core studies. Work has been done to determine the impact of different modes of natural circulation on the overall plant and to estimate RHR reliability. Preliminary results indicate that

1. Natural circulation in the primary helium only improves the reliability of helium circulation and thereby short-term RHR. However, in a short period of time, heat removal via an external water loop is required. If the water loop requires operation of active components such as pumps, this equipment is sufficiently unreliable, so that overall plant RHR reliability is not substantially improved. Natural circulation throughout the plant, including BOP equipment, is needed to improve overall plant RHR reliability.

2. Providing natural circulation capability in the normal BOP water/steam system (steam piping, condenser, feedwater system, circulating water system, etc.) is considered impractical. Natural circulation on the cooling water side is best done with a small circuit designed for that purpose. This may be the existing core auxiliary cooling system (CACS) circuit or a new circuit added parallel to the main steam/feedwater system.

3. Consideration of natural circulation cooling as a "last ditch" RHR mode (i.e., after all forced circulation has failed) improves reliability by eliminating the need for (and hence unreliability of) controls and instrumentation. That is, once the valves are open and natural circulation is functioning with all forced circulation modes inoperative, there is nothing the operator needs to do or can do to improve cooling further. In addition, higher temperatures are allowed in a "last ditch" mode; this greatly increases natural circulation rates. (The plant need not be operational after this extreme event, and limited damage is allowed.)

4. Use of the CACS rather than the main loops is preferred if "last ditch" cooling is adopted to avoid the number of switching operations required. Thus, the current sequence of forced circulation actions ends in the CACS; staying there for natural circulation rather than switching back to the main loops is preferred.

9.1.1.2. Impact of Licensing Criteria Changes. Licensing criteria have been changed to require a second safety class long-term RHR system for pressurized cooling (i.e. one in addition to the CACS). This second system has a major impact on the natural circulation RHR potential. It is expected that when a second RHR system independent of the CACS is added, reliability targets will easily be met for down-flow cores. The criterion requiring a second safety class system reduces the incentive to improve RHR reliability by selecting an up-flow core with natural circulation potential. However, the diversity benefits of natural circulation

are undimished and still provide significant incentive.

9.1.1.3. Relief Valve Operation. Analyses of helium heat-up during natural circulation with an up-flow core indicate that the relief valves will not open. Therefore, the effectiveness of pressurized natural circulation cooling is not jeopardized by depressurization through the relief valves. Steam ingress accidents may open the relief valves, and depending on the reliability analysis results, additional measures which ensure that the relief valves close again, as designed, may be required.

9.1.2. Main Circulator Drive Study

The electric drive circulator assembly has a first critical speed at approximately 50% of full speed. Although the equipment design appears feasible based on bearing design work and dynamic analyses, consideration was given to avoiding operation near critical speed. Plant part-load operation was examined using the ground rule that circulator speed must remain at 60% or above. Efficiency losses at the extreme 25% plant load point were modest, i.e., 1.65 percentage points. However, reactor inlet temperature (also circulator outlet temperature) increased 110°C (198°F), and the boiling zone in the steam generator moved to the economizer section. Therefore, although this is a feasible operating procedure, it causes significant design problems.

9.1.3. Residual Heat Removal

The impact of changes of RHR criteria on the overall plant was examined. In particular, the requirement to provide a second safety class RHR system in addition to the CACS for long-term pressurized cooling has a large impact. Although the concept for this second system has yet to be formally selected, it is assumed that it utilizes a CACS-type water circuit and main loop steam generators and circulators. The controls, separation requirements, diversity requirements, and upgrading of main loop equipment will add complexity to the overall plant.

9.1.4. Primary Coolant System

Primary coolant volumes and helium inventory were calculated for the latest demonstration plant design. The amount of helium in the plant has significantly increased, which will have a cascading (positive) effect on containment pressure during DBDA, CACS design, and RHR.

9.1.5. Parametric Model for the Steam and Circulating Water Systems

Development of a parametric scaling model of the BOP systems and structures was initiated. This is part of a larger activity to develop methods for performing trade-off studies for variations in system parameters about a base case. The purpose of this model is to provide the mathematical relationships required to size BOP systems and structures according to their required duty when NSS power level and design parameters change. The model must also define the changes caused by varying the values of the independent design variables specific to the BOP, such as the amount of steam-to-steam reheat used.

The approach taken uses a base case - alternate case method. The sizing of the alternate case BOP systems and structures is established by scaling from the base or reference case data. This approach is much simpler than attempting to design every BOP component "from the ground up," yet it has the advantage of being founded on base case design and performance data developed using much more sophisticated design tools. The components which make up the various steam systems and the circulating water system are the first BOP systems to be modeled. The major systems and components defined by the model are listed below.

1. Main turbine
    a. Main steam piping and valves.
    b. Steam-to-steam reheaters.

2. Condensate and feedwater system.
    a. Condensate pump.
    b. Low-pressure feedwater heater train.
    c. Deaerator.
    d. Feedwater pump.
    e. High-pressure feedwater heater.
    f. Piping and valves.

3. Circulating water system.
    a. Condenser.
    b. Cooling tower.
    c. Pond.
    d. Circulating water pumps.
    e. Cooling loop for generator and its auxiliaries.
    f. Piping and valves.

4. Extraction steam system.

5. Turbine vent and drain system.

6. Auxiliary steam supply system.

The model is a "first generation" analysis tool, and simplifying assumptions are used where appropriate.

9.2. SYSTEMS INTEGRATION

The number of control/shutdown assemblies was changed from 27 to 19.

10. COMPONENT DEVELOPMENT (180a No. 00585)

10.1. REACTOR VESSEL

The scope of this subtask is to ensure that the design of the PCRV and related components which contribute to the integrity of the pressure boundary is satisfactory and to test critical component configurations to make certain that they attain the design objectives. This subtask will demonstrate by analyses and tests that the PCRV and its penetrations and closures meet the design criteria, and it will ensure that (1) the design of the thermal barrier satisfactorily protects the liner and PCRV from the effects of high temperatures, and (2) the flow restrictors for the large penetrations can be developed to limit the flow of helium from the primary coolant systems to acceptable levels in the event of structural failure of a penetration or closure component.

During the last quarter, seven PCRV arrangements (Figs. 10-1 through 10-7 of Ref. 10-1) were prepared showing the up-flow core configurations for the safety evaluation of RHR schemes. A requirement for the PCRVs used for RHR arrangements is that the core auxiliary heat exchanger must be located at a specified height above the reactor core to permit natural convection cooling of the core. The PCRV arrangements were reviewed, and two arrangements (Figs. 10-3 and 10-6 of Ref. 10-1) were chosen for use as the basis for preparing revised PCRV configurations with up-to-date reactor components. The revised PCRV configurations are shown in Figs. 10-1 and 10-2.

During this quarter, the two PCRV configurations shown in Figs. 10-1 and 10-2 were evaluated so that one could be selected for the preparation of a more detailed PCRV arrangement. The configuration in Fig. 10-1 was chosen for further development because the coolant ducting was less complex than that of the configuration in Fig. 10-2, which has a primary

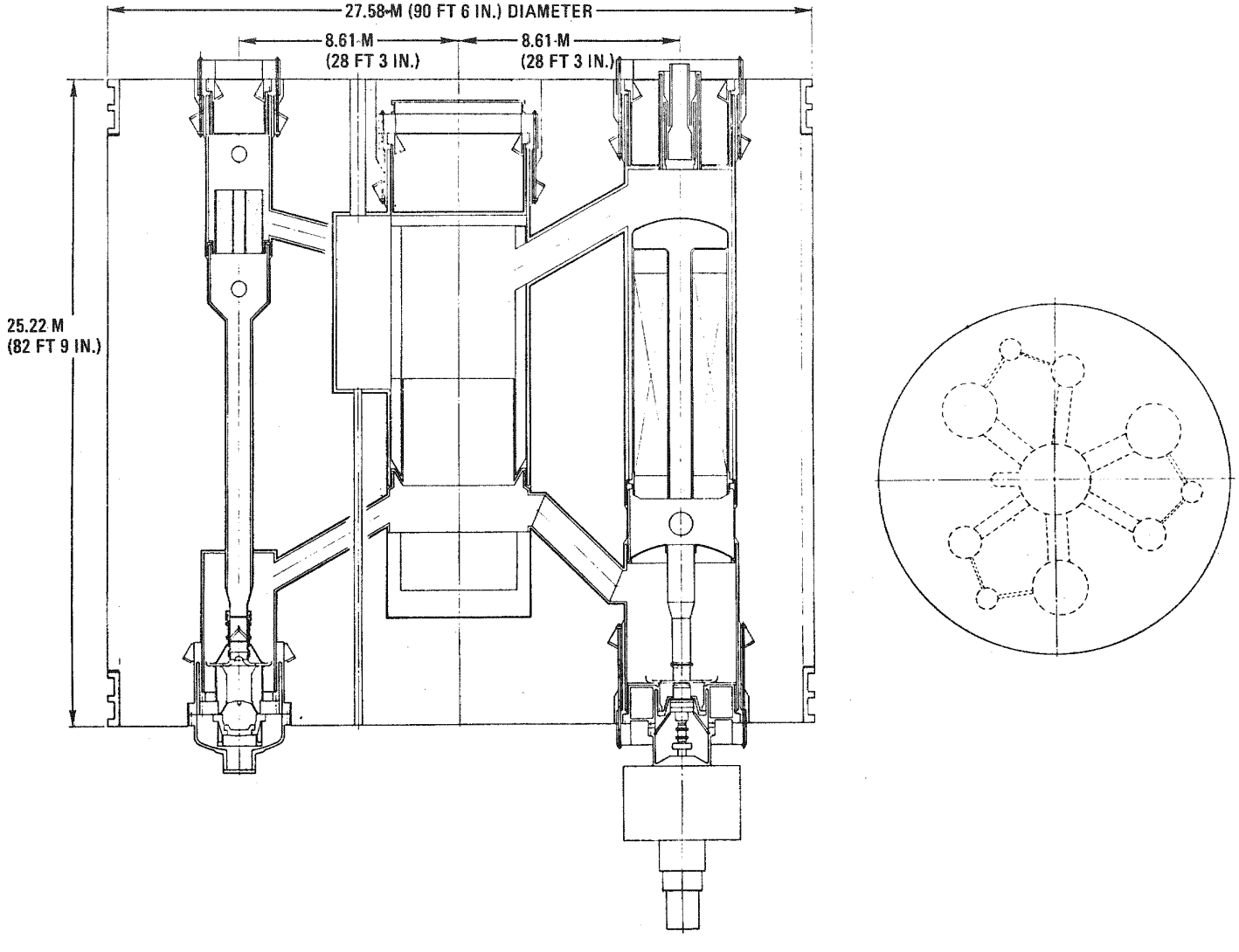

Fig. 10-1. 300-MW(e) GCFR PCRV configuration with up-flow core, concept No. 4A

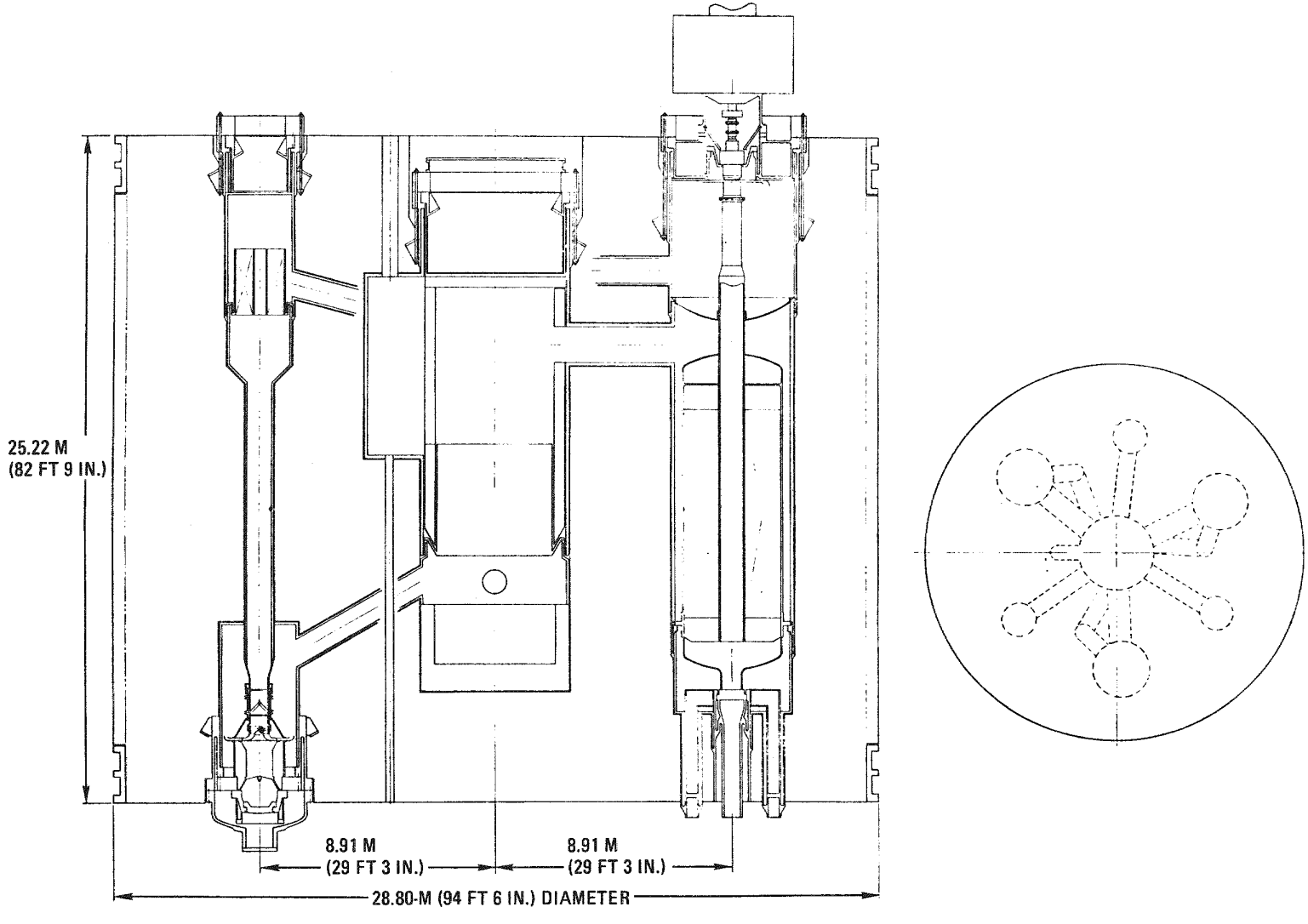

Fig. 10-2. 300-MW(e) GCFR PCRV configuration with up-flow core, concept No. 7A

coolant return duct with two 90-deg bends. The configuration in Fig. 10-2 is based on in-vessel fuel handling, i.e., manipulation through the fixed closure plug over the reactor cavity by a fuel transfer machine located within the reactor core cavity. A study was planned to determine the overall advantages and disadvantages of ex-vessel fuel handling in which a fuel transfer machine located outside the pressure vessel would manipulate the fuel assembly inside the reactor core cavity through a rotating plug. Figure 10-3, shows the PCRV configuration which would result from utilizing the ex-vessel fuel handling concept; this configuration has the rotating plug located directly above the reactor core. The two fuel handling concepts were evaluated to determine the scheme which would be used in advancing the design of PCRVs; the ex-vessel fuel handling concept was chosen and will be used in up-flow core studies.

The use of electric drives for the helium circulators requires high-horsepower motors which are large and heavy and thus have handling and mounting problems. This leads to the premise that horizontal mounting of the drives would be beneficial to the reactor design. Figure 10-4 shows a concept in which the large circulator drives are horizontally mounted at the base of the PCRV. This concept was examined, and it was determined that there may be advantages in mounting and servicing the motor. However, the disadvantages which result from preventing circumferential prestressing in this area of the PCRV and the penetration of the motors through the walls of the containment building were serious enough to cause the study to be discontinued. Figure 10-5 shows a PCRV arrangement which uses the rotating refueling plug for the ex-vessel fuel handling scheme and incorporates the latest design information and up-to-date configurations for the reactor internals and coolant loop components.

A considerable effort was expended on the PCRV closures for the up-flow/down-flow plant evaluation. Much of this effort was devoted to development of a suitable core cavity closure which would permit in-line, ex-vessel refueling. Early studies were associated with evaluating two different closure concepts, each of which involved a concrete plug which

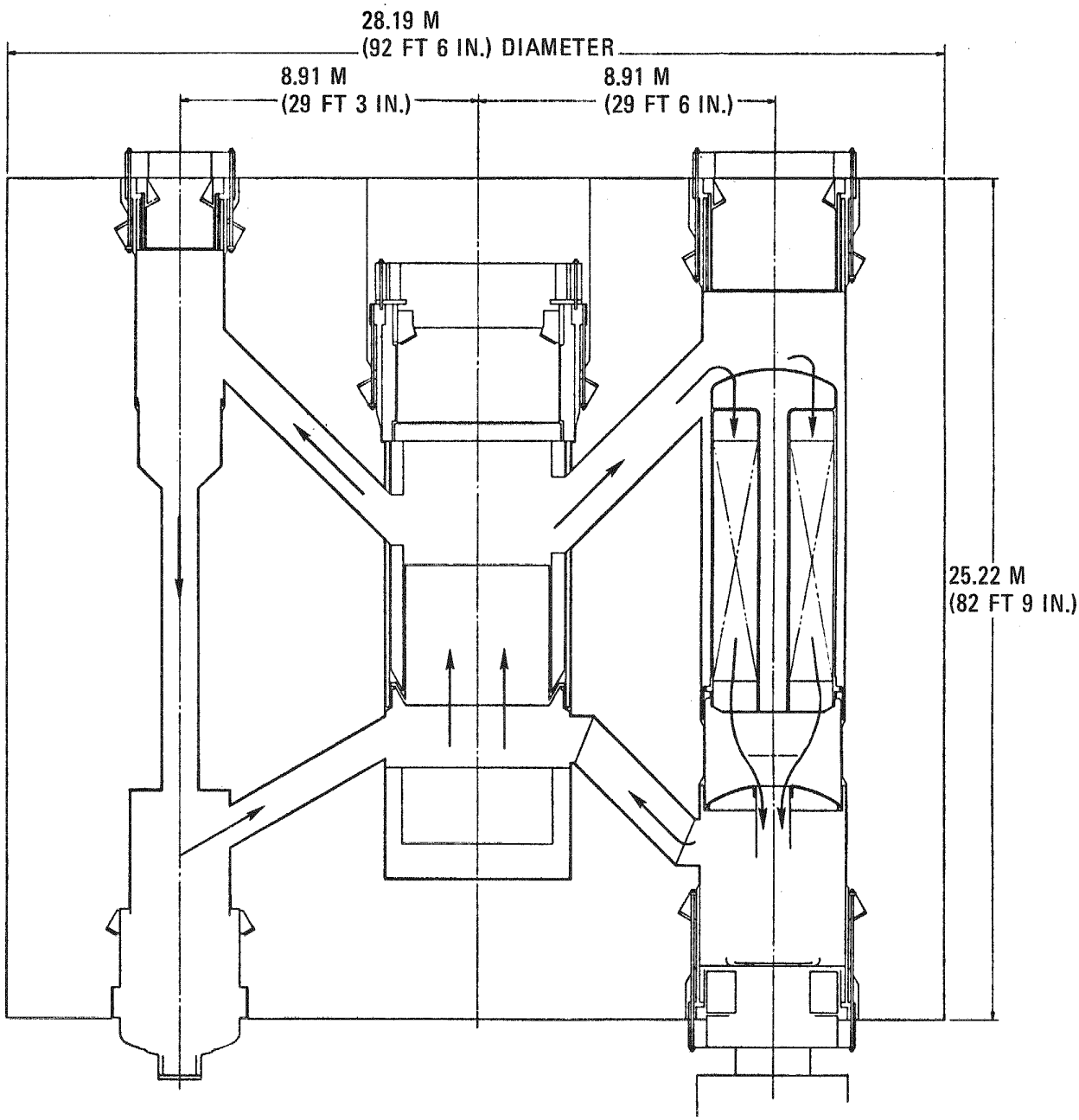

Fig. 10-3. 300-MW(e) GCFR PCRV up-flow core with rotating plug

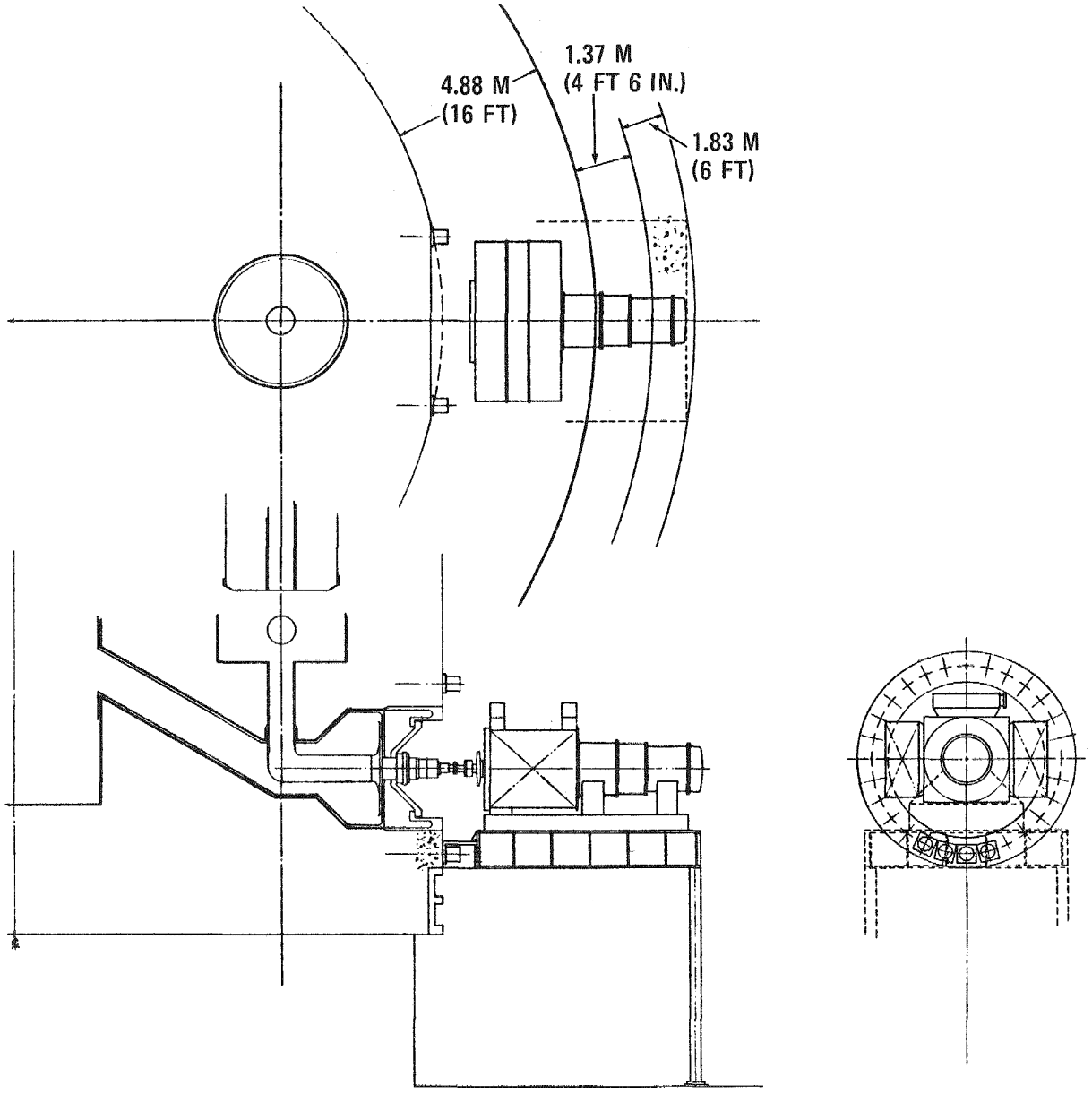

Fig. 10-4. 300-MW(e) GCFR PCRV with horizontally mounted helium circulator

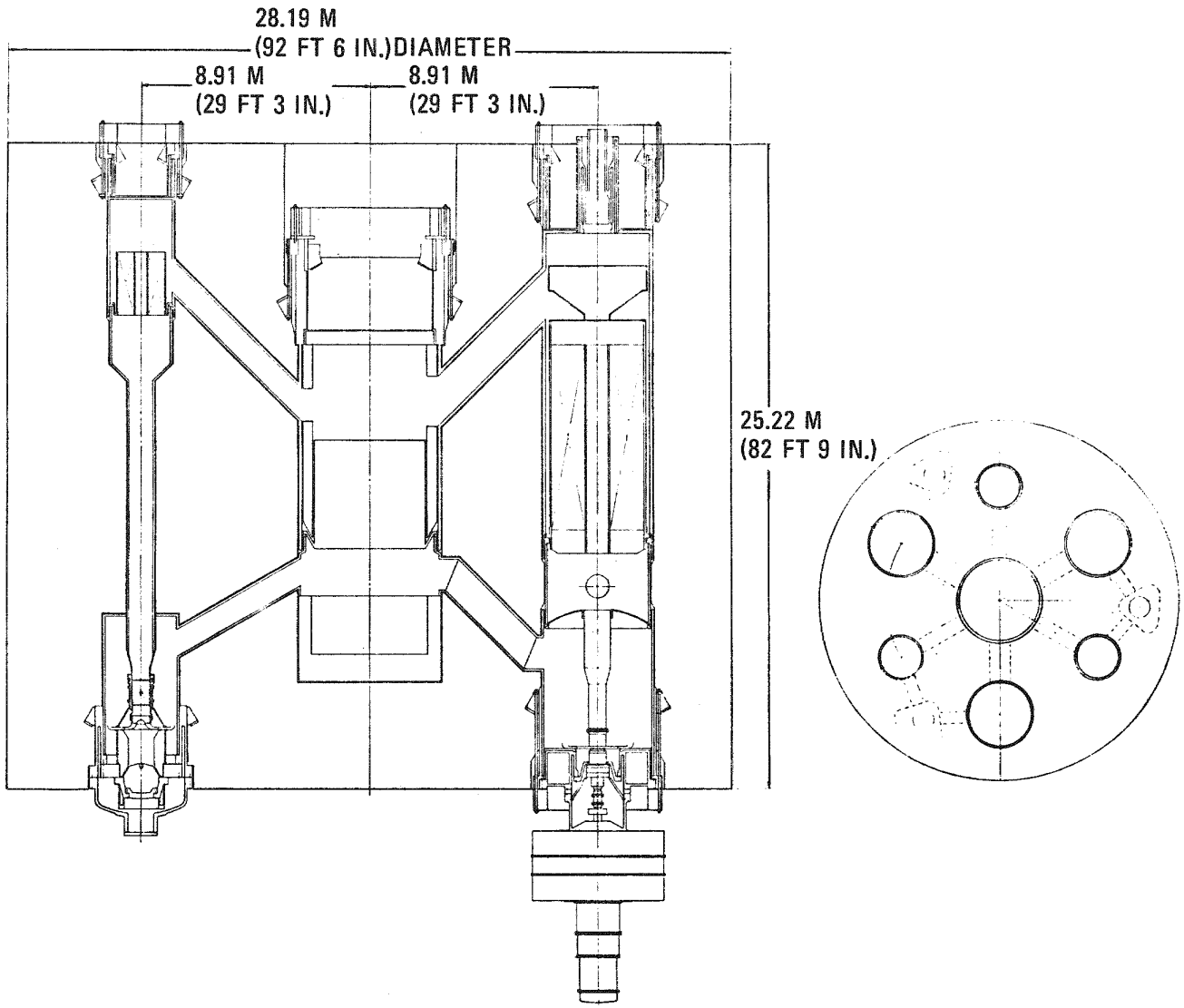

Fig. 10-5. 300-MW(e) GCFR PCRV arrangement with rotating refueling plug

could be moved during refueling through a system of drives and bearings to position a refueling penetration directly above any fuel or blanket assembly. These concepts were based in part on the rotating plug approach used in LMFBR plants. The first concept had a central plug which could be translated in one direction and then rotated. All drives and bearings were located outside the primary coolant pressure boundary. The second concept had an offset plug which could be rotated about two vertical axes, its own and that of the core centerline. Gears and bearings were within the primary coolant pressure boundary, and both arrangements utilized a welded steel hold-down ring beam bolted to a 15.24-cm (6-in.) thick penetration with O-rings and inflatable seals for leak-tightness.

To obtain the benefits of both concepts, a set of design objectives was formulated for the movable plug, and a new concept which satisfied these objectives was developed. The new concept consisted of an offset plug which rotated about its own axis, but which had all drive and bearing elements outside the pressure boundary. This shortened the load path and simplified the structure to a suitable arrangement for the demonstration plant. After a shielding analysis was performed, the design was further modified to minimize the gaps between the plug and penetration wall, to eliminate any direct streaming paths to seal areas, and to provide sufficient shielding material for access to areas above the closure. Scaling of the movable plug was considered, and it was found that a commercial size plant concrete plug would become massive. Therefore, an alternate approach might be required, and investigations were initiated on the use of a fixed, welded-in-place closure in conjunction with ex-vessel refueling.

Other work on the up-flow plant included design of steam generator and auxiliary cooling loop cavity closures. The upper closures for these components are considered to be fixed concrete plugs which are held down by prestressed concrete rings that are directly anchored to the PCRV with

prestressing tendons. A continuous steel liner on all surfaces of the closure in contact with primary coolant and a welded membrane seal between closures and their penetrations provide leak-tightness. These designs are similar to those designs developed previously for HTGR closures. The lower steam generator cavity closures are formed by the circulators and are bolted to a steel penetration, and concentric O-ring seals are used for leak-tightness. The lower auxiliary circulator closure is also formed by the circulator and is sized to permit installation of the radial flow diffuser from beneath the PCRV. An extension of the penetration and a separate cover are used to form a limited-leakage flow restrictor.

A preliminary comparison of the closures for the up-flow and down-flow plants was made, and the differences between the closures are shown in Table 10-1. The preliminary comparison indicates that from a closure viewpoint, the down-flow plant is preferable because it does not require a movable core cavity closure. The feasibility of the movable closure remains to be demonstrated because of uncertainties associated with its ability to be sealed and scaled.

As a part of the ORNL closure test program, a two-dimensional elastic analysis of the reactor core cavity closure was performed by ORNL. The effects of steel penetrations and the internal pressure in these penetrations were considered, and the results of the analysis indicate that for a 4.9-m (15-ft) diameter closure with 37 penetrations [355.6 mm (14 in.) schedule 60], a closure depth of 2286 mm (90 in.) meets working stress criteria. The results will be used as an aid in the design of the first test model of the reactor core cavity closure.

The design and R&D effort required to demonstrate the containment capability of the PCRV in the event of a core disruptive accident (CDA) with an energy release of 100 MW/s was reviewed, and the following required efforts were identified: (1) determination of PCRV loading as a consequence of a CDA; (2) dynamic analysis of the PCRV during a CDA;

TABLE 10-1
MAJOR GCFR CLOSURES

Location	Up-Flow Plant	Down-Flow Plant
Core cavity	Indexing concrete plug with control rod penetrations	Stationary concrete plug with control rod penetrations
Steam generator upper closure	Concrete plug with superheat penetration in plug	Steel plug with circulator penetration in plug
Steam generator lower penetration	Circulator penetration closure and flow restrictor	Feedwater and superheat penetration closures and flow restrictors
Auxiliary cooling loop upper closure	Concrete plug	Steel circulator closure and flow restrictor
Auxiliary cooling loop lower closure	Steel circulator closure and flow restrictor	None

(3) depending on the results of (1) and (2), dynamic testing of a PCRV under simulated CDA loading; (4) development of a pressure relief valve design for a CDA; and (5) preliminary study of the generation and impact of missiles and the effectiveness of thermal barriers, shielding, and other internal components for absorbing a CDA energy release. Potential design modifications for a large CDA energy release were suggested for the PCRV, closure, closure hold-down, closure seals, and pressure relief valve.

Conceptual design studies for a molten core retention system continued, with emphasis on the up-flow core configuration. Conceptual layouts have been developed for six basic ceramic crucible concept variations which are crucibles constructed primarily from high-purity magnesia brick selected for its extremely high melting point, elevated temperature strength, shielding effectiveness, and resistance to molten metal attack. The crucible construction is similar to that used in high-temperature furnace linings in the metal, cement, and other industries. The basic characteristics of the preferred ceramic crucible configuration are as follows:

1. The crucible is constructed of a combination of two layers of low-porosity magnesia bricks over a layer of standard 16.5%-porosity magnesia brick. High-density bricks are used in the upper layers to resist elevated temperature thermochemical attack and thermal shock. The lower, more cost-effective layer functions as a refractory insulator and shield. Some initial loss of material in the upper layer is expected, but should not cause loss of function since a solid crust of fuel is expected to form at the crucible-fuel interface.

2. Bricks are bonded together with thin magnesia mortar joints. These bonded bricks will enable the structure to remain tight at elevated temperatures in the event of cracking.

3. Expansion gaps adjacent to the liner are filled with Kaowool (or similar material), which offers resistance to helium permeation flow during normal operation and becomes compressed during PAFC to allow greater heat removal capability.

4. A layer of steel plates is located on the crucible floor to reduce mechanical damage due to falling debris and to aid in reducing thermal shock to the magnesia bricks.

5. The crucible thickness is 609.6 mm (24 in.) at its lower sidewall, where it can interface with molten fuel, and tapers to 457.2 mm (18 in.) thick along the remainder of the debris height.

6. 50.8 mm (2 in.) of encapsulated boronated graphite is included in the 457.2-mm (18-in.) sidewall to meet shielding requirements.

10.2. CONTROL AND LOCKING MECHANISMS

The initial conceptual design phase of the control rod drive system for the up-flow core study was completed during this quarter. The effects of two refueling schemes on the control rod drive and instrument tree installation geometry were evaluated. These two schemes are (1) center offset, dual-rotating top-head cavity closure plugs with fuel axially transferred through specific control rod drive penetrations and (2) single, fixed, top-head cavity closure plug with in-vessel transfer of fuel exiting downward alongside the core.

The center offset dual-rotating closure plugs allow the most favorable control rod drive and instrument tree installation geometry and minimize the complexity of the core-refueling operation interface. Only a few control rod drives must be removed from their penetrations to allow refueling access to the entire core. Since the core assemblies

are withdrawn and inserted directly in line with the central axis of a specific penetration, the upper cavity plenum height is greatly reduced and thereby allows for a shorter and more compact control rod drive configuration.

An alignment and stabilizing structure for the bottom ends of the control rod drives and instrument trees is also readily accommodated. An open grid-type structure which spans the top of the core and is laterally registered in the circumferential core restraint barrel is utilized. The alignment structure is also tied to the inner rotating plug. By slightly raising the guide structure, making it free of its connection to the core restraint barrel, it is allowed to move in conjunction with the displacement of the inner plug during refueling. Clear refueling access through a control rod drive penetration and control rod drive register opening in the alignment structure is thereby maintained.

A much taller plenum height above the core is required for the fixed, single, top-head closure plug concept. The added plenum height is necessary to allow complete withdrawal and lateral transfer of a fuel assembly above the core, since direct axial access through control rod drive penetrations is not possible with a fixed top-head closure. The main effect on the control rod drives is added length to the driveline and guide shroud members. The in-vessel refueling scheme requires that the plenum above the core be completely unobstructed. This means that all control rod drives and instrument trees have to be raised clear of this region or completely removed and stored elsewhere. The guide and stabilizing grid structure employed in the rotating plug concept also has to be raised the full upper plenum height to provide clearance for the refueling operation.

There are essentially no special requirements imposed on the control rod drive mechanisms by the up-flow core concept compared with the reference down-flow core concept. The control rod regulating stroke, direction, speed, and trip functions are identical for the up-flow and

down-flow cores. The primary differences are in the temperature operating environment of the control rod driveline member and the support and guide structure arrangement.

The linear actuator mechanism and electrical power and control components are arranged and contained in a configuration which is identical to that for the down-flow core control rod drive concept. This portion of the drive is more sensitive to high temperature and is located in penetrations embedded in the cooled concrete depth of the PCRV top-head plug. The portion of the control rod drive arrangement that will be exposed to the higher-temperature [∿538° versus ∿316°C (∿1000° versus ∿600°F)] environment of the up-flow core is the driveline member connected to the control rod, the support, and guide structures. The driveline consists of coaxially arranged tubular members operating in a push-pull manner to actuate a pawl-type mechanism for coupling to the control rod at the lower end. Inconel 718 was considered as the material for these components. This material was selected for the FFTF and LMFBR driveline and latching mechanisms, which operate in a temperature and radiation environment similar to that of the GCFR up-flow core. The combination of Inconel 718 and chromium carbide-nichrome was also considered for surfaces subject to frictional wear. The guide and support structure material is 316 stainless steel, as originally anticipated for the down-flow core concept.

For the down-flow core, the control rod drives are supported and contained within the lock actuator and thermocouple guide structures. These structures are axially supported at the top of the core support grid plate and are free to thermally grow upward in the PCRV top-head penetrations. The top-head penetration diameters are dictated by the circumferential area outside the control rod drive housing required to accommodate the core lock actuator mechanisms.

For the up-flow core, lock actuator mechanisms are not required at the control rod drive installations. The circumferential area around the control rod drive must only accommodate the thermocouple guide tubes.

Since the thermocouple guide tubes require less cross-sectional area than the lock actuators, the penetration diameter can be somewhat less [304.8 versus 355.6 mm (12 versus 14 in.)].

In the down-flow concept, the control rod drives can be separately removed from the lock actuator assemblies. The lock actuator assemblies must remain in place to retain the core assemblies in case it is necessary to service or replace a control rod drive. In the up-flow concept, the control rod drive, its guide, support tube, and thermocouple access tubes can be removed as a single unit since no core-locking function is incorporated in the installation. These entire drive assemblies are axially supported on a honeycomb grid-type auxiliary structure located a short distance above and spanning the top of the core and are free to grow thermally in the upward direction, similar to the down-flow core installations.

10.3. FUEL HANDLING DEVELOPMENT

Conceptual studies of methods for refueling an up-flow core through the top head have been developed in more detail and refueling time estimates compiled. Concepts for both in-vessel refueling and refueling through a rotatable top-head plug have been evaluated, and three preferred concepts have emerged: two have a fixed top head and one has a rotatable plug in the top head.

The first concept provides a means of transferring assemblies through a penetration immediately above the "patch," or region of seven assemblies, to be serviced and requires a penetration for each region of seven fuel, blanket, and shield assemblies. In the case of a commercial-sized plant, this could result in over 100 penetrations in the top closure head. The machine used to accomplish this function is installed in a penetration by a loading cask through an isolation valve attached to the penetration. This cask is subsequently replaced by a fuel transfer cask. The fuel handling machine has an offset capability

in excess of one assembly pitch and places the removed assembly in a position where it can be regrappled by and raised into the fuel transfer cask.

The second concept also provides a fixed head, but it requires only the penetrations needed for control rod drives and instrument trees together with one larger, dedicated peripheral penetration. After all control rod drive and instrument tree assemblies have been raised to the top of the refueling plenum, a folding beam arrangement is installed through the central penetration. When this beam is deployed, its end is supported by a radial rail attached to the underside of the top head. A fuel handling machine is installed through the dedicated penetration and transferred to the radial arm. By rotating the arm and traverse of the machine, the grapple can be axially aligned with any one of the core assemblies. An inclined conveyor moves the assemblies directly to the storage pool via an intermediate transfer cask located below the PCRV.

The third concept consists of a rotatable plug configuration which has two eccentric components. The primary, or inner, component is the plug, which contains all the required control rod drive and instrument tree penetrations together with two dedicated penetrations. The center of rotation of the assembly is offset from the center of the reactor core by one half the total required eccentricity. Surrounding the plug assembly is a secondary eccentric component in the form of an annulus which, when separately rotated, causes displacement of the plug assembly, resulting in the required total displacement of the penetrations. The primary and secondary components are supported on ball bearings during rotation, and each component is separately driven by an electric motor and gear reducer.

The fuel handling machine is carried above the rotating plug on a polar bridge arrangement in such a manner that the machine can be positioned over the appropriate penetration. The fuel handling machine consists of two telescoping sleeves, each actuated by a pair of ball

screws. An assembly grapple head is coupled to the inner screw-driven sleeve by a latching arrangement and is also attached to a secondary hoist. The penetration through which access to the core is to be made is first cleared and an isolation valve installed. The plug assembly is then rotated to place the axis of the penetration directly over the axis of the appropriate core assembly. Next, the fuel handling machine is moved into position and sealed to the isolation valve.

After the fuel handling machine has been sealed to the isolation valve and the interspace purged, the outer sleeve is driven downward until it contacts the six assemblies surrounding the assembly to be withdrawn. This restrains the adjacent assemblies in case frictional forces develop during withdrawal, which could raise them along with the grappled assembly. The outer sleeve also serves as a guide for the inner sleeve, which is lowered into position along with the grapple head. Once the core assembly has been grappled, the sleeves along with the grapple and assembly are retracted in reverse sequence, the isolation valves are closed, and the fuel handling machine is disconnected. The fuel handling machine is then moved to an inclined conveyor arrangement which is directly routed to the storage pool. From this position, the grapple head is uncoupled from the inner sleeve, and the assembly is lowered down the conveyor by the secondary hoist.

The fuel handling machine described above results in substantial axial forces being available from the screw-driven component to withdraw and insert assemblies. A longer, oriented travel through the transfer chute is provided by the secondary hoist.

10.4. CORE SUPPORT STRUCTURE

The purpose of this subtask is to ensure the availability of the structural analysis methods and materials mechanical behavior required to assess the structural integrity of the GCFR core support structure under

all anticipated operational and safety-related loading conditions. Work accomplished during the last quarter included preparation of conceptual drawings of three different core support methods for the up-flow configuration. During this quarter, input was provided on the up-flow core study, scoping stress and dynamic analyses were completed to validate the initial concept (Fig. 10-6), and conceptual designs for a down-flow core seismic restraint were initiated.

10.4.1. Stress and Dynamic Analyses of Up-Flow Core Support Structure

The stress due to static and pressure loading is acceptable; however, in this preliminary design, there is thermal stress slightly above the acceptable limit at the connection between the grid plate and core support cone (point A on Fig. 10-6). Simplified dynamic analysis indicated that the fundamental frequencies were low (9.4 Hz vertical and 12 Hz horizontal) and may be in the range of the PCRV natural frequency. Modifications of the core support structure initial conceptual design will be necessary to resolve this problem.

10.4.2. Interim Up-Flow Core Study Input

The up-flow core offers the following core support structure advantages:

1. Thinner material and hence expected better uniformity of properties throughout the thickness.
2. Reduced cost and complexity due to elimination of insulation on the core support cylinder.
3. Simplified secondary core support.

The areas requiring further study are

1. Manufacture of the sandwich-type grid plate.
2. The thermal stress and natural frequency problems mentioned in Section 10.4.1.

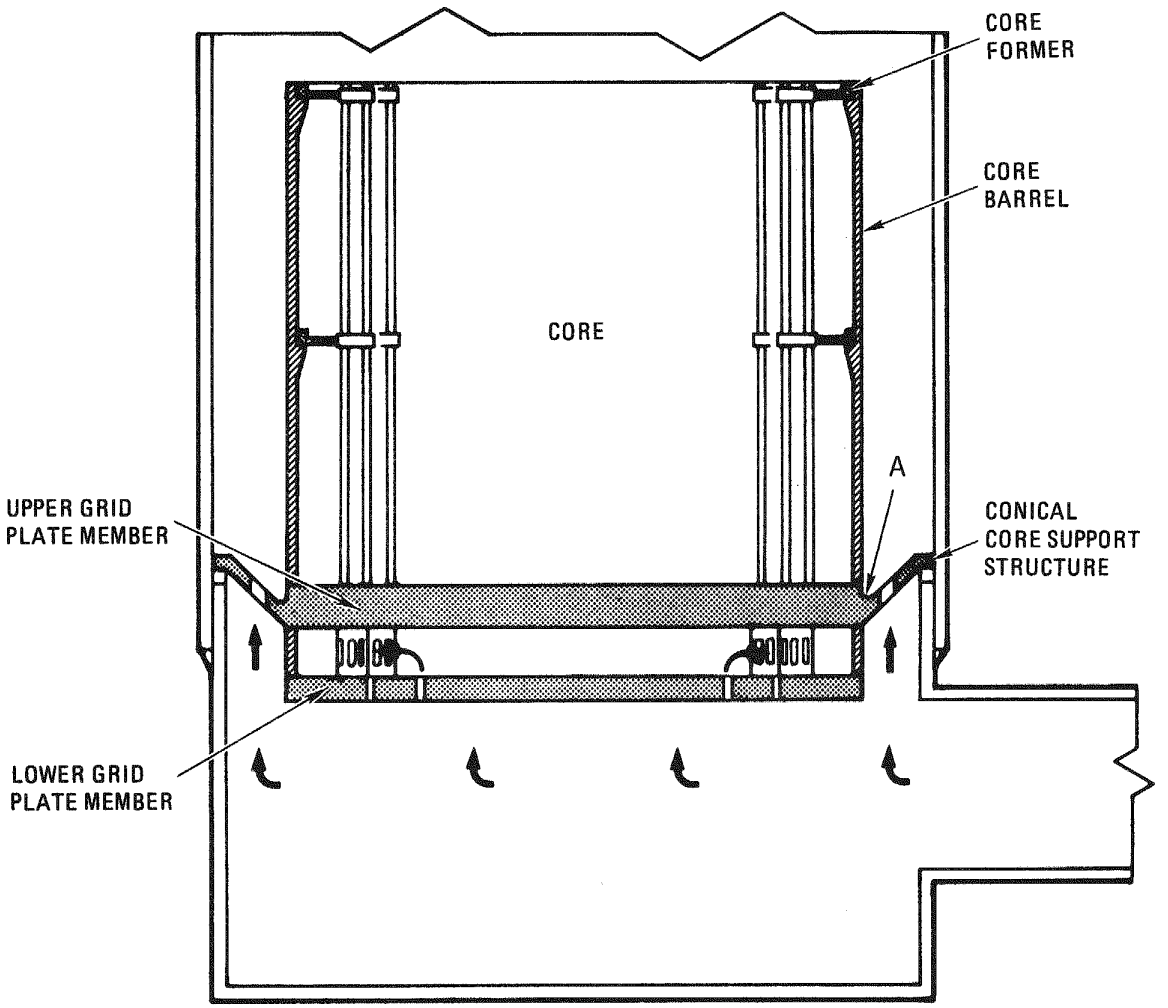

Fig. 10-6. Conceptual up-flow core configuration

10.5. REACTOR SHIELDING ASSEMBLIES

The purpose of this subtask is to design and develop analytical methods and experimental programs to evaluate the reference design of the reactor shields. This evaluation is expected to cover nonuniform temperature distribution, material behavior, seismic effects, hydrodynamic tests, and structural analysis. Alternate shield configurations will also be studied so that a satisfactory and optimized shield design can be developed.

During the previous quarter preliminary thermal analyses of the reference design radial shielding and the up-flow radial shielding were performed. The analyses indicate excessively high temperatures in the reference design shielding and temperatures close to acceptable levels in the up-flow radial shielding.

During this quarter a sizing stress analysis of the reference design radial shielding supports and secondary core supports was performed (Fig. 10-7). Three loading conditions were investigated:

1. Normal static radial shield load plus load due to normal core support cylinder (CSC) failure mode, where normal CSC failure mode is defined as sudden, complete, circumferential failure of the CSC with the load applied equally to all 12 secondary core supports.

2. Normal sustained radial shield load plus load due to tilted failure mode of the CSC, where tilted failure mode is defined as sudden failure of a 180 deg section of the CSC circumference with the load applied to one secondary core support and one pair of outer radial shield supports. These supports are permitted to yield, and the load is taken over and supported by an additional set of supports on each side of the initially contacted units.

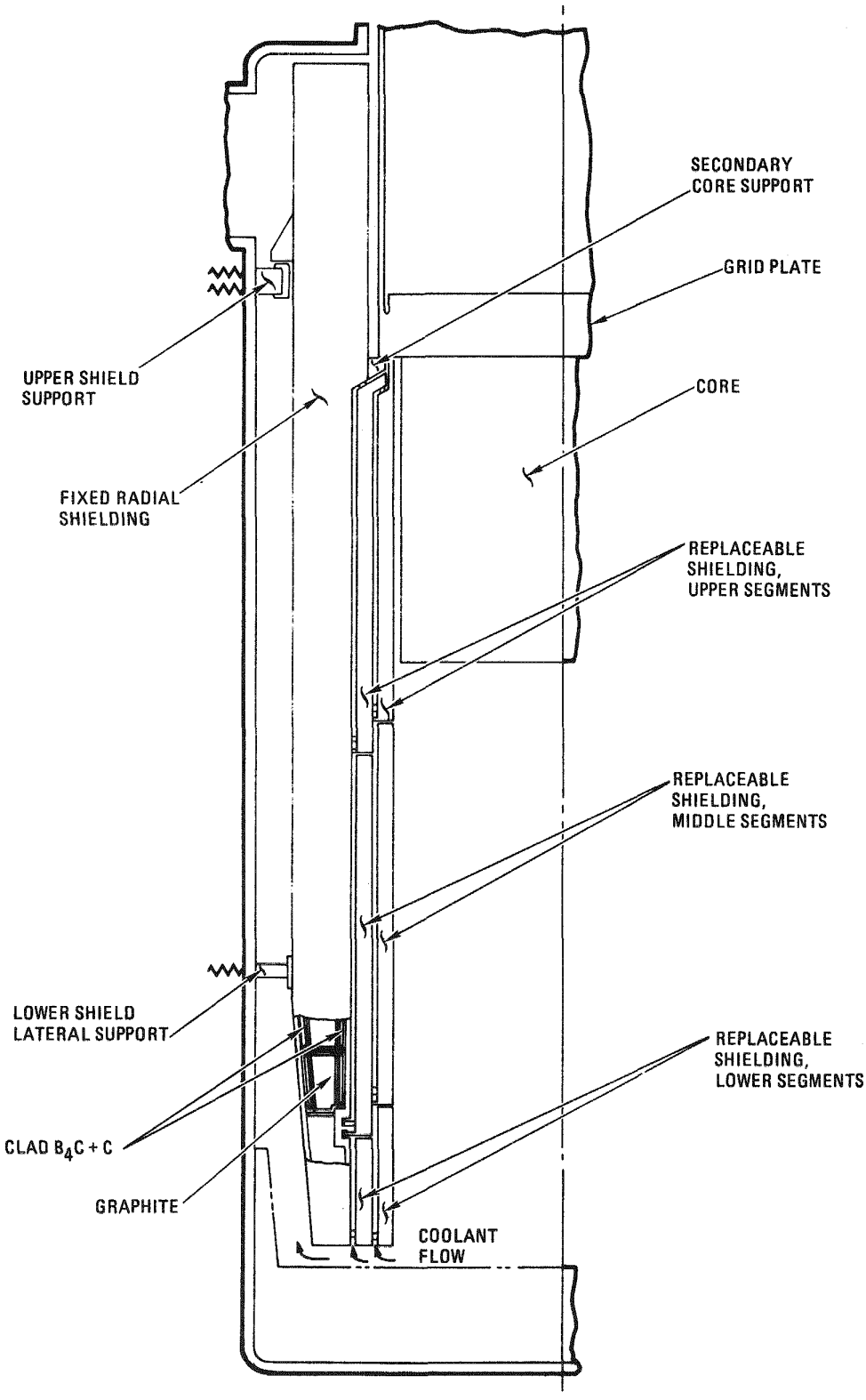

Fig. 10-7. Lower plenum shielding reference design

3. Installation load where the total load of one outer radial shield segment may be supported by only one of the two support structures; this load may be suddenly applied.

This analysis verified the design feasibility of the concept and resulted in acceptably sized load-carrying members.

10.6. MAIN HELIUM CIRCULATOR, VALVE AND SERVICE SYSTEM

The purpose of this subtask is to develop the helium circulator, its service system, and the main loop isolation valve to demonstrate performance and reliability by testing under anticipated operating conditions. The overall objective for FY-78 was to continue first-of-a-kind conceptual design and performance analysis of the circulator reference design configuration (external steam drive), the service system, the loop isolation valve, and the alternate electric drive selected from studies made in FY-77. Preliminary layouts of the circulator components will be made and requirements established for bearings, shaft critical speeds, seal flow rates, helium buffer systems, drains, jet pumps, inlet and diffuser configurations, shaft coupling and rotor dynamics, aerodynamic performance, and model test requirements for the compressor and diffuser. The work outlined will provide input to the circulator pretest analysis task for determination of test facility requirements and evaluation of alternate circulator and drive systems.

10.6.1. Main Helium Circulator

Figure 10-8 shows the recommended reference design layout for the main helium circulator. It incorporates a 3600-rpm electric motor drive, a common thrust bearing in a separate housing above the motor, and a high-pressure rotating shaft seal design. The brake is a Westinghouse pneumatically actuated brake which stops the electric motor and the circulator from 360 to 0 rpm. The brake is also used to keep the circulator from rotating when the circulator is shut down. Details of the design are given in Ref. 10-1.

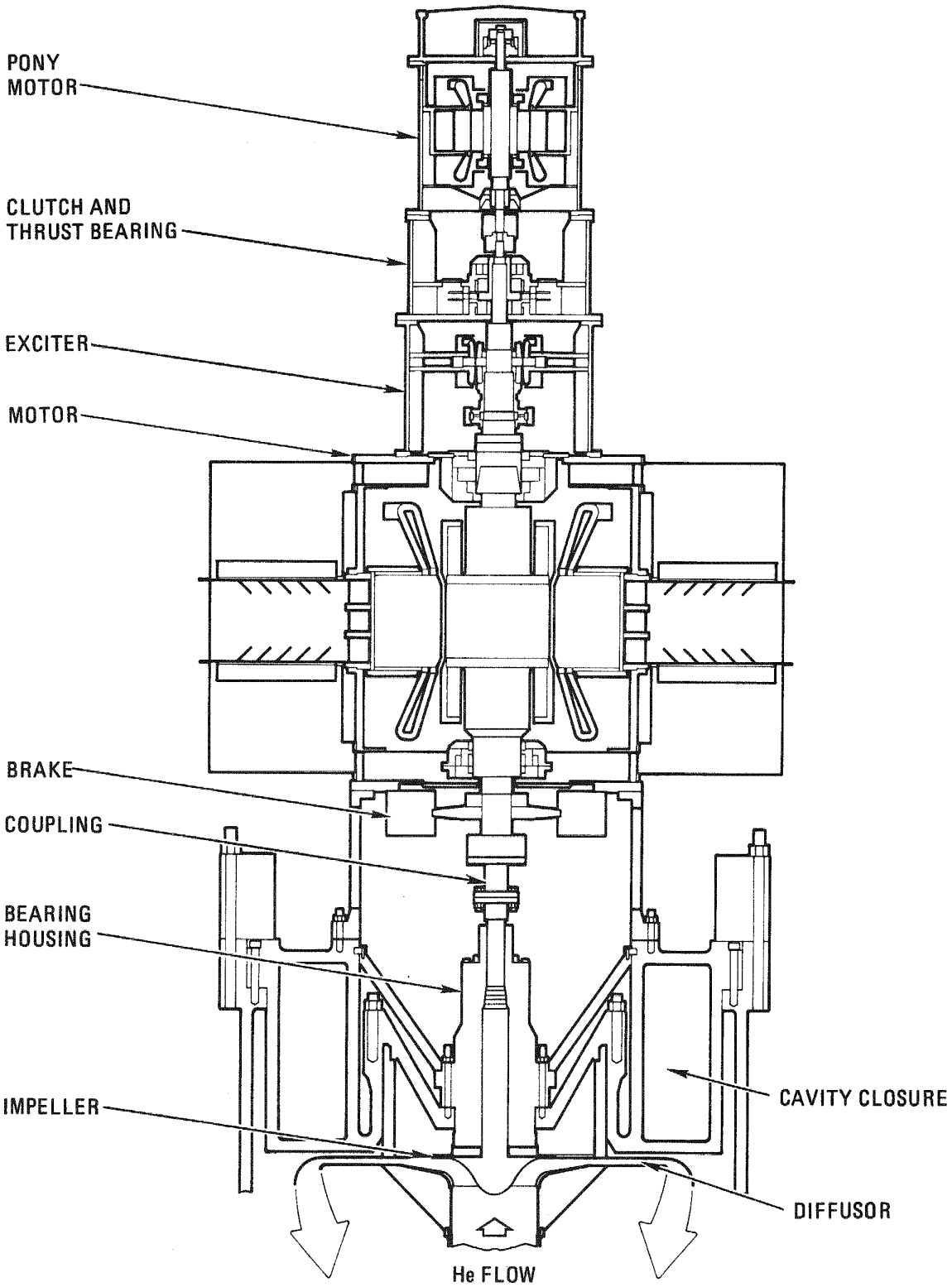

Fig. 10-8. GCFR main helium circulator

10.6.2. Shaft and Bearings

The five-bearing design of the combined circulator and electric drive motor, coupled through a solid shaft coupling, was analyzed at GA and compared with the results in Ref. 10-2 of Westinghouse. The results of the comparisons are shown in Figs. 10-9 through 10-12. There was generally good agreement between the Westinghouse and GA data. Reference 10-2 included the deflection of various shaft sections for certain bearing stiffness and damping plus the bearing housing damping and stiffness. Basically, these values were combined as springs and dampers in series. To achieve the condition of no calculated natural frequencies below 115% of maximum speed, bearing and support stiffnesses on the order of 2×10^9 N/m (10 million lb/in.) are required at the motor guide bearings (Fig. 10-12). Theoretical calculations indicate that such a bearing stiffness can be achieved by use of hydrostatic bearings requiring approximately 1.05 kg/s (1000 gpm) of oil at 15.85 MPa (2300 psi) per bearing. This would require approximately one 2014-kW (2700-hp) pump for the two main guide bearings. The structures supporting the bearings would also have to be at least this stiff. It was decided to use bearings which are flexibly supported but highly damped to achieve the desired natural frequency and minimize the response amplification. With hydrodynamic bearings and damped supports, the effect of a given unbalance will be as acceptable with a rigid body mode within the operating range as a system using hydrostatic bearings and a very rigid structure externally braced to the foundation to attain a rigid body mode greater than 115% of the rated operating speed. Operation above the first mode with the required damping to limit displacement amplitudes is an accepted commercial technique. However, further analysis must be done to investigate the effects of bearing damping and stiffness on the latest composite configuration.

10.6.3. Electric Motor Drive Design Recommendations

Large high-speed vertical motors and variable-frequency power supplies are not, in themselves, a new technology. Ample background exists to guide

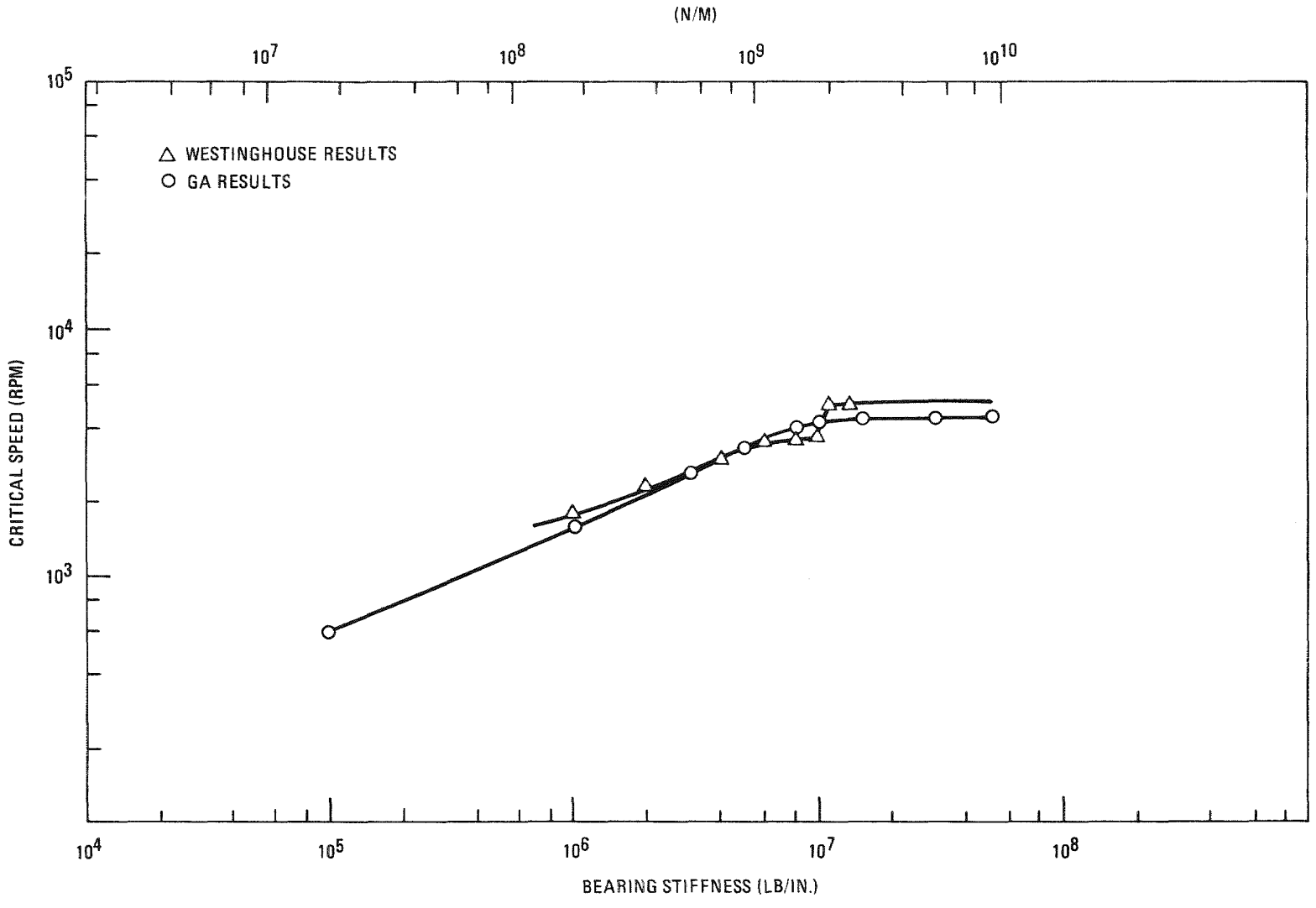

Fig. 10-9. Comparison of Westinghouse and GA results (all bearings have same stiffness and zero damping)

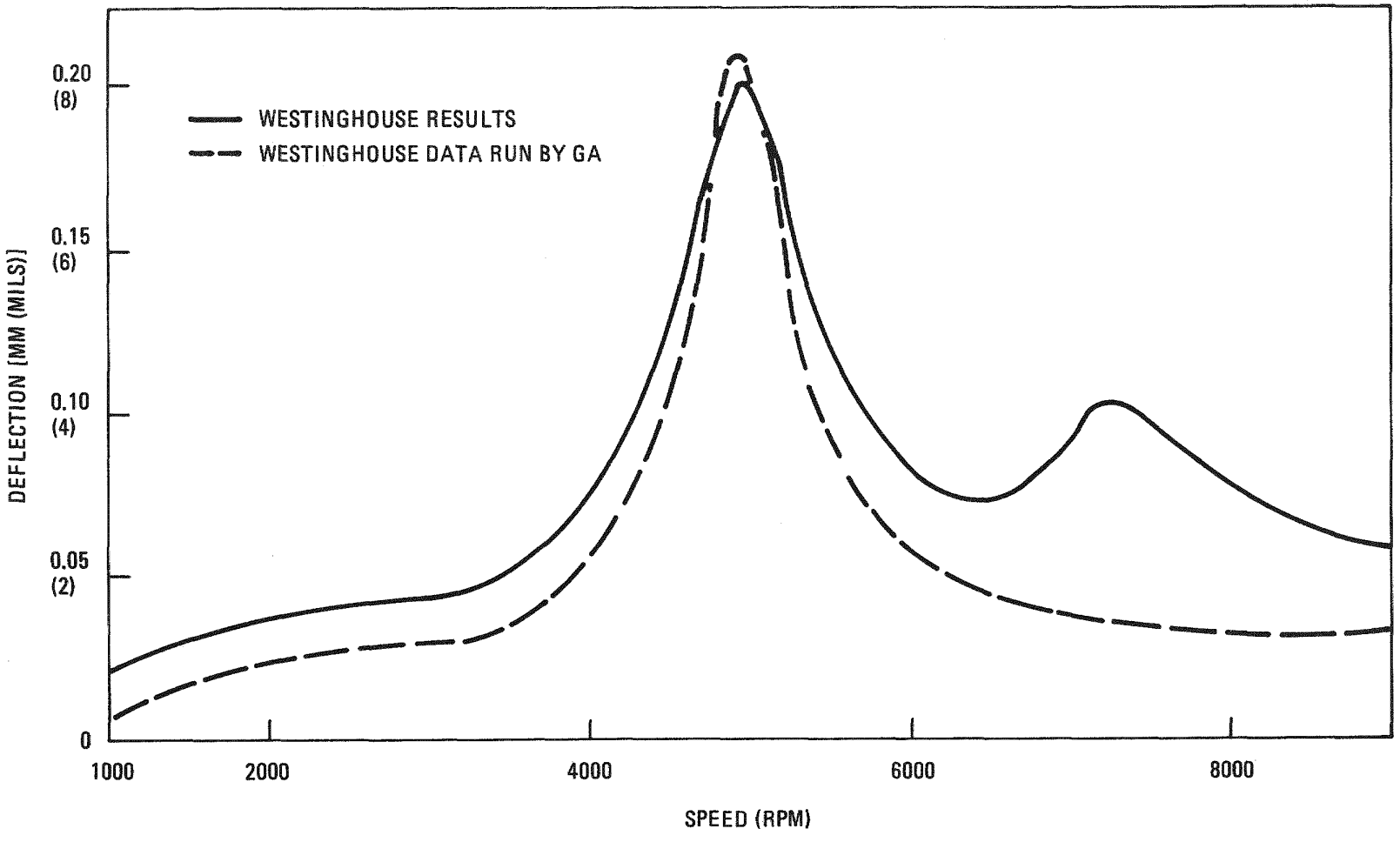

Fig. 10-10. Comparison of Westinghouse and GA results for the exciter

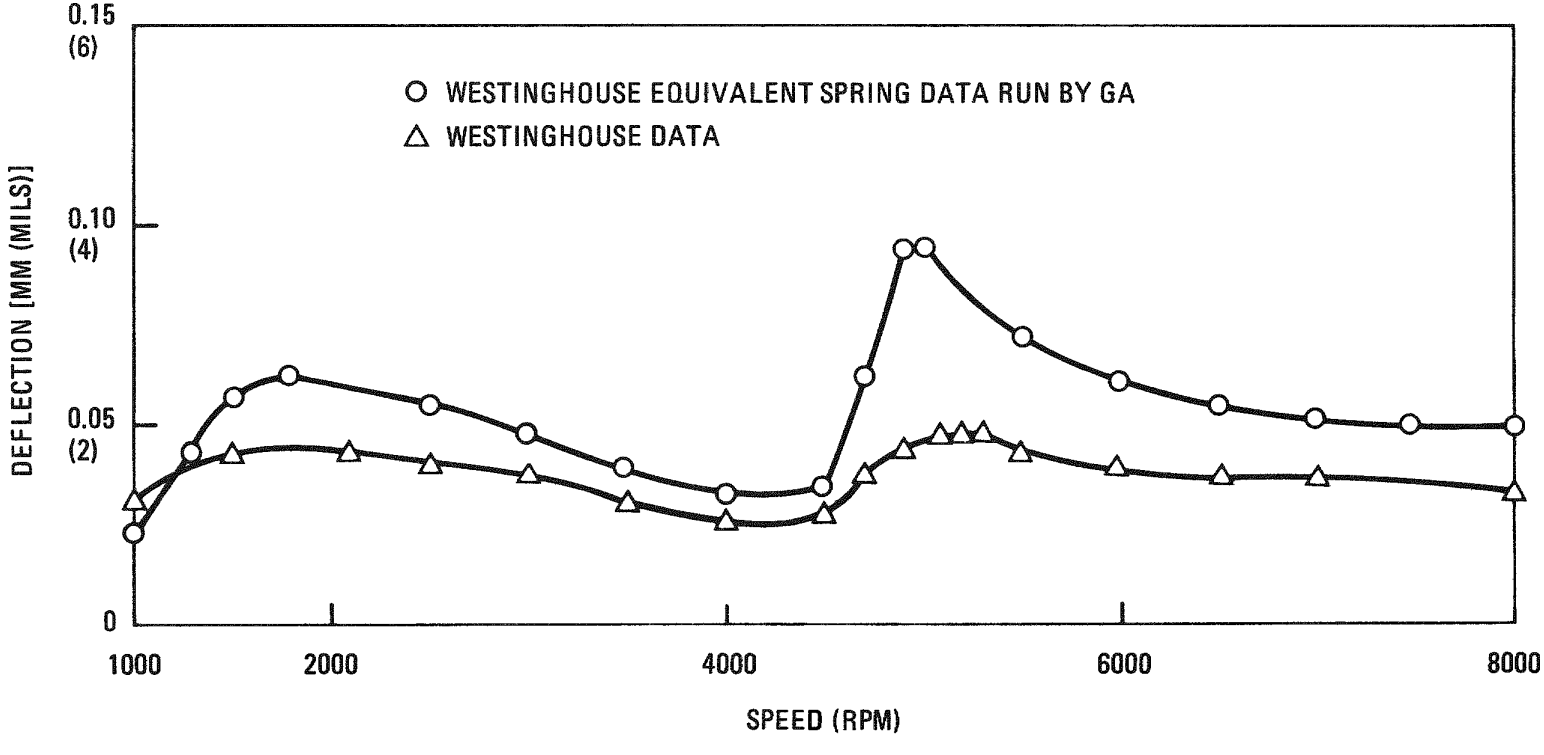

Fig. 10-11. Comparison of GA results with Westinghouse data for the motor rotor

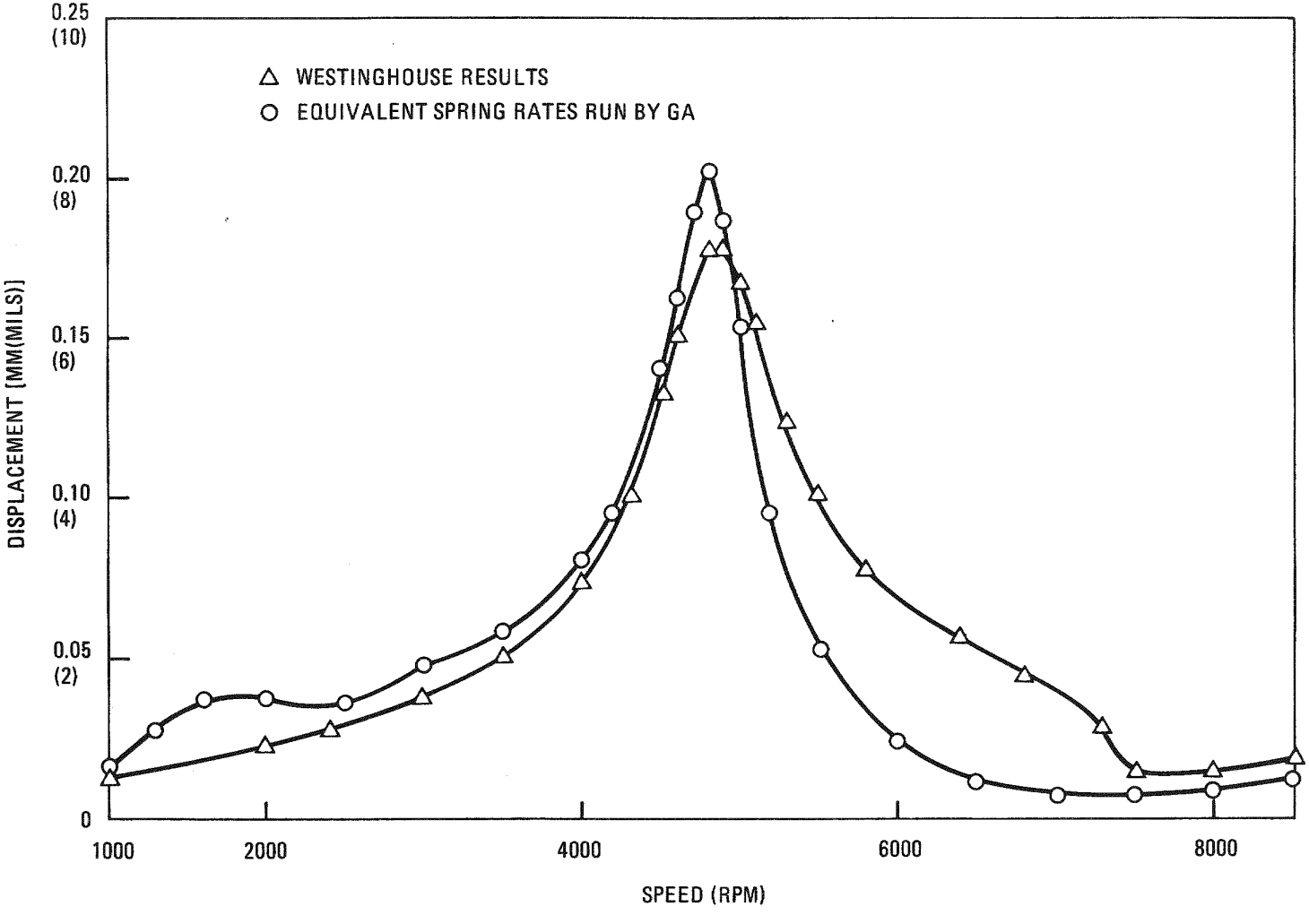

Fig. 10-12. Comparison of Westinghouse and GA results for the coupling

the choice of design dimensions and parameters so that equipment which meets the GCFR's requirements is designed. The main and pony motors and associated controllers were evaluated from a broad range of optional configurations. The recommended main motor is a 17,300-kW synchronous motor with brushless exciter and it is externally mounted at containment pressure. This motor will be designed for variable-speed operation and will be rated for full-power operation at 3600 rpm. The motor will be totally enclosed by missile-proof housing and will be cooled by water-to-air heat exchangers located inside the housing. This motor will be designed as an extension of modern turbine generator technology, with the major difference being the vertical orientation and variable-speed operation. Even with these unique features, the reliability of the motor is expected to be better than that for small turbine generators. Such machines operate with exceptional reliability as long as adequate margin is designed into the machine and its auxiliaries, the machine is operated within its design specifications, and proper preventive maintenance is performed.

The electric machine rotor that is most fully developed for high-speed aplications, in which the highest possible reliability and service continuity are essential, is the round rotor used in turbine generators. This type is commonly used at operating speeds of 3600 rpm (overspeed at 4320 rpm), but at ratings which are over 100 times larger than that required by the GCFR main circulators. Solid rotor turbo-type technology is therefore a suitable base for the development of the required drive motors. Although this type of rotor can be adapted to induction motor design, it is most suited to synchronous motor applications. Even though solid rotor turbo-type machines are predominantly used as generators, a substantial number have, over the years, been applied as motors, e.g., for compressor drives and wind tunnels.

The advent of practical and economical solid-state variable-frequency supplies has greatly simplified the starting and variable-speed operation of synchronous motors with solid rotors. For the highest reliability, a brushless excitation system is required. Control systems for this

excitation system are available as standard packages and provide protection against overloading, underexcitation, etc. This control package also incorporates static components mounted on modules or boards for ease of maintenance. For the present application, where starting from a standstill is required, a refinement of the standard brushless excitation system is required.

10.6.4. Motor Reliability

The design of the motors recommended for this application is based upon a combination of the designs of existing equipment. Thus, a reliability/availability/maintainability estimate must be made using the experience obtained from the apparatus upon which the motor is based. Reliability and availability data have been developed by Edison Electric Institute (EEI) (Ref. 10-2). The motor categories are not definitive at this time; however, the data for small turbine generators are of interest. These machines are more complicated than the proposed motors since they have hydrogen cooling and its associated seal systems, and most have a commutator-type exciter. Thus, the motors should be expected to have a better record than the approximately 40,000-h mean time between failures reported for small turbine generators for all causes, which includes lack of proper maintenance and operator error.

A study was made of 139 industrial horizontal motors rated from 920 to 11,190 kW (1,250 to 15,000 hp). One hundred and six of these motors were identical [3,730 kW (5,000 hp) and 1800 rpm]. These are mostly outdoor units operating under severe environmental conditions in pipeline pumping service. The actual mean time between failures for the motors was 260,000 h. A survey conducted by the Doble Engineering Company (Ref. 10-2) of motors rated 746 kW (1,000 hp) and larger indicated that in a group of 1,929 motors, 33 failed during the 1-yr period of 1975. This converts to a mean time between failures of 330,000 h at the 99% confidence level. Thus, a conservative expected mean time between failures should be at least on the order of 100,000 h for vertical

circulator motors and should approach 350,000 h with maturity. This reliability growth can be attained by careful attention to detail during design and manufacturing and by correcting any deficiencies found during prototype testing and initial operation.

Reactor coolant pump induction motors have been built or are being built for Westinghouse pressurized water reactor plants and PWR plants being constructed by Atomic Energy Canada Limited, Babcock and Wilcox, and Combustion Engineering. These motors are in the power range of 2,984 to 8,206 kW (4,000 to 11,000 hp) and are vertical machines which use guide bearings and lubrication and frame construction features which are applicable to the GCFR.

10.6.5. Motor and Controller Experience

Many horizontal, high-speed, cylindrical-rotor synchronous motors have been built whose rotor and stator construction features are applicable to the GCFR. In addition, hundreds of brushless exciters for 1800- and 3600-rpm cylindrical rotor turbine generators, salient pole generators, and synchronous motors have been built whose technology is applicable to the GCFR project. Many millions of kilowatts of thyristor power supplies have been used for power conversion for dc motors with heavy duty drive applications. The thyristor power supplies use the same basic elements as that recommended for the GCFR variable-frequency application. Actual reliability/availability figures have not been collected on this type of apparatus; however, users indicate that the service has been very acceptable. In an actual application of variable-frequency operation, only one thyristor failure occurred out of 576 devices in service for 18 months, which indicates that thyristor mean time between failures can be expected to be much greater than 1×10^6 h. The failure did not cause a forced outage because thyristors are normally shorted when they fail, and sufficient units were used in series to allow continued operation until a planned maintenance period. The time to repair a thyristor is estimated to be less than 4 h.

10.7. STEAM GENERATOR

The function of the steam generator is to transfer heat from the reactor primary coolant (helium) to the secondary coolant (water/steam) during normal plant operation. The steam generator will be subject to cyclic or repeated steady and transient operating conditions in its 30 yr of design life. The objective of this task is therefore to design and develop a steam generator which meets the operational, performance, and safety requirements of the GCFR.

In the reference down-flow core plant configuration, the steam generator features a bottom-fed, bottom-exhaust arrangement. In this design, water enters from the bottom of the bundle, and the steam is routed down through a straight tube section and exhausts from a tube sheet located at the bottom of the PCRV. In the up-flow core configuration presently being studied, the location of the steam exit is at the top of the PCRV. Such a steam generator is generally a bottom-fed, top-exhaust arrangement.

During this quarter the main task was to provide design and analysis support for the up-flow core study. The major work accomplished included (1) production of a top-exhaust steam generator general arrangement drawing for the PCRV layout (Fig. 10-13) and (2) performing a feasibility study of the top-exhaust steam generator. Figure 10-13 shows that the helical bundle is basically the same size as that of the down-flow core, since the system conditions are identical. The bundle and shroud assembly is bolted to the main support flange at the bottom end of the bundle, and the expansion loops are provided on top of the bundle. Tubes are routed behind a helium flow shield such that no expansion loop tube will be exposed to the hot helium flow from the cross duct. Feedwater flows into the steam generator through a side penetration so that interference with the circulator assembly below the steam generator is avoided. The superheater tube sheet at the top of the PCRV is anchored to the concrete plug, which is designed to be removable.

NOTES: UNLESS OTHERWISE SPECIFIED

1. ALL DIMENSIONS ARE NOMINAL COLD.

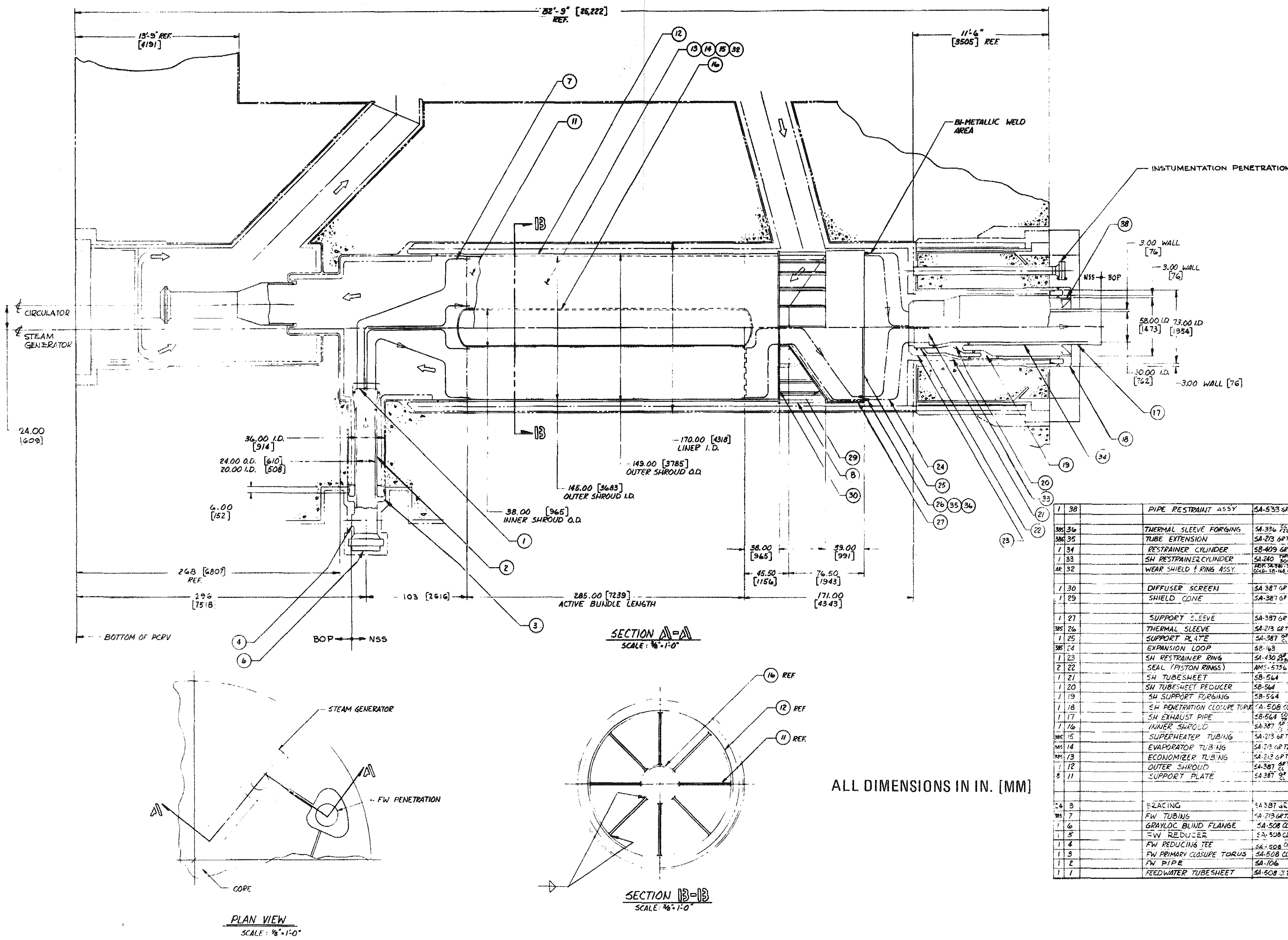

1	38		PIPE RESTRAINT ASSY	SA-533 GR B	1" × 9" LG	110
						9E
385	36		THERMAL SLEEVE FORGING	SA-336 CL F22	1½" × 6 × 15.30 D	2VE
385	35		TUBE EXTENSION	SA-213 GR T22	.906 OD × 17 LG	2VE
1	34		RESTRAINER CYLINDER	SB-409 GR 1	3" THK	110
1	33		SH RESTRAINER CYLINDER	SA-240 TYPE 304	2" THK	110
AR	32		WEAR SHIELD & RING ASSY.	HOT-SA-240-304 COLD-SB-168, 422		9E
						5E
1	30		DIFFUSER SCREEN	SA-387 GR 22	1" THK	9E
1	29		SHIELD CONE	SA-387 GR 22	½" THK	9E
1	27		SUPPORT SLEEVE	SA-387 GR 22	½" THK	9E
385	26		THERMAL SLEEVE	SA-213 GR T22	1¼ OD × 5" LG	2B
1	25		SUPPORT PLATE	SA-387 GR 22 CL 1	2" THK	6E
385	24		EXPANSION LOOP	SB-163	1" O D	2VE
1	23		SH RESTRAINER RING	SA-430 GR FP304	10" THK × 24" LG	110
2	22		SEAL (PISTON RINGS)	AMS-5736	42" DIA	9E
1	21		SH TUBESHEET	SB-564	15" THK × 42" DIA	2PT
1	20		SH TUBESHEET REDUCER	SB-564	11" THK × 41 LG	2UT
1	19		SH SUPPORT FORGING	SB-564	8" THK × 30" LG	2UT
1	18		SH PENETRATION CLOSURE TORUS	SA-508 CL 2	9" THK × 16" LG	2UT
1	17		SH EXHAUST PIPE	SB-564 SOL TR	3" THK	2UT
1	16		INNER SHROUD	SA-387 GR 22 CL 1	1" THK	6E
385	15		SUPERHEATER TUBING	SA-213 GR T22	1" O D	2VE
385	14		EVAPORATOR TUBING	SA-213 GR T22	1" OD	2VE
385	13		ECONOMIZER TUBING	SA-213 GR T22	1" OD	2VE
1	12		OUTER SHROUD	SA-387 GR 22 CL 1	2" THK	6E
5	11		SUPPORT PLATE	SA-387 GR 22 CL 1	1.5" THK	6E
24	8		BRACING	SA-387 GR 22	4 × 4 H BEAM	
385	7		FW TUBING	SA-213 GR T22	1" O D	2VE
1	6		GRAYLOC BLIND FLANGE	SA-508 CL 2	20" I D	
1	5		FW REDUCER	SA-508 CL 2	20 × 24	
1	4		FW REDUCING TEE	SA-508 CL 2	24 × 24 × 12	1UT
1	3		FW PRIMARY CLOSURE TORUS	SA-508 CL 2	10" THK × 13" LG	1UT
1	2		FW PIPE	SA-106	2" THK	1UT
1	1		FEEDWATER TUBESHEET	SA-508 CL 2	7" THK	1MT

ALL DIMENSIONS IN IN. [MM]

Fig. 10-13. General arrangement of top exhaust steam generator

The design feasibility investigation focused on the dominant problem areas of the expansion loop design. In a top-exhaust steam generator design, the tubes connected to the top superheater tube sheet tend to expand in the opposite direction of the tubes connected to the bottom feedwater tube sheet. The effects of the two thermal expansion modes are combined with respect to the expansion loops. Therefore, increased flexibility must be provided for the expansion loops. However, flexibility raises seismic stress. Thus the feasibility study sought a design which would satisfy both seismic and thermal expansion requirements. Furthermore, the natural frequency of the expansion loop assembly is required to be higher than that of the supporting structure to avoid resonance during a seismic event.

A series of parametric analyses were performed to determine the effect of geometry and design on thermal seismic stress and natural frequency response. Figure 10-14 summarizes the final set of calculations with fixed horizontal span and vertical height. The results indicate that the tube material for the expansion loops must be alloy 800H so that the allowable value will not be exceeded by the total combined thermal, seismic, and dead weight loads. To maintain the assembly frequency higher than that of the bundle, which was estimated at 16 Hz, the expansion loop horizontal restraints must be provided at both ends of the horizontal span and the unsupported arc length below the expansion loops has to be limited. The study indicates that a top-exhaust steam generator with alloy 800H expansion loops is conceptually feasible and should be studied at a more detailed level of design and analysis.

10.8. AUXILIARY CIRCULATOR, VALVE AND SERVICE SYSTEM

A revised design of the GCFR auxiliary circulator and an alternate design of the auxiliary circulator using a hydraulic drive have been completed. A revised drawing of the auxiliary loop isolation valve is shown in Fig. 10-15.

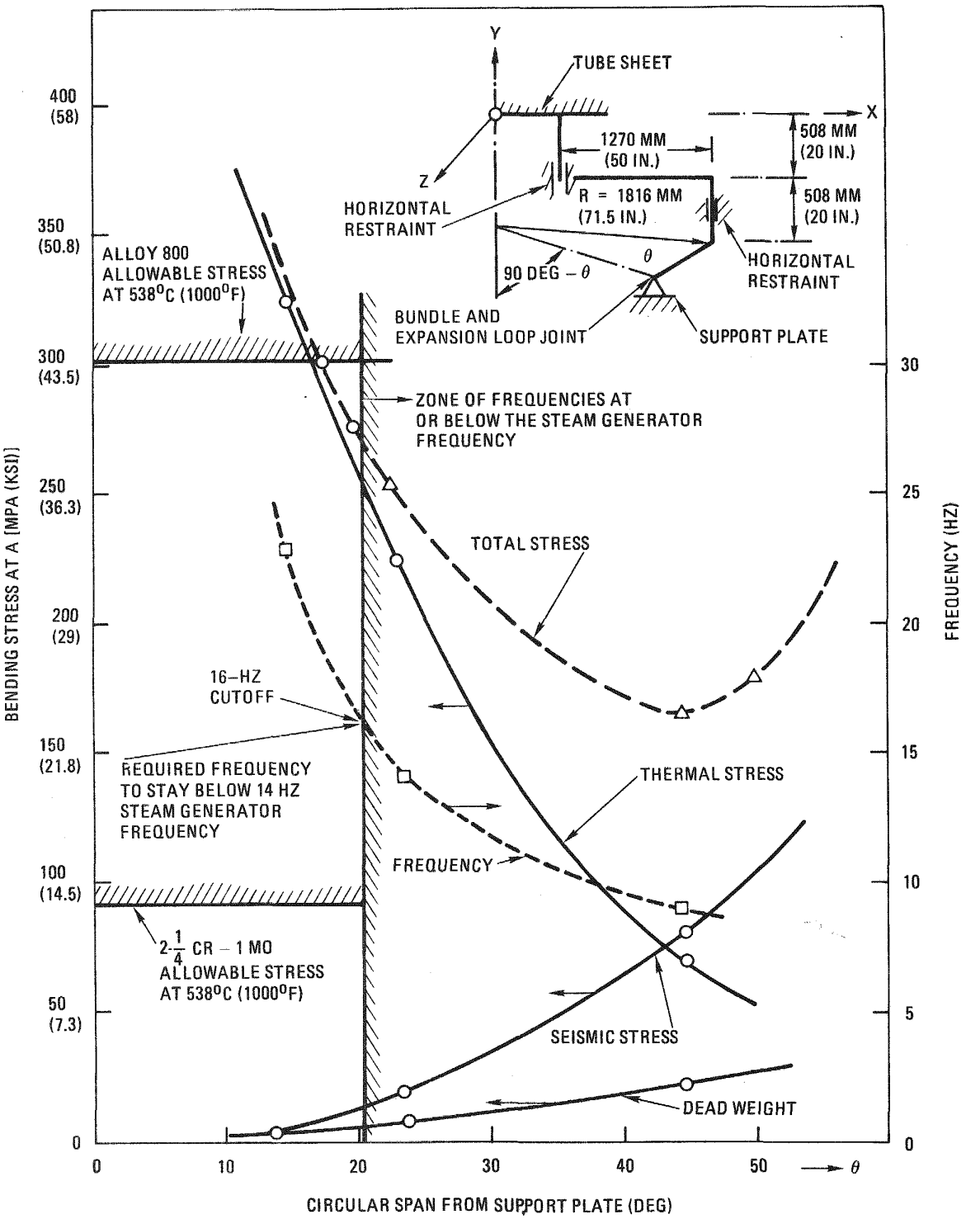

Fig. 10-14. Expansion loop stresses and frequencies with respect to geometry and allowable values

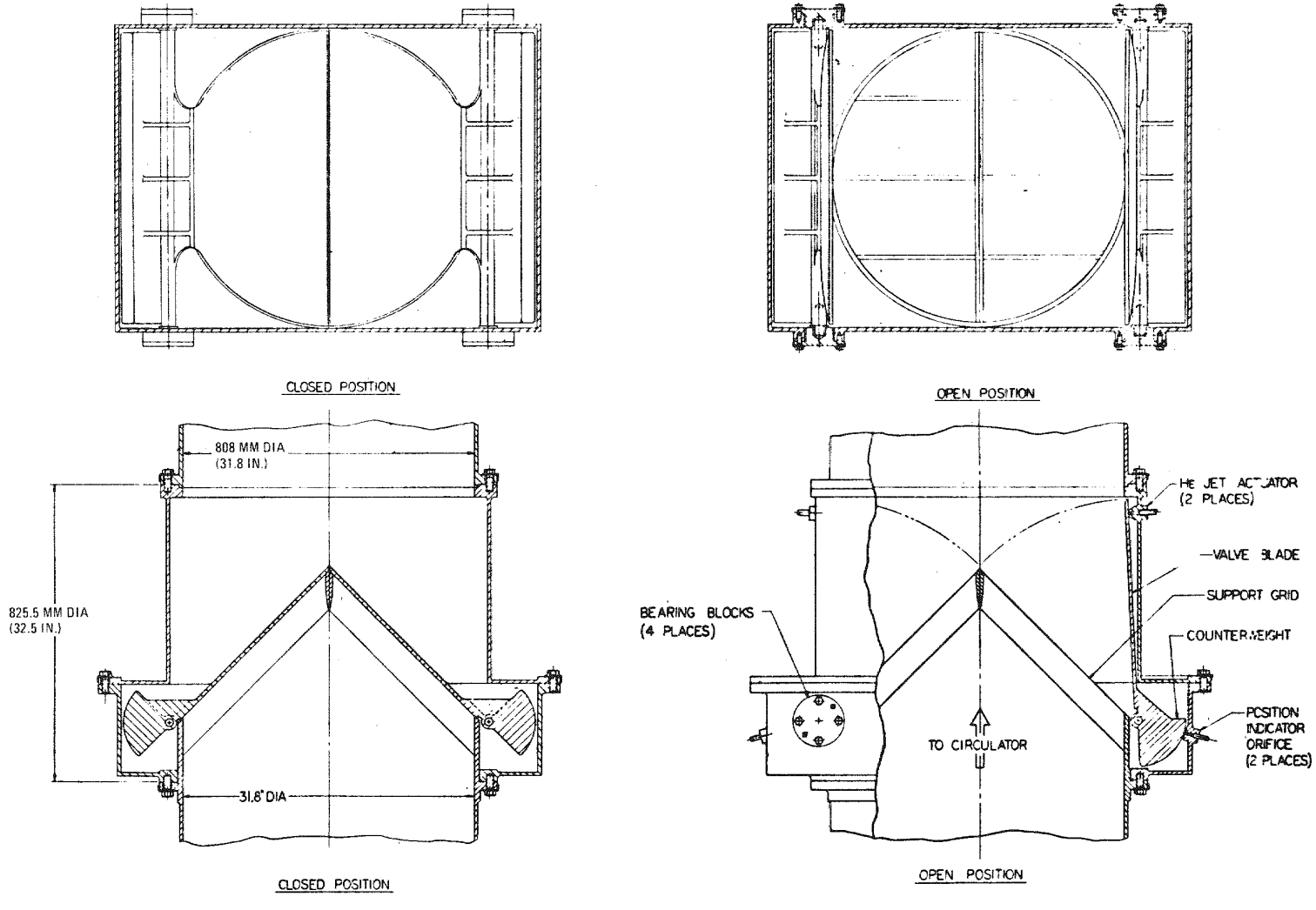

Fig. 10-15. GCFR auxiliary loop isolation valve

10.8.1. Aerodynamic Design and Performance

The compressor for the auxiliary circulator was redesigned to meet operation requirements under DBDA conditions with no air ingress. For these conditions, RHR requires a flow of 5.393 kg/s (11.897 lb/s), and the required pressure rise in the auxiliary circulator compressor is 10.12 kPa (1.47 psi). The full design point conditions are

Inlet total pressure [kPa (psi)]	154.43 (22.4)
Inlet total temperature [°C (°F)]	231 (437)
Outlet total pressure [kPa (psi)]	164.55 (23.87)
Mass flow rate [kg/s (lb/s)]	5.393 (11.897)

Using the design charts of Ref. 10-3, the following design parameters are obtained for a rotor with a radially oriented vane exit:

$$\text{Optimum head rise coefficient} = 2gH_{is}/U_{opt}^2 = 1.45,$$

$$\text{Optimum flow coefficient} = C_m/U_{opt} = 0.295,$$

where C_m = mean inlet meridional velocity,

U_{opt} = rotor tip speed (optimum),

H_{is} = isentropic head rise.

The rotor dimensions in Table 10-1 were based on these values with the additional assumption of constant average meridional velocity. The number of rotor vanes was obtained from Ref. 10-3.

To obtain the highest possible efficiency at the design point, a vaned diffuser was designed for the compressor. The inner radius of the vanes was set at 1.15 times the turbine tip radius, and the outer radius was set at 1.7 times the turbine tip radius. Conventional circular arc vanes were used, and the exit angle and curvature of the vanes were set

using the methods of Ref. 10-3 to provide an equivalent two-dimensional diffuser divergence angle at 8 deg. The details of the diffuser design are given in Table 10-2.

The design point and off-design performance of the compressor was calculated using the computer program PREDM (Ref. 10-4). The curvatures of the hub and shroud profiles, which are required for the program input, were obtained from a preliminary layout of the meridional profile of the rotor. The vane inlet angles calculated by the program for these curvatures are shown in Table 10-2, together with the design point efficiency. The off-design performance of the compressor is presented in the form of dimensional and nondimensional variables. A typical nondimensional plot of the off-design performance is given in Fig. 10-16. The variables are

$$\text{Pressure rise coefficient } \psi = g\,\Delta P/\rho U_{tip}^2,$$

$$\text{Flow coefficient } \phi = Q/A_{tip}U_{tip},$$

where A_{tip} = rotor frontal area [m^2 (ft^2)],

g = 1.0 $kg \cdot m \cdot s^{-2}N^{-1}$ (32.2 $lbm \cdot ft/s^{-2} \cdot lb^{-1}$),

ΔP = pressure rise [Pa (lbf/ft^2)],

U_{tip} = rotor tip speed [m/s (ft/s)],

Q = volumetric flow rate [m^3/s (ft^3/s)],

ρ = gas density [kg/m^3 (lbm/ft^3)].

The results are given for speeds from 20% of design speed. Note that over the range 40% to 120% design speed the curves lie close enough together that the performance of the compressor could be represented by a single curve of ψ versus ϕ. The deviation of the curves at the lower speed is caused by Reynolds number effects not included in the formulation of ψ and ϕ.

TABLE 10-2
GCFR AUXILIARY CIRCULATOR COMPRESSOR DESIGN

Rotor	
Tip diameter [mm (in.)]	1608 (63.30)
Inlet shroud diameter [mm (in.)]	822.5 (32.38)
Inlet hub diameter [mm (in.)]	402 (15.82)
Tip vane width [mm (in.)]	76.1 (2.996)
Vane passage axial length [mm (in.)]	250 (9.84)
Inlet shroud vane angle [deg (from axial)]	39.3
Inlet hub vane angle [deg (from axial)]	68.5
Number of vanes	21
Diffuser (stator)	
Inner radius of vanes [mm (in.)]	924.6 (36.42)
Outer radius of vanes [mm (in.)]	1367 (53.81)
Inlet angle of vanes [deg (from radial)]	70.4
Outlet angle of vanes [deg (from radial)]	53.0
Radius of curvature of vanes [mm (in.)]	2297 (90.43)
Number of vanes	35
Design point performance	
Inlet total pressure [kPa (psi)]	154.43 (22.4)
Inlet total temperature [°C (°F)]	231 (437)
Outlet total pressure [kPa (psi)]	164.55 (23.87)
Outlet total temperature [°C (°F)]	247 (476)
Compressor efficiency (%)	79.94

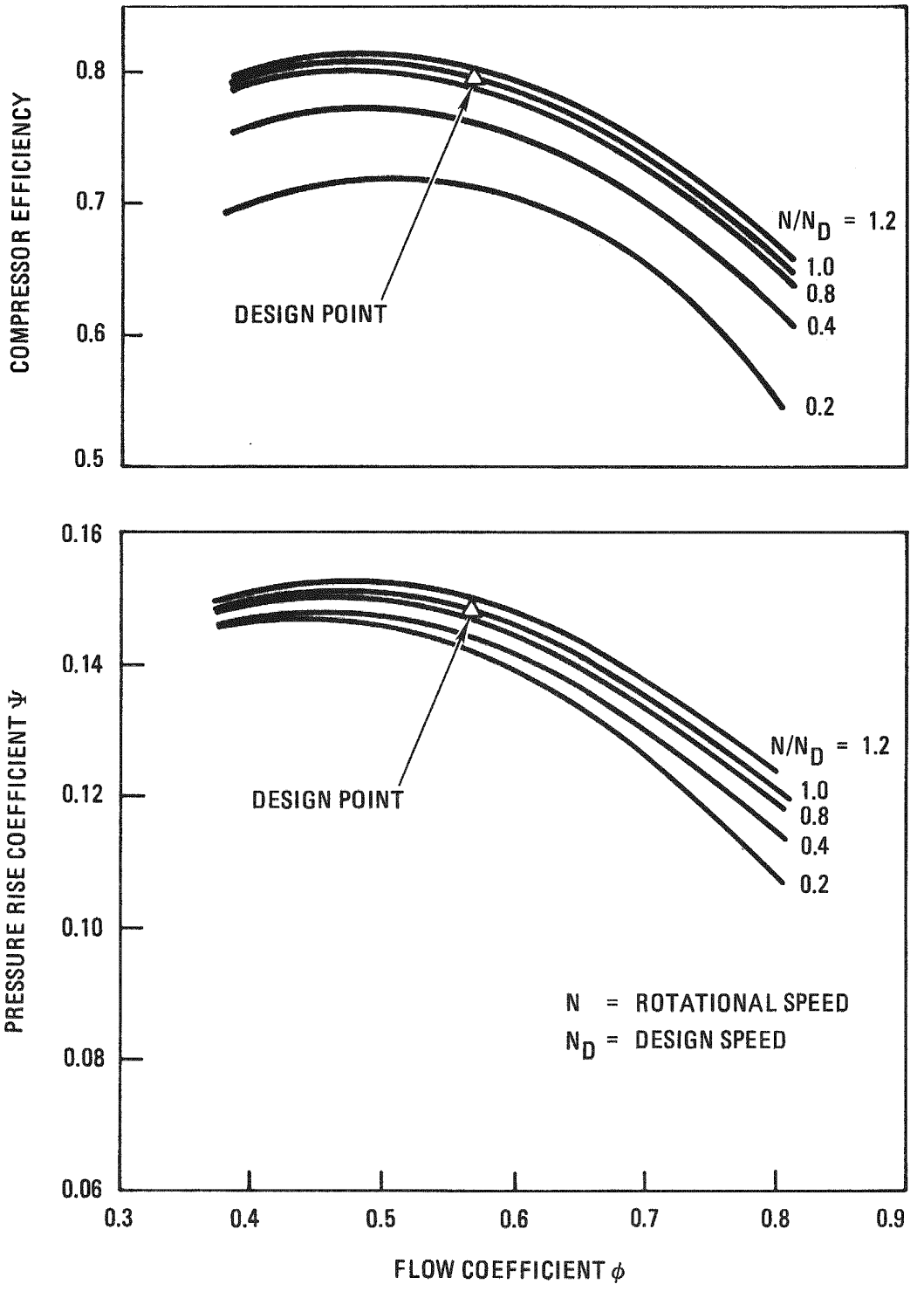

Fig. 10-16. Compressor performance (nondimensional parameters); GCFR auxiliary circulator designed for DBDA (no air ingress)

Figure 10-17 shows the auxiliary circulator. The required cavity diameter for a 3600-rpm impeller is 3.35 m (11 ft). To achieve the requisite margin between operating speed and fundamental critical speed, it was necessary to increase the shaft diameter between bearings. A shaft diameter of 209.55 mm (8.25 in.) and a bearing span of 1.4 m (45 in.) were chosen. The rotor is vertically mounted, and the thrust load is taken by a pair of tandem-mounted ball bearings at the compressor end. The upper end alignment is provided by a roller bearing. The stiffnesses required of the upper and lower end bearings are 1.75×10^8 N/m (1×10^6 lb/in.) and 8.75×10^8 N/m (5×10^6 lb/in.), respectively. Figure 10-18 shows the details of the shaft system, and the critical speed map (Fig. 10-19) shows the variation of critical speed with bearing stiffness. As can be seen, the critical speed value chosen, i.e., 4350 rpm, is not significantly smaller than the fundamental critical speed with rigid bearings (4850 rpm). It may be necessary to further stiffen the shaft [229 to 241.3 mm (9 to ∿9-1/2 in.) diameter], but the resulting change in the design of the motor has to be investigated before this can be done.

10.8.2. Rotor Dynamics of the Hydraulic Drive Auxiliary Circulator

It was concluded that an operating speed of 5000 rpm, which was determined to be optimum for the compressor from a specific speed viewpoint, provided an adequate margin to the onset of the first critical speed. The cavity diameter is 2.9 m (9.5 ft). Table 10-3 gives the principal dimensions of the circulator, and Fig. 10-20 shows the details of the shaft system. The shaft diameter between bearings is 247.65 mm (9-3/4 in.), and the bearing span between centers is 9144 mm (36 in.). It is possible to achieve a critical speed of approximately 6000 rpm using bearing stiffnesses of 0.875×10^9 N/m (5×10^6 lb/in.). The critical speed map (Fig. 10-21) shows the variation of critical speed with bearing stiffness. If it is assumed that the asymptotic value of the critical speed is the fundamental critical speed on rigid bearings,

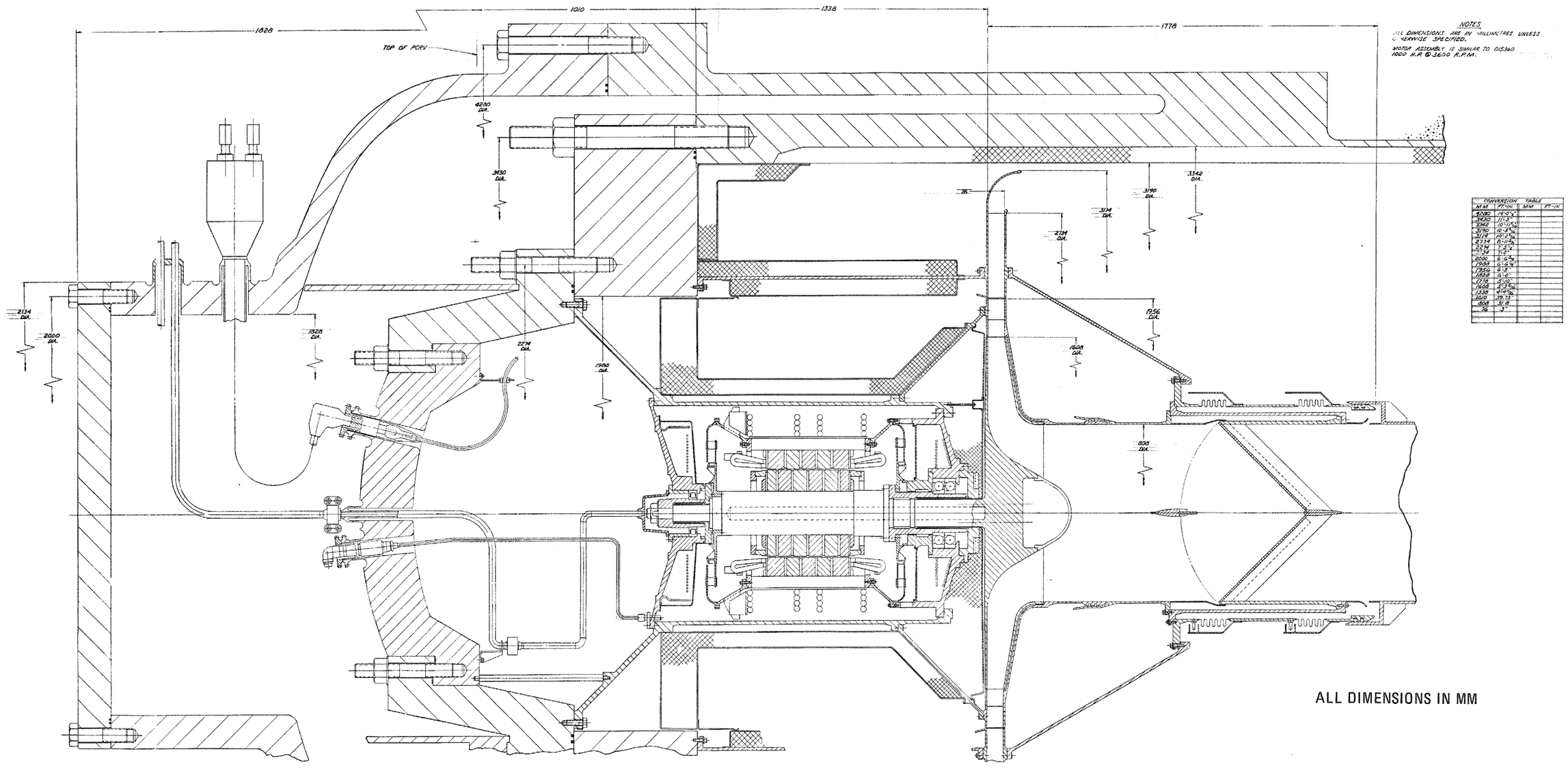

ALL DIMENSIONS IN MM

Fig. 10-17. Auxiliary circulator electr drive

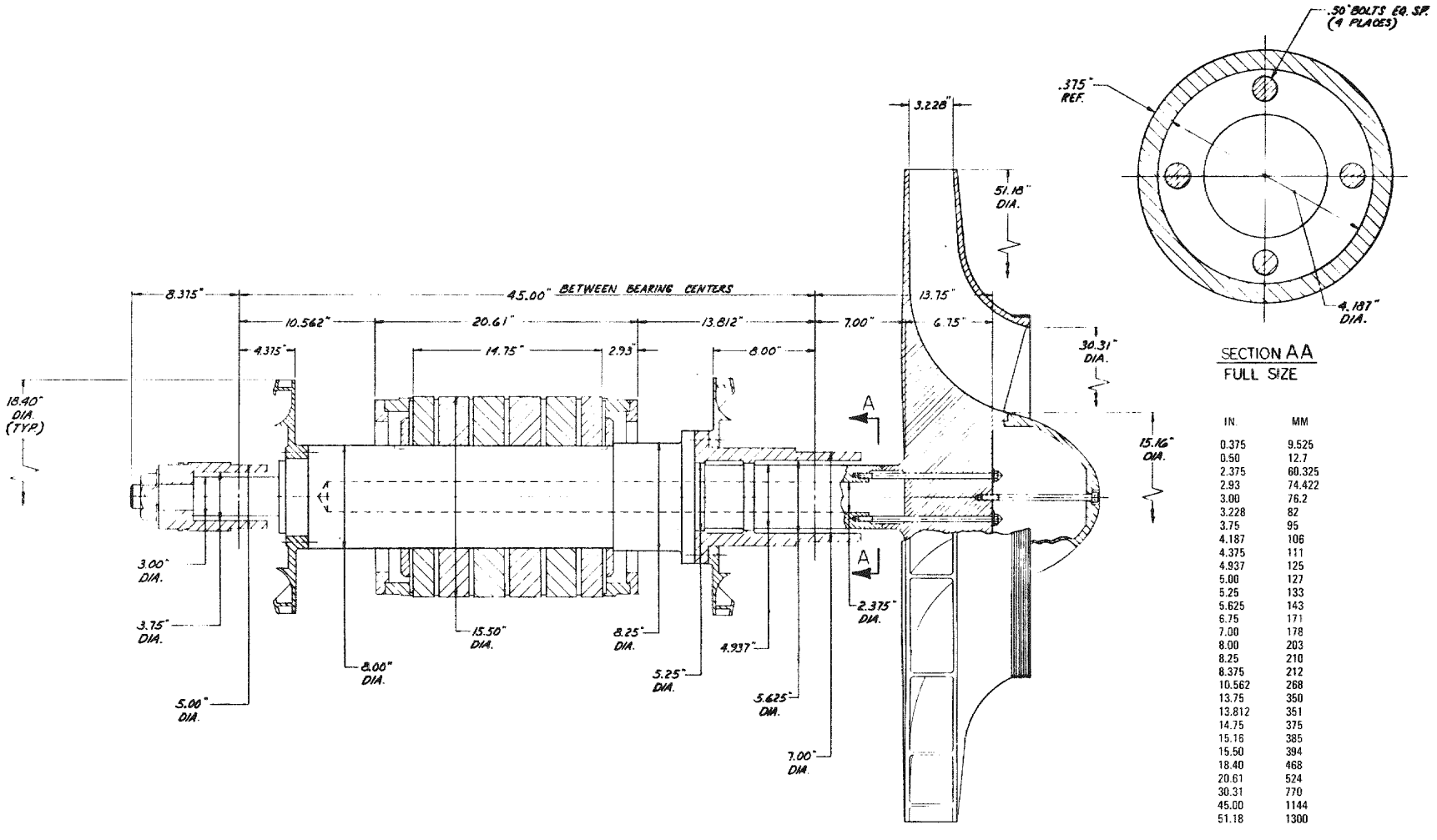

IN.	MM
0.375	9.525
0.50	12.7
2.375	60.325
2.93	74.422
3.00	76.2
3.228	82
3.75	95
4.187	106
4.375	111
4.937	125
5.00	127
5.25	133
5.625	143
6.75	171
7.00	178
8.00	203
8.25	210
8.375	212
10.562	268
13.75	350
13.812	351
14.75	375
15.16	385
15.50	394
18.40	468
20.61	524
30.31	770
45.00	1144
51.18	1300

Fig. 10-18. Auxiliary circulator shaft assembly

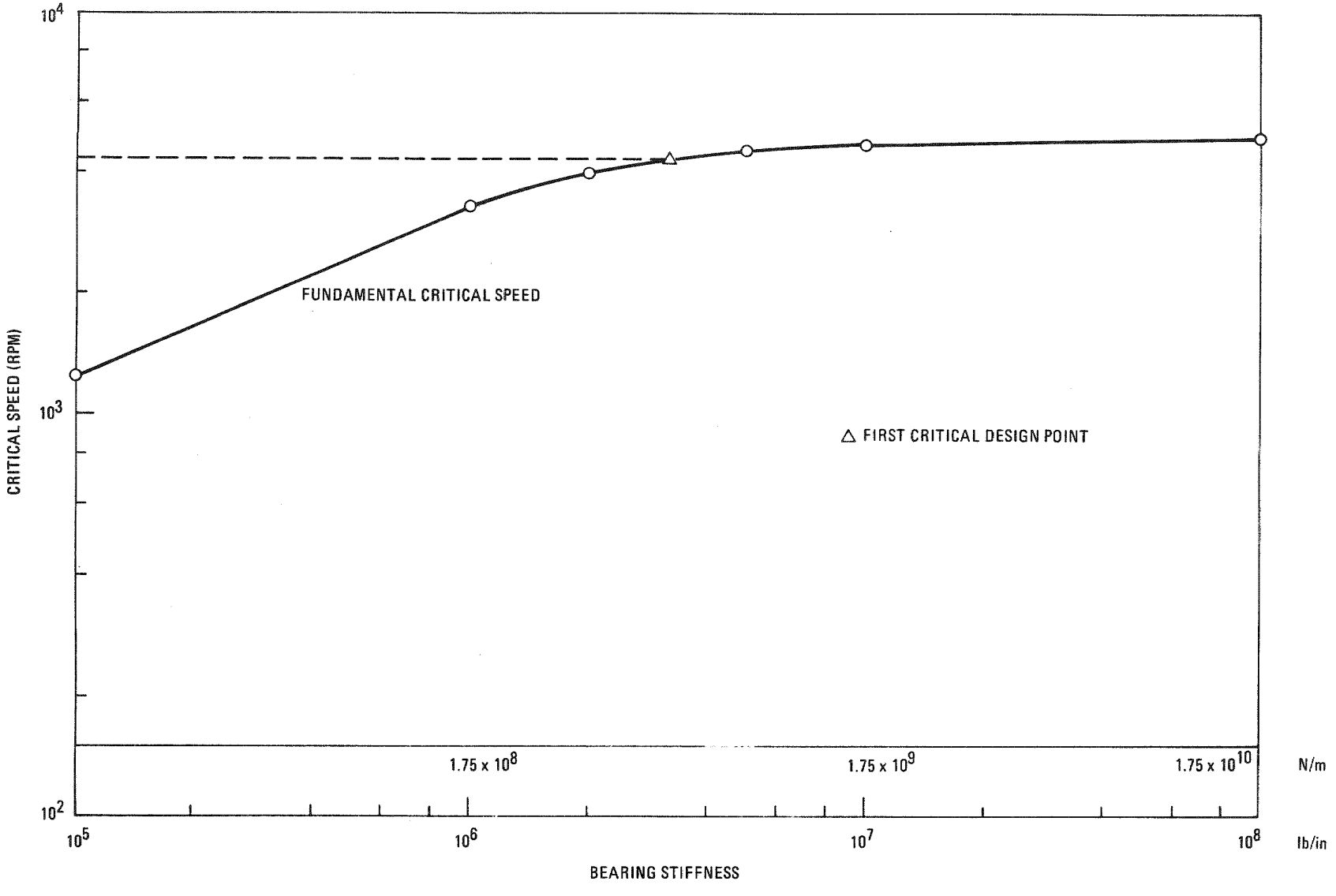

Fig. 10-19. Critical speed map for GCFR electric drive auxiliary circulator

TABLE 10-3
MAIN PARAMETERS OF GCFR HYDRAULIC DRIVE
AUXILIARY CIRCULATOR

Rotational speed (rpm)	5000
Tip diameter [m (in.)]	1.02 (40.2)
Eye diameter [m (in.)]	0.71 (27.88)
Hub diameter [mm (in.)]	240 (9.63)
Tip width [mm (in.)]	140 (5.55)
Shaft diameter [mm (in.)]	247.7 (9.75)
Turbine tip diameter [mm (in.)]	203.2 (8.0)
Turbine eye diameter [mm (in.)]	101.6 (4.0)
Bearing span [m (ft.)]	0.91 (36.0)
Cavity diameter [m (ft)]	0.24 (9.5)

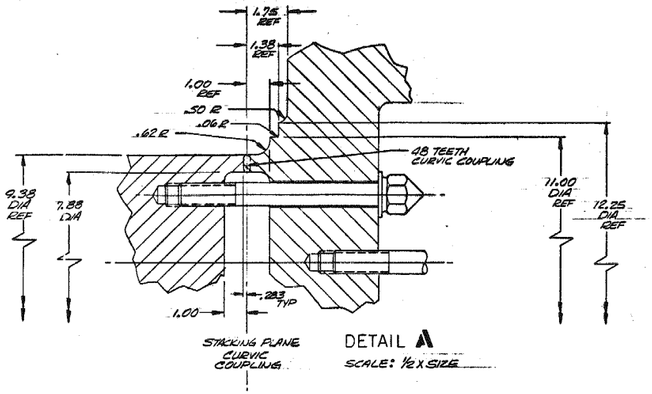

DETAIL A

SCALE: ½ X SIZE

NOTES:

1. GENERAL DATA:
   RPM 5000 RPM MAX
   HORSE POWER 750 HP
   MATERIAL 400 SERIES STAINLESS STEEL
2. THIS DRAWING REFLECTS THE SHAFT ASSY CONFIGURATION USED FOR THE "SCCR AUXILIARY CIRCULATOR, HYDRAULIC DRIVE". FOR INTERFACE INFORMATION REFER TO DRAWING 028446.

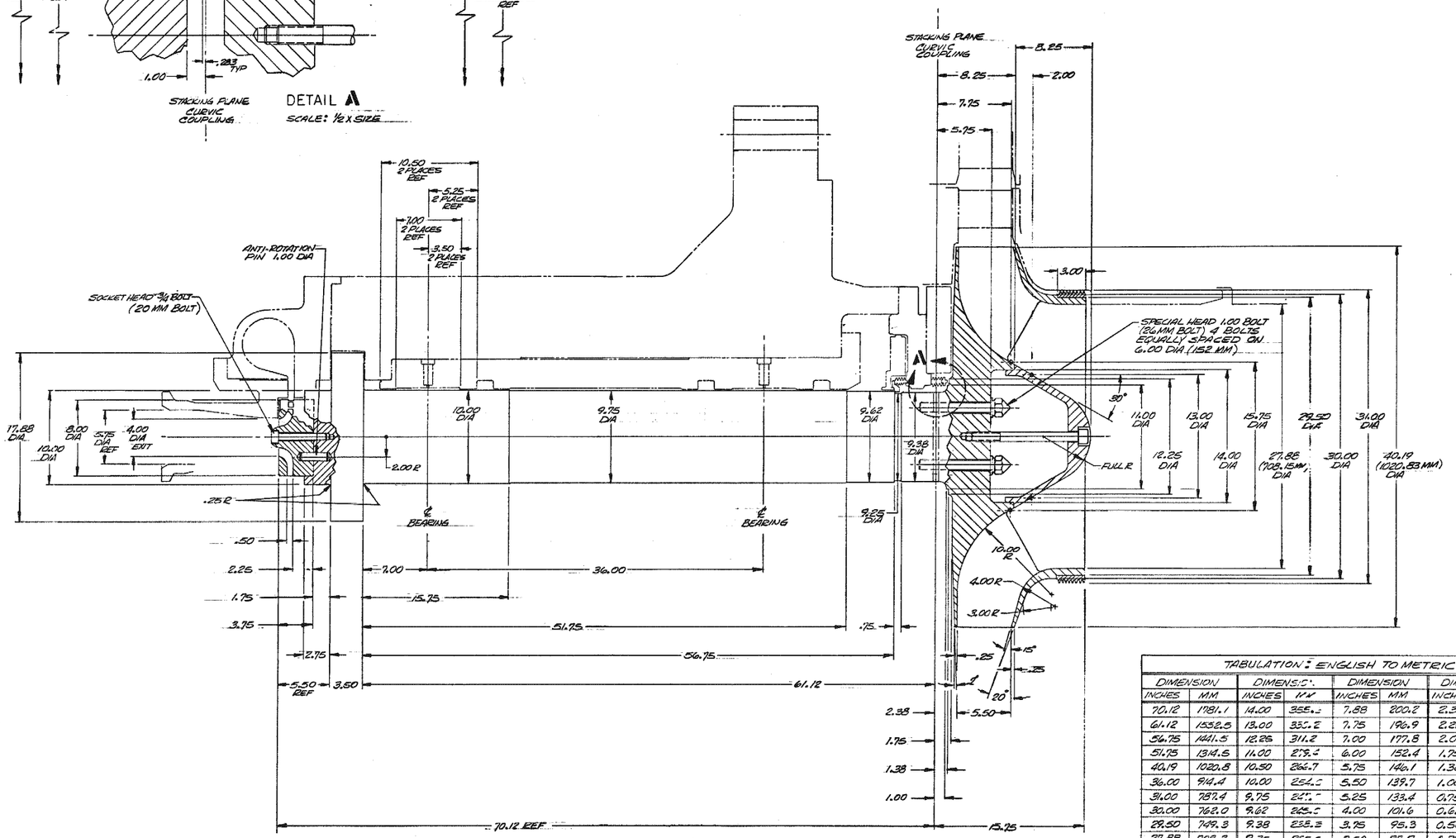

ALL DIMENISONS IN INCHES

TABULATION: ENGLISH TO METRIC

DIMENSION		DIMENSION		DIMENSION		DIMENSION		ANGLE	
INCHES	MM	INCHES	MM	INCHES	MM	INCHES	MM	DEG	RAD
70.12	1781.1	14.00	355.6	7.88	200.2	2.38	60.5	20	0.349
61.12	1552.5	13.00	330.2	7.75	196.9	2.25	57.2	15	0.262
56.75	1441.5	12.25	311.2	7.00	177.8	2.00	50.8	2	0.035
51.75	1314.5	11.00	279.4	6.00	152.4	1.75	44.5		
40.19	1020.8	10.50	266.7	5.75	146.1	1.38	35.1		
36.00	914.4	10.00	254.0	5.50	139.7	1.00	25.4		
31.00	787.4	9.75	247.7	5.25	133.4	0.75	19.1		
30.00	762.0	9.62	244.3	4.00	101.6	0.62	15.8		
28.50	749.3	9.38	238.3	3.75	95.3	0.50	12.7		
27.88	708.2	9.25	235.0	3.50	88.9	0.283	7.19		
17.88	454.2	8.25	209.6	3.00	76.2	0.25	6.4		
15.75	400.1	8.00	203.2	2.75	69.9	0.06	1.5		

Fig. 10-20. Hydraulic drive auxiliary circulator

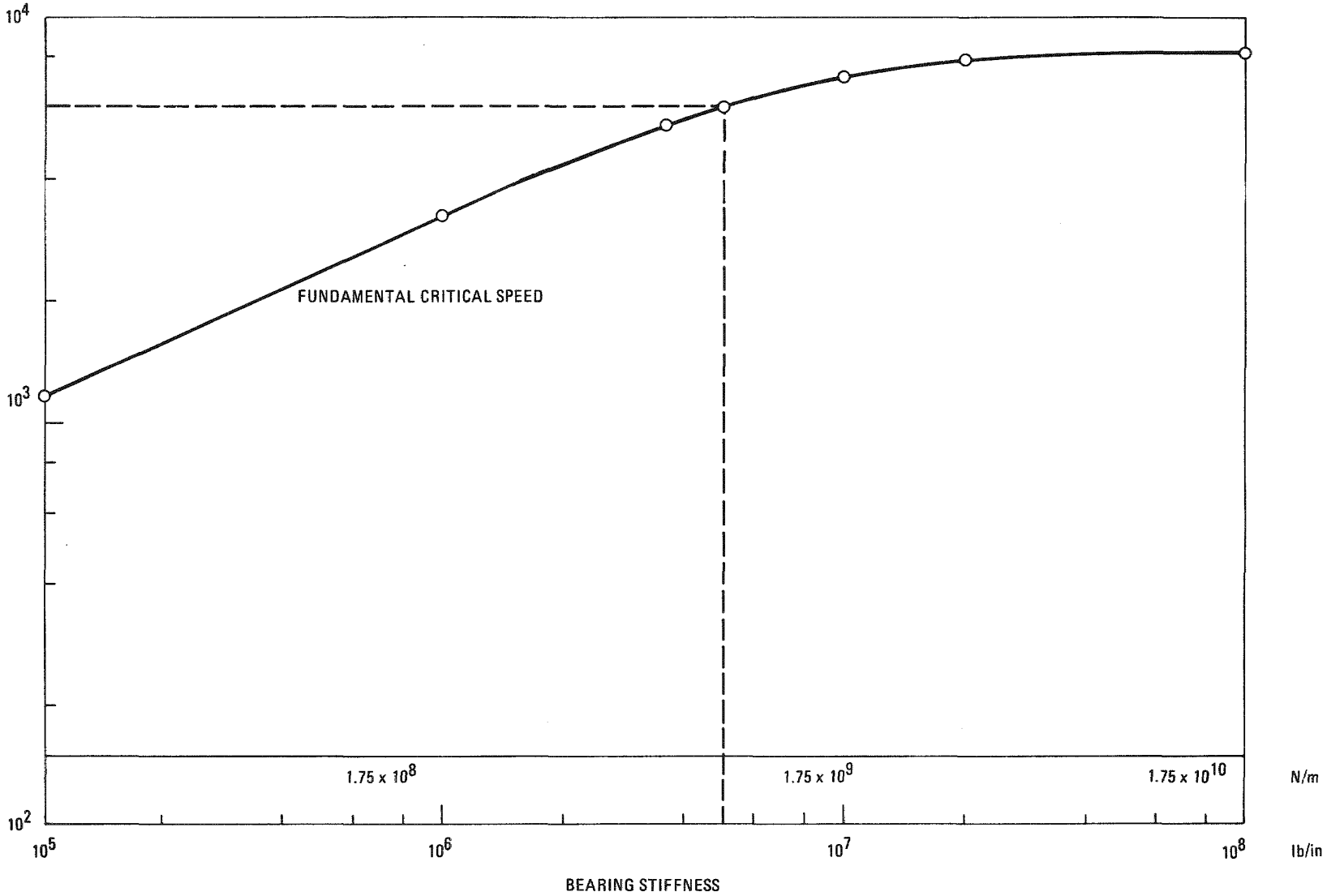

Fig. 10-21. Critical speed map for GCFR hydraulic drive auxiliary circulator

the ratio of the bearing stiffness to the shaft stiffness can be found from

$$\frac{2\,K_b}{K_s} = \frac{1}{\left(\frac{\omega_r}{\omega}\right)^2 - 1} \quad ,$$

where ω_r = rigid bearing critical speed,

ω = critical speed with flexible bearings.

If ω_r = 874.41 rad/s, then ω = 628.32 rad/s, so that $2K_b/K_s$ = 1.07. This is an acceptable value and ensures that a significant proportion of the strain energy of vibration is concentrated in the bearings rather than in the shaft itself. This bearing stiffness is achievable on a 248-mm (9-3/4 in.) shaft.

10.8.3. Core Auxiliary Heat Exchanger

The core auxiliary heat exchanger (CAHE) is designed to remove residual heat from the core during reactor shutdown and/or refueling operations. The purpose of this task is to develop a CAHE to meet the performance, safety, and reliability criteria of the core auxiliary cooling system (CACS).

One of the apparent advantages of an up-flow core plant configuration is the natural convection through the CAHE in case of an emergency. The hot helium will rise to the top of the PCRV, where the CAHE will cool the helium. The cold, or denser, helium falls down through the CAHE by gravity and returns to the core, forming a natural circulation loop for emergency cooling. To achieve a maximum natural circulation effect, the elevation difference between the CAHE and the core should be as large as possible. Because of such considerations, a helical type tube bundle was selected for the up-flow core CAHE study. In general, a helical CAHE is the most compact design of all those under consideration, and therefore it can be placed as high as allowed by the PCRV configuration.

The major concern associated with a helical CAHE is that the large temperature difference between the tube and the bundle support plates generates a large tube thermal expansion bending stress (or bear hug stress). The scope of the task during this quarter was to determine a bundle support method which has an acceptable level of thermal expansion bending stress. A combined heat transfer and structural analysis was beyond the scope of this task, and it is therefore impossible at this time to definitely determine the feasibility of the helical bundle CAHE for the up-flow core.

Three tube bundle support methods were compared based on relative tube thermal stress levels. The simplified analytical methods are based on techniques developed for steam generators. Based on a preliminary comparison of these concepts, it was concluded that helical bundles with radially free plates could provide an acceptable design (Fig. 10-22). Even in this case, the tube thermal bending stresses are satisfactory only if plate temperatures are strongly controlled by the tubes; i.e., closely spaced tubes with good plate contact will be necessary. A more detailed and expanded scope of analysis will be formulated to establish more definitely the feasibility of the CAHE for use in the up-flow core plant configuration.

10.9. HELIUM PROCESSING COMPONENTS

A development plan (Ref. 10-5) was prepared for the helium purification system. This plan details the engineering and design verification and support (DV&S) work necessary to complete the design of the system. The DV&S work will include bench-scale tests in the laboratory to establish the capability of filter media for removing particulates from high-temperature helium. This DV&S work is not required to establish feasibility but rather to determine optimum operating conditions and to size processing components. In addition, base line data have been prepared for the helium purification, pressure equalization, and gas waste systems.

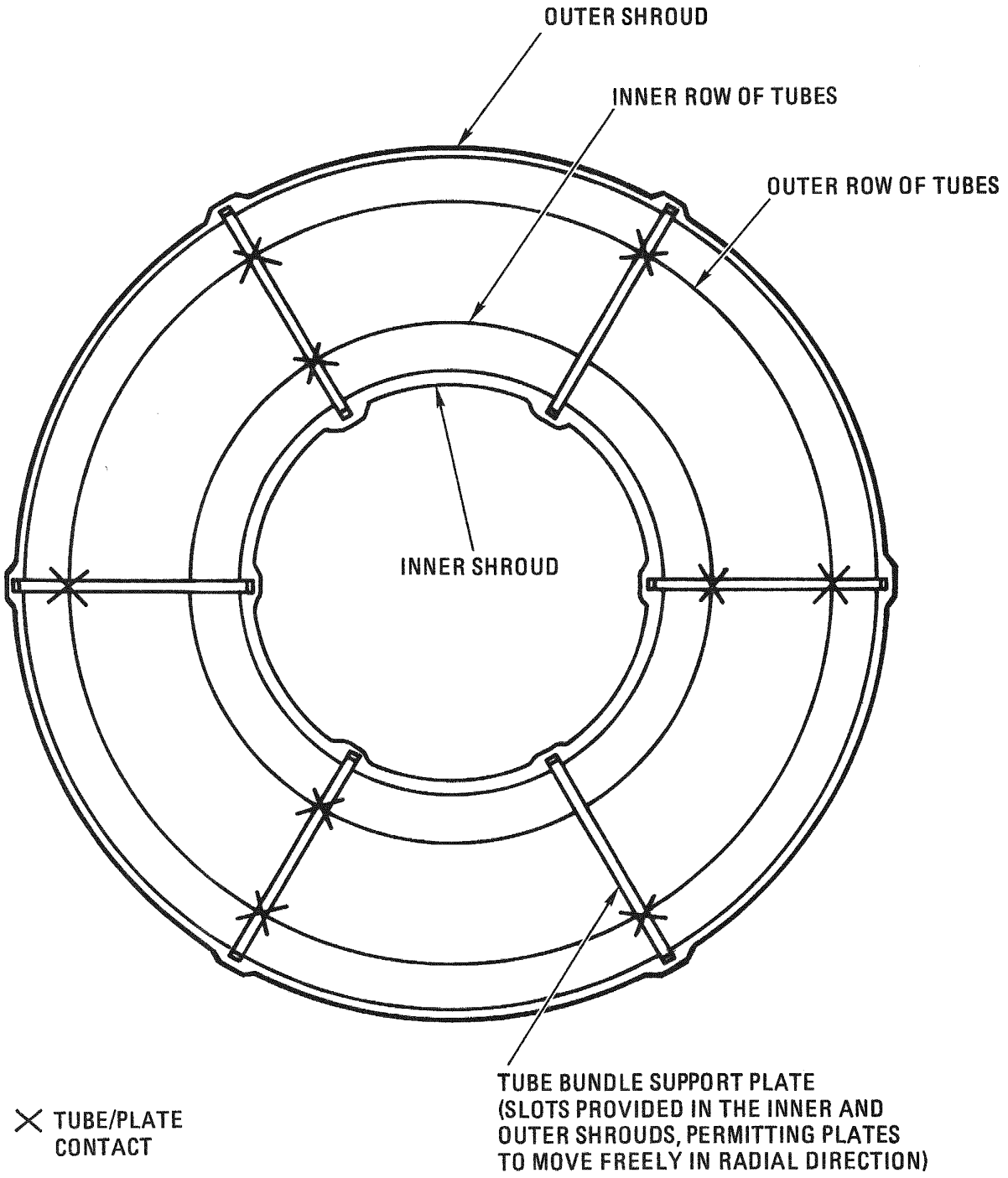

Fig. 10-22. Radially free support plate concept for core auxiliary heat exchangers

10.10. CONTROL AND ELECTRIC COMPONENTS

10.10.1. Main Circulator Electric Drive Study

Westinghouse completed phase 1 of the electric drive study (Ref. 10-6) and has initiated work on phase 2. During phase 1 it was found that the motor design for operation to 4500 rpm with first critical speed outside the operating speed range presents several technical problems such as

1. The requirement for hydrostatic bearings with lubrication supplied at high pressure from a separate, complex service system. These bearings would require a major development program.

2. A rotor which is at the limit of the present state of the art for design and materials.

3. Bearings requiring a very rigid structure which is externally braced against the PCRV.

Although this design is technically feasible, its increased risk, expense, and service system complexity make it undesirable. In addition, this design cannot be extrapolated to larger motors.

As a result of the above considerations, it was agreed that Westinghouse should proceed to develop the design based upon a maximum speed of 3600 rpm with the first critical speed within the operating range. This motor would use external squeeze film and damped tilting pad bearings and could operate at the critical speed without significant vibration amplitude. Westinghouse suggested that commercial plant motors would have to be built this way because preliminary studies indicate the impossibility of having the first critical speed outside the operating range for these large motors.

The controller proposed by Westinghouse is an adjustable-frequency power supply using line-commutated converters with a direct current link. Each controller consists of two parallel systems, each capable of driving the motor, although at reduced speed. The input transformers to these parallel systems are phase shifted to reduce the harmonic currents flowing into the power system. Cooling of the controller is by a closed water system, which results in a considerable reduction in dimensions and other benefits such as reduced acoustic and electromagnetic noise emissions. This type of controller represents a well known technology which is in widespread use throughout the world.

Phase 2 of the electric drive study will refine and optimize the preliminary design of the motor and controller developed in phase 1. In addition, phase 2 will

1. Investigate the feasibility and design of a submerged motor.

2. Investigate the feasibility and design of both external and submerged large commercial plant motors and controllers.

3. Investigate the feasibility of increasing motor voltage and reducing overall length of the motor.

4. Investigate motor mechanical braking, maintenance, in-service inspection, Class I qualification, and potential problems of electromagnetic interference.

5. Define scope, costs, and schedule of the development program required for the proposed damped motor bearing system.

10.10.2. Separation of IE Power Sources: Safety Residual Heat Removal System

The electrical design of the RHR system requires the safety classification of a portion of the main loop cooling system (i.e., the shutdown

cooling system) and the CACS in accordance with the following criteria:

1. No single event shall cause a loss of more than one shutdown cooling system loop and shall not cause the loss of any CACS loops.

2. No single event shall cause the loss of more than one CACS loop and shall not cause the loss of any shutdown cooling system loops.

Figures 10-23 and 10-24 illustrate the separation of IE power sources required to meet these criteria. Six independent IE power systems are needed to power the equipment and the instrumentation and controls of the shutdown cooling system and CACS. Each IE power system includes

1. A standby generator to furnish power on loss of off-site and turbine generator (non-IE) power.

2. A power distribution system to distribute non-IE power and standby generator power.

3. A IE direct current power subsystem.

For the purpose of diversity, it is proposed to use diesel-driven standby generators to power the CACS and gas turbine standby generators to power the shutdown cooling system.

Table 10-4 shows the separation of IE equipment within the shutdown cooling system, CACS, and plant protection system. The table indicates a need for six separation divisions.

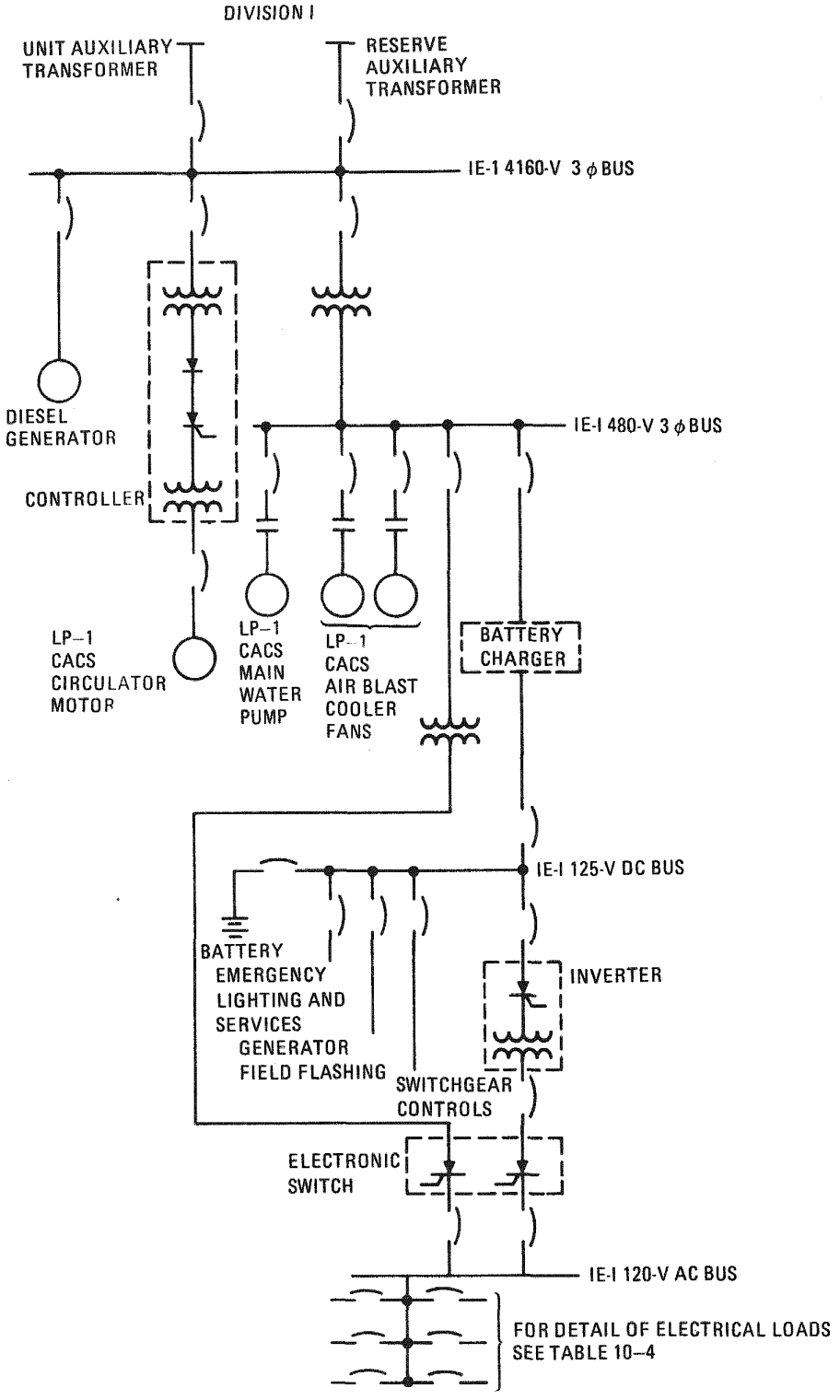

Fig. 10-23. IE power system for loop 1 of core auxiliary cooling system (typical of loops 2 and 3; loop 2 is IE Division II, loop 3 is IE Division 3)

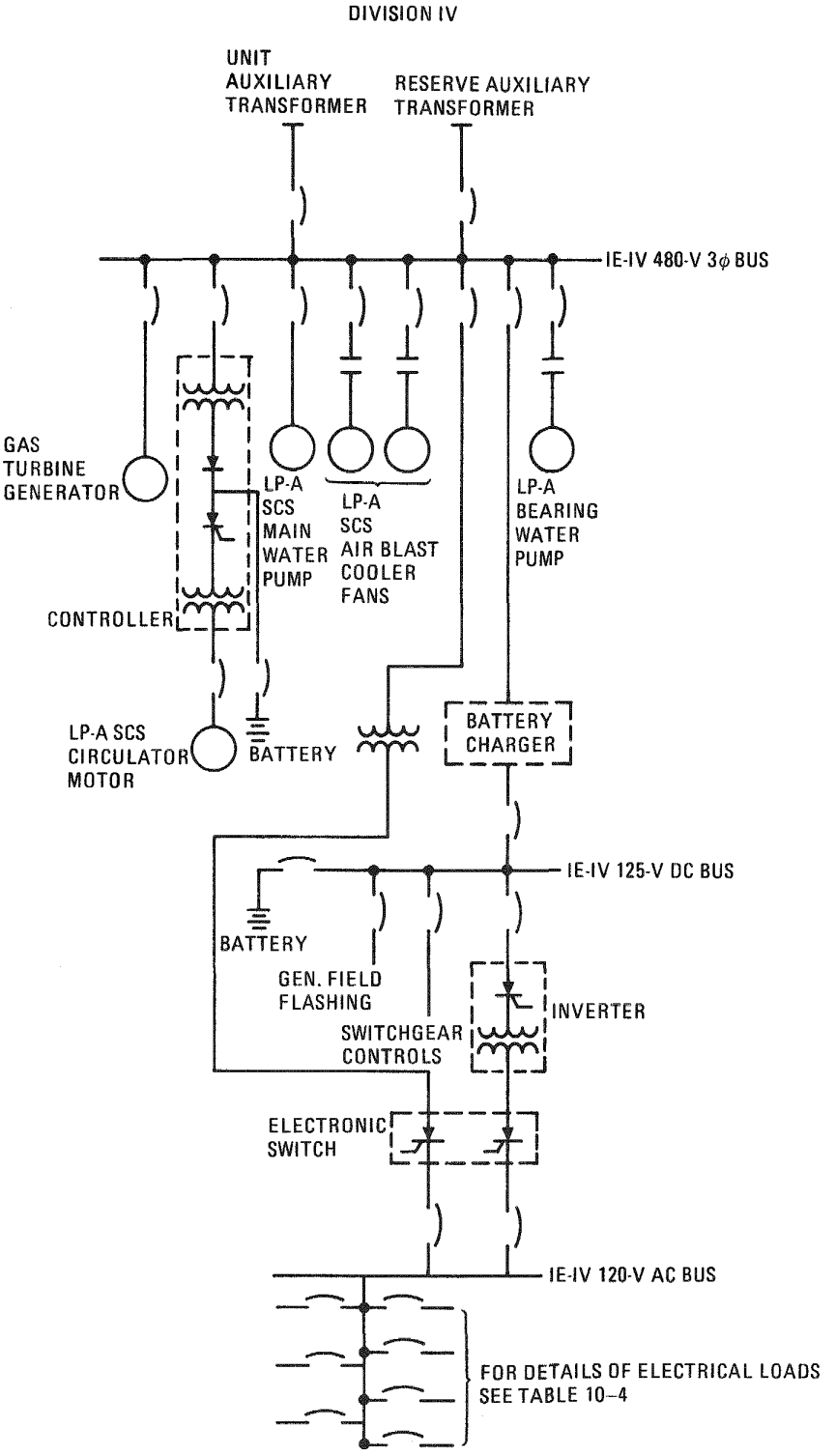

Fig. 10-24. IE power system for loop A of shutdown cooling system (typical of loops B and C; loop B is IE Division V, loop C is IE Division VI)

TABLE 10-4
CLASS IE SEPARATION

I	II	III	IV	V	VI
Primary reactor trip sensors and logic (CH-A)[a]	Primary reactor trip sensors and logic (CH-B)	Primary reactor trip sensors and logic (CH-C)	Secondary reactor trip sensors and logic (CH-D)	Secondary reactor trip sensors and logic (CH-E)	Secondary reactor trip sensors and logic (CH-F)
Control rod in-limit indication (CH-A)	Control rod in-limit indication (CH-B)		Steam generator isolation and dump, loops A, B, and C (CH-D)	Steam generator isolation and dump, loops A, B, and C (CH-E)	Steam generator isolation and dump, loops A, B, and C (CH-F)
Core region outlet temperature, thermocouple (CH-A)	Core region outlet temperature, thermocouple (CH-B)		Main loop shutdown, loops A, B, and C, sensors (CH-D)	Main loop shutdown, loops A, B, and C, sensors (CH-E)	Main loop shutdown, loops A, B, and C, sensors (CH-F)
CACS loops 1, 2, and 3, sensors and logic (CH-A)	CACS loops 1, 2, and 3, sensors and logic (CH-B)	CACS loops 1, 2, and 3, sensors and logic (CH-C)	Main loop shutdown output logic (CH-D)	Main loop shutdown output logic (CH-E)	
CACS loop 1 initiation logic	CACS loop 2 initiation logic	CACS loop 3 initiation logic	Safety rod position (CH-D)	Safety rod position (CH-E)	
CACS loop 1 controls	CACS loop 2 controls	CACS loop 3 controls	Shutdown cooling system loops A, B, and C, sensors and logic (CH-D)	Shutdown cooling system loops A, B, and C, sensors and logic (CH-E)	Shutdown cooling system loops A, B, and C, sensors and logic (CH-F)
CACS loop 1 circulator motor and water loop components	CACS loop 2 circulator motor and water loop components	CACS loop 3 circulator motor and water loop components	Shutdown cooling system loop A initiation logic	Shutdown cooling system loop B initiation logic	Shutdown cooling system loop C initiation logic
			Shutdown cooling system loop A controls	Shutdown cooling system loop B controls	Shutdown cooling system loop C controls
			Shutdown cooling system loop A pony motor and water loop components	Shutdown cooling system loop B pony motor and water loop components	Shutdown cooling system loop C pony motor and water loop components

[a] CH-A = channel A.

10.10.3. Plant Protection System Trip on Core Reactivity and Delayed Neutron Activity

The present plant protection system reactor trip parameters include trips on core reactivity and detection of delayed neutrons in a gas sample of primary coolant from the PCRV. The purpose of the reactivity anomaly trip is to shut down the reactor on core reactivity changes of a few cents which do not correlate with the plant power demand. Reactivity changes of this magnitude occur during the early stage of a core assembly heat-up due to flow blockage, and reactor trip would prevent fuel damage in one or more assemblies. Because of the complexity of this measurement, it can only be implemented by a sophisticated computer system such as the data acquisition and process system, with the end result being operator alarm rather than reactor trip.

Monitoring of fission product activity in the PCRV allows reactor trip upon detection of failed fuel rod(s) in a core assembly and, in that respect, is similar to the reactivity anomaly trip. In this case, the mode of detection is objectionable for two reasons: (1) the equipment is not readily available, (2) the reliability of the BF_3 neutron detectors is questionable. On the other hand, equipment for monitoring beta particles in primary coolant is readily available, and one vendor is in the process of qualifying the instrument to perform safety-related functions. Accident analysis leading to the selection of these two reactor trips will be reviewed to assess the possibility of deleting the reactivity anomaly trip from the plant protection system and substituting a beta monitor for the delayed neutron coolant activity monitor (detection of reactivity anomalies will be performed by the data acquisition and processing system).

10.10.4. Plant Protection System Response to Six Accident Cases

A number of plant protection system parameters were examined in response to six unprotected plant transients: (1) loss of feedwater flow, (2) loss of primary cooling, (3) slow primary coolant depressurization,

(4) DBDA, (5) single rod withdrawal, and (6) single loop trip without rod setback. These can be controlled without plant damage by the following reactor trip parameters:

1. Primary coolant pressure.
2. Main stream pressure.
3. Feedwater flow.
4. Neutronic power to helium flow ratio (P/F ratio).
5. Helium circulator speed.
6. Neutron flux level.
7. Reactor period.
8. Containment pressure.

To speed up the response of the plant protection system and provide diversity of trip functions (particularly in the cases of loss of primary cooling and DBDA, which require reactor trip at 3.2 and 7.2 s after onset of accident, respectively), additional trip parameters are being considered:

1. Primary coolant volumetric flow.
2. Time rate of decrease of helium flow.
3. Time rate of decrease of circulator speed.
4. Loss of circulator drive power.

The effect of instrument accuracy and response time at the trip set points and on plant safety and availability was examined and is illustrated in Figs. 10-25 and 10-26. This was accomplished by using the basic requirements of IEEE Standard 603 and the NRC Regulatory Guide 1.105.

REFERENCES

10-1. "Gas Cooled Fast Breeder Reactor Progress Report for the Period May 1, 1978 Through July 31, 1978," DOE Report GA-A15054, General Atomic Company, August 1978.

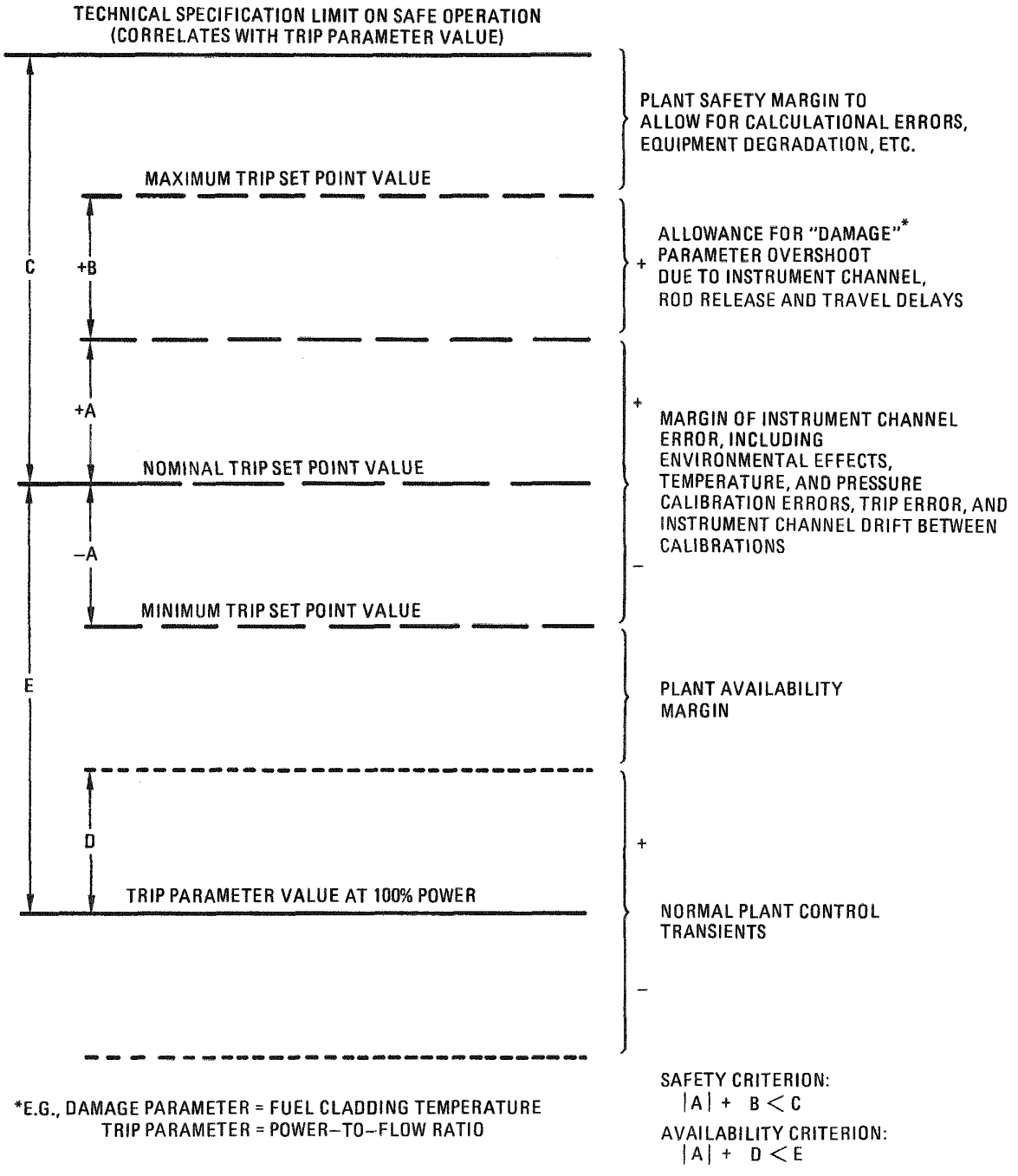

Fig. 10-25. Trip on increase of trip parameter

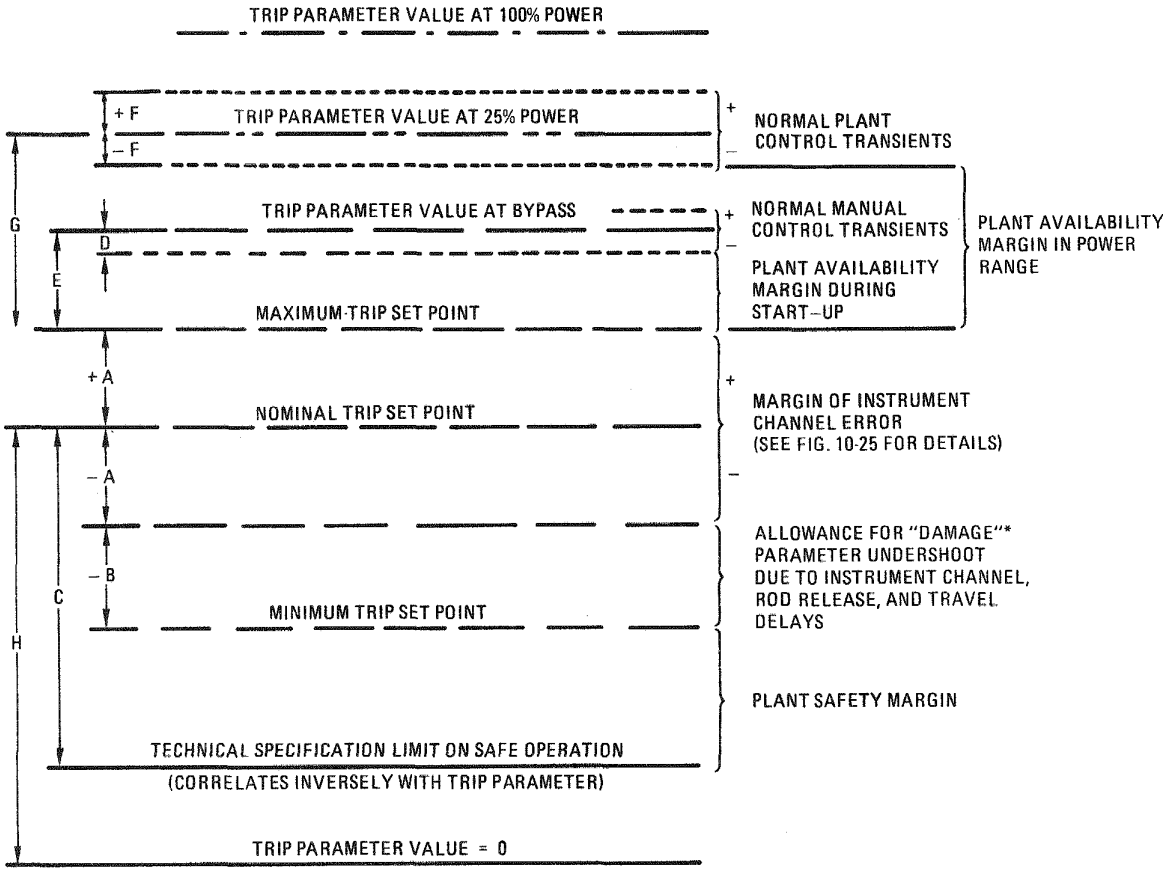

Fig. 10-26. Trip on decrease of trip parameter

10-2. "GCFR Main Helium Circulator Electric Motor Drive Study," Westinghouse LRA Report 6878, June 8, 1978.

10-3. Eckert, B., Kroener's Taschenbuch der Maschinentechnik, v. II, part 2, Kroener, Stuttgart, 1956, Chapter 22.

10-4. "Program PREDM: Multistage Centrifugal Compressor Performance Evaluation," Northern Research and Engineering Report 900AXA-1, July 1, 1974.

10-5. Lengyel, G., "GCFR Helium Purification Development Plan," General Atomic Company, unpublished data, September 26, 1978.

10-6. "GCFR Main Helium Circulator Electric Motor Drive Study," Westinghouse LRA Report 6878, June 8, 1978 (Rev. July 20, 1978).

11. CIRCULATOR TEST FACILITY (189a No. 00586)

The objective of this task is to develop a facility for the development and qualification testing of the GCFR main helium circulator. The scope of this task involves (1) evaluation of alternative test facility concepts in terms of technical feasibility and cost; (2) identification of the most promising test facility concept; (3) determination of an architect/engineer conceptual design; and (4) final design, construction, and checkout of the facility.

During the last quarter, a conceptual design report was prepared (Ref. 11-1) which described the features and costs of a GCFR circulator test facility.

The facility design is based on a site in Sorrento Valley, which adjoins GA. The facility (Fig. 11-1) is on an 85 x 146 m plot of land and consists of a 32 x 36 m building, a switchyard, a transformer station, an air-cooled heat exchanger, a gas storage area, and required driveways and parking areas.

The facility building contains a helium test loop and its associated support systems. The test loop (Fig. 11-2) is contained within a heavy-walled pressure vessel which is internally partitioned to form a continuous helium flow path. The circulator and its drive motor are mounted at the top of the vessel. A diffuser assembly mounted in the upper head of the vessel expands the circulator discharge into the flow circuit and six flow restrictor valves are used to simulate the development plant primary cooling circuit flow resistance. A helium/Dowtherm G heat exchanger, arranged around the inner wall of the vessel, removes the heat generated by compression of the helium.

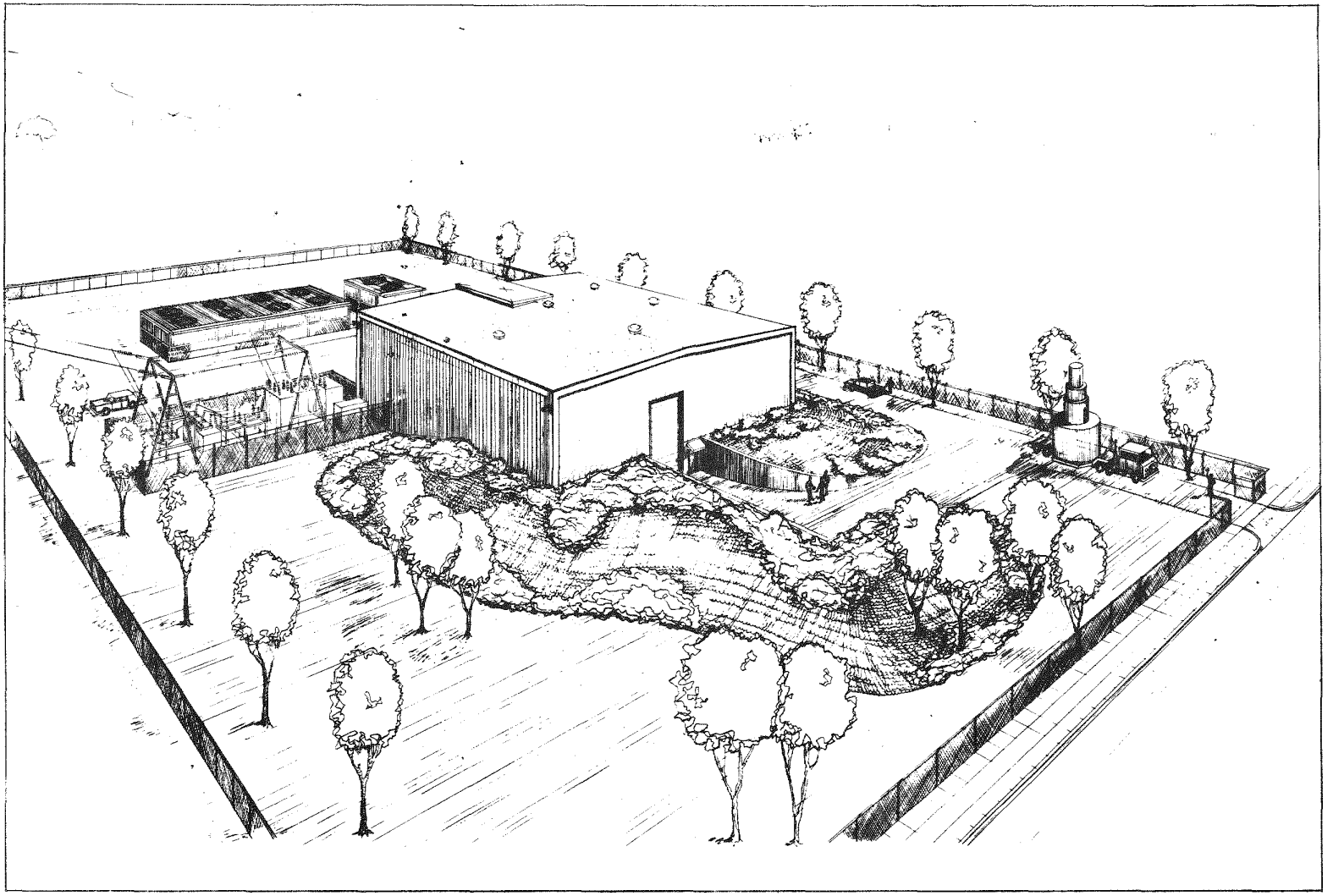

Fig. 11-1. GCFR helium circulator test facility

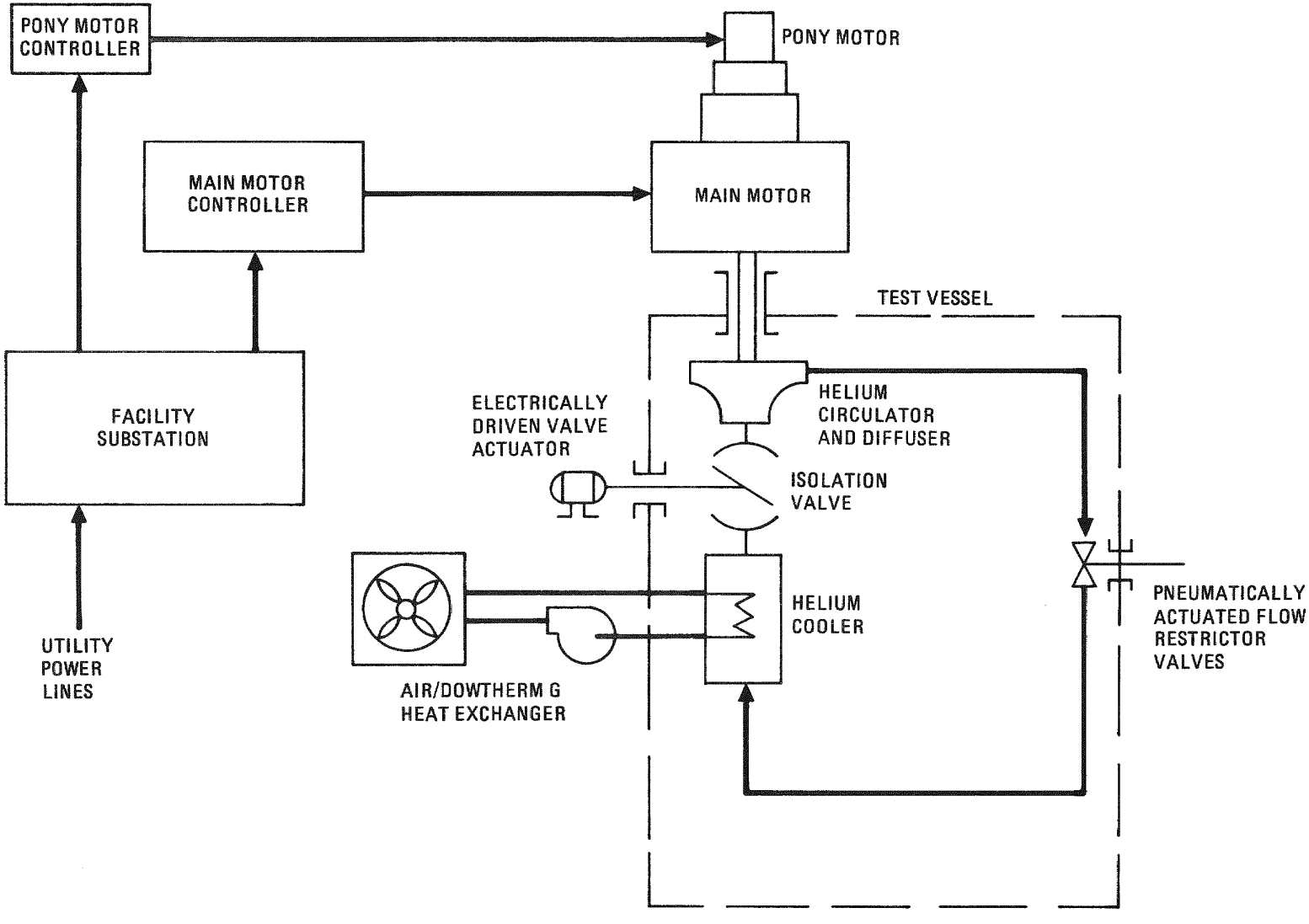

Fig. 11-2. Schematic diagram of GCFR helium circulator test facility

The circulator drive consists of a main motor and a pony motor. The main motor is a 24,000-hp brushless exciter, synchronous machine rated for full-power operation at 3600 rpm. The pony motor, which is coupled to the top end of the main motor shaft, is a three-phase induction motor rated at 300 hp and designed for operation over a speed range of 150 to 1800 rpm. An overrunning clutch is built into the pony motor to prevent rotation when the main motor is operating. The main motor controller is a large solid-state thyristor device which converts 60-Hz alternating current to direct current and then reconverts it to variable-frequency alternating current to power and control the circulator motor. Electrical power for the pony motor is supplied by a separate controller.

The facility building is a steel-framed structure with insulated metal siding and roofing. It has a high central main bay flanked by two-story sections. A test pit is located at one end of the central bay to house the test vessel, and a motor disassembly pit is located adjacent to the test pit. Storage space for a motor and a radial compressor assembly is also included in the central bay area. A 90,710-kg overhead crane runs the full length of the central bay. The remainder of the ground floor is occupied by (1) a high-ceiling, controlled-environment room for disassembly and maintenance work; (2) a mechanical equipment room which houses an air compressor; (3) heating, ventilation and air conditioning (HVAC) and water treatment equipment; (4) a control room and an office; (5) a forklift truck room; (6) a small machine shop; and (7) a storage room and locker and toilet facilities. The second floor is occupied by an electrical equipment room which contains switchgear, motor control centers and panel boards, a battery room, and a room with main and pony motor controllers.

The facility described in Ref. 11-1 was produced on a schedule which did not permit a full cost optimization. Consequently, efforts are currently being directed toward updating the design, which will improve the cost effectiveness of the facility. A statement of work describing the work to be done has been prepared and sent to Ralph M. Parsons Company

for a cost estimate, and Parsons has been requested to do the following:

1. Update the facility design to reflect the latest circulator, electric motor, service system, and motor controller requirements.

2. Investigate areas of potential cost reduction and evaluate their merit.

3. Produce an updated design report describing the changes and associated costs.

These activities are scheduled for completion by late December.

REFERENCE

11-1. "Gas-Cooled Fast Breeder Reactor - Conceptual Design for a Helium Circulator Test Facility," DOE Report GA-A14999, General Atomic Company, June 1978.

12. PLANT DYNAMICS (189a No. 00586)

12.1. CONTROL SYSTEMS

To provide a basis for analyzing plant/control system interaction, an on-load control system is being developed for the three-loop demonstration plant. This plant, incorporating the electric-motor-driven helium circulators, and the location of the measured quantities used for control are schematically shown in Fig. 12-1. The structure of the control system is shown in Fig. 12-2. At present, the steam reheat, low-pressure turbine, electrical generator, and condensate control functions are not being considered. The objectives of this control system are (1) to maintain set point values of main steam temperature and pressure in the main steam header upstream of the high-pressure turbine throttle valves, (2) to regulate reactor power relative to main turbine load, and (3) to balance the plant load between the three steam generators. The system satisfies these objectives by (1) using the reactor control rods to control reactor power and main steam temperature, (2) adjusting the boiler feed pump turbine valve area to control feedwater flow and main steam pressure, and (3) varying the speed of the helium circulator motors to maintain helium flow proportional to feedwater flow and to balance the thermal load of the three steam generators.

12.1.1. Main Steam Temperature and Neutron Flux Control

The inlet temperature to the high-pressure turbine is controlled throughout the normal load range by adjusting reactor power. This is accomplished by measuring the steam temperature at the turbine inlet, conditioning the signal, and generating a neutron flux demand signal which, when added to a flux signal derived from turbine first-stage pressure, forms the flux controller demand. The flux controller then adjusts the position of the control rods to vary reactor power. The flux demand

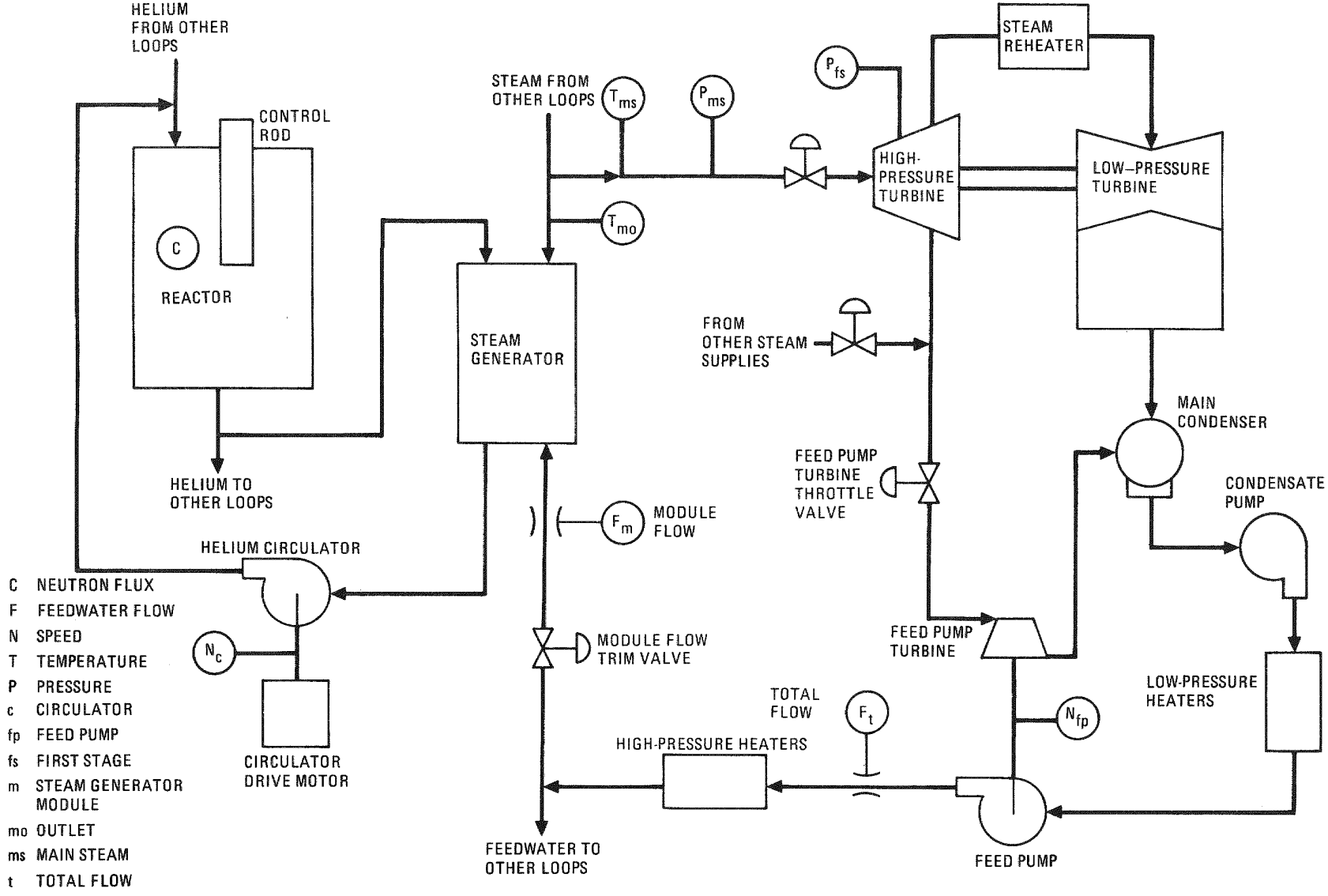

Fig. 12-1. Plant schematic indicating control system measurements

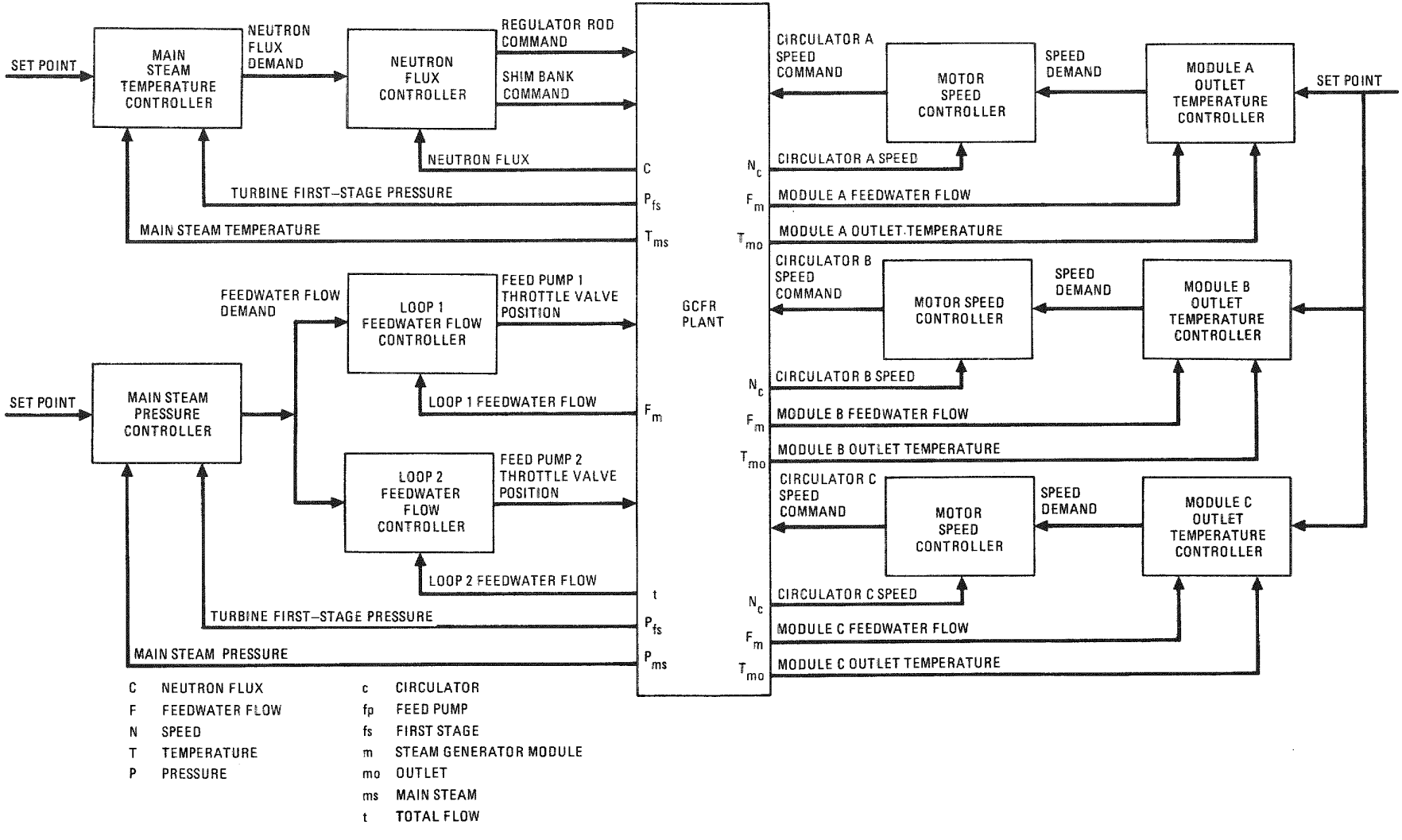

Fig. 12-2. Control system structure

is limited to prevent excessive flux excursions, and the output of the temperature controller is limited so that the neutron flux demand cannot substantially vary from the value commanded by the flux signal. These features are desirable to prevent large excursions in reactor power in the event of a controller or sensor failure.

12.1.2. Main Steam Pressure and Feedwater Flow Control

The pressure of the steam at the inlet of the high-pressure turbine stop valves is controlled throughout the normal load range by manipulating feedwater flow. A total feedwater flow demand is generated from a turbine load signal and the main steam pressure controller output. During load changes, the steam mass flow rate (equivalent to load) is varied using the turbine throttle valves. To maintain a constant main steam pressure at the inlet of the throttle valves, a steam/feedwater mass flow rate balance must be preserved. Thus, for a change in load or other secondary disturbance, the load signal (as measured by the turbine first-stage pressure) adjusts the feedwater flow rate in anticipation of a change in main steam pressure. The pressure controller then "fine tunes" the main steam pressure to its set point value. The feedwater flow controller compares the feedwater flow command with measured feedwater flow and maintains the flow at its demanded value. The compensated feedwater flow signal controls the position of the feed pump turbine valve, which in turn varies the speed in each steam-driven feed pump to produce the required feedwater flow.

12.1.3. Steam Generator Module Outlet Temperature and Helium Circulator Speed Control

The circulator speed demand signal contains two components. One is a functional relationship designed to maintain helium flow through each steam generator in a fixed proportion to the feedwater flow through that steam generator for the normal plant load range. The other is based on a set point computed to be the average of the three measured steam generator outlet steam temperatures. This average temperature is compared with the actual outlet temperature in a particular loop to obtain the temperature

error signal for that particular loop. In effect, this temperature error signal acts as a trim function on the helium flow to maintain the steam temperature at the outlet of each steam generator module near the average outlet temperature for the three modules.

Circulator speed is regulated by a closed-loop motor speed controller. Both the amplitude and frequency of the voltage applied to the motor are varied to control motor speed. Mechanization of this controller is strongly dependent on the characteristics of the particular motor designed for this application. At present, the motor is assumed to have an ideal speed controller.

12.2. SEISMIC ENGINEERING

A detailed seismic model comprising the reactor confinement, reactor containment building, PCRV, core, core support, and various equipment has been generated, and the seismic analysis of this model is in progress.

12.3. FLOW-INDUCED AND ACOUSTICALLY INDUCED VIBRATIONS

There was no activity on this subtask during this quarter.

13. REACTOR SAFETY, ENVIRONMENT, AND RISK ANALYSIS (189a No. 00589)

The purpose of this task is to investigate and quantify GCFR safety characteristics. A liaison and coordination subtask integrates the DOE-sponsored GCFR safety work at GA and the national laboratories into a national GCFR safety program which is responsive to the need for GCFR safety research. A GCFR safety program plan is being developed to define the safety research and schedule needed for a 300-MW(e) plant. Safety research at GA includes probabilistic accident analysis, core accident consequence analysis, postaccident fuel containment (PAFC) analyses, and radiological/environmental analyses. During this quarter the relative safety of the up-flow and down-flow GCFR concepts was assessed.

13.1. REACTOR SAFETY PROGRAM COORDINATION

13.1.1. Safety Evaluation of Up-Flow Core

The safety characteristics of the up-flow core are determined to a large degree by both the opposite direction of the core coolant flow and gravity and the support of the core from below. Since the heat sink is located at a higher elevation than the core, cold helium with a relatively high density flows in the direction of gravity, inducing the potential for natural coolant circulation as a backup heat removal mechanism and increasing core cooling reliability after shutdown. In the event of a core disruptive accident (CDA), however, debris generated in the core and ejected from the fuel assembly by the coolant stream would be returned by gravity to the core and deposited on the core against any residual helium flow. The massive lower core support structure would aid in accumulating the debris. This mechanism may lead to a potential for radial core damage propagration and recriticality. Another aspect of a bottom-supported core is related to PAFC in a reactor vessel designed without bottom penetrations.

The safety characteristics of a GCFR with a bottom-supported core and upward coolant flow direction are discussed below. An important aspect when comparing the up-flow versus down-flow core is the experience gained from established reactors. This is especially true for safety-related questions. Thermal reactors [advanced gas-cooled reactor (AGR), boiling water reactor (BWR), and pressurized water reactor (PWR)] and fast reactors have an impressive record of safe operation for bottom-supported fuel assemblies with up-flow cooling. Although experience under different conditions and in different reactor types cannot be directly applied to the GCFR, it should be taken into account in a comparative evaluation.

For the safety assessment, it was assumed that the up-flow configuration has a standing core located at the bottom of the core cavity and the reactor is refueled from the top of the core.

13.1.2. General Safety Assessment

During normal operation, gravity-induced cooling effects have no influence on the performance of the reactor. At very low flow rates (below the operational envelope), substantial redistribution of the coolant flow in a down-flow core may result in partial flow reversal and instabilities. Cladding temperatures could exceed safety limits under these conditions. A comparable effect does not exist in the up-flow core. However, flow instabilities in the down-flow core occur only at a very low flow rate, such that cladding melting is predicted prior to the onset of flow instabilities.

The reactivity feedback of fuel assembly bowing at power is negative in top-supported, cantilevered core without bottom or lateral restraint. A lateral core restraint results in a complex pattern of interaction between the core assemblies with reactivity effects that are more difficult to predict. Clamping planes are selected such that negative reactivity effects result from increases in core temperatures.

With respect to seismic excitation, the high natural frequency of a laterally restrained core offers the advantage of a low sensitivity to motion induced by earthquakes. The absence of a shear plane between the core and the control rods in the down-flow core improves the reliability of shutdown during an earthquake with strong lateral acceleration components.

The consequences of a depressurization accident depend only moderately on the coolant flow direction in the core. In the event of a leak in the central cavity, helium at core outlet temperature is discharged into the containment building. This results in a smaller depressurization rate, a higher containment atmosphere temperature after blowdown, initially a higher coolant back pressure, and lower cladding temperatures during depressurization. Since the maximum cladding temperatures in the core are reached after the end of blowdown, the influence of the location of the leak on the severity of the accident is not expected to be very strong. If a mechanical fuel assembly hold-down is provided, the pressure difference across the reactor core induced by the depressurization cannot cause assemblies to move or jeopardize the integrity of the core.

During refueling, the impact of an accidentally dropped fuel assembly would cause damage to other assemblies in a bottom-supported up-flow core. However, cooling of the lost assembly would be better if the assembly came to rest on top of the up-flow core rather than on the bottom of the PCRV as in the down-flow version.

13.2. PROBABILISTIC SAFETY ANALYSIS: RELIABILITY EVALUATION OF RESIDUAL HEAT REMOVAL BY NATURAL CIRCULATION

The incremental reliability advantage of residual heat removal (RHR) by natural circulation is an important parameter in comparing up-flow and down-flow designs. A meaningful estimate of the improvement in RHR reliability due to natural circulation requires a reliability analysis of the dominant event sequences that lead to a demand for RHR by natural convection systems. These reliability estimates must be related to a broad spectrum

of plant conditions to determine the net RHR reliability improvement for natural circulation. Event sequences leading to a demand for natural circulation to prevent core meltdown can be grouped into three categories as follows:

1. Failure of RHR support systems needed for forced circulation RHR but not needed for natural circulation RHR (i.e., circulator support systems, etc.).

2. Loss of all electrical power for circulating helium, water, and air (i.e., loss of off-site power, turbine generator power, emergency diesel power, and 2-h battery power).

3. Common mode failure of all components for circulating helium, water, or air in both the main loop and the core auxiliary cooling system (CACS) loops.

The limited analysis performed to date indicates that a significant improvement in long-term main loop RHR reliability owing to a natural circulation capability can only be accomplished if the main loop RHR systems are made to be fully naturally circulating between the core and the ultimate heat sink with only structural components shared. Natural circulation on the helium side alone will not significantly enhance reliability. In the context of the current main loop RHR design, this would require natural circulation of the primary, secondary, and tertiary heat removal systems with all actions required to establish circulation accomplished with stored energy such as batteries or accumulators. The major limitation of a main loop natural circulation RHR concept for a pressurized PCRV is the unavailability of the steam generator.

A natural circulation capability on only the helium side can improve short-term main loop RHR reliability by extending the inherently reliable main loop RHR time from main circulator coast-down time to steam generator depletion time. By providing a reliable water supply which depends only

on stored energy (tank with battery-powered shutdown feed pump or stored gas tank pressurizer), the inherently reliable main loop RHR function can be extended to several hours if steam release to the atmosphere is the ultimate heat sink.

13.3. CORE ACCIDENT ANALYSIS

13.3.1. Core Disruptive Accident Consequences for Up-Flow Versus Down-Flow Concepts

The comparison of the up-flow and down-flow core designs with respect to core disruptive accident (CDA) consequences includes an assessment of expected accident consequences as well as an assessment of the potential for consequence mitigation by core design features selected to enhance early accident termination. Accordingly, the CDA assessment includes the following elements:

1. By quantitative and qualitative assessment, determination of a range of fuel vapor fractions and energy releases for the up-flow and down-flow configurations with no consideration of accident mitigation features.

2. Determination of the feasibility of employing recriticality-averting [protective loss of flow (PLOF) accident] features for both configurations.

3. Assessment of the differences in damage propagation potential and likelihood of complete assembly flow blockage.

This strategy recognizes that accident consequences can be significantly reduced by early draining of molten fuel and steel from the core.

Consequences will be assessed in terms of fuel vaporization and energy release. This assessment will consider the following four event classes that lead to CDA conditions:

1. PLOF.

2. Loss of flow (LOF).

3. Transient overpower (TOP).

4. Complete flow blockages in a single assembly.

The CDA assessment program is shown in Fig. 13-1.

13.3.2. Protective Loss of Flow Accident Analysis

A PLOF is an accident initiated by a loss of all forced circulation in the GCFR either while the reactor is shut down or concurrent with reactor shutdown. Figure 13-2 summarizes the expected sequence of events and the key uncertainties which limit a complete understanding of the accident sequence and consequences and highlights the differences and similarities between the up-flow and down-flow concepts.

Following loss of power to the main helium circulators, they coast down under their own inertia. The CACS is presumed to be inoperative, but shutdown has occurred, so that power generation is due to decay heat. The times at which various phenomena occur are given their relative values only; they are estimates based on a 40-s coast-down from full to laminar flow and then an instantaneous flow reduction to zero. Approximately 2 min after the initiating event, the cladding begins to melt. In a down-flow core, any residual flow would aid gravity in the flow of a molten cladding film downward toward the lower axial blanket. Possible natural convection flow in an up-flow concept would not generate enough drag forces to overcome the downward pull of gravity. The cladding would ultimately reach the lower axial blanket where it would freeze. The amount of cladding which would melt in the core over a period of 3 to 4 min would be sufficient to block all coolant channels in the core except, perhaps, the channels bounded by duct walls.

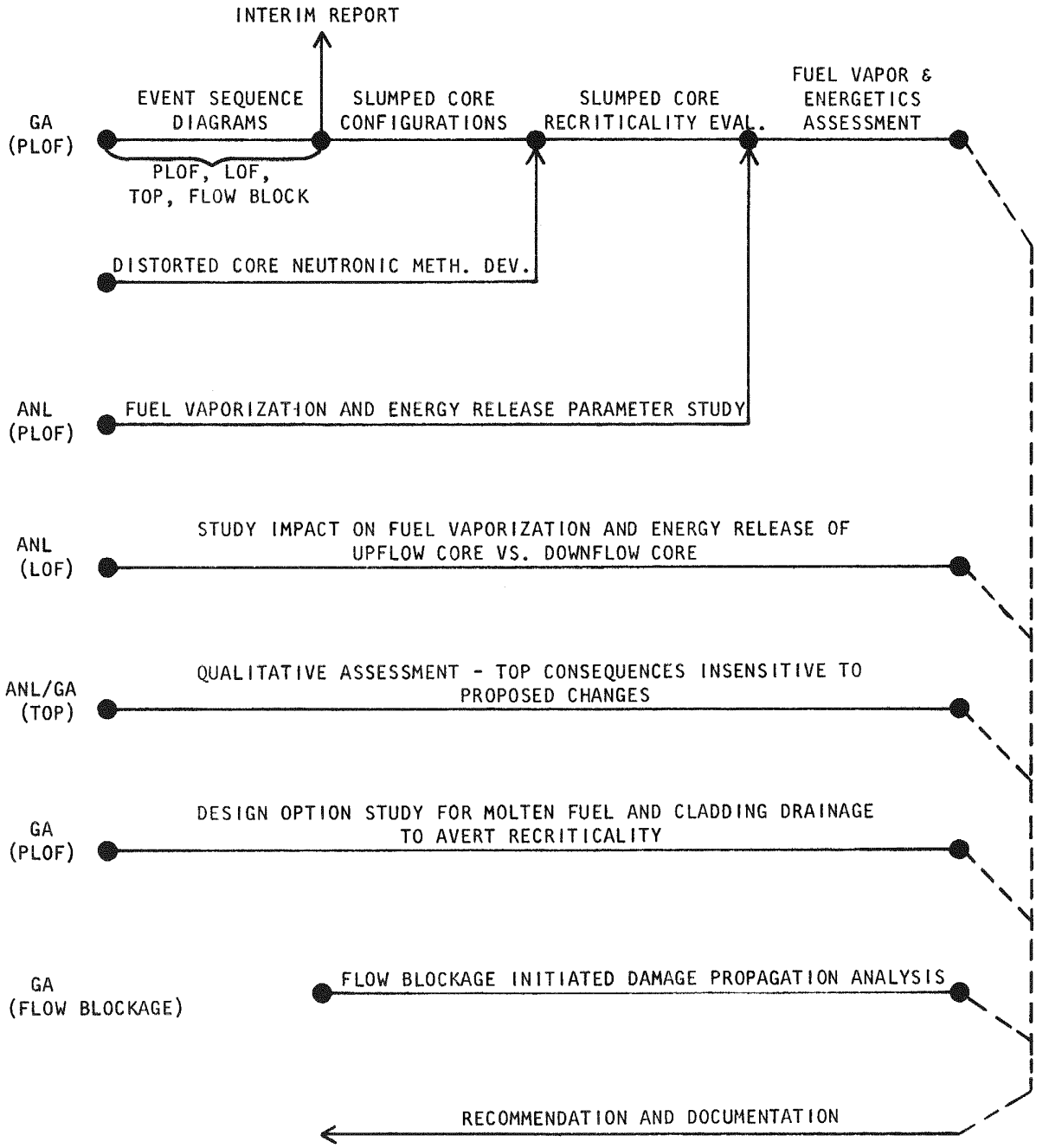

Fig. 13-1. Up-flow/down-flow core disruptive accident assessment program

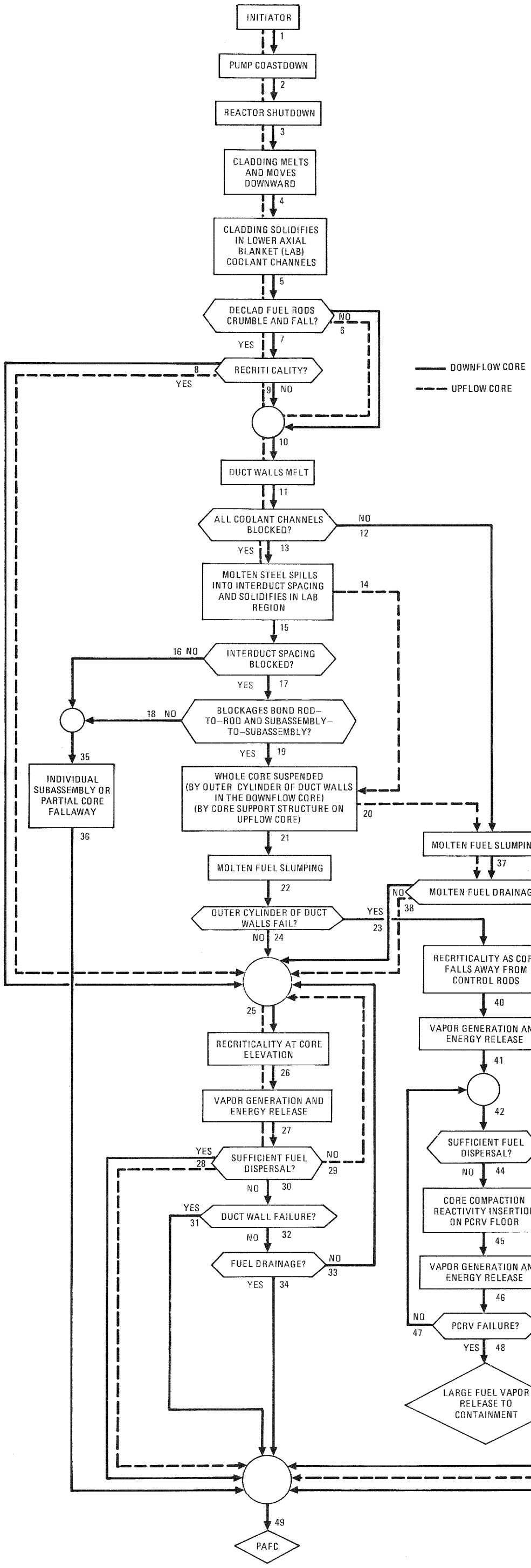

Fig. 13-2. PLOF event sequence diagram

Following decladding of the core, fuel columns would be left standing, at least temporarily. While they stood, the direct radiative heat transfer to the duct walls would cause the duct walls to melt. In the absence of any flow, the hottest duct wall would begin to melt within 4 min. The axial and azimuthal progression of the melt front in the duct walls would provide sufficient molten steel to block the remaining open channels in the lower axial blanket. An important difference between a top-mounted core (down-flow) and a bottom-supported core (up-flow) may be in the possibility of providing drainage paths for molten steel (and later molten fuel) to prevent blockage. The top-mounted core may more readily provide such drainage paths than the bottom-supported core because of the lack of a large lower core support structure.

Following decladding of the core rods, some of the fuel columns would be subjected to large temperature gradients across their diameters. The resultant thermal bowing and the interaction with the end supports, duct wall, and other rods might cause the fuel columns to break and/or crumble. Thus, there is a possibility of early recriticality. This is a current uncertainty in determining the sequence of events. The remaining description assumes that early recriticality would not occur and that the lower axial blanket channels would become completely blocked by solidified cladding.

Molten steel from the melting duct walls would fill the lower axial blanket coolant channels and backfill the void spaces in the core. Back-filling would continue until the molten steel level reached the elevation of the duct wall hole. Thereupon the molten steel would spill into the interduct spacing, flow down the outer duct wall face, and refreeze below the core level. Ample molten steel inventory would be available to completely block the flow paths between ducts at a level below the core bottom. If the blockages occurred, they might bond one subassembly to another such that, in the extreme, the entire down-flow core might become suspended by the outer cylinder of the duct walls adjacent to the radial blanket. However, whole-core suspension is not a foregone conclusion in

a down-flow core. Blockages may be prevented by design features that enhance molten steel drainage. Even without such design, asymmetric heat-up may allow groups of subassemblies to fall to the PCRV cavity floor. The core support structure in the up-flow concept would prevent subassembly relocation and make design provisions for steel drainage more difficult to achieve.

At about 6 min into the accident, well after the bulk of steel relocation and freezing, fuel would begin to melt and slump. The GCFR up-flow concept would allow collection of the slumped fuel upon steel blockages or solidifying of molten fuel-induced channel blockages somewhere between the core bottom and the core support plate. In the absence of design provisions which prevent blockages, fuel slumping, compaction, and loss of control poison due to dissociation by thermal attack will lead to a recriticality. In a standing core, drainage will be difficult to achieve, and similar to the LOF accident in an LMFBR, a "boiled-up" core scenario with repeated energy release events may be envisioned. In the extreme, the down-flow core may also produce this scenario. However, design provisions which ensure open flow paths for molten fuel and steel drainage are relatively easy to attain with minimal performance penalties. Recriticality may, therefore, be completely averted with a down-flow core concept.

In the absence of design provisions for fuel drainage, the down-flow core would be subject to another recriticality sequence. The whole core could become suspended by the interaction of steel blockages such that the support would be provided by a cylinder created by the duct walls adjacent to the radial blanket. These duct walls would eventually reach a temperature at which they could no longer support the total core weight. This could occur as soon as 8 to 9 min after accident initiation. The core could then fall away from the control rods, through the space between the core and PCRV floor, and impact upon the PCRV floor. This hypothetical situation could conceivably cause a fuel compaction such that large amounts of fuel vapor and thermal energy would be generated.

Based on the current status of the evaluation, the up-flow core concept is expected to lead inevitably to fuel-slumping-induced recriticality and a "boiled-up" core with substantial fuel vapor generation. This would occur as a result of a PLOF in the absence of features specifically designed to eliminate this situation. This may also be true for the down-flow concept. However, a first recriticality burst of sufficient magnitude may open flow paths by dynamic failure of the blockages, and dynamic failure of duct walls may occur from the first burst. The down-flow core also has the potential for fallaway of the whole core or portions of the core. It is expected that specific provisions for molten steel and fuel drainage will be easier to design for the down-flow concept without substantial performance and/or cost penalties. If successful, these provisions would eliminate recriticality, leading directly to PAFC conditions with little or no vapor generation.

13.3.3. Loss of Flow Analysis

A loss of flow accident is a circumstance in which concurrent failures are postulated in the primary coolant circulation and reactor shutdown systems. Loss of heat removal from the core may arise from faults in either the helium circulation equipment or the feedwater system. Figure 13-3 summarizes the expected sequence of events and key uncertainties which prevent an adequate quantification of the accident consequences. Figure 13-3 also highlights the differences and similarities between the up-flow and down-flow concepts.

Loss of flow accidents starting from full power would proceed to cladding melting but not duct melting prior to fuel melting. The cladding would relocate downward in a down-flow core, generating a positive feedback of less than \$5/s, and would cause an order of magnitude or more increase in power; however, it would not induce a prompt-critical burst. The rate of cladding relocation might be influenced by residual flow during a depressurization or by circulator coast-down. The up-flow core would provide a retardation of the rate of downward cladding relocation owing to circulator coast-down, and residual flow in the down-flow core

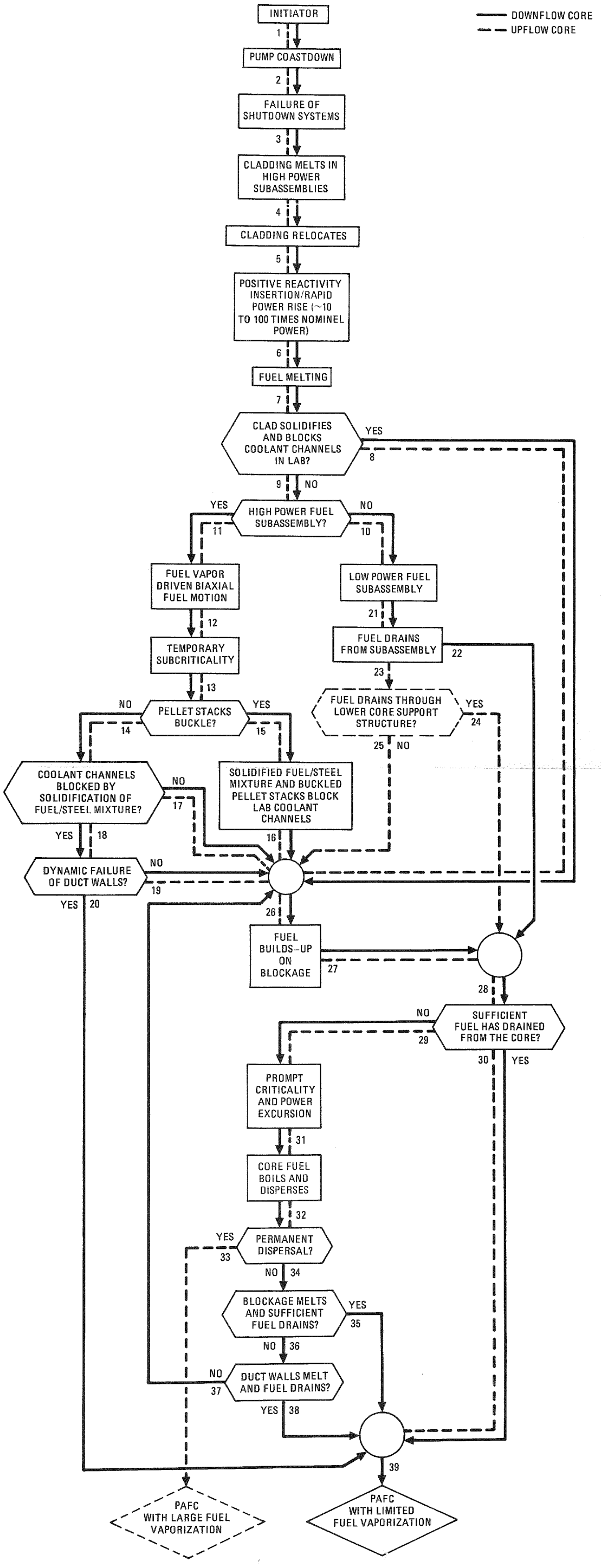

Fig. 13-3. LOF event sequence diagram

would enhance the downward flow of molten steel. Fuel melting follows cladding melting closely in time, and cladding refreezing in the lower axial blanket is not expected. In high-power subassemblies fuel vaporization would rapidly drive molten fuel up and down the flow channels. A temporarily subcritical state is expected because of this early fuel dispersal. The combination of intermixed molten fuel and steel ejected through the axial blanket section would cause the fuel/steel mixture to solidify and block lower axial blanket coolant channels.

On the other hand, low-power subassemblies might have a combination of melting rates and temperatures which would prohibit steel blockages from forming in the lower axial blanket and would allow molten fuel to drain through the subassembly. If a sufficient number of such subassemblies prevailed, the core could be rendered permanently subcritical. A distinction between the up-flow and down-flow core is that in the up-flow core, any draining fuel must drain through the cold inlet blanket and the lower core support structure to ensure permanent subcriticality. Another difference is in the potential for accident mitigation in the down-flow core by duct wall failure due to melting or by dynamic duct wall failure leading to either drainage through the interassembly spacing or fallaway of a subassembly. In high-power subassemblies, refreezing on the duct wall of the very rapidly moving fuel/steel mixture could impart sufficient momentum to fail the duct wall. More likely, however, is melt-through of the duct wall by contact with molten fuel after blockage and subsequent drainage through the interassembly spacing. Because of the massive, cold, lower core support structure in the up-flow concept, neither mechanism is potentially accident-mitigating.

In the event of fuel/steel blockages in the high-power subassemblies and insufficient or delayed drainage from low-power subassemblies, a prompt critical burst and boiled-up core sequence could be expected when the molten fuel which was driven upward returns. In the up-flow core, the only accident termination mechanism from this scenario is dispersal or ejection of sufficient fuel to allow the remaining molten fuel to be subcritical. This could lead to large fuel vapor fractions. The down-flow

core may terminate the accident, by melting through blockages in the lower axial blanket or by duct wall melting and drainage. The ultimate consequences of an LOP (e.g., fraction of fuel vaporized) appear to hinge on the ability to remove fuel from the core. It is currently believed that more timely fuel removal methods would be available for a down-flow concept during an LOF accident than for an up-flow concept.

13.3.4. Transient Overpower Analysis

A TOP accident is one in which there is power-to-flow mismatch at full-power operation occurs because of a postulated reactivity insertion rate with concurrent failure of the plant protection system. Figure 13-4 summarizes the expected sequence of events and the key uncertainties which prevent an adequate understanding of the accident sequence and consequences.

It is customary to characterize TOP in terms of input reactivity ramp rates, although Doppler and fuel expansion feedbacks limit total feedback. The input ramp rate determines the rate at which reactor power rises, which in turn determines many of the characteristics of the accident. Values which have been considered for the GCFR range from \$0.10/s to \$10/s. Regardless of input ramp rate, calculated TOP is characterized by a rise in power with an assumed constant coolant flow. For slow ramps, quasi-steady-state thermal conditions would be obtained, and for fast ramps, the fuel would essentially be adiabatically heated. In either case, the cladding would be subjected to temperature and loading transients that would eventually lead to failure. Potential loading mechanisms include differential thermal expansion of fuel and cladding, loading of cladding by released fission gas or dissolved helium gas, and fuel swelling due to gases entrapped within the fuel. In addition, failure of cladding due to melt-through is a possibility at very low ramp rates. At failure, the fuel rod would usually contain some molten fuel at a high pressure compared with the coolant pressure. When cladding failure occurred, this pressurized molten fuel would be ejected through the breach into the coolant channel, and it would then interact hydrodynamically and thermally with the coolant. The nature of this interaction

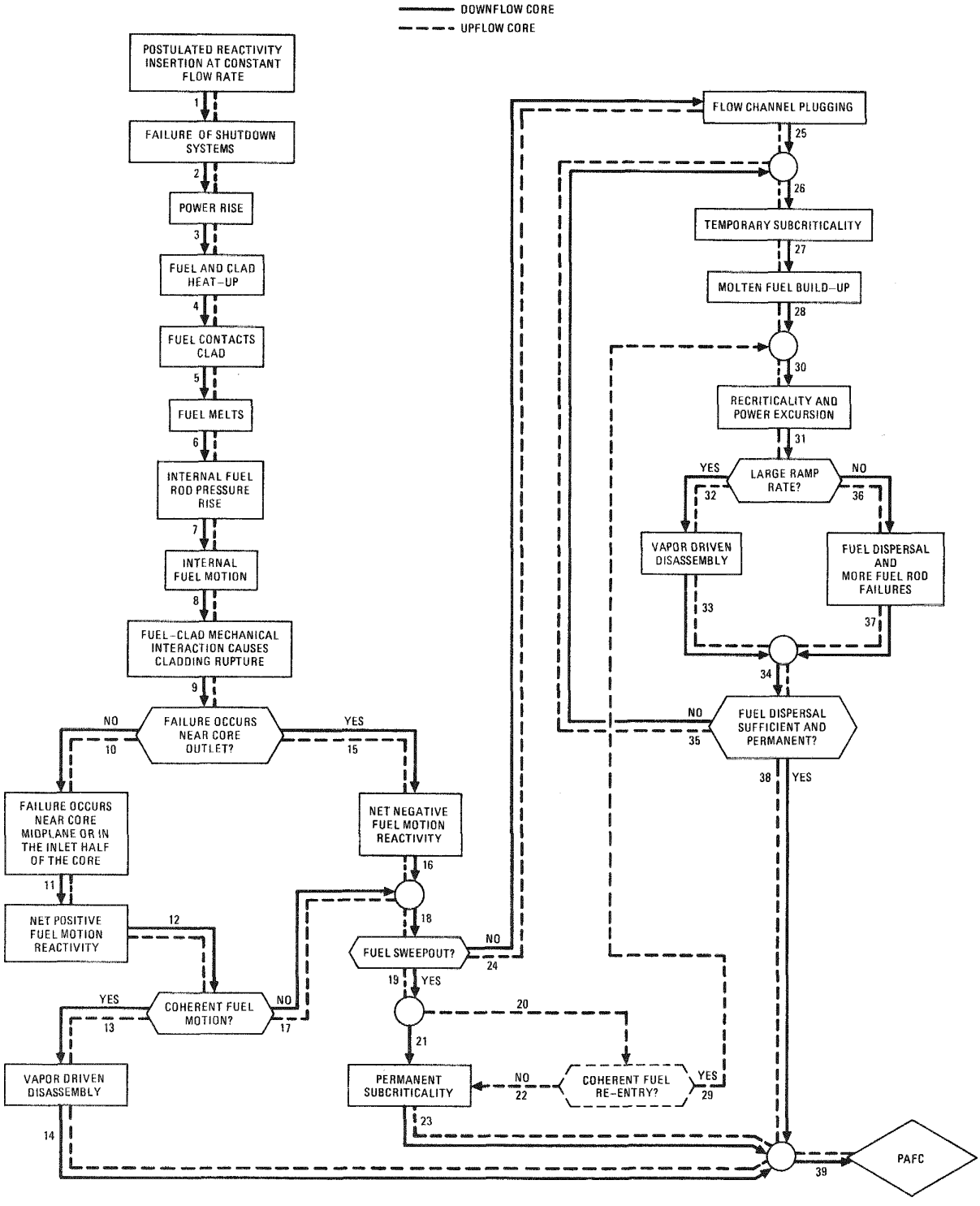

Fig. 13-4. TOP event sequence diagram

would determine the degree of fuel fragmentation and, to some extent, the subsequent motion. Hydrodynamic and thermal interaction between the coolant, fuel, and channel boundaries would determine the extent to which fuel could undergo sweep-out leading to its removal from the reactor core.

Since full coolant flow is maintained, core damage could be limited if neutronic shutdown were calculated to occur. Shutdown could be achieved if fuel removal occurred in relatively few subassemblies. Accident termination would occur when the core configuration was subcritical and coolable. Assurance of this mode of accident termination depends on the occurrence of several sequential events, all of which are currently expected on the basis of analysis. First, the time and location of failure would have to be such that initial fuel motion would produce shutdown rather than reactivity addition. This means that failure would have to occur in the downstream half of the core after substantial molten fuel generation so that fuel motion would occur promptly upon failure and be away from the core midplane. Second, the fuel fragmentation and sweep-out process would have to be effective so that fuel would be removed from the failure site to beyond the core boundaries to maximize the reactivity removal rate and ensure that fuel re-entry did not occur. One uncertainty is the molten or solid fuel fragment size in relation to channel plugging at spacer grid locations. In addition, the up-flow core has the uncertainty of ensuring that the entire mass of fuel does not re-enter the core from the upper axial blanket or upper plenum if coolant flow blockages occur. Furthermore, both concepts should ensure that any channel plugging due to released fuel must be such that the ability to cool the damaged subassemblies can be maintained. If this cannot be done, general meltdown of damaged subassemblies and recriticality may occur.

Assessment of the energetics of an unprotected TOP accident is closely related to the issues surrounding the extent of core damage. If the phenomena leading to shutdown with limited core damage occur and the ability to cool damaged assemblies is maintained, the accident will be energetically benign. However, if the time and location of failure are

unfavorable (near the core midplane or toward the inlet), the fuel motion accompanying cladding failure will produce increased reactivity and the potential for an energetic nuclear excursion. Furthermore, if permanent fuel removal from the core region is not assured, assemblage of a second critical configuration may result in a subsequent increase in the potential for core disassembly. However, it is believed that the energetics from a TOP initiator will not exceed that from an LOF initiator. Because the anticipated TOP event sequence for the up-flow and down-flow concepts is very similar, the TOP sequence is not expected to affect the choice of concept.

13.3.5. Single-Assembly Blockage Analysis

An incident initiated at full power and full flow by complete flow blockage of an individual subassembly is of interest because of the potential for damage propagation from one subassembly to another. It is expected that the probability of such an occurrence would be exceedingly low for both the up-flow and down-flow core. It is also expected that instrumentation would be provided to enable reactor shutdown prior to the spreading of damage to an adjacent subassembly. Analyses indicate that over 90% of the subassembly inlet flow area must be blocked to cause cladding melting. Nevertheless, Fig. 13-5 presumes a complete flow blockage at full-power operation and no plant protection system function.

The sequence of events within the blocked subassembly is similar to that for an unprotected LOF accident in a low-power subassembly. The damage propagation mechanisms are blockage of flow channels because of cladding relocation and solidification and thermal attack by molten fuel. If these mechanisms cause melt-through of the duct wall of unblocked subassemblies, the uncertainty of the events would be similar to that of fuel sweep-out in a TOP.

Cladding would begin to melt within a few seconds following a complete flow blockage of an individual subassembly. Fuel would begin to melt soon after, and the time delay between these two events would determine whether

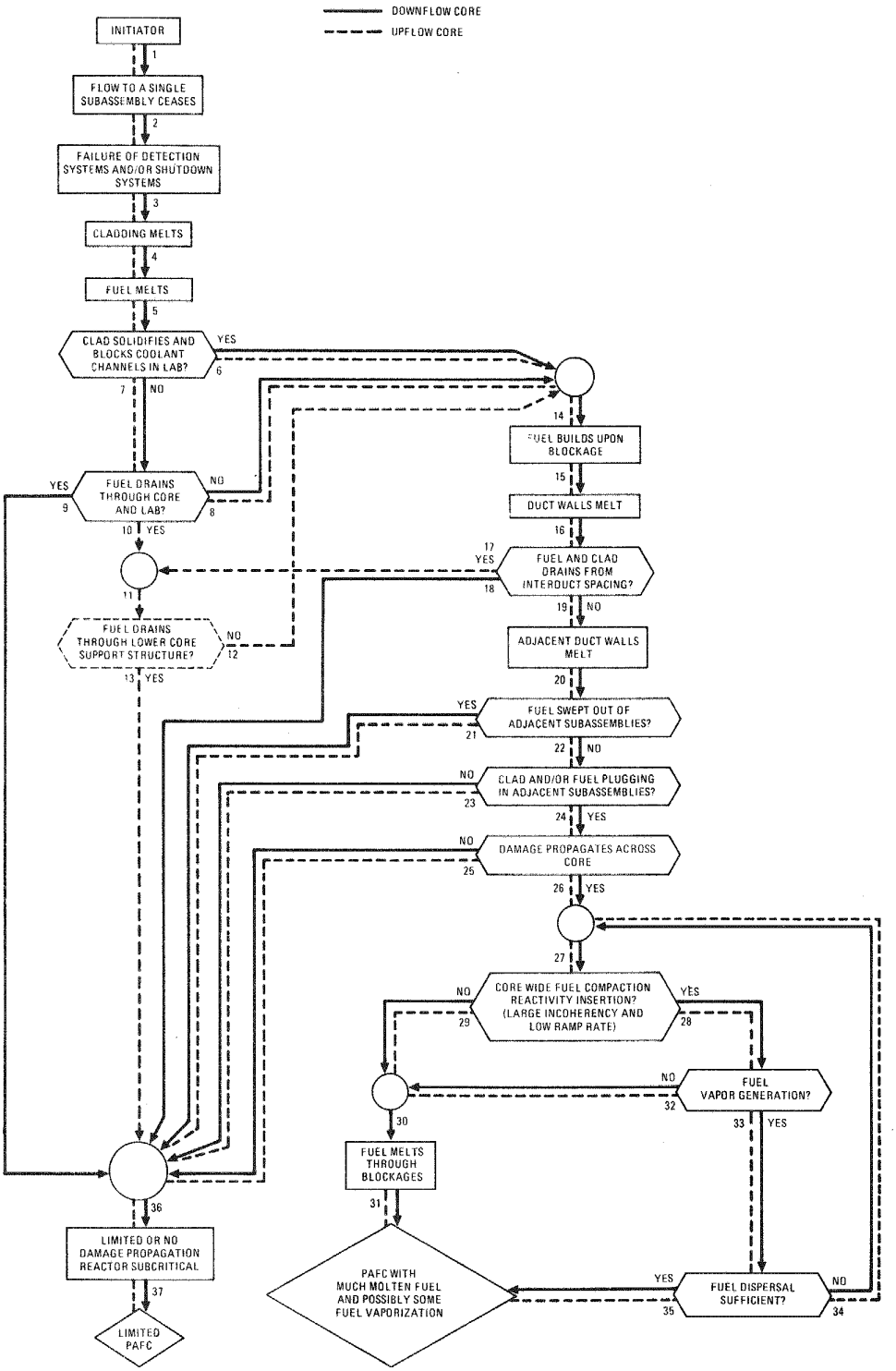

Fig. 13-5. Total flow blockage of an individual subassembly

the cladding would solidify in the lower axial blanket. If fuel and cladding flowed simultaneously, the most likely sequence would be fuel/cladding mixture drainage through the lower axial blanket and the lower subassembly grid. Alternatively, temporary freezing could occur on the lower subassembly grid. This grid or the duct wall would subsequently fail owing to continued buildup of molten fuel. The molten fuel/cladding mixture only has to drain through the subassembly in a down-flow core to eliminate the possibility of damage propagation and end the accident by means of negative reactivity insertion. The same argument cannot be presumed for the up-flow core. The molten fuel would have to either drain through the lower core support structure or fail to block the inlet flow orifices of adjacent subassemblies. Such blockage can occur because of lateral spreading on the support structure.

If cladding blockages form in a down-flow or up-flow core, lateral molten fuel spreading can contact the duct walls and cause them to fail. If molten material could not drain through the interduct spacing (and through the lower support structure in an up-flow core), the adjacent duct walls of surrounding subassemblies may eventually melt. Since these subassemblies would have full flow, molten fuel would be expected to be swept out of the subassemblies in both concepts, similar to the situation after cladding failure during a TOP. Also similar to a TOP, it is only when fuel sweep-out could not effectively be attained that damage could spread beyond the adjacent duct walls. An up-flow core would have the additional potential damage propagation mechanism of lateral fuel spreading and buildup on the lower core support structure. This could cause eventual blockage of the inlet orifices of adjacent subassemblies, thereby producing multiple subassembly flow blockages. The effect of reactor shutdown on the flow blockage accident sequence will be assessed during the next quarter.

13.4. POST ACCIDENT FUEL CONTAINMENT*

During the preliminary phase of the up-flow/down-flow core design studies, a scoping PAFC study was completed. Some potential problems for

*For the up-flow core.

further study were defined, initial PAFC conditions were developed based on different meltdown scenarios, and the major differences between the up-flow and down-flow designs were assessed.

13.4.1. Initial PAFC Conditions

Three distinct initial PAFC conditions may develop:

1. If only molten fuel and molten stainless steel from the core and axial blankets drain through the grid plate, only a small pool of fuel and stainless steel is formed above the cavity floor.

2. If the radial blanket also melts and drains through the grid plate, a larger pool will form above the cavity floor but it will develop at a slower rate.

3. If the core support grid plate fails during the accident sequence owing to exposure to high-temperature fuel, a large molten pool containing the core, blankets, shielding assemblies, and the grid plate might develop.

Detailed analyses are planned to predict the conditions most likely to occur. For conditions 1 and 2, the grid plate with the core barrel and shielding assemblies may still melt down because of thermal radiation from the debris pool formed above the cavity floor.

13.4.2. Retention Volume Required

If a core retention device is designed according to the most conservative meltdown condition (i.e., full-core meltdown including the grid plate and shielding assemblies), a total mass of more than 30 m^3 (three

times the amount of core debris for the down-flow core) must be contained. A 2.5-m thickness of core debris may be accumulated above the cavity floor, and thus a big space must be provided for this debris mass.

13.4.3. Upward Heat Removal

A 0.6-m layer of graphite from the 2.5-m-thick core debris resulting from a full core meltdown is formed above the debris pool. Therefore, upward heat removal is likely to be insignificant and will be insensitive to helium convection (forced or natural). The heat capacity of the reactor internal structures may be able to absorb all the upward-flowing heat.

For the partial core meltdown case (with shielding assemblies and grid plate remaining), the graphite layer is less than 0.1 m. Therefore, a significant amount of decay heat can still be removed through the solid graphite layer. If helium convection cannot be restored with a proper time limit, the grid plate will melt and the inventory of a full-core meltdown is obtained. Whether this is an expected event sequence needs to be studied further.

13.4.4. Potential Reduction of Retention Volume

If upward heat removal does not depend on helium convection, blockage of the helium flow path may be permitted and core retention volume can be greatly reduced with a minimum dropping distance for core debris.

13.4.5. Stored Heat Effect and the Possibility of Fuel Boiling

With a full core meltdown, the increased core debris (stainless steel and graphite) would certainly enhance the stored heat effect, i.e., the grace period without emergency cooling would be extended. However, with a total debris thickness of 2.5 m, the fuel region at the bottom of the core debris would reach a very high temperature, i.e., above the melting point. Compared with a partial or full core meltdown in a down-flow core, there are greater possibilities for fuel boiling.

13.4.6. Steel Bath Core Retention Concept

With a full core meltdown, the volume of steel is three times that of the fuel and blanket. Therefore, if a molten fuel pool has not yet formed at the bottom of the debris, there is a greater chance that a pool of stainless steel may be formed first. The fuel and blanket could be in the form of solid pieces submerged in the steel bath. As a result, fuel boiling could be suppressed.

13.4.7. Emphasis in PAFC System Design

During normal operation, the gamma heating rate in the lower shield of the up-flow core is about one-tenth of that in the down-flow core. The requirement for the lower shield is thus very much relaxed. Furthermore, in the lower plenum region, the low helium inlet temperature reduces the requirement for the thermal barrier in the lower cavity region. Therefore, in the core catcher design (as well as the lower shield design), more consideration can be given to PAFC conditions instead of normal operating conditions.

13.4.8. Downward Heat Removal and Refueling Penetration

Top refueling, a natural choice for the up-flow core, seems to be the most promising factor for PAFC. Since penetration of molten fuel through the refueling port is always a problem with the bottom penetration design, top refueling would tend to make downward heat removal and core catcher design simpler.

13.4.9. Planned PAFC Analysis

Several PAFC analyses have been planned for the up-flow core design:

1. A one-dimensional up/down heat split analysis to examine the downward melting progression and estimate the required amount

of upward heat removal. A condition without cooling will also be considered to determine the effect of stored heat.

2. Two-dimensional upward heat removal analysis to ascertain whether the grid plate with the core barrel will melt down owing to thermal radiation from the debris pool surface after a partial core meltdown.

3. An assessment of core retention concepts to determine suitable schemes for up-flow core configurations.

13.5. ENGINEERING RELIABILITY INTEGRATION

There was no activity on this subtask during this quarter.

13.6. GAS-COOLED REACTOR RELIABILITY BANK

There was no activity on this subtask during this quarter.

14. GCFR SAFETY TEST PROGRAM (189a No. 00588)

Two large-scale experimental test programs are being established to support the development and verification of GCFR accident analysis methods. The GRIST-2 facility is an in-pile transient helium test facility to be installed in the TREAT Upgrade reactor for testing of GCFR fuel under rapid, high-power transient conditions predicted to occur during unprotected LOF and reactivity insertion transients (TOP). The DMFT program is an out-of-pile test program to investigate the behavior of cladding and assembly duct walls during PLOF accident sequences. Its major objective is to characterize postmelt cladding and duct motion within an assembly and between assemblies.

14.1. GRIST-2 PROGRAM

Concerns have been raised over the projected cost of the total GRIST-2 test program, and more cost-effective alternatives may have to be considered. GRIST-2 is a test program for verifying methods of analysis of beyond design basis accidents. It consists of two basic elements, test fuel procurement and the GRIST-2 transient test program. Since the test program requirements have not been defined to the point where the quantity of test fuel and the test fuel requirements have been fully established, it is not meaningful to examine options for varying these requirements. However, the two most fundamental options can be considered: (1) a GRIST-2 program without a test fuel preirradiation program or (2) no GRIST-2 program at all.

The GRIST-2 code verification program will enable the degree of conservatism in the accident consequences to be justifiably minimized. A lack of such code verification is thus likely to increase the containment requirements, and the savings associated with a reduced GRIST-2 or

no GRIST-2 approach must be evaluated against these increased requirements. In addition, licensing feasibility and the prospects of public acceptance of a reactor system that cannot eliminate large core vaporization fractions and energy releases, even though the consequences are contained, must also be considered.

Option 1 would eliminate the requirement for prototypical GCFR fuel preirradiation. All important test transient phenomena must be preserved for option 1 to be viable. A program has been outlined that could accomplish this objective. It considers simultaneous preirradiation in EBR-II of fuel rods under typical GCFR and LMFBR conditions as well as fabrication of fresh fuel with out-of-pile preconditioning. All three types of fuel and cladding would be subjected to microscopic analysis, cladding pressurization tests, direct electric heating transient tests, and TREAT tests in stagnant helium to investigate differences in fuel behavior. The technical feasibility of such a program still needs to be assessed in detail. It is not certain that the fuel preirradiation requirement for GRIST-2 can indeed be waived on the basis of such a test program, and a 2- to 3-yr delay in the GRIST-2 program could result if selection of a preirradiation facility and conceptual design did not proceed in parallel. However, a significant increase in the preconstruction permit experimental data base for fuel behavior would be accomplished and could have a significant licensing payoff for a demonstration plant.

Option 2 would entirely eliminate the GRIST-2 program for the demonstration plant. The bounding core disruptive accidents would have to be accepted and adequate containment capability demonstrated in order for option 2 to be viable. It is likely that a GRIST-2 type program would be required for licensing commercial plants. Furthermore, the cost of a substitute program for demonstrating containment ability may be very high, and even if containment could be demonstrated, concern of the acceptability of a reactor which cannot eliminate large amounts of fuel aerosols still remains.

14.2. GRIST-2 PRELIMINARY TEST PLAN FUEL FABRICATION AND PREIRRADIATION REQUIREMENTS

Documentation of the preliminary GRIST-2 test plan and fuel fabrication and preirradiation requirements was completed (Ref. 14-1). This work was undertaken by GA under the old GRIST-2 program organization. ANL has been assigned the responsibility for GRIST-2 test planning and will be responsible for completing the test fuel requirements for GRIST-2, which will constitute the basis for the fuel fabrication and preirradiation task for which GA has responsibility.

The test plan is designed for a 5-yr testing period prior to the operating license for a GCFR demonstration plant and includes 16 tests. The major parameters varied in the tests are

Type of transient: LOF, TOP

Type of fuel: UO_2, mixed oxide

Fuel preconditioning: fresh fuel, short preirradiation (1 month nominal), long preirradiation (1 yr nominal)

Preirradiation power: high, low

LOF fuel failure state: melted, vaporized

TOP ramp rate: \$0.10/s, \$1/s

Bundle size: 3, 7, 19 rods

The test plan outline for the 5-yr test period is shown in Table 14-1. A description of each test, its purpose, and a priority ranking are shown.

The proposed GRIST-2 test schedule is shown on Fig. 14-1. Because of tight schedule requirements, grouping of three to five tests into a test package is proposed whereby one test approval package (experiment plan, safety analysis report, request for approval in principle) and one test report would be prepared. This restriction would be lifted if the test schedule could be expanded. Based on the test plan and test schedule, the test fuel preirradiation schedule shown in Fig. 14-2 was

TABLE 14-1
GRIST-2 PRELIMINARY TEST PLAN OUTLINE (FIRST 5 YEARS)

Test Designation	Type	Bundle Size	Test Fuel Condition	Fuel Type	Pin Power Type	LOF Fuel Failure State	TOP Ramp Rate	Priority
			Phase I. Fresh Fuel Tests					
GL1	LOF	7	No preconditioning	UO_2	N.A.	Molten		1
GL2	LOF	7	No preconditioning	UO_2	N.A.	Vapor		1
GT1	TOP	7	No preconditioning	UO_2	N.A.		1 $/sec	1
			Phase II. Preconditioned BOL Fuel Tests					
GT2	TOP	7	1 mo. preirradiation	Mixed-oxide	LPP		1 $/sec	2
GT3	TOP	7	1 mo. preirradiation, restructured	Mixed-oxide	HPP		1 $/sec	1
GL3	LOF	7	1 mo. preirradiation	Mixed-oxide	LPP	Molten		1
GL4	LOF	7	1 mo. preirradiation, restructured	Mixed-oxide	HPP	Vapor		1
			Phase III. Preirradiated Fuel Tests					
GL5	LOF	7	9 mo. preirradiation	Mixed-oxide	HPP	Molten		2
GL6	LOF	7	9 mo. preirradiation	Mixed-oxide	HPP	Vapor		1
GL7	LOF	3	15 mo. preirradiation	Mixed-oxide	LPP	Just melting		1
GL8	LOF	7	15 mo. preirradiation	Mixed-oxide	LPP	Molten		1
GT4	TOP	3	9 mo. preirradiation	Mixed-oxide	HPP	Pin failure	1 $/sec	1
GT5	TOP	7	9 mo. preirradiation	Mixed-oxide	HPP		1 $/sec	1
GT6	TOP	7	15 mo. preirradiation	Mixed-oxide	LPP		1 $/sec	2
GT7	TOP	7	9 mo. preirradiation	Mixed-oxide	HPP		10 ¢/sec	1
GT8	TOP	7	15 mo. preirradiation	Mixed-oxide	LPP		10 ¢/sec	2
			Phase IV. Scaling Tests					
GL9	LOF	19	No preconditioning	UO_2	N.A.	Molten		2
GT9	TOP	19	No preconditioning	UO_2	N.A.		1 $/sec	2

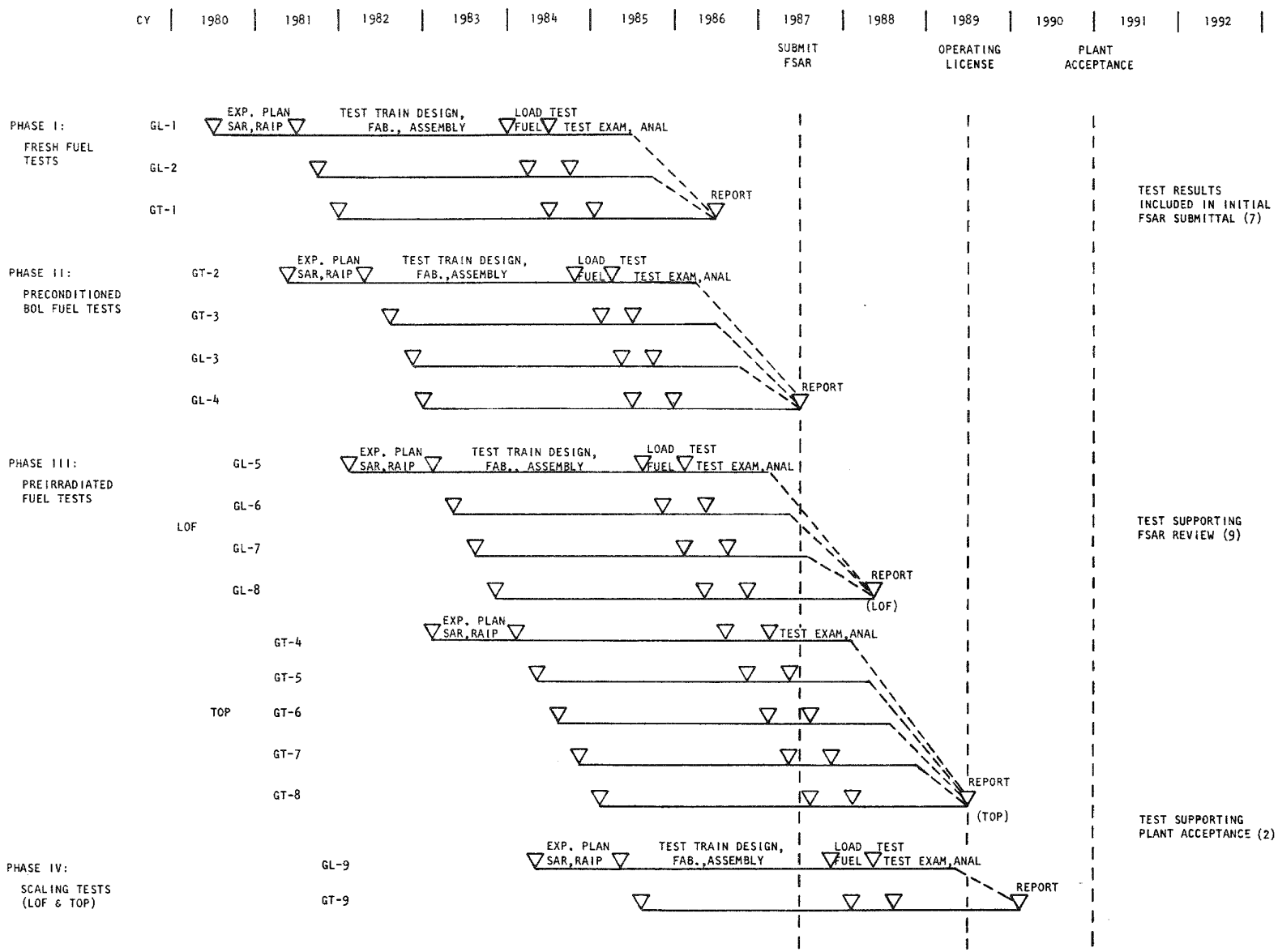

Fig. 14-1. Proposed GRIST-2 testing schedule to meet needs of tests outlined in preliminary test plan

IRRADIATION PARAMETERS					
			PREIRRADIATED RODS		
BURNUP	POWER	FUEL TYPE	BUNDLE SIZE	TEST RODS	SIBLING RODS
LO	HI	$(Pu,U)O_2$	19	14	5
LO	LO	$(Pu,U)O_2$	19	14	5
HI	HI	$(Pu,U)O_2$	19	17	2
HI	LO	$(Pu,U)O_2$	27	24	3
HI	HI	$(Pu,U)O_2$	19	14	5
TOTAL IRRADIATED RODS			103	83	20

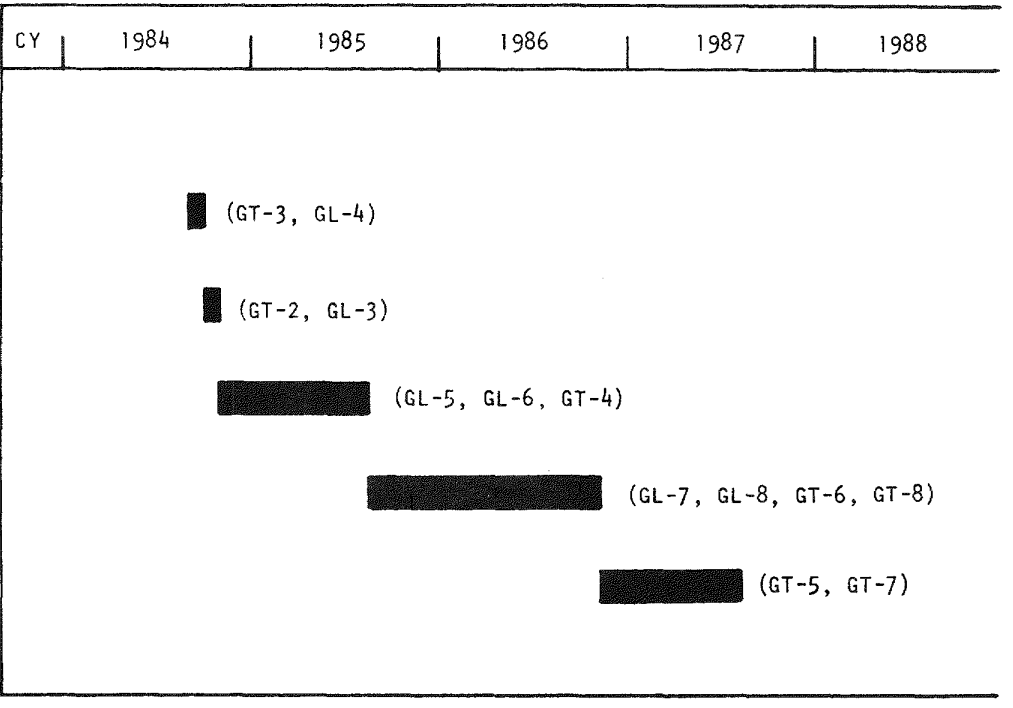

Fig. 14-2. Fuel preirradiation program to support tests outlined in preliminary GRIST-2 test plan

developed. To meet these fuel needs on a time scale compatible with the test plan, a break in an preirradiation bundle size of 27 rods is needed. If a specific GCFR preirradiation facility is required, it will be necessary to commence test reactor selection in FY-79 and conceptual design in FY-80 to meet the GRIST-2 base schedule shown in Fig. 14-3. The new plant acceptance date has eased the schedule pressure on the GRIST program.

In order for GA to proceed with the test fuel task, it is necessary to specify the test fuel requirements fully. Under the new GRIST-2 program organization, ANL is responsible for test planning. The need date for the test fuel specification is May 1, 1979. The major test fuel preirradiation requirements which need to be resolved are listed in Table 14-2. A preliminary list of fuel requirements for each GRIST-2 test is shown in Table 14-3 (the specific requirements which have not been firmly established but which need to be set by May 1, 1979 are labelled TBD). The GRIST-2 preliminary test plan and requirements for fuel fabrication and preirradiation completes GA's responsibilities for GRIST-2 test planning.

14.3. DUCT MELTING AND FALLAWAY TEST PROGRAM

The following were accomplished during this quarter: (1) a major milestone in the DMFT program was passed with the completion of testing of the first full-length subgroup test assembly (FLS-1); (2) the DMFT Program Management Plan (Ref. 14-1) was prepared; and (3) fabrication was initiated of prototypical ducts, rods, and spacers for the first guarded core module test expected in late 1979.

14.3.1. FLS-1 Experiment

Seven scheduled tests using FLS-1 at LASL were completed. The electrical fault that aborted the fourth test (FLS 1-4) was repaired by replacing the lower electrode. Tests FLS 1-5 and FLS 1-6, which were repeats of FLS 1-1 and FLS 1-4, respectively, suggest that some changes

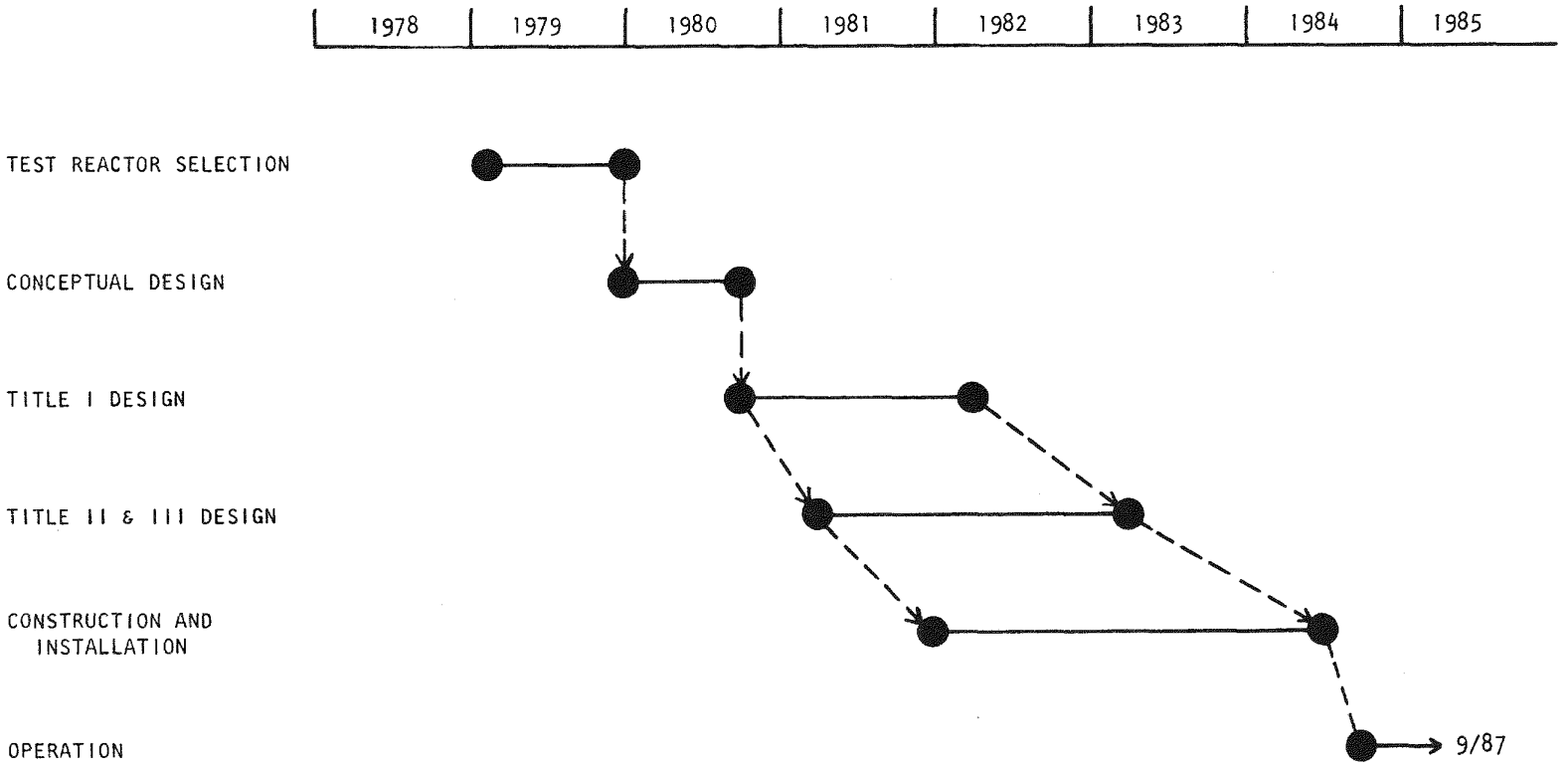

Fig. 14-3. Estimated schedule for designing and constructing a preirradiation loop facility for the GRIST-2 program

TABLE 14-2
PREIRRADIATION REQUIREMENTS THAT NEED FURTHER DEFINITION
PRIOR TO INITIATING PREIRRADIATION FACILITIES SURVEY

Item	Transient Test Requirement Needing Definition or Clarification	Possible Effect on Preirradiation Program	Comments, Possible Solutions, and/or Alternatives to Consider
A. Fuel enrichment	Range of enrichments needed to properly conduct LOF and TOP tests	If TOP test rods are required to be preirradiated in a fast flux facility, it may not be possible to obtain highly enriched irradiated fuel because of excessively high heat generation rates produced during preirradiation.	1. If fast neutron flux irradiations are required, determine possibility of using prototypic enrichments in running GRIST-2 TOP tests. 2. Alternatives to fast flux irradiation: a. Preirradiate only cladding material in fast neutron spectrum and assemble pellets into rods afterwards. b. Investigate alternate means of inducing mechanical property changes to cladding which would simulate irradiation effects, i.e., extra work-hardening, heat treating in He atmosphere, etc.
B. Enrichment grading (matching of preirradiation and test conditions)	Need and acceptability of enrichment grading to maintain flat power profile across bundle during transient testing in GRIST-2. Effects on power transient with or without enrichment grading.	Almost certainly, enrichment grading will be necessary during preirradiation to achieve uniform power and temperature profiles across bundle. In this event, a requirement for no enrichment grading in GRIST-2 would result in need for additional irradiation to obtain sufficient rods for single enrichment experiment. Conversely, requirements for enrichment grading in GRIST-2 need to be consistent with enrichment grading requirements for preirradiations.	ANL currently indicates that enrichment grading is prohibited because of possible distortion of test result interpretations due to maldistribution of primary fissions in fuel having different enrichments. Range of permissible variations in enrichment needs to be determined to avoid excessive uncertainty in hodoscope detection of fuel motion due to variations in primary fission coming from fuel having different enrichments.
C. Fast vs thermal flux preirradiations for TOP tests	Define need for fast flux irradiation for rods to be used in TOP accident studies.	If fast flux preirradiations are required, cost of GRIST-2 preirradiation program could possibly double because of need for additional preirradiation loop facility.	1. Determine if alternate means are available to simulate fast flux irradiation damage to cladding (see comment 2 for item A). 2. Investigate possibility of using FTR driver fuel rods for TOP tests.

TABLE 14-2 (continued)

Item	Transient Test Requirement Needing Definition or Clarification	Possible Effect on Preirradiation Program	Comments, Possible Solutions, and/or Alternatives to Consider
D. Helium pressure			
1. Helium sorption effects in fuel	1a. Need for preconditioning fresh fuel to build in helium, which may be rapidly dissolved in fuel during first days of irradiation.	1a,b. Would require all fresh fuel tests to receive short period (~1 mo) preirradiation prior to testing in GRIST-2. Requirement has minor scheduling impact but significant cost impact on preirradiation rod procurement effort.	1a,b. Determine possibility of saturating fuel in high-pressure helium to obtain desired quantity of dissolved gas within fuel grain structure.
	1b. Need to define proper helium and fission gas environment during both long- and short-term preirradiations.	1b. May require simulating PES.	1b. Alternatives to be considered after requirement is established.
2. Prototypicality of internal and external helium environment	2. Need to establish prototypic helium content and strain in cladding.	2. Require preirradiations to be run in high-pressure helium loop with PES.	2a. Determine possibility of soaking fuel rod in He before testing in GRIST-2. b. Investigate alternate means of embrittling He cladding, e.g., giving cladding special heat treatment. c. Determine acceptability of preirradiation in a high-pressure nonhelium environment with high helium internal pressure. d. Determine acceptability of preirradiating fuel rods in sodium-bonded capsules, i.e., tests having prototypic internal helium rod pressures but cooled externally by sodium bond.
E. Fuel rod length	Need to define acceptable ranges of fuel rod lengths for core upper axial blanket and lower axial blanket regions.	Length of rods will influence selection of preirradiation reactor as well as design of preirradiation loop facility.	For cases where either upper axial blanket or lower axial blanket does not meet requirements, determine feasibility of reconstituting rods after preirradiation to obtain proper blanket length.
F. Radial and axial temperature profiles in rods during preirradiation	Need to define acceptable limits on uniformity of restructuring and gas distribution in test fuel.	Influences test reactor selection as well as design and location of loop within test reactor.	Alternatives to be considered after requirement is established.
G. Burnup to fast fluence ratio	Define acceptable limits on burnup as function of fast neutron fluence for TOP rod irradiation.	Influences test reactor selection; may require fast flux reactor preirradiation.	Investigate alternative means of inducing prototypic cladding damage as function of burnup (see items A and C).

TABLE 14-3
LIST OF FUEL REQUIREMENTS NEEDING DEFINITION IN ORDER TO DEFINE
THE SCOPE OF THE GRIST-2 FUEL FABRICATION AND PREIRRADIATION TASK

Test Type	No. of Rods		Type of Rods		Test Fuel Rod Condition	Cladding Preconditioning	Preirradiation Conditions				Tests
	Test	Sibling	Composition	Enrichment			Rod Power	Burnup (at. %)	Fast Fluence	Prototypic Fuel Preconditioning[a]	
LOF	33	7	UO_2	High	Fresh	(b)	NA	NA	NA	NA	GL1, GL2, GL9
TOP	26	4	UO_2	TBD	Fresh	TBD	NA	NA	NA	NA	GT1, GT9
TOP	7	(c)	Mixed-oxide	TBD	Preirradiated	TBD	Low	<<1	TBD	TBD	GT2
TOP	7	(c)	Mixed-oxide	TBD	Preirradiated	TBD	High	<<1	TBD	TBD	GT3
LOF	7	(c)	Mixed-oxide	TBD	Preirradiated	(b)	Low	<<1	TBD	TBD	GL3
LOF	7	(c)	Mixed-oxide	TBD	Preirradiated	(b)	High	<<1	TBD	TBD	GL4
LOF	14	(c)	Mixed-oxide	TBD	Preirradiated	(b)	High	∿3	TBD	TBD	GL5, GL6
LOF	10	(c)	Mixed-oxide	TBD	Preirradiated	(b)	Low	∿3	TBD	TBD	GL7, GL8
TOP	17	(c)	Mixed-oxide	TBD	Preirradiated	TBD	High	∿3	TBD	TBD	GT4, GT5, GT7
TOP	14	(c)	Mixed-oxide	TBD	Preirradiated	TBD	Low	∿3	TBD	TBD	GT6, GT8

[a] Prototypic fuel preconditioning includes requirements on rod helium pressures, radial and axial gradients in power and temperature, need for PES, etc.

[b] Condition of cladding is not considered to influence fuel rod behavior during LOF accident since cladding is molten before any fuel motion is assumed to occur.

[c] Number of sibling pins available to characterize fuel rod prior to testing will depend upon choice of preirradiation bundle size and grouping of rod types to be preirradiated together.

may have occurred in the test assembly. The destructive test FLS 1-7 used a simplified power transient. The heater rods maintained their integrity for a period of time which was longer than predicted. The test was terminated with 18 failed heater rods and limited duct melting. The precise nature of the original FLS 1-4 electrode failure has been discussed along with observed post-FLS 1-4 duct bowing, the evidence for reversed FLS 1-7 duct bowing, radiographs of the duct internals, and the next steps in post-test examination. Destructive duct wall cutaway was accomplished, and the nature of the cladding blockage, the surprising elevation of the duct hole (noted previously), and the apparent early failure of several heater rods were considered.

14.3.2. FLS-1 Analytical Support

Pretest analysis for all the FLS-1 tests did not accurately predict the experimental measurements. Variations in actual execution of the low-pressure test require reanalysis. The predictions for the high-pressure tests were inadequate because important physical phenomena were not adequately modeled. The dominant differences are under investigation; however, the major inadequacy in the predictive model appears to be the lack of natural-convection-induced heat transport. The azimuthal asymmetry evident in the post-test examination may be due to experimental anomalies not expected in the real GCFR core.

REFERENCES

14-1. Tang, I. M., D. P. Harmon, and A. Torri, "GRIST-2 Preliminary Test Plan and Fuel Fabrication and Preirradiation Requirements," DOE Report GA-A15121, General Atomic Company, to be published.

14-2. Moore, R. A., "Request for Review of DMFT Program Management Plan," General Atomic Company, unpublished data, September 18, 1978.

15. GCFR NUCLEAR ISLAND DESIGN (189a No. 00615)

The purpose of this subtask is to develop preliminary system designs and general arrangements of the nuclear island so that the feasibility of several nuclear island concepts can be evaluated and the major dimensions of the buildings established.

During this quarter, the following was accomplished:

1. The feasibility of converting the main helium circulator from a vertical to a horizontal position for the up-flow core concept, in which the circulators are located at the bottom of the PCRV, was investigated.

2. A study was conducted to determine the impact of the in-vessel and ex-vessel refueling schemes associated with the up-flow core on the nuclear island design. Both schemes are feasible; however, adoption of either results in major changes to the originally proposed reactor service building arrangement.

3. The proposed criteria to be used for the core cooling system design have been discussed, and a possible shutdown cooling system and rough estimates of its costs have been examined.

4. Demonstration plant containment building configurations for the reference (down-flow core) plant and the up-flow core concepts were analyzed to determine the effects of containment back pressure on CACS performance and drive motor horsepower requirements.

5. A meeting was held with an architect-engineering firm to obtain its unofficial review of the current BOP design. The reactor building configuration (steel containment with a surrounding reinforced concrete confinement) was questioned, and the reasons for the choice of this particular design were explained, specifically the Nuclear Regulatory Commission (NRC) requirement for a postulated 1% fuel (plutonium) release to the containment. Construction problems associated with a concrete "haunch" and refueling penetration at the base of the building were also discussed, and it was concluded that the present steel containment design is practical and acceptable.

16. ALTERNATE DESIGN STUDY (189a No. 00759)

The objective of this task is to develop and evaluate alternate design concepts for the GCFR 300-MW(e) plant NSSS configuration, components, and related plant facilities and equipment.

16.1. ALTERNATE RESIDUAL HEAT REMOVAL SYSTEM STUDY

The purpose of this subtask is to study and evaluate alternate RHR concepts with the objective of improving the RHR system of the present reference design or developing RHR concepts that would be applicable to the reference design and larger GCFR plants. Particular emphasis has been placed on improving the reliability and availability of the RHR system by providing diversity and reducing system complexity.

During this quarter the progress of the first phase of this design study was documented (Ref. 16-1). A ground rule for this study was that it should principally be directed to the down-flow core design but should include a maximum degree of commonality to make it applicable to the up-flow core. It was also decided that investigation of natural convection cooling should not be included, at least initially, since it is presently being investigated in the up-flow core design studies.

16.1.1. Residual Heat Removal Requirements

The RHR capability provides a means of removing residual heat from the reactor system (including the core and other internals) for the following conditions:

1. Scheduled reactor shutdown (pressurized).
2. Reactor trip (pressurized).

3. Refueling (unpressurized).
4. DBDA (depressurized).

The RHR systems are specifically required to limit the maximum cladding temperature to provide an adequate safety margin for all operating and specified accident conditions.

16.1.2. Reference Design

For the GCFR baseline reference design (Ref. 16-2), the primary RHR capability is provided by the main loops. The CACS also provides an alternate cooling source which is independent of the main loops whenever main loop cooling is insufficient or not available. The CACS consists of the core auxiliary heat exchanger (CAHE), auxiliary circulators, and the core auxiliary cooling water system (CACWS). In the CAHE core, residual heat is transported by forced helium circulation on the shell side and forced water circulation on the tube side. The heat in the CACWS is ultimately rejected to the atmosphere utilizing air blast heat exchangers.

In the previous reference design (Ref. 16-2) the main circulators were driven by series steam-driven turbines; electric-motor-driven main circulators are proposed for the present reference design. In both designs, the auxiliary circulators are driven by electric motors. In the alternate design study, electrically-driven and steam-driven circulators were included in some of the concepts to provide added diversity. However, this should not be construed as a proposal to use a steam drive in place of the electric drive as currently specified for the reference design main circulator.

16.2. ALTERNATE RHR CONCEPTS

A number of alternate RHR system concepts were developed for evaluation (Table 16-1), covering a wide range of configurations for the main and auxiliary loops, including independent and combined series and parallel flow concepts. Some of these concepts could be incorporated into

TABLE 16-1
ALTERNATE RHR CONFIGURATIONS

Configuration	Description
1a	Reference design (steam-driven circulators)
1b	Modified reference design with parallel flow steam-driven main circulators
2	Running auxiliary heat removal system (GBR-4 design)
3	Series heat exchangers/parallel circulators
4	Series heat exchangers/series circulators
5	Parallel heat exchangers/parallel circulators
6	Parallel heat exchangers/series circulators
7	Series heat exchangers/one circulator
8	CACS loop without CAHE
9	Modified backup design with diverse main feed pumps
10	Boiling CAHE with in-house power

the reference design demonstration plant with relatively minor design perturbations, while others, particularly those using the series steam generator and CAHE and series or parallel flow circulators, would impose considerable NSS configuration changes. Emphasis was placed on the series heat exchanger configurations, since they offer the possibility of being able to simplify the main to auxiliary loop transfer procedure and are also expected to simplify the PCRV design by reducing the number of cavities. This is of particular interest for large multiloop plant systems where space in the PCRV becomes a critical concern. The reference design was also included in the evaluation as a benchmark.

16.2.1. Screening Evaluation

A preliminary screening evaluation of the alternate RHR concepts was performed to limit the number of most promising candidates to two or three which could be more fully explored and analyzed in the next phase of the design study. Five major categories were identified, and each category was subdivided to define important considerations contributing to the design. Appropriate weighting factors were assigned to each category in terms of importance as given below:

Category	Weighting Factor
Safety and licensing	35
Performance	20
Development and commercialization	20
Operation and maintenance	15
Power plant cost	10
Total	100

The highest weighting factor was assigned to safety and licensing. This category was subdivided into six subcategories: (1) diversity, (2) reliability, (3) level of redundancy, (4) complexity, (5) plant control, and (6) diverse power supply. Each subcategory was assigned a points index for the design requirements and associated bases for evaluation. Other

categories were also divided, with each having appropriate maximum points assigned to each subcategory. After assigning appropriate rating points to each subcategory, the sum for each category was obtained and combined with the appropriate weighting factor to obtain the overall evaluation rating.

16.2.2. Candidate Concepts

All RHR concepts were evaluated based on the screening procedure as outlined above. The three most promising concepts were selected and are proposed for evaluation:

1. A revised reference design in which safety-related components are added to provide reactor cooling during pressurized cooldown or refueling in the event of main turbine trip and nonavailability of the main condenser. This cooling system, identified as the shutdown cooling system, is intended to provide core cooling during the time interval between main loop coast-down and CACS start-up.

2. A configuration which incorporates series steam generators and CAHE with parallel series flow circulators (two per loop). The steam generator and CAHE for each loop would be located in the same PCRV cavity. The circulators would probably be located in separate cavities to accommodate the circulator, diffuser, and valve geometry.

3. A steaming core auxiliary boiler (CAHE) concept which produces steam for in-house turbine generator sets which in turn would provide auxiliary power for essential RHR safety backup systems. A possible option of steam-to-steam reheat for the main turbine is also offered by this concept.

A number of other, more radical means of providing additional and more diverse methods of RHR have been suggested and are reviewed in the study.

REFERENCES

16-1. Macken, T., "Interim Report on RHR Concept for GCFR," General Atomic Company, unpublished data, August 22, 1978.

16-2. "300-MW(e) Gas-Cooled Fast Breeder Reactor Demonstration Plant," General Atomic Company Report GA-A13045, July 15, 1974.

17. ALTERNATE FUEL CYCLES (189a No. 00761)

The purpose of this task is to determine the characteristics of a GCFR fueled with a variety of fissile and fertile materials. These characteristics will be used to evaluate various reactor fuel strategies which could be employed to improve the proliferation resistance and/or energy capability of future nuclear power systems. A general outline for the study was established previously, and the preliminary analysis and evaluation phase has been completed (Ref. 17-1). Preliminary fuel strategy studies indicate that the fuel cycles of greatest interest for the GCFR are

1. Pu/U core with U or Th blankets.
2. Pu/Th core with Th blankets.
3. (Low-enriched) U-233/Th core with Th blankets.

Core material and configuration studies are being performed during the second phase of the program to identify the optimum states for the various parameters for each fuel composition.

During this quarter, approximate parametric studies have continued on two of the fuel cycles of interest (Pu and Pu/Th cores). The design characteristics of large core designs for the Nonproliferation Alternate Systems Assessment Program (NASAP) have been documented, and fuel strategy studies have been initiated to help identify the optimum core characteristics for the various roles which a fast breeder reactor may be required to fulfill.

17.1. APPROXIMATE SENSITIVITY ANALYSIS

Earlier parametric studies which provided guidance for the GCFR NASAP mass flow submittals indicated several limitations in the core performance code CALIOP (Ref. 17-2) used to approximate many core design parameters.

Modifications have been made to make several improvements in CALIOP, including:

1. A method of radially zoning the core to consider the noncylindrical geometry of the zone boundaries.

2. A depletion routine (with fission products) to follow core reactivity.

3. A fuel enrichment search which will produce the desired end-of-cycle core multiplication.

4. A means of separating net fissile production (and species) in the core and blanket.

The improved CALIOP code is being tested to verify the adequacy of the revised version.

As part of the effort to verify and calibrate the improved analytical techniques, a series of revised sensitivity calculations have been made to more precisely determine the appropriate rod diameter for a large-scale GCFR. Figure 17-1 presents breeding ratio, specific power, and doubling time as a function of fuel rod diameter for a 1200-MW(e) GCFR. As in previous (less precise) studies, the breeding ratio increases monotonically with fuel rod diameter, reactor rating decreases monotonically with rod size, and doubling time passes through a rather flat minimum between a rod diameter of 8 and 9 mm. Since doubling time does not consider the total amount of power being doubled initially, total energy potential is not necessarily maximized by minimizing doubling time.

The fuel rod diameter resulting in the maximum GCFR energy availability from a finite Pu reserve is illustrated in Fig. 17-2. For the case shown, a given U_3O_8 resource (2×10^6 tonnes) is assumed to be used to fuel 400 GW(e) of LWR, and the resulting Pu is available for use in a fast breeder reactor.

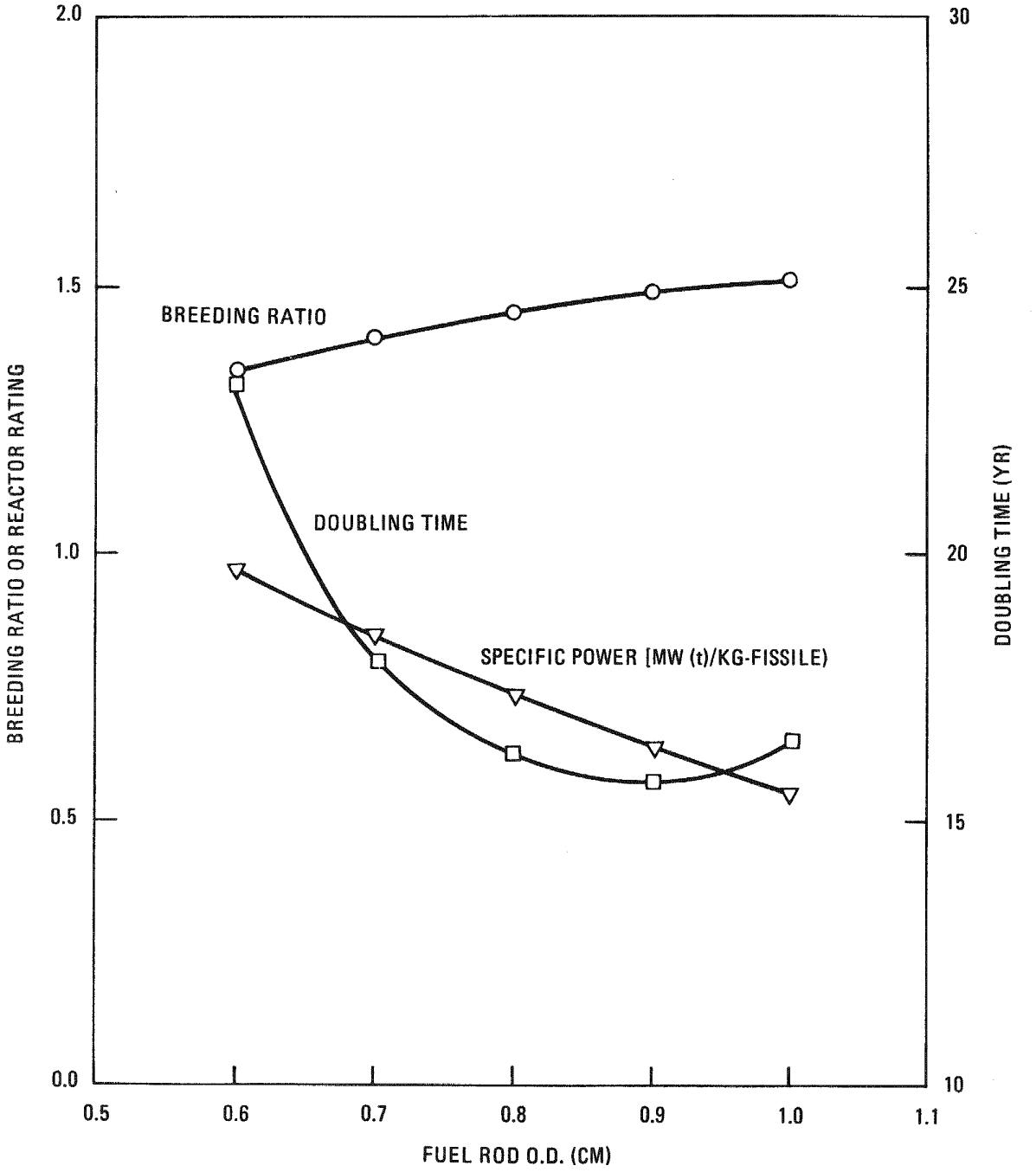

Fig. 17-1. Characteristics of 1200-MW(e) GCFR, $Pu/U/U/UO_2$

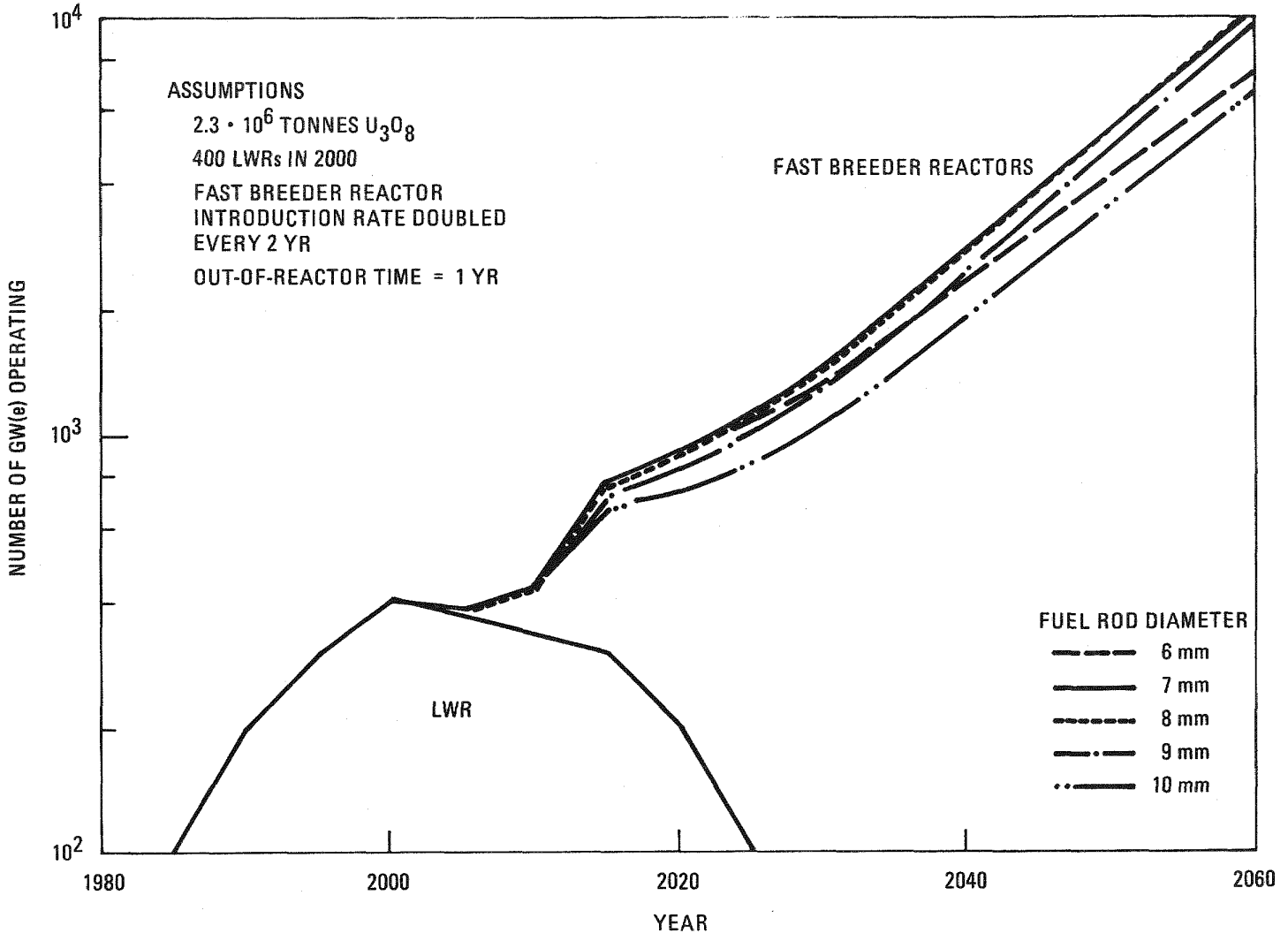

Fig. 17-2. Energy potential of a Pu/U/U/U GCFR influenced by fuel rod diameter

Figure 17-2 indicates that a fuel rod diameter of 7 to 8 mm will result in the maximum energy potential. Based on this analysis, the 8-mm rod selected for the GCFR NASAP submittals can be judged to be approximately optimum for nonsymbiotic breeder systems.

17.2. DETAILED MASS FLOW INFORMATION

As indicated previously, two GCFR NASAP submittals (Refs. 17-3, 17-4) have been made. Both contained complete mass flow information for Pu/U and Pu/Th GCFR core designs. Table 17-1 compares the mass flow characteristics of the two designs. The second submittal was prepared to meet revised ground rules and reduced the linear heat rate by approximately 15%. Reducing the linear heat rate produces an increase in specific inventory and fissile gain. A slight increase in doubling time can also be anticipated.

17.3. ALTERNATE FUEL CYCLE MATERIALS

Little progress has been made on this subtask during the current quarter. Descrepancies between various sets of thermodynamic data on actinide carbides are being resolved.

REFERENCES

17-1. Hamilton, C. J., "A Preliminary Study of Alternate Fuel Cycles for the Gas-Cooled Fast Breeder Reactor," General Atomic Report GA-A14536, August 1977.

17-2. Thompson, W. I., "CALIOP - A Multichannel Design Code for Gas-Cooled Fast Reactors," General Atomic Company, unpublished data.

17-3. Broido, J. H., General Atomic Company, private communication, May 24, 1978.

17-4. Broido, J. H., General Atomic Company, private communication, June 14, 1978.

TABLE 17-1
COMPARISON OF GCFR ROUND 1 AND ROUND 2 PHYSICS PARAMETERS IN THE NASAP STUDY

	$Pu/UO_2/UO_2/UO_2$ Case 2		$Pu/UO_2/ThO_2/ThO_2$ Case 8		$Pu/ThO_2/ThO_2/ThO_2$ Case 12	
	Round 1	Round 2	Round 1	Round 2	Round 1	Round 2
Breeding ratio	1.51	1.54	1.48	1.51	1.41	1.40
Fuel volume fraction	0.27	0.27	0.27	0.27	0.34	0.36
Core height (cm)	110	127	110	127	110	127
Core enrichment	0.137	0.128	0.142	0.132	0.149	0.145
Specific power [MW(t)/kg fissile]	0.870	0.767	0.795	0.740	0.501	0.464
Specific inventory [kg/MW(e)]	3.30	3.57	3.45	3.70	5.47	5.91
Fissile gain [kg/MW(e)-yr]	0.304	0.330	0.272	0.292	0.208	0.230
Fissile gain/specific inventory (%)	9.21	9.24	7.88	7.89	3.80	3.89
Peak linear heat rate (kW/ft)	17.2	14.1	19.0	15.1	17.2	14.2
Cladding thickness (cm)	0.043	0.043	0.043	0.043	0.043	0.054
Gap between fuel elements (cm)	0.99	1.46	0.99	1.46	1.11	1.64